
**Inter-Agency Agreement to Conduct Scientific Studies
Relevant to the Stormwater Treatment Areas**

A-6-a: DRAFT Comprehensive Interim Report

Agreement No. 4600003125

SUBMITTED ON:
September 23, 2015

PREPARED FOR:
South Florida Water Management District and Everglades Agricultural Area
Environmental Protection District

PREPARED BY:
DB Environmental, Inc.



Table Of Contents

1	Executive Summary	1-1
1.1	Previous PSTA Research	1-1
1.2	Existing Knowledge Gaps	1-2
1.3	Current Research	1-2
1.3.1	STA-3/4 PSTA Cell	1-2
1.3.2	Mesocosm and Microcosm Studies	1-4
1.4	The State of PSTA Research	1-6
2	Introduction and Background	2-1
2.1	Description of Periphyton-based Stormwater Treatment Areas	2-2
2.2	Previous PSTA Research	2-3
2.2.1	Limitations of early PSTA research	2-5
2.3	Study Plan Objectives and Outstanding PSTA Research Questions	2-6
2.4	Opportunities with the STA-3/4 PSTA Facility, and Complementary Ongoing Investigations	2-8
2.4.1	STA-3/4 PSTA Cell	2-8
2.4.2	PSTA microcosm and mesocosm studies	2-10
2.5	Report organization	2-10
3	STA-3/4 PSTA Cell	3-11
3.1	Treatment Performance	3-11
3.2	Comparison to muck-based systems	3-12
3.3	Internal Water Quality Surveys	3-14
3.3.1	Introduction	3-14
3.3.2	Methods	3-14
3.3.3	Response of surface water TP and phosphatase enzymes to flow pulses	3-17
3.3.4	Water quality profiles	3-26
3.3.5	Discussion	3-29
3.4	Sediments	3-30
3.4.1	Introduction	3-30
3.4.2	Methods	3-30
3.4.3	Results and Discussion	3-31
3.5	Macrophytes	3-34
3.5.1	Introduction	3-34
3.5.2	Methods	3-35
3.5.3	Results	3-36
3.5.4	Discussion	3-44
3.6	Periphyton	3-45

3.6.1	Introduction	3-45
3.6.2	Periphyton on Natural Substrates	3-45
3.6.3	Periphyton on Artificial Substrates: Glass Slide Periphytometers	3-54
3.6.4	Periphyton Taxonomy	3-63
3.6.5	Discussion	3-69
4	Mesocosm and Microcosm Studies	4-1
4.1	Quantifying Operational Boundaries: Water Depth Effects on Water Column Phosphorus and Vegetation Communities	4-1
4.1.1	Introduction	4-1
4.1.2	Methods	4-1
4.1.3	Water Quality	4-8
4.1.4	Biological Response	4-26
4.2	PSTA Substrate Effects on Vegetation and Water Column Chemistry	4-37
4.2.1	Introduction	4-37
4.2.2	Methods	4-37
4.2.3	Results	4-39
4.2.4	Discussion	4-49
4.3	Substrate and Macrophyte Interactions	4-51
4.3.1	Introduction	4-51
4.3.2	Methods	4-51
4.3.3	Results	4-52
4.3.4	Discussion	4-55
4.4	Investigations with Low-P Muck Soils and a Limerock Cap	4-56
4.4.1	Introduction	4-56
4.4.2	Methods	4-56
4.4.3	Results	4-59
4.4.4	Discussion	4-75
4.5	Use of Limerock Cap to Reduce Flux from High P Soils	4-75
4.5.1	Background	4-75
4.5.2	Methods	4-75
4.5.3	Results	4-77
4.5.4	Discussion	4-83
5	References	5-1

List Of Figures

Figure 1.	Location map of STA-3/4 and PSTA Project, including the Upper and Lower SAV Cells, the PSTA Cell, and related water control structures.	2-8
Figure 2.	Periphyton growing on <i>Chara</i> sp. and <i>Eleocharis</i> stems in the STA-3/4 PSTA Cell.....	2-9
Figure 3.	Mean annual total phosphorus (TP) concentrations in the inflow and outflow waters from the PSTA Cell during the period of record (Andreotta et al, 2015).....	3-11
Figure 4.	Correlations between annual P loading rate, inflow and outflow P concentrations, and the fraction of outflow water added to the cell from sources other than inflow structures.	3-12
Figure 5.	Box and whisker plots (top) and cumulative distribution functions (bottom) of water TP concentrations in outflow culvert grab samples collected between January 2008 - February 2014 by the District from STA-3/4 Cell 2B, Cell 3B and the PSTA Cell.....	3-13
Figure 6.	Flow and stage as measured at the PSTA Cell inflow and outflow structures, and the surface water TP concentration at each structure during the period from January 2012 - July 2014.	3-15
Figure 7.	PSTA Cell monitoring and sampling locations.	3-16
Figure 8.	Average daily flow and stage as measured at the PSTA Cell inflow and outflow structures, and the surface water TP concentration at each structure during the period of the first managed pulse: June 1 - August 25, 2012.....	3-18
Figure 9.	Total phosphorus concentrations and alkaline phosphatase activity along internal transects within the PSTA Cell during Pulse #1 (August 2, 2012), compared to sampling events before and after the pulse.....	3-19
Figure 10.	Flow and stage as measured at the PSTA Cell inflow and outflow structures, and the surface water TP concentration at each structure during the period of the second managed pulse: October 1 - December 1, 2012.	3-20
Figure 11.	Total phosphorus concentrations and alkaline phosphatase activity (APA) along internal transects within the PSTA Cell during Pulse #2 (October 25, 2012), compared to sampling events before and after the pulse.	3-21
Figure 12.	Flow and stage as measured at the PSTA Cell inflow and outflow structures, and the surface water TP concentration at each structure during the period from June 1 - July 14, 2014. The arrows note internal water quality sampling events.	3-23
Figure 13.	Comparison of total phosphorus concentrations in the surface waters of the PSTA Cell for three sampling dates, before, during and after a period of high flows (flows peaked just prior to 6/26/14).....	3-24

Figure 14.	Comparison of alkaline phosphatase activity (APA) in the surface waters of the PSTA Cell for three sampling dates, before, during and after a period of high flows.	3-24
Figure 15.	Chlorophyll a concentrations (pheophytin-corrected) in the surface waters of the PSTA Cell for three sampling dates, before, during and after a period of high flows.	3-25
Figure 16.	Phosphorus species concentrations in the surface water at inflow and outflow structures, and three internal transects within the cell, on June 26, 2014.	3-25
Figure 17.	Longitudinal profile of total phosphorus concentrations through the PSTA Cell, as well as the upstream Upper SAV Cell and Cell 2A, in the central flow way of STA-3/4, on June 26, 2014.	3-27
Figure 18.	Enzyme activity in the surface waters along internal transects through the PSTA Cell and the upstream Upper SAV Cell, as well as at inflow and outflow structures, on June 26, 2014.	3-27
Figure 19.	Internal profiles of total phosphorus (TP) for 16 sampling events between May 2012 and July 2014.	3-28
Figure 20.	Average (\pm SE) total phosphorus concentrations and alkaline phosphatase activity (APA) in surface waters of the PSTA Cell, based on multiple internal water sampling events under different flow conditions: No flow (N=2), moderate flow (N = 11) and high flow (N=3).	3-29
Figure 21.	Internal locations within the STA-3/4 PSTA Cell where sediments were assessed for accrual depth, chemistry and P flux studies.	3-32
Figure 22.	Spatial survey of the depth of the accrued sediment layer in the STA-3/4 PSTA Cell, based on a field survey on May 15, 2014 of 13 internal transects each with three stations where the accrued depth was measured.	3-32
Figure 23.	Phosphorus content, depth, bulk density and P storage of the newly accrued sediment layer along three transects within the PSTA Cell, in May 2014.	3-33
Figure 24.	Enzyme activity in the newly-accrued sediment layer along three transects within the PSTA Cell in May 2014. Values denote the mean \pm SE of three stations along each transect.	3-34
Figure 25.	Stages in the STA-3/4 PSTA Cell during the period from May 1, 2010 through August 1, 2015, and dates of 11 SAV surveys within the cell during that time.	3-35
Figure 26.	Relative density and distribution of <i>Chara</i> in the PSTA Cell for each of 111 semi-quantitative vegetation surveys between July 2011 and June 2015.	3-37
Figure 27.	Relative density and distribution of <i>Potamogeton</i> in the PSTA Cell for each of 11 semi-quantitative vegetation surveys between July 2011 and June 2015.	3-38
Figure 28.	Relative density and distribution of <i>Najas guadalupensis</i> in the PSTA Cell for each of 11 semi-quantitative vegetation surveys between July 2011 and June 2015.	3-39

Figure 29.	Percent cover of three SAV species (under moderately dense conditions, or greater) in the STA-3/4 PSTA Cell over time.....	3-39
Figure 30.	Density and distribution of submerged macrophyte species in the PSTA Cell and Upper SAV Cell (“Head Cell”) during a survey on June 19, 2014.....	3-40
Figure 31.	Density and distribution of <i>Utricularia</i> species in the PSTA Cell and Upper SAV Cell (“Head Cell”) during a survey on June 19, 2014.....	3-40
Figure 32.	Density and distribution of emergent macrophyte species in the PSTA Cell and Upper SAV Cell (“Head Cell”) during a survey on June 19, 2014.....	3-41
Figure 33.	Comparison of SAV biomass along inflow, mid, and outflow transects through the PSTA Cell on 3 dates.....	3-43
Figure 34.	Changes in tissue P content over time along internal transects within the PSTA cell.....	3-43
Figure 35.	Recent plant tissue P concentrations are shown relative to an earlier sampling event in August 2010.....	3-44
Figure 36.	Periphyton growth on <i>Chara</i> in the PSTA Cell.....	3-46
Figure 37.	Areal biomass of epiphytes growing on <i>Chara</i> tissues in the PSTA Cell, on two sampling dates.....	3-47
Figure 38.	Phosphorus content of periphyton growing on <i>Chara</i> tissues in the PSTA Cell, on two sampling dates. Values represent individual grab samples.....	3-47
Figure 39.	Nitrogen content of periphyton growing on <i>Chara</i> tissues in the PSTA Cell, on two sampling dates. Values represent individual grab samples.....	3-48
Figure 40.	Phosphorus content of periphyton and its associated host macrophyte, along three internal transects within the PSTA Cell, in 2015 (top) and 2015 (bottom).	3-50
Figure 41.	Comparison of tissue composition of five macrophyte species found within the PSTA Cell on June 24, 2015.....	3-51
Figure 42.	Comparison of the nutrient composition of periphyton tissues associated with five macrophyte species found within the PSTA Cell on June 24, 2015.....	3-52
Figure 43.	Phosphorus concentrations of periphyton associated with <i>Chara</i> along inflow, mid and outflow transects within the PSTA Cell, on five dates between August 2013 and June 2015.....	3-53
Figure 44.	Periphytometers retrieved on August 8, 2013, from the middle of the PSTA Cell (Station G-2) after a 6-week deployment.....	3-55
Figure 45.	Areal biomass of slide periphyton after 2, 4, and 6 weeks of exposure to <i>in situ</i> conditions at three locations in the STA-3/4 PSTA Cell.....	3-56
Figure 46.	Change in nutrient content of periphyton growing on glass slides, during two 6-week deployment periods in summer 2013 and winter 2014.....	3-57
Figure 47.	Nutrient ratios in the periphyton grown on glass slides in the PSTA cell.....	3-58

Figure 48.	Tissue phosphorus contents in periphyton growing on glass slides, collected along internal transects within the PSTA Cell, on two dates before and after a flow pulse.	3-59
Figure 49.	Areal biomass of periphyton grown on glass slides along transects internal to the PSTA Cell, before and after a flow pulse.....	3-59
Figure 50.	Chlorophyll a contents for periphyton grown on glass slides along transects internal to the PSTA Cell, before and after a flow pulse.....	3-60
Figure 51.	Monoesterase alkaline phosphatase activity (APA) of periphyton along transects internal to the PSTA Cell, before and after a flow pulse.	3-60
Figure 52.	Alkaline phosphatase (monoesterase) activity (APA) associated with periphyton growing on glass slides on January 29, 2014.....	3-61
Figure 53.	Enzyme activity associated with periphyton growing on <i>Chara</i> tissues on January 2, 2014.	3-62
Figure 54.	Enzyme activity of periphyton growing on a variety of naturally-occurring substrates in the PSTA Cell, on January 2, 2014.....	3-62
Figure 55.	Periphyton assemblage from the STA-3/4 PSTA cell. Photo by Michael Hein (400X).....	3-64
Figure 56.	Relative abundance of the most dominant Cyanobacteria genera observed on glass slides retrieved January 29, 2014, after 6 weeks of deployment in the STA-3/4 PSTA Cell.	3-65
Figure 57.	Relative abundance of dominant diatom species observed on glass slides retrieved January 29, 2014, after 6 weeks of deployment in the STA-3/4 PSTA Cell.....	3-66
Figure 58.	Relative dominance of three diatom species found in periphyton grown on natural substrates (<i>Chara</i> and <i>Eleocharis</i>), at three locations within the PSTA Cell.....	3-66
Figure 59.	Relative dominance of cyanobacteria genera found in periphyton grown on natural substrates (<i>Chara</i> and <i>Eleocharis</i>), at three locations within the PSTA Cell.....	3-67
Figure 60.	Relative dominance of diatoms in the slide periphyton samples collected June 19, 2014 from inflow, middle and outflow transects within the PSTA Cell.....	3-68
Figure 61.	Relative dominance of cyanobacteria in the slide periphyton samples collected June 19, 2014 from inflow, middle and outflow transects within the PSTA Cell.....	3-69
Figure 62.	Mesocosms were established at a range of water depths to explore the effects of operating conditions on P removal effectiveness and biological community response.	4-2
Figure 63.	Process train configuration for static depth and variable depth mesocosms.	4-3

Figure 64.	Water depth schedules for each of four depth treatments during the monitoring period (December 12, 2013 – April 1, 2015).	4-4
Figure 65.	Periphyton in mesocosms has developed on the benthic surface, as well as tank walls, plant surfaces, and in some areas, benthic mats have separated to form floating mats (left image). The middle image shows a sampling collar used to define the area for benthic periphyton sampling, and a recess for measuring photosynthetically active radiation (PAR) at the benthic surface. The benthic periphyton mat shown in the right image was removed from the outflow region of a mesocosm on May 29, 2014.	4-6
Figure 66.	Sampling grid used for relative macrophyte density evaluations.	4-8
Figure 67.	Inflow phosphorus (P) loading rate to each flow way during the period of record (December 18, 2013 – April 1, 2015).....	4-8
Figure 68.	Surface water total phosphorus (TP) concentrations and alkaline phosphatase activity (APA) for inflow and outflow waters (D = fourth tank in series) from mesocosms operated at static depths of 23 and 46 cm.	4-9
Figure 69.	Concentrations of three forms of nitrogen in the inflow and outflow waters from mesocosms operated at static water depths of 23 cm and 46 cm.	4-10
Figure 70.	Dissolved organic matter characterization of the outflow waters from mesocosms operated at 23 cm and 46 cm water depths.	4-12
Figure 71.	Response of surface water TP concentrations to increased water depths, measured at the midpoint and outflows from mesocosms operated at depths between 46 and 69 cm.	4-13
Figure 72.	Response of surface water TP concentrations to increased water depths, measured at the midpoint and outflows from mesocosms operated at depths between 46 and 92 cm.	4-14
Figure 73.	Average (\pm SE) inflow and midpoint surface water total phosphorus (TP) concentrations (top panel) and outflow concentrations (lower panel) from process trains operated at static depth (46 cm) or variable depths during the period between March 2014 and January 2015.	4-16
Figure 74.	Characteristics of the dissolved organic matter in inflow and outflow waters from mesocosms operated at static or variable depths.....	4-17
Figure 75.	Nitrogen concentrations in inflow and outflow waters from mesocosms operated at static or variable depths.....	4-18
Figure 76.	Inflow, midpoint and outflow concentrations of total phosphorus (TP) for mesocosm flow ways operated at either static depths (23 cm or 46 cm) or variable depths (46-69 cm or 46-92 cm).....	4-19
Figure 77.	Inflow concentrations of phosphorus species are compared to midpoint concentrations (upper panel) and outflow concentrations (lower panel) for mesocosm flow ways operated at either static depths (23 cm or 46 cm) or variable depths (46-69 cm or 46-92 cm).....	4-20

Figure 78.	Average total phosphorus concentrations in the inflow waters and outflow-region surface waters of flow ways operated at either 23 cm or 46 cm depths, for the period December 2013 – April 1, 2015.	4-21
Figure 79.	A comparison of total phosphorus concentrations in the inflow, midpoint, and outflows from the four treatments.	4-22
Figure 80.	Alkaline phosphatase activity (APA) in the surface waters of inflow, midpoint and outflow waters during the period of record between February 2014 and April 2015.	4-23
Figure 81.	A comparison of dissolved organic phosphorus (DOP) concentrations in the inflow and outflows from the four treatments.	4-24
Figure 82.	A comparison of particulate phosphorus (PP) concentrations in the inflow and outflows from the four treatments.	4-25
Figure 83.	Light remaining at the sediment surface, as a fraction of the ambient light available above the water column, in the outflow region of mesocosms operated under four depth treatments.	4-27
Figure 84.	Areal biomass development on the benthic surface of mesocosms operated at either 23 cm or 46 cm water depths.	4-28
Figure 85.	Areal biomass of benthic periphyton grown in mesocosms operated at either static water depth (23 or 46 cm) or variable water depth, on three sampling dates (Top panels).	4-29
Figure 86.	Relative density of benthic periphyton in each of four tanks in series of process trains operated at static water depths of either 23 cm or 46 cm.	4-30
Figure 87.	Relative density of <i>Chara</i> in each of four tanks in series of process trains operated at static water depths of either 23 cm or 46 cm.	4-31
Figure 88.	Relative density of <i>Potamogeton</i> in each of four tanks in series of process trains operated at static water depths of either 23 cm or 46 cm.	4-32
Figure 89.	Relative density of benthic periphyton in the first tank in series (top panel) of process trains operated at variable water depths of either 46-69 cm or 46-92 cm. (bottom panel).	4-34
Figure 90.	Relative density of <i>Chara</i> in the first tank in series (top panel) of process trains operated at variable water depths of either 46-69 cm or 46-92 cm. (bottom panel).	4-35
Figure 91.	Relative density of <i>Potamogeton illinoensis</i> in the first tank in series (top panel) of process trains operated at variable water depths of either 46-69 cm or 46-92 cm. (bottom panel).	4-36
Figure 92.	Photo of the experimental soil-water columns, and inflow water reservoir (left). Photos on the right depict the mixture of macrophytes (<i>Chara</i>) and algae in three of the treatments.	4-38

Figure 93.	Total phosphorus (TP) and total nitrogen (TN) contents of sediments collected May 31 and August 22, 2012 from the outflow regions of the PSTA Cell and Lower SAV Cell, respectively.	4-40
Figure 94.	Total phosphorus (TP) concentrations in the inflow waters to experimental columns and in the surface waters above PSTA sediment and exposed limerock (LR) substrate treatments, during the period of record (November 28, 2012 – September 11, 2013).....	4-41
Figure 95.	Total phosphorus (TP) concentrations in the inflow waters to experimental columns and the surface waters above two substrate treatments, during the period of record (November 28, 2012 – September 11, 2013).	4-42
Figure 96.	Dissolved organic phosphorus (DOP) concentrations in the inflow waters to experimental columns and in the surface waters above PSTA sediment and exposed limerock (LR) substrate treatments, during the period of record (November 28, 2012 – September 11, 2013).....	4-42
Figure 97.	Dissolved organic phosphorus (DOP) concentrations in the inflow waters to experimental columns and in the surface waters above two muck substrate treatments, during the period of record (November 28, 2012 – September 11, 2013).....	4-43
Figure 98.	Particulate phosphorus (PP) concentrations in the inflow waters to experimental columns and in the surface waters above PSTA sediment and exposed limerock (LR) substrate treatments, during the period of record (November 28, 2012 – September 11, 2013).....	4-43
Figure 99.	Particulate phosphorus (PP) concentrations in the inflow waters to experimental columns and in the surface waters above two muck substrate treatments, during the period of record (November 28, 2012 – September 11, 2013).....	4-44
Figure 100.	Alkaline phosphatase activity (APA) in the surface waters above PSTA sediment and exposed limerock (LR) substrate treatments, during the period of record (November 28, 2012 – September 11, 2013).....	4-44
Figure 101.	Alkaline phosphatase activity (APA) in the inflow waters to experimental columns and the surface waters above two substrate treatments, during the period of record (November 28, 2012 – September 11, 2013).	4-45
Figure 102.	A comparison of water column TP concentrations in flow-through columns established on PSTA sediments and muck soils from Cell 3B of STA-3/4, during the period from April 10 – September 11, 2013.	4-46
Figure 103.	Average (\pm SE) inflow or water column total phosphorus (TP) concentrations in triplicate columns established on limerock (LR), muck sediments (STA-3/4 Cell 3B), or PSTA sediments, for the period April 10 – September 11, 2013 (N=23).....	4-46

Figure 104.	Enzyme hydrolysis rate of inflow and outflow waters in columns established on 3 substrate types, over the period of record (May 15, 2013 – September 11, 2013; N= 11 bi-weekly sampling events).....	4-47
Figure 105.	Areal biomass of periphyton growing on the walls of experimental columns established on three substrates: exposed limerock (LR), PSTA sediment, and muck sediments from STA-3/4 Cell 3B.....	4-47
Figure 106.	Enzyme (monoesterase) activity in periphyton (June 2013) collected from the fiberglass walls of experimental columns established on three substrates: exposed limerock (LR), PSTA sediments, and muck soils from STA-3/4 Cell 3B.	4-48
Figure 107.	Soil enzyme activity at the end of the study period (September 2013) in the upper 5 cm soil layer in experimental columns under three substrate treatments: exposed limerock (LR), PSTA sediments, and muck soils from STA-3/4 Cell 3B. Monoesterase (APA) and diesterase (PDE) activity was normalized to the dry weight of the soil as assayed.	4-48
Figure 108.	Average total phosphorus (TP) concentrations in the inflow water to experimental columns and the surface water above substrate treatments, during two consecutive phases of operation. Also shown is the P content as measured in the upper 5 cm of the soil at the conclusion of Phase II.	4-50
Figure 109.	Surface water Total P concentrations in cores incubated outdoors with one of three substrates (limerock (LR), PSTA sediment, or muck), and one of three vegetation treatments, during a 12-week study period.	4-53
Figure 110.	Total phosphorus content in soils from the PSTA Cell and the outflow region of STA 2 Cell 3 (Muck).....	4-54
Figure 111.	Chemical composition and dry weights of <i>Chara</i> , and <i>Potamogeton</i> tissues in cores incubated outdoors for 84 days, compared to the initial conditions of the inoculum, as a function of sediment type.	4-55
Figure 112.	Mesocosms were established on unfarmed low-phosphorus muck soils with and without a “cap” of limerock gravel placed onto the sediment surface prior to flooding.....	4-57
Figure 113.	Mean total phosphorus (TP) concentrations in the inflow waters and outflow waters of triplicate mesocosms established with or without limerock added as a cap over muck soils, for the period of operation prior to draw-down (May 2011 – April 2014).....	4-59
Figure 114.	Long-term mean total phosphorus (TP) concentrations from mesocosms for three periods of operation: an initial period of low P loading (May 2011 – January 2013), higher P loading (February 2013 – April 2014), and a post-drawdown period (June 2014 – February 2015).....	4-60
Figure 115.	Mean surface water outflow dissolved organic phosphorus (DOP) and particulate phosphorus (PP) concentration for mesocosms established with limerock added as a cap to muck soils.	4-61

Figure 116.	Average enzyme hydrolysis rates for monoesterase (APA) and diesterase (PDE) in the inflow and outflow waters of mesocosms with or without limerock added as a cap over muck soils.....	4-62
Figure 117.	Average dissolved organic carbon (DOC) concentrations in the inflow and outflow waters of mesocosms with or without limerock added as a cap over muck soils.	4-63
Figure 118.	Average dissolved calcium concentrations in the inflow and outflow waters of mesocosms with or without limerock added as a cap over muck soils.	4-63
Figure 119.	Dissolved organic phosphorus (DOP) and particulate phosphorus (PP) concentrations in the surface waters of muck-based mesocosms with or without a limerock cap, during a 3.8-year period of operations.	4-64
Figure 120.	Soil characteristics in the accrued layer and at discrete depth intervals for cores collected on October 22, 2013, from mesocosms where the P removal performance of un-amended muck soils is compared to treatments with a limerock (LR) cap.	4-66
Figure 121.	Alkaline phosphatase activity (APA), phosphodiesterase (PDE) activity and pH measured in the newly-accrued sediments and underlying muck soils collected from outdoor mesocosms on October 22, 2013, after 2.5 years of flow through operations.....	4-67
Figure 122.	Change (amount of reduction) in sediment thickness (top panel) and sediment oxidation-reduction potential during a 42-day drawdown period.....	4-68
Figure 123.	Average total phosphorus (TP) concentrations in the inflow and outflow waters of mesocosms established on low-P muck soils with and without a limerock cap, for the period prior to and following a drawdown of water levels in each mesocosm.....	4-70
Figure 124.	Plant tissue characteristics on three sampling dates. Values represent the average (\pm SE) of grab samples from triplicate mesocosms under each treatment.....	4-72
Figure 125.	Macrophyte biomass in muck-based mesocosms with and without a limerock cap, on April 7 2014, just prior to vegetation sampling and drawdown.....	4-72
Figure 126.	Average (\pm SE) standing crop biomass of submerged aquatic vegetation (primarily <i>Chara</i> and <i>Potamogeton</i>) in triplicate mesocosms with or without a limerock (LR) cap above muck soils, as determined April 9, 2014 after three years of flow-through operations.....	4-73
Figure 127.	Standing crop biomass of the two dominant SAV species at the conclusion of the study on February 2, 2015.....	4-73
Figure 128.	Standing crop biomass and total phosphorus content of submerged aquatic vegetation (SAV) tissues on February 2, 2015, at the end of the period of operations.	4-74

Figure 129. Enzyme activity of epiphytic algae on <i>Chara</i> and <i>Potamogeton</i> grown in outdoor mesocosms established on a low-phosphorus muck soil with or without a limerock (LR) cap.	4-74
Figure 130. Four limerock treatments were applied to the muck soils: 0, +5, +10, +15 cm limerock gravel amendments.	4-76
Figure 131. Soil incubation treatments (from left to right): PSTA sediments, STA muck soil without limerock, and STA soil with a 5-cm limerock cap.	4-76
Figure 132. Mean soil total phosphorus (TP) content of three soils used in the incubation.	4-78
Figure 133. Mean dissolved oxygen (DO) concentrations in control cores containing muck soils or PSTA accrued sediments during the 12-week study.	4-79
Figure 134. Soluble reactive phosphorus (SRP) concentrations in the overlying water above three soil types.....	4-80
Figure 135. Soluble reactive phosphorus concentrations in the surface waters overlying STA muck soils during six consecutive batch cycles of 14 days each.	4-81
Figure 136. Soluble reactive phosphorus concentrations in the surface waters overlying Farm Muck soils during 6 consecutive batch cycles of 14 days each.	4-81
Figure 137. Soluble reactive phosphorus (SRP) concentrations in the porewater of the limerock layer in treatments with 15 cm LR added as a cap above two muck soil types. Error bars denote the standard error around the mean for triplicate cores under each treatment.	4-82
Figure 138. Porewater calcium concentrations in the limerock layer above two muck soil types incubated for six two-week cycles.	4-83
Figure 139. Porewater pH values from limerock over two muck soil types incubated for six two-week cycles.	4-83

List Of Tables

Table 1.	Operational periods, size, and number of experimental units in various PSTA research platforms.....	2-1
Table 2.	Total phosphorus (TP) concentrations in the inflow and outflow waters of various PSTA systems operated at a range of water depths. Also shown are comparable configurations on muck, peat and sand substrates.	2-4
Table 3.	Hydrologic parameters during and prior to 16 surface water sampling events along transects within the PSTA Cell.....	3-16
Table 4.	Analytical methods used for surface water analysis.	3-17
Table 5.	Chemical composition of the accrued sediment layer in the PSTA Cell in May 2014.....	3-33
Table 6.	Macrophyte standing crop estimated from replicate throws of a sampling frame (0.5 m x 0.5 m) at three stations along internal transects in the PSTA Cell, on July 7, 2014.....	3-42
Table 7.	Standing crop biomass and nutrient content of back-end SAV communities from a previous study in STA-1W (DBE 2002).	3-42
Table 8.	Chemical composition of periphyton grown on naturally-occurring substrates in the PSTA Cell on two dates. n.d = not determined.	3-49
Table 9.	Periphyton areal biomass estimates from this study and two similar studies conducted in the Everglades National Park (ENP) and Water Conservation Area (WCA) 2A.	3-56
Table 10.	A comparison of periphyton phosphorus and nitrogen contents from slides and natural substrates in this study, with estimates from the interior region of Water Conservation Area 2A.	3-58
Table 11.	Relative dominance (%) of taxonomic groups in slide periphyton samples.	3-67
Table 12.	Operational targets for experimental flow ways assigned to one of four depth treatments.....	4-4
Table 13.	Analytical methods and method detection limits (MDLs) for inflow and outflow waters collected from the mesocosms.	4-5
Table 14.	Porewater constituents on May 23, 2014, one day after initial reflooding of the dried soils in mesocosms containing low-P soils with or without a limerock cap. Also shown are the surface water concentrations for each treatment, as measured during reflooding on May 22, 2014.	4-69

1 Executive Summary

The existing vegetation communities in the Everglades Stormwater Treatment Areas (STAs) may not consistently achieve outflow total phosphorus (TP) concentrations low enough to comply with current water quality-based effluent limits (WQBEL) specified in the STA operating permit. A multi-year Science Research Plan therefore has been established to better define the efficacy of concepts for enhancing STA performance, including technologies and approaches that may be feasible as a final STA polishing step in the removal of phosphorus from surface waters.

The Periphyton-based Stormwater Treatment Area (PSTA) is one such concept. Periphyton constitutes a considerable portion of the total biomass of the unimpacted, ultra-oligotrophic Everglades, and the organisms comprising periphyton mats are exceptionally efficient at scavenging TP from the water column, driving native concentrations to 4 µg/L or lower, which lends empirical credence to the notion that PSTA systems can achieve very low P concentrations. As a stormwater treatment technology, PSTA systems are united by a single feature: periphyton as a significant primary producer. Typically, periphyton growth in PSTA systems is encouraged by several design features, including a benthic surface dominated by calcitic minerals, typically limerock; limited densities of emergent macrophytes, to reduce shading; and shallow water depths, to support light penetration. Synergistically, these characteristics may offer additional advantages over traditional muck-based systems, by reducing sediment P diffusive efflux and “mining” by macrophytes, and by supporting UV photolysis of recalcitrant dissolved organic P (DOP) molecules.

Several small-scale PSTA applications have consistently produced ultra-low outflow P levels (i.e., below WQBEL thresholds). If the key processes that promote such outflow TP levels can be characterized, and the sustainability of treatment better assured, then PSTA may prove to be a superior final-stage treatment system, compared to existing muck-based treatment areas. This document is an update of a prior mid-project report (DBE October 2014), and serves to: review previous studies of PSTA technology; define existing knowledge gaps that are constraining broader implementation of PSTA technology; and report data from current PSTA studies, and evaluate those results with respect to the knowledge gaps.

1.1 Previous PSTA Research

Modification of the benthic surface (muck removal or limerock addition) to support periphyton growth is expected to be the costliest aspect of construction of a full-scale PSTA facility. Many of the early PSTA studies were designed to examine the effects of substrate character on outflow TP concentration. This points to a key knowledge gap: Does the establishment of a limerock or shell rock substrate in the treatment wetland provide a strong likelihood of attaining annual mean outflow TP levels of 13 µg/L and lower? The previous studies that we examined were

conducted across a variety of scales (2 m² - 40 ha) and tested substrates including muck, sand, local limerock and shell rock, and imported limerock. Across all studies by all investigators, muck-free, calcitic substrates produced long-term (i.e., life of the project) outflow concentrations at or below 13 µg/L in only 8 of 20 treatment groups. Of course, this general assessment pools studies using diverse inflow waters, hydraulic loading rates and operating depths, but it does indicate that the removal of muck alone does not guarantee acceptable performance. The prior PSTA investigations (not including those with the STA-3/4 PSTA Cell) also produced other useful information, particularly by characterizing construction challenges (the importance of elevation control during construction) and operational issues (seepage and flow quantification, types of macrophyte and periphyton) pertaining to PSTA community development.

1.2 Existing Knowledge Gaps

We identified three major shortcomings prevalent in previous PSTA research efforts: 1) durations were short, typically 12 - 27 months; 2) limerock substrates were “raw” (i.e., freshly scraped or quarried, rather than covered by mature periphyton communities and accrued sediment), and; 3) replication of treatments was poor. Given these limitations, we identified the following knowledge gaps, framed as research questions, that persist despite the earlier PSTA research, and that are sufficiently severe so as to compromise the promulgation of an engineering feasibility analysis of the technology at this time.

1. What operational conditions (water depth, inflow P loading rates and TP concentrations) facilitate or compromise PSTA P removal performance?
2. How does the accumulation of new sediment over the original calcium-based substrate affect outflow TP concentrations and sustainability of P removal performance?
3. What is the expected trajectory of macrophyte and periphyton growth over time, and what metrics are available to evaluate the effectiveness of vegetation and associated microbial communities for P removal?
4. Is either a limerock cap, or stable, low-P muck soils a viable alternative to complete muck removal?
5. What footprint is needed for a PSTA wetland situated at the back-end of an STA flow path?

1.3 Current Research

The current research initiative, in contrast with previous work, has taken advantage of the longest running PSTA platform to date by intensively sampling the STA-3/4 PSTA Cell, and has incorporated novel experimental platforms at several scales (15-cm diameter cores up to 7.6 m² mesocosms) designed to address the specific research questions outlined above.

1.3.1 STA-3/4 PSTA Cell

The STA-3/4 PSTA cell has provided effective treatment performance since its inception, with annual average inflow TP levels ranging from 14 - 27 µg/L and mean annual outflow levels

ranging from 8 – 13 µg/L. Our ongoing work in the STA-3/4 PSTA Cell has included wet- and dry-season sampling of surface water, sediment, plants and periphyton along fixed internal transects; deployment of periphytometers at three internal locations, and monitoring water quality and periphyton before, during and after flow pulse events. This work is being complemented by additional research and monitoring efforts by District scientists.

This work has offered insight on each of the five guiding research questions. For example, we observed that short (ca. 1 week) flow pulses, mimicking those provided to the full-scale STA flow paths (on a relative basis), had no detrimental effect on outflow TP concentrations (Key Question #1). Alkaline phosphatase activity (APA) is an indicator of P limitation and a measure of the ability for naturally occurring monoesterase enzymes to increase bioavailability of recalcitrant P compounds. While water column APA was depressed and/or diluted during high flow conditions, levels increased in the days following the pulses, indicating that a temporary increase in P loading during high flows does not curtail enzyme production by biota. Another concern, that flow pulses will create flow velocities high enough to disrupt the sediments and biomass, has proven unfounded within the current PSTA cell. In the largest pulse test, thought to be representative (on a relative basis) of high pulses in the full-scale STA flow paths, the biota and sediments remained intact and well-functioning. Indeed, direct measurements of enzyme activity in periphyton communities before and after the largest flow pulse demonstrated no reduction in activity as a result of the pulse.

Other factors controlling enzyme activity, and the removal of DOP and PP within PSTA cells, are still under investigation. Sixteen internal water quality surveys have been performed in the PSTA cell since July 2011 and have typically shown declining or flat TP profiles, and gradually increasing phosphatase enzyme activities, within the wetland. Full-scale PSTA systems, therefore, can exhibit a reasonable ability to succeed under naturally variable flow conditions.

With respect to Key Question #2, studies both within the PSTA cell and in mesocosms are yielding insight into the characteristics of sediments that accrue over time. As of May 2014, an average of 7.8 ± 0.5 cm of marl sediments have accumulated in the PSTA cell, with a cell-wide average (\pm one standard error) chemical composition of 257 ± 33 mg/kg P, $0.9 \pm 0.1\%$ N and $24.5 \pm 1.6\%$ Ca. Alkaline phosphatase activity was relatively high in the inflow region sediments, with activity declining towards the outflow region.

Long-term PSTA cell monitoring (11 semi-quantitative monitoring events; three quantitative monitoring events) indicates that submerged plant cover has been generally stable in recent years (Key Question #3). *Chara* sp. is the dominant macrophyte, followed in importance by *Potamogeton illinoensis*. Our semi-quantitative PSTA cell vegetation monitoring efforts were initiated immediately following a drawdown event that eliminated most of the SAV standing crop. Our survey results show that recovery of the PSTA cell SAV community from drawdown was rapid. PSTA cell SAV communities generally have exhibited a comparable standing crop biomass (mean of 441 g/m²), but lower P content (mean of 219 mg/kg), relative to SAV

communities at the outflow region of muck-based cells (e.g., in STA-2 and STA-1W). Periphyton is abundant throughout the PSTA Cell, with P-sensitive diatoms and cyanobacteria dominating the assemblage. Prior to 2014, periphyton P concentrations (95 - 247 mg/kg) were found to be typical of other south Florida ultra-low P marsh environments, whereas the areal periphyton biomass values measured on natural substrates in the PSTA cell (4.4 - 170 mg/cm²) are at the upper end of values reported in other studies. In 2014 and 2015, higher epiphyton tissue P levels (up to 580 mg/kg) were observed in summer months. It is unclear whether this increase in tissue P is related to seasonal (e.g., possibly flow related) variability, or to a gradual P enrichment of the tissues. Moreover, initial PSTA cell data suggest that the type of macrophyte species may influence the P content of the associated epiphyton. Additional PSTA cell sampling, and on-going research using replicated mesocosms will provide additional insights into the effects of factors such as depth and P loading on PSTA periphyton assemblages, and on mechanisms that may enable the STA-3/4 PSTA Cell to provide lower outflow TP levels than muck-based STA flow ways.

1.3.2 Mesocosm and Microcosm Studies

Small-scale PSTA studies have been initiated to provide PSTA design/operational guidance, and insight into the sustainability of PSTA sediments. Flow-through mesocosm treatment trains were constructed near the STA-1W outflow for a long term study to assess effects of P loading and water depth on P removal performance, and on the characteristics of the biological communities. Four depth treatments (fixed depths of 23 cm and 46 cm; variable depths of 46 - 69 cm and 46 - 92 cm) were established in triplicate, using local limerock gravel as a substrate. The periphyton and macrophyte (*Chara* spp. and *Potamogeton illinoensis*) communities were established successfully. The mesocosms are being monitored for surface water constituents including P species and enzyme activity, plant and periphyton cover, light penetration, and benthic periphyton biomass.

From December 2013 - April 2015, all of the water depth treatments have provided comparable performance, reducing inflows of 21 µg/L TP to 8 µg/L TP, at a P loading rate (PLR) of 0.33 gP/m²-yr. At the two greatest water depths, we did observe a very slight reduction in performance (i.e., 1 to 2 µg/L higher TP than that for the two shallower depths) at the midpoint of the process trains. Moreover, benthic periphyton mat density was reduced by the deep-water conditions that occurred in the higher, variable-depth treatments between May and September 2014, but this effect was evident only in the upstream tanks, a factor that may explain the slightly elevated water column TP levels at the mid-point of the process trains. These initial findings suggest robust, sustainable performance at depths of 23 and 46 cm, and only a modest penalty, if any, to TP removal performance for depth increases up to 69 and 92 cm. The water depth evaluation trials are continuing.

Both the 23 cm and 46 cm water depth treatments consist of four tanks in series, which facilitates insight into effects of various loading rates on PSTA systems. The first tank in series

has reduced the average 21 $\mu\text{g/L}$ TP levels to a mean of 14 $\mu\text{g/L}$, at a PLR of 1.3 $\text{gP/m}^2\text{-yr}$. TP outflows from the 2nd, 3rd and 4th tanks in series have averaged 11, 9 and 8 $\mu\text{g/L}$, at respective PLRs of 0.7, 0.4, and 0.3 $\text{gP/m}^2\text{-yr}$. Continued operation of this mesocosm platform should produce guidance for establishing target operating depths and PLRs for full-scale PSTA deployments (Key Question #1), with process-level understanding of light effects and P loading on periphyton growth, enzyme production and P uptake (Question #3).

In a second study, we established a flow-through mesocosm study, using muck soils obtained from an unfarmed parcel of land adjacent to STA-1W, to investigate whether unenriched (Low-P: ~ 180 mg/kg) muck soil could serve as a suitable PSTA substrate. As a second treatment, we added a “cap” of limerock over this same muck, to assess whether the presence of CaCO_3 or some other limerock constituent would enhance development of a desirable benthic community, which in turn would lead to reduced outflow P levels. Long-term outflow TP concentrations for both treatments were identical. Both the limerock cap and the unamended muck supported elevated enzyme activities, and removed P from the recalcitrant P pools. This indicates that a limerock substrate, per se, is not necessary to obtain ultra-low (≤ 13 $\mu\text{g/L}$) TP concentrations (Key Question #4), but that the organic substrate, if present, must contain sufficiently low total P levels (and presumably, small pools of labile P).

This same concept was tested using an enriched muck collected from a farm field, as well as STA muck soils and PSTA sediments. Lime rock caps of 5 cm, 10 cm and 15 cm were placed above the two muck substrate types in small incubation cores, which were then (along with the PSTA substrate cores) flooded with a low P water. The farm muck exhibited considerable P release, with a lower release occurring from the STA cores. The limerock cap was effective at both reducing P flux from the farm muck, and increasing P uptake by the STA muck, across a range of cap depths (5-15 cm). Porewater SRP and calcium enrichment and lower pH values within the LR layer were observed above farm muck soils.

In order to evaluate the long-term effectiveness of a limerock cap, a follow-up study is planned using larger flow-through mesocosms. This platform will incorporate macrophytes and evaluate the potential adverse effects of macrophyte P uptake from soils (i.e., “mining”) on water column P concentration reduction above limerock-capped muck soils.

In a third study, outdoor soil-water columns were constructed with one of four substrate types: a bare limerock substrate; limerock covered with accrued-layer marl sediments from the PSTA cell; intact muck core with accrued sediment layer removed, and intact muck core with top 10 cm removed. These columns were operated under continuous flow-through conditions for 11 months. During a second phase, initiated after about four months, whole, intact cores from a well-performing muck-based cell (STA-3/4 Cell 3B) were added as an additional treatment. Generally, the bare limerock substrate produced consistently low TP concentrations (≤ 12 $\mu\text{g/L}$), whereas TP concentrations across all the muck treatments averaged 15-17 $\mu\text{g/L}$. The performance of the PSTA sediment was variable (13-16 $\mu\text{g/L}$), and apparently depended

somewhat on the precise collection location in the PSTA Cell. The variable performance of PSTA sediments indicated that the effect of the accrued layer in the PSTA cell is yet poorly defined, and requires further investigation (Key Question #2). Although the removal of upper muck layers in this study exposed lower-P strata (425 to 450 mg/kg), P removal performance was not substantially improved. The effective TP removal observed for the prior mesocosm study (described above) on an unfarmed, muck substrate (~ 180 mg P/Kg), suggests that partial muck removal (or soil inversion) on previously farmed lands may only be effective if the TP levels in the underlying muck are quite low (Key Question #4). This will be a key topic for further investigation, due to its potential for providing substantial construction cost savings in PSTA systems.

Substrate and macrophyte interactions were investigated in more detail in a fourth study, using intact soil cores. Phosphorus removal and growth/composition of *Chara* and *Potamogeton* were compared to that of un-vegetated controls, in cores containing either exposed limerock, limerock covered with PSTA sediment, or muck soils from the outflow region of STA 2 Cell 3, a well-performing SAV-dominated flow way. Overlying water in triplicate cores under each treatment was exchanged every two weeks for 12 weeks, before macrophyte tissues were harvested, dried, and weighed to assess biomass increase. Tissue P contents of the dried material were compared to the P contents of the inoculum, which had been collected from the PSTA Cell. The findings showed lowest water P concentrations were obtained over raw limerock substrate, followed by PSTA sediments, and then muck cores. The presence of *Chara* typically improved water column P removal over unvegetated conditions, but there was little water quality improvement in cores containing *Potamogeton*, possibly due to soil P “mining” by this deeply rooted SAV species. The final *Chara* and *Potamogeton* biomass and P contents were highest on muck (compared to PSTA sediments or limerock). Emerging evidence suggests that higher macrophyte (and potentially, periphyton) P contents could be a contributing factor to the inferior particulate P (PP) and dissolved organic P (DOP) removal by muck-based systems, compared to PSTA systems.

1.4 The State of PSTA Research

As a final-stage polishing feature, the PSTA concept shows promise. PSTA systems in ongoing field- and mesocosm-scale experiments have reliably produced TP concentrations at or below 13 µg/L. Current and recent research has begun to close the remaining major knowledge gaps, especially those related to the effects of substrate type and character. Ongoing projects appear poised to provide definitive design/operational guidance, particularly regarding operational water depths and P loading rates, which will be essential to PSTA feasibility studies and address the final Key Question (#5) of appropriate sizing of PSTA footprint for STAs.

2 Introduction and Background

This report is an update on the “state of the science” of the Periphyton Stormwater Treatment Area (PSTA) phosphorus (P) removal technology. PSTA is the name applied in south Florida to shallow treatment wetlands that incorporate a limerock substrate (achieved either by scraping existing muck soil, or by adding a limerock cap over muck). Such wetlands, provided with low to moderate P loading rates, are thought to be able to achieve ultra-low outflow TP concentrations. PSTA has long been under consideration as a potential polishing step for STAs, to enable existing STA configurations to achieve lower outflow TP levels than the range of 14-16 µg/L currently attainable by back-end submerged aquatic vegetation (SAV) communities (Juston and DeBusk, 2011). Considerable research has been conducted during the past 15 years on the PSTA technology, using multiple platforms ranging from 2 m² up to 40 ha (Table 1). Three literature/data reviews have been performed (Kadlec and Walker 2003, Goforth 2011, Wetland Solutions, Inc. (WSI) and ANAMAR, 2011), that summarize PSTA performance from these platforms. This report attempts to synthesize the findings of those earlier efforts as a foundation upon which to construct an appropriate approach forward.

The existing vegetation communities in the Everglades Stormwater Treatment Areas (STAs) may not consistently achieve outflow total phosphorus (TP) concentrations low enough to comply with current water quality-based effluent limits (WQBEL) specified in the STA operating permit. A multi-year Science Plan therefore has been established to better define the efficacy of any concept that may be feasible as a final polishing step in the removal of TP from stormwater entering the Everglades. PSTA is one such concept. In this document, we review key previous findings, and we discuss investigations currently underway that will provide critical data on PSTA capabilities and constraints that will in turn support cost and technical feasibility analyses. The suitability of current research activities in answering key questions about PSTA is also addressed in this document, and additional research needs are highlighted.

Table 1. Operational periods, size, and number of experimental units in various PSTA research platforms.

Project	Size	Units	Operational Period	Months	Source
Porta-PSTA	6-18 m ²	24	4/1999-2/2001	22	CH2MHill 2003a
Shallow Raceway	13 m ²	3	7/1998-2/2000	19	DeBusk et al. 2004
DB Mesocosms	2 m ²	4	7/1999-7/2005	72	DeBusk et al. 2011
Flying Cow Road Test Facility	93 m ²	4	4/2006-7/2008	27	WSI/ANAMAR 2011
Wellington	500 m ²	2	9/2001-2/2003	17	CH2MHill 2003b
Test Cells	0.2 ha	3	2/1999-3/2000 and 4/2000-4/2001	12	CH2MHill 2003a
PSTA Field Scale Demonstration	2 ha	4	8/2001-9/2002	14	CH2MHill 2003a
STA 1E Cells	18.6 ha	3	10/2008-12/2008 and 2/2010-12/2010	12	WSI/ANAMAR 2011
STA 3/4 PSTA Project	40 ha	1	WY2008-WY2014	84	SFER 2014

2.1 Description of Periphyton-based Stormwater Treatment Areas

Presence of a periphyton community adapted to low water column P concentrations is considered the central element that leads to superior P removal performance by the PSTA technology. Periphyton communities are complex assemblages of cyanobacteria, eubacteria, diatoms and eukaryotic algae and are found in lakes, streams and wetlands, including the marshes of the Everglades (McCormick and O'Dell 1996). Several characteristics of periphyton communities make them well suited for biological treatment of surface waters in wetlands (Dodds 2003). Floating and benthic calcareous periphyton mats are a key component of the ultra-oligotrophic Everglades marshes (Browder et al., 1994), and are thought to be capable of reducing water column TP to extremely low levels. Periphyton typically has a high affinity for P and responds to P inputs more rapidly than other wetland components (macrophytes, soils) and thus is important in the uptake and storage of P (McCormick et al., 1996). Typically, periphyton growth in PSTA systems is encouraged by several design features, including a benthic surface dominated by calcitic minerals, typically limerock; limited densities of emergent macrophytes, to reduce shading; and shallow water depths, to support light penetration.

Periphyton-based systems appear to produce lower particulate P (PP) and dissolved organic P (DOP) concentrations, relative to muck-based EAV and SAV marshes. Phosphorus in those pools is less available for biological uptake or chemical sorption than soluble reactive P (SRP), and so more difficult to remove in treatment wetlands. Under certain conditions, however, PP and DOP can be broken down through hydrolysis reactions into more bioavailable forms of P. Phosphatase enzymes are naturally-produced proteins that catalyze these hydrolysis reactions, effectively increasing the transformation of selected DOP and PP molecules into more bioavailable P forms. Phosphatases are found internally within organisms and as extracellular moieties within the aquatic environment (Wetzel 1991). In ultra-oligotrophic south Florida marshes, periphyton mats are thought to be a key locus for production of these enzymes.

It is believed that excessive inputs to a wetland of readily available P (such as SRP), either through inflow waters or via sediment-to-water column flux from enriched sediments, can constrain the development of periphyton adapted to low-P conditions, as well as the production of phosphatase enzymes. Hence, the presence of a limerock substrate in PSTA systems, which is thought to curtail substrate P transport to the water column via diffusive flux or macrophyte "mining", is expected to facilitate the development and enhanced P removal function of periphyton communities. Finally, it has been suggested that periodic drydown benefits both the robustness, and P removal performance of periphyton in PSTA systems (Doren and Jones, 1996 in WSI/ANAMAR, 2011).

PSTA systems also are thought to require relatively shallow water conditions for optimum performance. Shallow conditions facilitate light penetration to the sediment (benthic) surface. In highly colored surface waters typical of the STAs, light is rapidly attenuated, so small increases

in water depth can dramatically reduce light penetration to the benthic surface. McCormick et al. (2006) noted that nearly all photosynthetically active radiation ($\lambda = 400\text{-}700\text{ nm}$) was attenuated within the upper 30 cm (1 ft) of the water column in STA-1W Cell 4. Shallow water depths may confer additional benefits to PSTA systems. Theoretically, lower depths increase the ratio of benthic (periphyton) surface area to water volume, increasing treatment contact. Also, shallow conditions may promote the breakdown of dissolved organic compounds (including DOP) by UV radiation (Wetzel et al., 1995).

The unique operating conditions in prior PSTA studies (e.g. Table 2) did not typically result in a vegetation community distinctly different from that of typical muck-based SAV cells. It is suspected, however, that the community composition, standing biomass and nutrient content of macrophytes and periphyton within PSTA wetlands differs from STA flow ways with the organic soil intact, but this has not been investigated in sufficient detail.

2.2 Previous PSTA Research

The original research on PSTA was initiated at a time when the expected outflow TP target concentration from the technology would be 10 $\mu\text{g/L}$. While the current WQBEL target for the STAs is slightly higher (outflow average of 13 $\mu\text{g/L}$ TP three out of five years), it is clear that to achieve an annual mean value of 13 $\mu\text{g/L}$, the wetland must be capable of providing sub-13 $\mu\text{g/L}$ outflow levels for a good portion of the operational period. This concentration range appears to be outside the long-term capability of SAV cells established on previously farmed lands (Juston and DeBusk, 2011).

A key question, when reviewing results from previous PSTA platforms, is “Does the establishment of a limerock or shell rock substrate in the treatment wetland provide a strong likelihood of attaining annual mean outflow TP levels of 13 $\mu\text{g/L}$ and lower?” Prior to the establishment of the STA-3/4 PSTA Cell, numerous investigations were performed at mesocosm, test cell and field scale using a number of inert substrates (e.g., limerock, shell rock and acid-rinsed sands), and these results are described below.

Eighteen mesocosm-scale PSTA treatments have been investigated at STA-1W, 14 of which contained an “inert” substrate, such as sand or limerock. Of these, only three achieved average outflow concentrations below 13 $\mu\text{g/L}$: a very shallow raceway (9 cm water depth) using local limerock reduced inflow levels of 18 $\mu\text{g/L}$ to 10 $\mu\text{g/L}$ over an 18-month period (DeBusk et al., 2004); a slightly deeper treatment (30 cm water depth) with an acid-rinsed sand substrate reduced inflow TPs of 19 $\mu\text{g/L}$ to 11 $\mu\text{g/L}$ (over 12 months) (CH2M-Hill 2003), and; a 60 cm depth shell rock substrate treatment reduced inflows from 19 $\mu\text{g/L}$ to 13 $\mu\text{g/L}$ over 12 months (CH2M-Hill 2003). Two STA-1E mesocosm treatments, one with a 12” Ft. Thompson limestone substrate and one with 6” of local limestone over 6” sand, performed relatively well, reducing inflow TP levels of ~25 $\mu\text{g/L}$ to 13 and 9 $\mu\text{g/L}$, respectively, over 27 months. It is unclear why the ~13 $\mu\text{g/L}$ TP “target” was achieved in only 21% (5 of 14) of the “inert substrate” mesocosm

treatments, but it indeed demonstrates that the presence of limerock does not guarantee that ultra-low P levels will be achieved.

Table 2. Total phosphorus (TP) concentrations in the inflow and outflow waters of various PSTA systems operated at a range of water depths. Also shown are comparable configurations on muck, peat and sand substrates.

Project Treatment	Substrate	Replicates	Optimal Performance Period* TP Inflow (µg/L)	TP Outflow (µg/L)	Nominal Water Depth (cm)
DB Mesocosms					
Raceways	Limerock	3	18	10	9
Meso-1	Limerock	2	32	17	40
Meso-2	Muck	2	32	15	40
Porta-PSTA					
PP 4	Shellrock	3	29	15	30
PP 15	Shellrock	3	23	15	30
PP 11	Shellrock (Larger tanks, 3X)	1	28	18	30
PP 2	Shellrock	3	19	13	60
PP 5	Shellrock (Higher flows, 2X)	3	25	16	60
PP 16	Shellrock (Variable flows, 0-1X)	3	23	17	0-30
PP 6	Shellrock (Variable flows, 0-2X)	3	24	14	0-60
PP 14	Limerock	3	23	14	30
PP 7	Sand	1	28	15	30
PP 8	Sand	1	19	16	60
PP 17	HCl-rinsed sand	1	23	11	30
PP 3	Peat	3	28	17	30
PP 1	Peat	3	19	14	60
PP 12	Peat (Larger tanks, 3X)	1	28	19	30
PP 13	Ca-amended peat	3	23	16	30
STA-1W Test Cells					
Test Cell 8	Shellrock over sand	1	25	13	60
	Shellrock over sand	1	22	12	30
Test Cell 3	Shellrock over sand	1	25	17	0-60
	Shellrock over sand	1	24	19	0-30
Test Cell 13	Peat over shellrock over sand	1	27	16	60
	Ca-amended peat over shellrock over sand	1	22	20	30
STA 2 Field Demonstration					
FSC-1	24" Limerock on peat	1	26	18	30
FSC-2	24" Limerock on peat	1	23	15	30
FSC-3	Peat removed to expose caprock	1	21	16	30
FSC-4	Peat	1	20	31	30
FCRTF					
Cell 1	1" lime sludge on 12" sand	1	27	17	15-60
Cell 2	12" Ft Thompson limestone	1	24	13	15-60
Cell 3	6" local limerock on 6" sand	1	26	9	15-60
Cell 4	6" Ft. Thompson limestone on 6" sand	1	24	14	15-60
STA 1E					
Cell A	1" lime sludge on 5" sand	1	8	10	30-45
Cell B	2" Miami Limestone over 4" local limerock	1	10	10	30-45
Cell C	6" local limerock	1	10	8	30-45

*TP results provided were from the optimal performance period, or post-startup period, as provided in project reports.

Similar, inconsistent attainment of ultra-low outflow TP targets has been observed for PSTA systems tested at larger scales. Three 0.2-ha cells at the STA-1W south test cell research facility were used to explore PSTA community development and P removal effectiveness. All cells were lined and filled with sand, then capped with shellrock and/or peat. Test Cell 13 had 80 cm sand, 30 cm shellrock, and 30 cm peat added as substrate. Test Cells 3 and 8 contained 1 m sand, with 30 cm shellrock. Test Cells 13 and 8 were operated at a static depth (60 cm, then later 30 cm) while Test Cell 3 was variable depth 0-60 cm at first, then 0-30cm. The static depth shellrock test cell had lowest outflow TP (12-13 $\mu\text{g/L}$) during the optimal performance period (12 months), whereas variable depth and peat substrate outflows were higher (17-18 $\mu\text{g/L}$ and 16-20 $\mu\text{g/L}$, respectively). Poor performance of the peat-based test cell was thought to be related to emergent macrophyte invasion.

The effects of scraping organic soils to expose bedrock were evaluated at the STA-2 Field Scale PSTA system (2 ha), with one replicate of each of the following four treatments: muck removed by scraping; limerock added as a 0.6 m thick cap over the muck soil; 0.6 m limerock cap plus internal levees increasing the flow path 3X, and; unaltered muck soils. Inflow TP was 20-26 $\mu\text{g/L}$ from a seepage return canal and piped from STA-2 Cell 3. The muck substrate treatment grew dense macrophytes, and exported P (outflow averaged 31 $\mu\text{g/L}$). By contrast, the limerock-based systems, whether scraped or with a limerock cap, reduced TP to 15-19 $\mu\text{g/L}$. The optimal performance period of these systems ("post-startup") was 241 days, with a total of 421 days in the period of record. While much effort was expended to construct and monitor these systems, the lack of replication and large uncertainties with respect to flow conditions and seepage, combined with low outflow TP concentrations in the range already achieved by well-performing, muck-based SAV-dominated STAs, limited the utility of the resulting data for scale-up of the PSTA concept for effective P removal.

More recently, in STA-1E, three 18.8 ha cells were constructed using local and imported inorganic materials, which were placed above sandy soils. A 2.5 cm layer of lime sludge was applied to Cell A, while Cells B and C each received 15 cm limerock above the native sand soils. Cell B had a 5 cm layer of Miami Limestone over 10 cm of local limerock, while Cell C had 15cm of local limerock. The cells operated for a limited time (data period was October - December 2008 and February to December 2010), inflow water average TP concentrations were very low (8-10 $\mu\text{g/L}$) and flow measurements were problematic (WSI/ANAMAR, 2011). Outflow concentrations were also 8 to 10 $\mu\text{g/L}$, and it was unclear whether these levels could be achieved if the wetland was challenged with higher inflow TP levels, such as those likely to exit a well-performing SAV wetland. Finally, no substrate difference was found in TP removal performance among the three calcium substrate types.

2.2.1 Limitations of early PSTA research

The prior PSTA investigations (not including those with the current STA-3/4 PSTA Facility) helped characterize construction challenges (the importance of elevation control during

construction) and operational issues (seepage and flow quantification, types of macrophyte and periphyton) pertaining to PSTA community development. However, we identified three major shortcomings prevalent in previous PSTA research efforts: 1) durations were short, typically 12 – 27 months; 2) limerock substrates were “raw” (i.e., freshly scraped or quarried, rather than covered by mature periphyton communities and accrued sediment, and; 3) replication of treatments was poor.

Short duration experiments are necessary and useful to generate new information quickly. Any full-scale PSTA implementation, however, will need to operate indefinitely for the continued protection of the Everglades. Short-term studies potentially miss two challenges of long-term operation. First, long-lived treatment wetlands inevitably face irregular, unpredictable perturbations, especially from the climate. The resilience of the PSTA technology to uncontrollable impacts (e.g. drought, hurricane, biological invasion) cannot be easily tested in short-term studies. Second, some treatment wetlands have demonstrated declining P removal performance after many years of operation (e.g. Orlando Easterly Wetland), which may require addition management intervention. This is difficult to predict with short-term experiments.

As noted previously, PSTA studies have operated on a variety of substrates, including peat, shellrock and sand (CH2M-Hill 2003, DeBusk et al., 2004, DeBusk et al., 2011), but most were of short duration (typically < 24 months). None of these prior investigations used “accrued” PSTA sediment; only the original inert material (i.e., the “starting substrate condition”) was utilized. A disadvantage to short-term experiments is that any initial substrate material present during establishment will be covered by accruing sediment material, which is more representative of long-term operational conditions. Hence, the long-term sustainability of the PSTA concept is ill defined. We address this through experimental work comparing newly-accrued sediment from the STA-3/4 PSTA Cell to exposed limerock substrates.

Several of the early projects were conducted with little or no experimental replication. This design can be useful for less-costly pilot or range-finding studies, but the results are not reliable for design or operational guidance. For example, the WSI/ANAMAR (2011) project produced very low outflow TP concentrations, but, without experimental replication, we cannot be confident that those results can be repeated (e.g. in a full-scale PSTA implementation). As outlined below, the currently ongoing PSTA research effort employs both replicated measurements and replicated experimental units to better define effects of design variables (e.g., substrate or macrophytes) and operational variables (e.g., depth and loading) on P dynamics and removal mechanisms.

2.3 Study Plan Objectives and Outstanding PSTA Research Questions

The PSTA Detailed Study Plan was developed in February 2014 with a primary objective of determining design and operational factors that contribute to the PSTA cell’s superior

performance, in order to facilitate large-scale replication of the success of this technology. Data gathered from the PSTA Cell will provide needed information on the effects of muck removal, as well as operational factors (water depth and hydraulic and P loading), on treatment performance. Alternate approaches to immobilize soil P, and specific mechanisms contributing to sustainable low-level TP removal, are to be tested in replicated mesocosm studies. These data are considered critical to any future feasibility analysis of using PSTA technology to improve STA back-end P removal performance.

Given the limitations of the prior PSTA studies, a number of key design, operational and sustainability questions remain unanswered. We identified the following knowledge gaps, framed as research questions, that persist despite the earlier PSTA research, and that are sufficiently severe so as to compromise the promulgation of an engineering feasibility analysis of the technology.

1. *What operational conditions (water depth, inflow P loading rates and TP concentrations) facilitate or compromise PSTA P removal performance?*

The establishment of envelopes for these operating conditions has proved key to the sustained success of the STAs and other large treatment wetlands. To date, most PSTA experiments, including the STA-3/4 PSTA Cell, have been conducted with fairly static water depths, P loads and concentrations, so the boundaries on these parameters have not been sufficiently explored.

2. *How does the accumulation of new sediment over the original calcium-based substrate affect outflow TP concentrations and sustainability of P removal performance?*

The STA-3/4 PSTA Cell has accrued conspicuous sediments that may be distinct in composition from sediment that accrues in muck systems. The effects of these sediments on macrophyte growth, sediment P flux and enzyme activity are yet unknown.

3. *What is the expected trajectory of macrophyte and periphyton growth over time, and what metrics are available to evaluate the effectiveness of vegetation and associated microbial communities for P removal?*

PSTA systems are designed to produce conditions novel to the STA network. It is not yet known how macrophytes, in particular, will respond. For example, boom-and-bust cycles have been observed of *Chara* in the STAs; a similar phenomenon in a PSTA system would likely impair P removal effectiveness.

4. *Is either a limerock cap, or stable, low-P muck soils a viable alternative to complete muck removal?*

Early work lacked process-level understanding of why these (potentially less-costly) alternatives to complete muck removal did or did not offer effective P removal.

5. *What footprint is needed for a PSTA wetland situated at the back-end of an STA flow path?*

Given the potential high costs associated with limerock-based PSTA systems, there is interest in minimizing the necessary footprint. With a sufficiently high (and sustainable) P uptake rate, a small PSTA region could potentially polish discharge water from a large STA. The necessary size will be dictated by a number of factors, including the performance of the upstream flow path EAV and SAV communities.

2.4 Opportunities with the STA-3/4 PSTA Facility, and Complementary Ongoing Investigations

2.4.1 STA-3/4 PSTA Cell

A “full-scale” PSTA demonstration area was constructed from 2004 to 2005 for the purpose of addressing uncertainties associated with large-scale implementation of periphyton-based treatment technology. The PSTA Project is located on a total of 400 acres in STA-3/4, and is comprised of a 200-acre Upper SAV Cell, a 100-acre Lower SAV Cell and a 100-acre PSTA Cell (Figure 1). The PSTA Cell is unique among existing STA treatment cells in that the peat layer was scraped and hauled away, exposing the underlying rock.

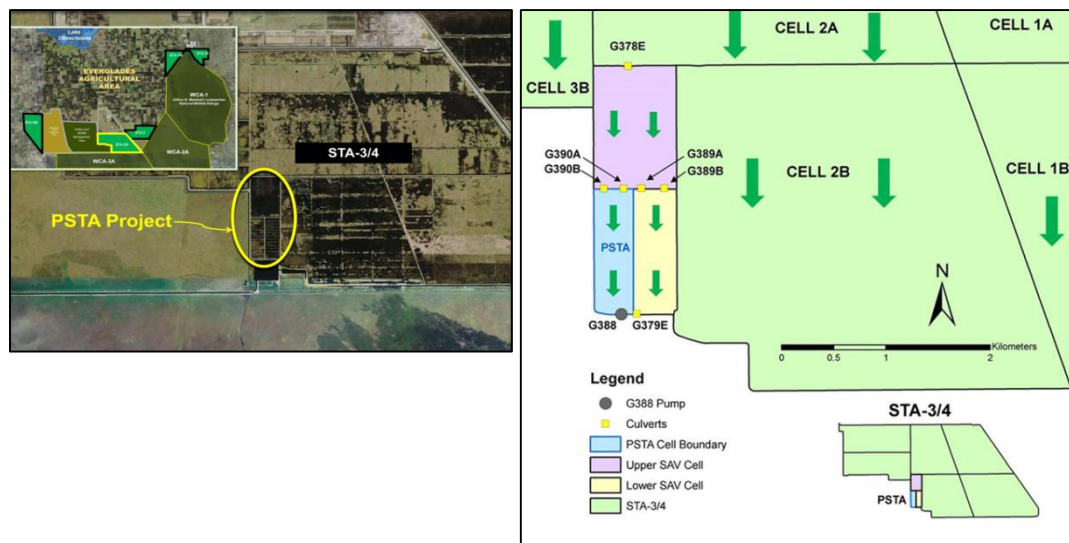


Figure 1. Location map of STA-3/4 and PSTA Project, including the Upper and Lower SAV Cells, the PSTA Cell, and related water control structures. Green arrows show flow direction.

The PSTA Cell has successfully developed into an oligotrophic, periphyton-rich wetland treatment cell. Due to favorable growing conditions, several species of submerged aquatic

vegetation (SAV) have also colonized the PSTA Cell. Over the years, visual observations suggest that the SAV community in the PSTA Cell has fluctuated slightly in terms of species composition, relative density, and coverage. Periphyton colonization of the benthic surface and surfaces of submerged and emergent macrophytes also appears to vary over time, and generally appears robust in most parts of the cell (Figure 2).



Figure 2. Periphyton growing on *Chara* sp. and *Eleocharis* stems in the STA-3/4 PSTA Cell.

The STA-3/4 PSTA Cell has shown promising performance by discharging outflow waters with ultra-low TP concentrations (findings are described in the next section of this report). Replicating the success of the PSTA Cell across other STA flow ways may improve the SFWMD’s ability to meet the WQBEL established to protect downstream marshes. However, questions remain regarding the factors contributing to this wetland’s low outflow TP concentrations. Under certain stage conditions, seepage into the cell is thought to occur at a high rate. If groundwater inflows into the wetland contain low TP concentrations, then the wetland’s observed low-level TP discharge concentrations could be an artifact of dilution by seepage, rather than the actual removal of P by biogeochemical processes. Another concern is that the wetland was not challenged sufficiently during its initial five years of operation: inflow volumes instead were rather steady, and low, which differs from the periodic high flow pulses received by the full-scale STA flow paths. Such pulse conditions with high hydraulic loading rates create short wetland hydraulic retention times (HRTs), which may impair treatment.

Additional investigations within the PSTA cell the past two years, for example subjecting the wetland to large flow pulses, have been performed to address the above concerns. More exhaustive studies of PSTA cell accrued sediments and vegetation (both macrophyte and periphyton) have also been conducted to better define the potential “unique” characteristics of the PSTA cell.

2.4.2 PSTA microcosm and mesocosm studies

Given that the STA-3/4 PSTA cell represents only one “experimental unit”, and that numerous design, operational, and sustainability questions remain to be addressed, complementary studies also are being performed using batch and flow-through soil/water mesocosms at various scales. These studies are focused on better understanding factors such as water depths and P loading rates on the performance and the biotic characteristics of PSTA communities, and on defining the P efflux potential of PSTA sediments. Finally, for both small-scale and full-scale PSTA investigations, more sophisticated analytical approaches (e.g., characterization of phosphatase enzyme activity of waters, periphyton and sediments) are being utilized that should provide an improved understanding of the key processes in PSTA systems that lead to ultra-low level outflow concentrations.

2.5 Report organization

Following the executive summary and introductory sections, the remainder of this report is divided into two main sections. In the first, we describe the performance of the STA-3/4 PSTA Cell and the results of recent intensive studies in that system. Descriptions of, and initial results from, ongoing microcosm- and mesocosm-scale experiments targeting specific PSTA design knowledge gaps comprise the second section.

3 STA-3/4 PSTA Cell

In this section, we provide a brief overview of STA-3/4 PSTA Cell (hereafter referred to as “PSTA Cell”) performance and hydrologic conditions during the study period, as background for synoptic surveys of the sediments, vegetation, and water quality. Key design and operational factors are discussed, including water depth and P loading rate ranges.

3.1 Treatment Performance

The PSTA Cell outflow TP concentrations ranged from 8-13 $\mu\text{g/L}$ during the past seven years (Andreotta et al., 2014, Andreotta et al, 2015, Figure 3). There was no correlation between flow-weighted mean outflow concentrations and annual inflow P loading rate, inflow volume, or the fraction of outflow volume not accounted for by inflows at the G390 structures (Figure 4). There was a weak positive correlation between inflow and outflow flow-weighted mean concentrations. Over the period of record, WY2009 had the lowest annual outflow TP concentration; it also had the lowest inflow TP concentration, lowest P loading rate and highest differential between inflow and outflow volumes (proxy for relative input of groundwater seepage). Across all six years, the outflow TP concentrations of the STA-3/4 PSTA Cell were below the background concentration (14-16 $\mu\text{g/L}$) of well-performing SAV-dominated cells on muck substrates (Juston and DeBusk, 2011).

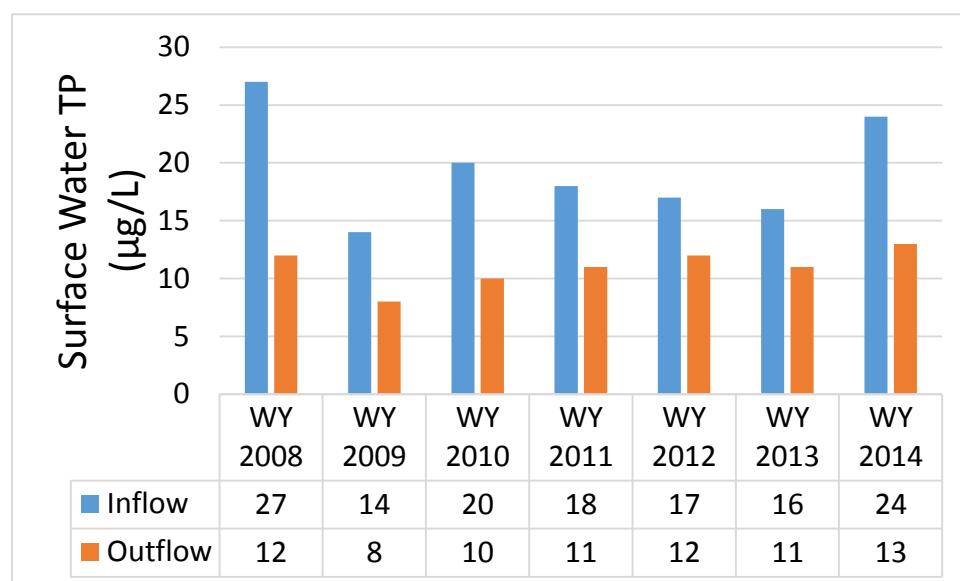


Figure 3. Mean annual total phosphorus (TP) concentrations in the inflow and outflow waters from the PSTA Cell during the period of record (Andreotta et al, 2015).

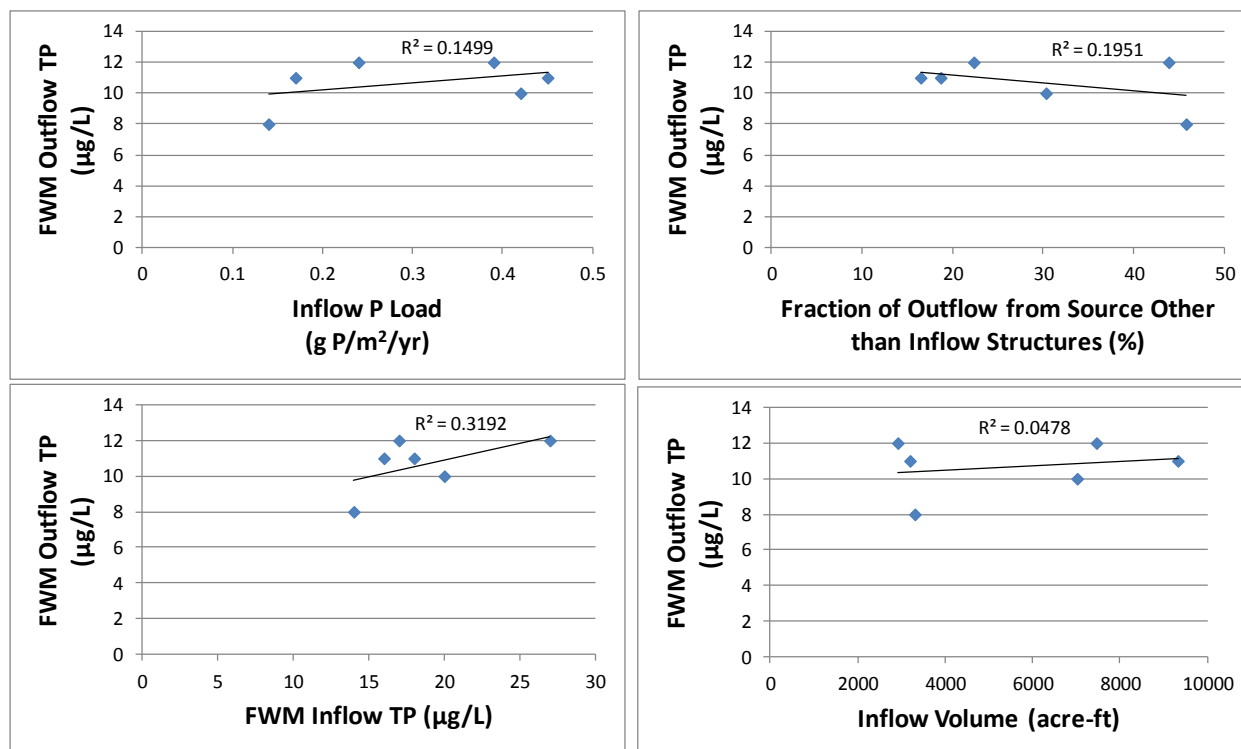


Figure 4. Correlations between annual P loading rate, inflow and outflow P concentrations, and the fraction of outflow water added to the cell from sources other than inflow structures. Values represent annual average or flow-weighted mean values as reported in the South Florida Environment Report Chapter 5 for six water years, WY2008-2013 (Andreotta et al., 2014).

3.2 Comparison to muck-based systems

It is important to consider, based on the performance data collected to date, whether the STA-3/4 PSTA Cell has actually produced lower outflow TP concentrations, compared to those of adjacent muck-based SAV cells. The distribution of outflow TP concentrations for the single PSTA cell outflow from January 2008 to February 2014 was compared to that of four monitored outflow structures in the adjacent full-scale SAV cells (two in Cell 2B, two in Cell 3B) for this same period. Mean outflow TP concentrations (calculated using grab samples collected only under flowing conditions) for Cell 2B, Cell 3B and the PSTA cell were 18, 13 and 11 µg/L, respectively. Respective median TP concentrations for these locations were 15, 12 and 10 µg/L (Figure 5). There have been additional concerns that the low P concentrations observed at the PSTA cell outflow are an artifact of ultra-low P groundwaters seeping into the cell. Since on a percentage basis the contribution of seepage waters would be minimized under higher flow conditions, we repeated this analysis using only outflow PSTA cell TP grab samples collected under “moderate to high flow” conditions. Using this approach, outflow mean and median TP values (9 and 8 µg/L, respectively) were even lower than under “all flowing” conditions (Figure

5), suggesting that the PSTA cell very likely does contain biota with the unique ability to reduce water column P to very low levels.

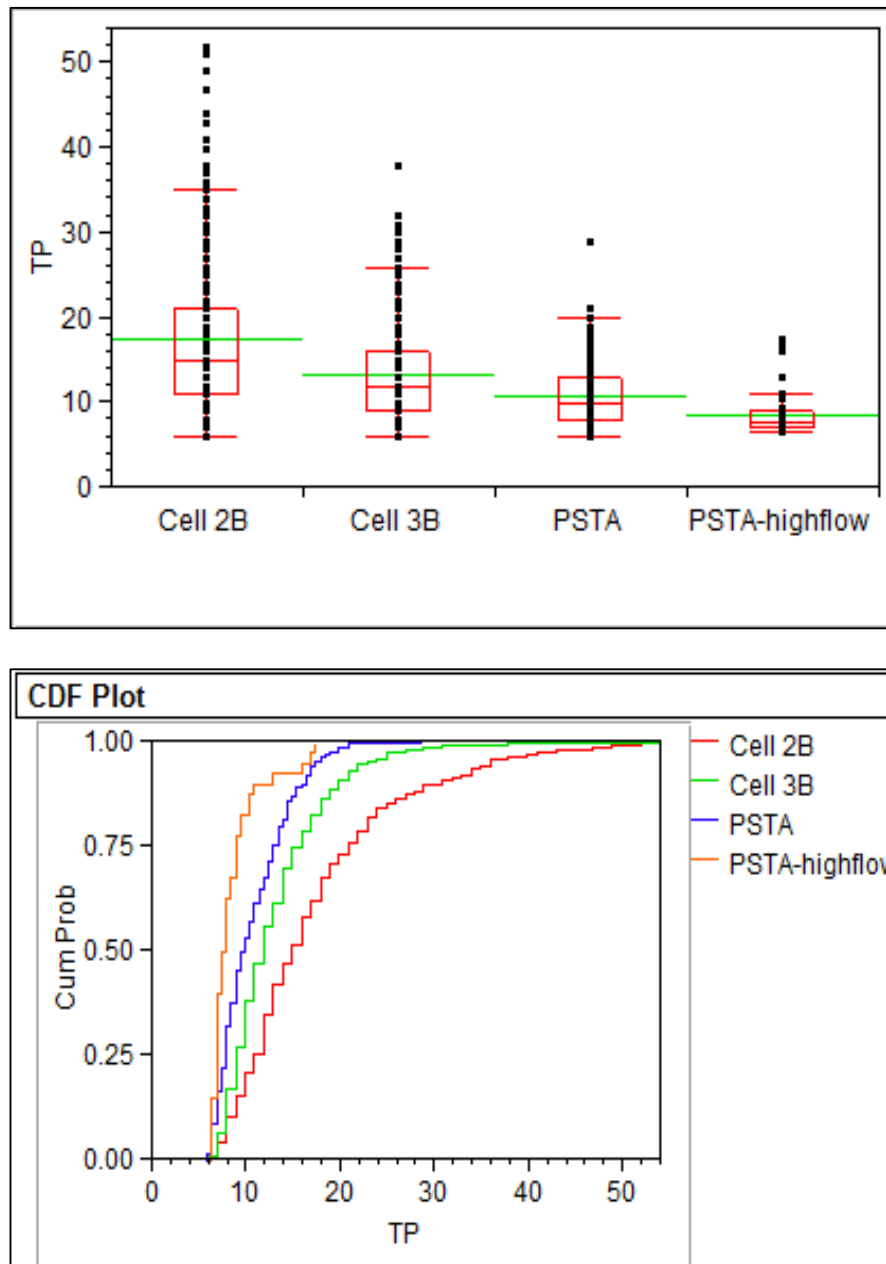


Figure 5. Box and whisker plots (top) and cumulative distribution functions (bottom) of water TP concentrations in outflow culvert grab samples collected between January 2008 - February 2014 by the District from STA-3/4 Cell 2B, Cell 3B and the PSTA Cell. Analyses represent flowing conditions only (TP values collected under non-flowing conditions were not considered in this analysis). Also included are TP plots for PSTA cell “moderate to high flow” conditions only (outflows > 21 cfs). The number of grab sample values used for the analyses were: Cell 2B, 325; Cell 3B, 323; PSTA, 210; and PSTA high flow, 40.

3.3 Internal Water Quality Surveys

3.3.1 Introduction

As noted above, the STA-3/4 PSTA Cell appears capable of producing uniquely low outflow TP concentrations, and it is important to understand how much of the wetland footprint is needed to achieve target TP levels under a range of hydraulic and P loading conditions. To better understand where P reductions are occurring, internal monitoring of surface water chemistry in the PSTA Cell has been conducted on 16 occasions since May 2012 (See Figure 6 and Table 3). Because our assessments are taking place within a narrow range of TP concentrations (typically 6 to 20 µg/L), we are utilizing phosphatase enzyme activity as a key metric for characterizing temporal and spatial changes in biotic responses to P deprivation or enrichment under the varying hydraulic (and P) loading conditions.

3.3.2 Methods

During internal sampling events, surface waters typically were sampled along five transects within the PSTA Cell, and analyzed for P species and phosphatase enzyme activities, including alkaline phosphatase activity (APA) and phospho-diesterase (PDE) activity (Figure 7). The three most recent internal profile sampling events included “Wet Season” characterizations in October 2013 and June 2014, and a “Dry Season” characterization in February 2014. For these recent efforts, an expanded suite of parameters, including nitrogen species, chlorophyll a, sulfate, dissolved organic carbon (DOC) concentrations and UV absorbance properties, was sampled along the middle transect in the PSTA Cell (Figure 7). Analytical methods for surface water are provided in Table 4.

On select occasions, including a recent survey during high flow conditions (June 26, 2014), samples were also collected in the Upper SAV Cell and selected upstream structures, to examine P gradients along the entire central flow way of STA-3/4 upstream of the PSTA Cell.

Our internal surveys often were scheduled to coincide with managed flow pulses, so that internal water quality data could be obtained before, during and after high flow pulse conditions. The hydrologic conditions during each of three managed pulse events, as well as the inflow and outflow TP concentrations and the timing of associated internal sampling events, are shown in Figures 8 (Pulse #1), 10 (Pulse #2), and 12 (Pulse #3) later in the document.

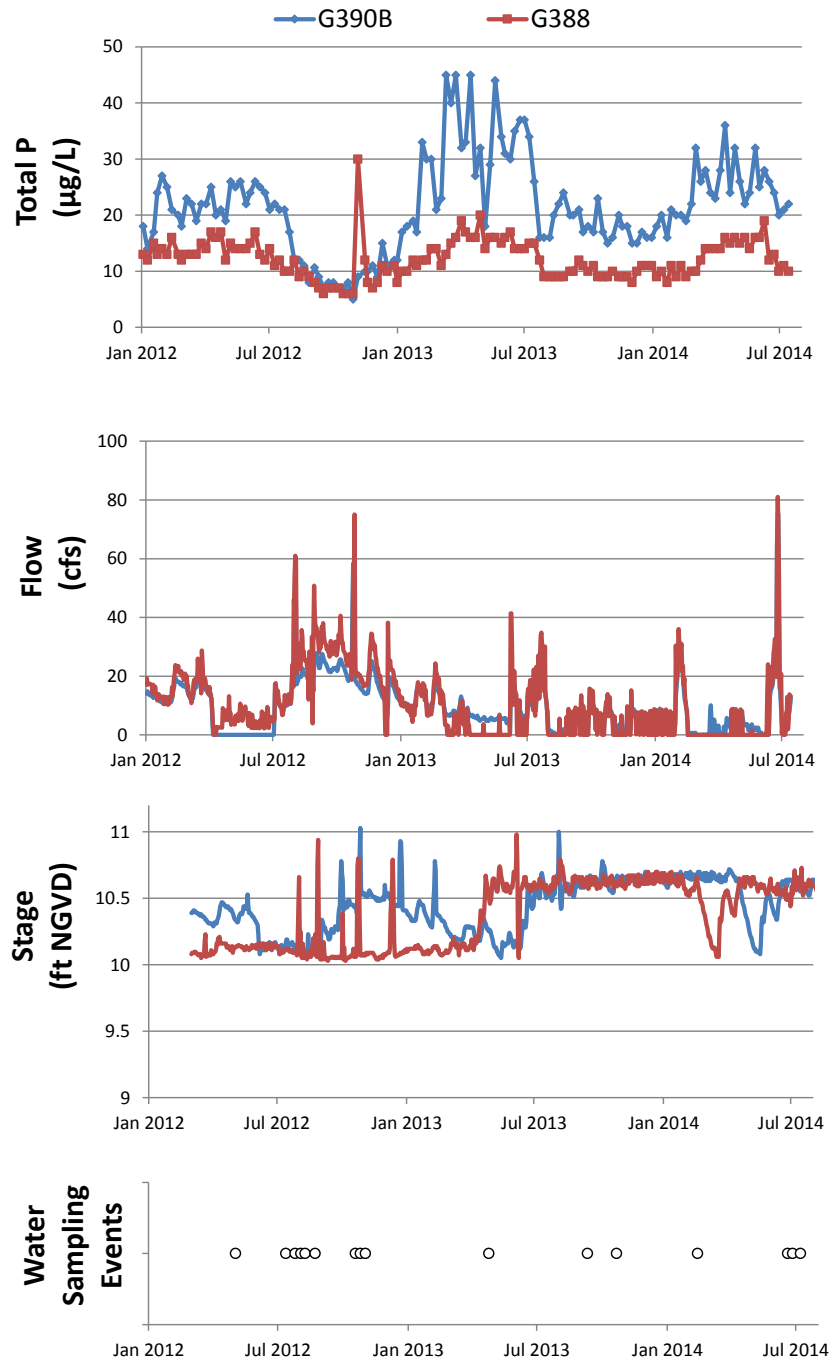


Figure 6. Flow and stage as measured at the PSTA Cell inflow and outflow structures, and the surface water TP concentration at each structure during the period from January 2012 - July 2014. Surface water sampling along internal transects was performed for 16 events during the same period.

Table 3. Hydrologic parameters during and prior to 16 surface water sampling events along transects within the PSTA Cell.

Monitoring Event	Sample Date	3-month		14-day Period Prior to Sampling		Day of Sampling				
		P Load	P Load	Inflow	Outflow	Inflow	Outflow	HRT Based on Inflow	HRT Based on Outflow	Depth
		g P/m ² /yr	g P/m ² /yr	cfs	cfs	cfs	cfs	days	days	m
Dry Season - No Inflow	5/2/2012	0.41	0.00	0	6	0	3	no flow	16	0.34
Flows Resumed to Cell	7/12/2012	0.06	0.36	8	10	9	10	6	6	0.36
Pulse #1 monitoring	7/25/2012	0.16	0.47	10	11	11	12	5	5	0.36
	8/2/2012	0.25	0.85	20	21	58	61	1	1	0.44
	8/8/2012	0.31	0.82	25	29	20	25	3	2	0.38
	8/22/2012	0.45	0.62	20	26	17	28	4	2	0.40
Pulse #2 monitoring	10/18/2012	0.44	0.35	22	30	19	27	3	2	0.38
	10/25/2012	0.42	0.44	27	29	56	55	2	2	0.57
	11/1/2012	0.40	0.41	27	31	17	21	4	3	0.38
Dry Season - No Outflow	4/24/2013	0.61	0.45	6	0	5	0	17	no flow	0.49
Wet Season monitoring	9/10/2013	0.25	0.13	3	3	7	8	12	10	0.49
Wet Season monitoring	10/21/2013	0.25	0.21	5	5	6	9	13	9	0.50
Dry Season	2/12/2014	0.35	0.85	19	24	12	14	6.9	5.8	0.49
Wet Season monitoring Pulse #3	6/19/2014	0.26	0.39	7	12	20	28	4.2	3.0	0.50
	6/26/2014	0.35	1.44	27	31	75	73	1.2	1.2	0.53
	7/7/2014	0.35	1.07	23	24	5	7	16	11	0.49

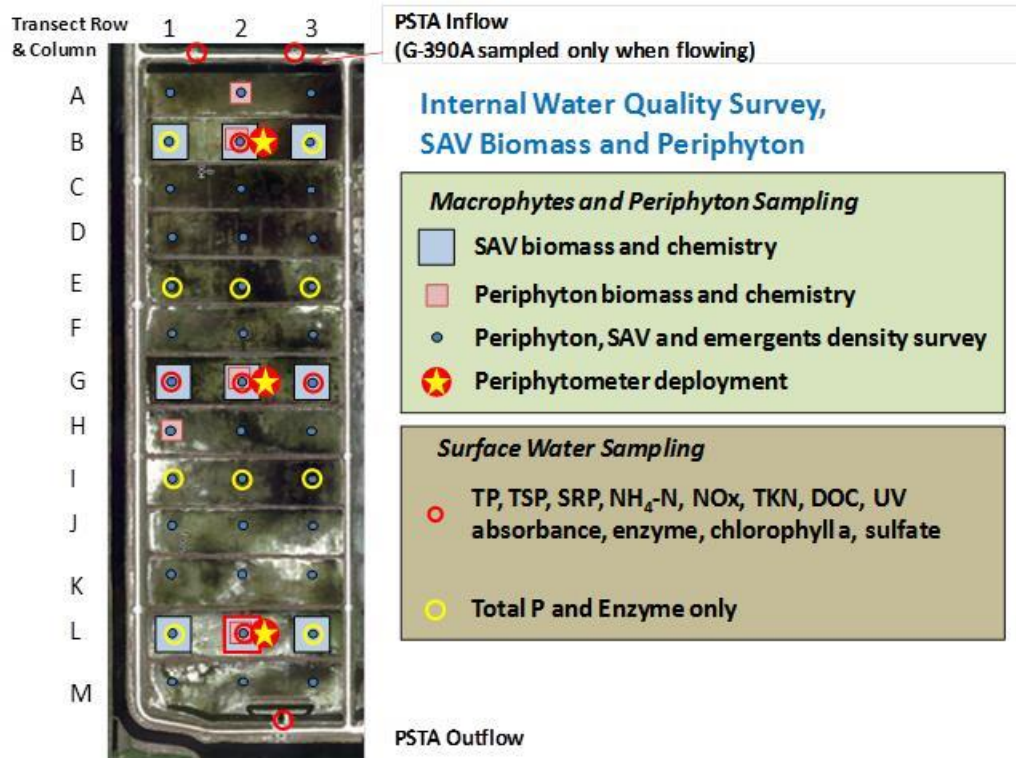


Figure 7. PSTA Cell monitoring and sampling locations.

Table 4. Analytical methods used for surface water analysis.

Parameter	Method
APA	DBE SOP-Enzyme Activity
PDE	DBE SOP-Enzyme Activity
TP	SM4500-P F
TSP	SM4500-P F
SRP	SM4500-P F
Ammonia-N	EPA 350.1 (1978)/SM4500-NH3 H (18th ed.)
TKN	EPA 351.2
NOx	SM 4500NO3 H-2000
Chlorophyll a	SM 10200H
Pheophytin a	SM 10200H
Uncorrected Chl a	SM 10200H
Sulfate	EPA 375.4/SM 426 C (15th ed.)
DOC	SM 5310B
UV 254	SM 5910 B
S275-295	Helms et al 2008
S350-400	Helms et al 2008

3.3.3 Response of surface water TP and phosphatase enzymes to flow pulses

In the following sections, the short-term response to three pulsed flow events in the PSTA Cell is described. Additionally, a summary of the internal TP profiles across all events is presented as a function of flow conditions. Details on additional parameters also are presented for our recent “Wet Season” sampling effort on June 26, 2014, which coincided with the third day of sustained high flows during Pulse #3 and captured internal profiles of water column constituents under the highest-flow conditions experienced in the PSTA Cell since operations began. Table 3 shows the hydrologic conditions during and prior to all 16 internal water quality sampling events. On the day of sampling, daily mean inflow rates ranged from 0 to 75 cfs across all events. Phosphorus mass loading rates, calculated for 14-day and 3-month periods prior to each event, ranged from 0 - 1.44 g P/m²/yr and 0 - 0.61 g P/m²/yr, respectively.

Water depth conditions in the PSTA Cell are controlled by the operation of pumps at the outflow structure G388, and vary little with changes in flow. These pumps become operational when the stage increases above a set value, and turn off when stage falls below a lower target stage level. For example, during the period of operations prior to April 2013, these thresholds were 10.2 ft NGVD to turn pumps on, and 9.8 ft NGVD to turn pumps off. Thus, water depths in the outflow region of the PSTA Cell varied by less than 0.4 ft, regardless of inflow rates. Mean bottom elevation (based on a District survey in 2013) was 8.7 ft NGVD, but did not account for the ~4” deep accrued sediment layer that is too soft to fully support the survey rod. More detail about the variability in water depth and sediment conditions is described in a later section. We used a bottom elevation of 9 ft NGVD, and the average of stage at inflow and

outflow structures, to estimate a mean daily water depth for the PSTA Cell for each sampling event. Depth and flow were then used to estimate a nominal hydraulic retention time.

3.3.3.1 Flow Pulse #1

The first flow pulse event conducted as part of this research effort occurred in early August 2012, when flows between 40 and 60 cfs were achieved for several days (Figure 8). Internal monitoring was conducted on July 12, August 2, and August 22 to characterize TP and APA in surface waters along five transects within the cell on each date. Inflow TP concentration to the PSTA Cell declined over the period, from 24 $\mu\text{g}/\text{L}$ to 10 $\mu\text{g}/\text{L}$. Prior to this period, the cell had not received inflow water since early April 2012. However, because the G388 pump structure was set to maintain outflow-region stage near 10 ft NGVD, approximately 5-10 cfs was discharged daily from the cell prior to the pulse.

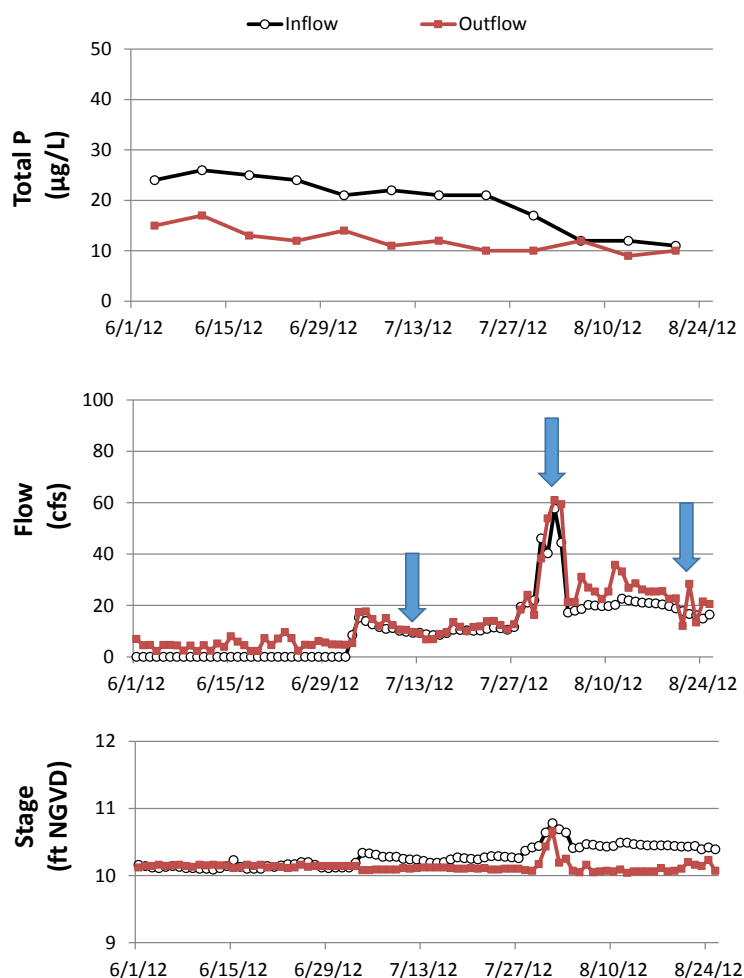


Figure 8. Average daily flow and stage as measured at the PSTA Cell inflow and outflow structures, and the surface water TP concentration at each structure during the period of the first managed pulse: June 1 – August 25, 2012. The arrows note internal water quality sampling events before during, and after the flow pulse.

Total phosphorus concentrations at each location within the PSTA cell were lower during the pulse event (8/2/12 sampling), as compared to the earlier sampling in July (Figure 9). The concentrations continued to decrease after the pulse and by August 22, each transect was exhibiting ultra-low TP concentrations (7-10 $\mu\text{g/L}$). Enzyme activity in the cell before the pulse was elevated in the inflow waters (1.5 μM MUF released/hr), but continued to increase with distance through the PSTA Cell. This increasing trend was also observed during and after the flow pulse, but APA was depressed to $\sim 50\%$ of the levels observed prior to the pulse.

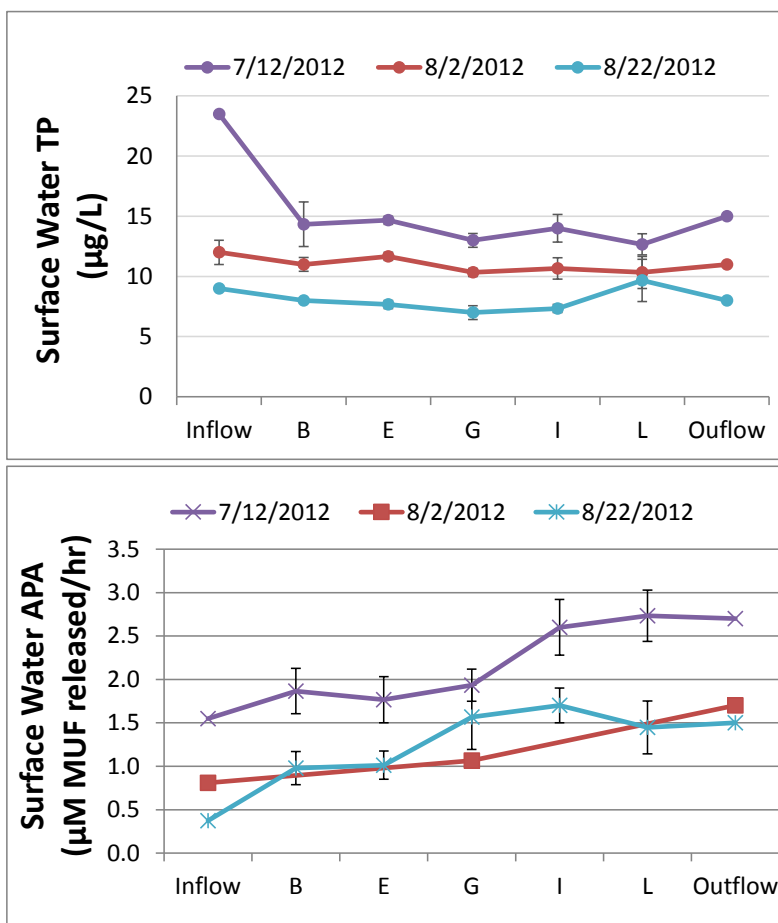


Figure 9. Total phosphorus concentrations and alkaline phosphatase activity along internal transects within the PSTA Cell during Pulse #1 (August 2, 2012), compared to sampling events before and after the pulse.

3.3.3.2 Flow Pulse #2

A second pulse event was conducted as an attempt to achieve higher flows into the PSTA Cell that might challenge the PSTA system under flow conditions more typical of other STA flow ways. The peak mean daily inflow rate during this pulse was 58 cfs, and was 56 cfs on the day

of our internal sampling event on October 25, 2012 (Figure 10). During Pulse #2, a slight increase in stage was implemented to ensure hydraulic connectivity between the surface water in the PSTA Cell and the outflow pump structure. This was achieved by increasing the on/off thresholds for Pump #2 operations from 10.2 ft/9.8 ft to 11.0 ft/10.5 ft during the pulse. Deeper water was thought to reduce hydraulic resistance from bottom roughness and vegetation, and improve conveyance of surface waters to the outflow pump location. While there was some concern that delivering sustained high flows could permanently disrupt the PSTA Cell's excellent performance by exceeding the mass P loading rate tolerated by periphyton community, this turned out to not be the case. Inflow concentrations at the time of Pulse #2 were extremely low: 6 $\mu\text{g/L}$ during the pulse on 10/25/12, and 6 $\mu\text{g/L}$ one week later (on 11/1/12) after the flows had returned to more typical rates (Figure 11). Nevertheless, the pulse event was a successful test of the ability of the PSTA cell (including sediments, periphyton and macrophyte communities) to withstand higher flows.

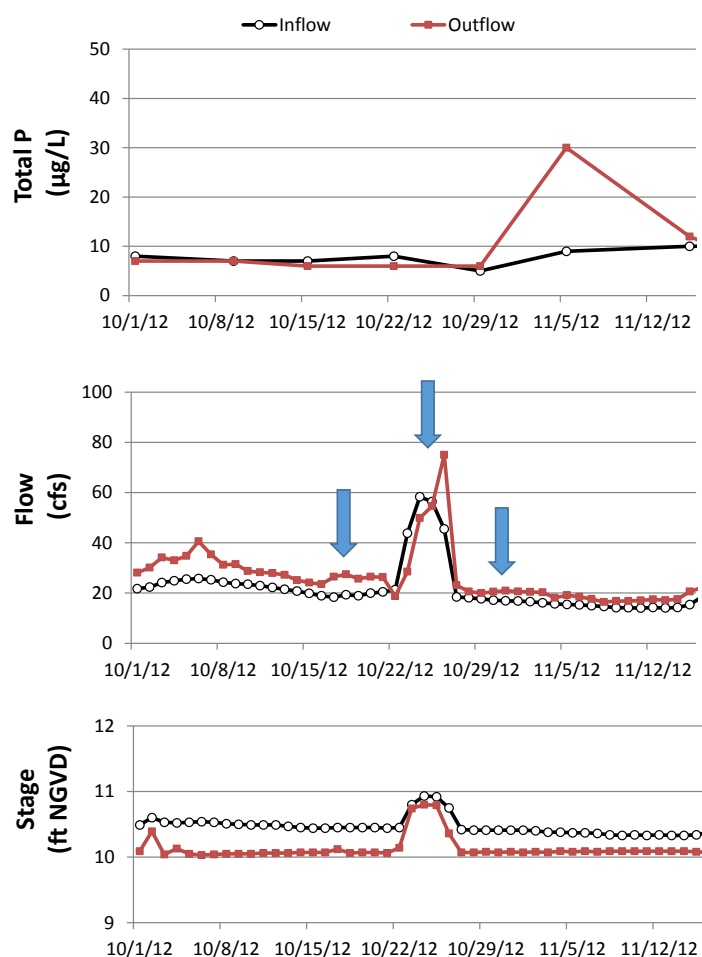


Figure 10. Flow and stage as measured at the PSTA Cell inflow and outflow structures, and the surface water TP concentration at each structure during the period of the second managed pulse: October 1 - December 1, 2012. The arrows note internal water quality sampling events before during, and after the flow pulse.

One week prior to the second pulse, TP concentrations showed a slight decrease through the cell, from inflow of 10 $\mu\text{g/L}$ to 6 $\mu\text{g/L}$ in the outflow region (L-transect), before increasing slightly to 8 $\mu\text{g/L}$ at the outflow structure (Figure 11). During the pulse, inflow concentrations dropped to 6 $\mu\text{g/L}$ while the internal transects showed slightly elevated P levels (6-8 $\mu\text{g/L}$), before decreasing back to 6 $\mu\text{g/L}$ at G388. After the pulse, TP concentrations declined from an inflow of 6 $\mu\text{g/L}$ to 5 $\mu\text{g/L}$ throughout the cell, before increasing to 7 $\mu\text{g/L}$ at G388. Meanwhile, APA was highest prior to the pulse, but increased with distance through the cell on all three sampling dates.

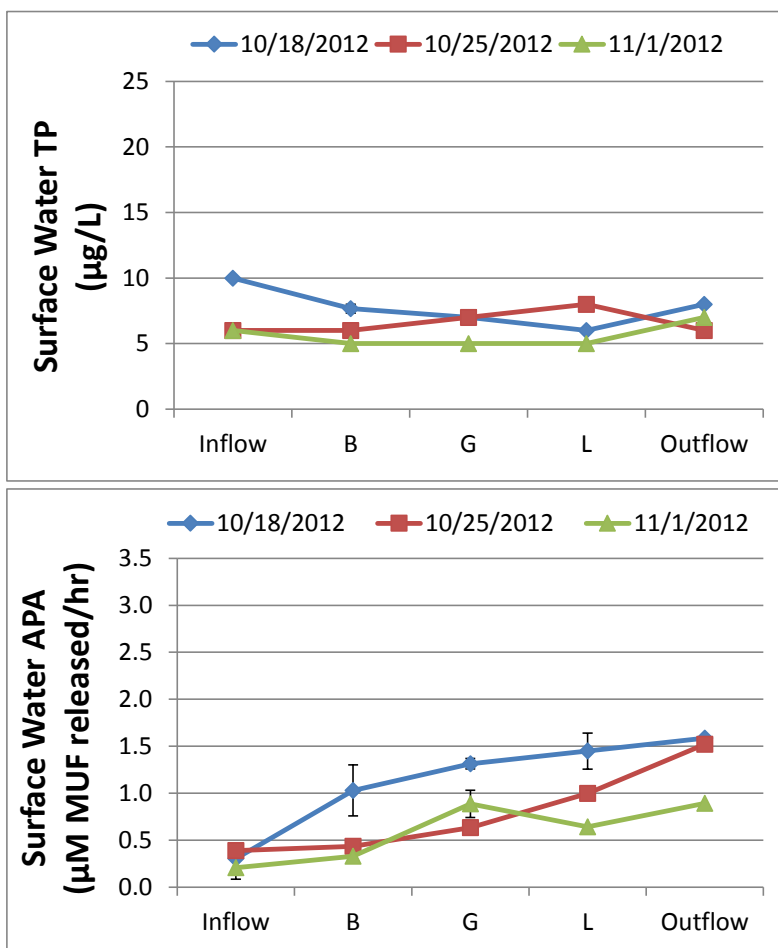


Figure 11. Total phosphorus concentrations and alkaline phosphatase activity (APA) along internal transects within the PSTA Cell during Pulse #2 (October 25, 2012), compared to sampling events before and after the pulse.

3.3.3.3 Flow Pulse #3

During June 2014, a third pulse event was conducted. As part of preparations for Pulse #3, the inflows to the PSTA Cell were curtailed after June 1, and stage in the Upper SAV Cell was increased to store the necessary water required to maintain high flow conditions for several days. Inflows to the PSTA Cell are gravity-fed through structure G390A and G390B, with G390A only open during higher flow conditions. Since April 2013, the PSTA Cell stage had been maintained ~0.5 ft higher than the level that the cell was operated at during the first two pulses. This was achieved by changing the on/off thresholds for G388 outflow pump operations from 10.2 ft/9.8 ft to 10.7 ft/10.3 ft, respectively. For the six-week period between June 1 and July 14, 2014, mean daily average stage values at the inflow structures ranged from 10.59 – 11.03 ft and from 10.44 – 10.71 ft (NGVD29) at the outflow structure (Figure 12). The Pulse #3 event achieved higher flow rates than the previous pulse events, in part by utilizing pump #1 at the G388 structure (pump #2 is normally all that is required to maintain desired stage and outflow), with a mean flow of 75 cfs on the day of our internal sampling on June 26, 2014 (Figure 12). Stage was maintained at 10.5 ft during Pulse #3.

In comparison to samples collected approximately one week before and one week after the flow pulse, there was no difference in outflow P concentration (10 µg/L) under high-flow conditions during Pulse #3 (Figure 13). Inflow waters were somewhat lower in TP during the pulse than either before or after the flow event. Nevertheless, a steady decline was observed as water passed through the PSTA Cell, highlighting the cell's ability to reduce P concentrations even where inflow TP concentrations are low.

In contrast to TP, the enzyme activities measured during the flow pulse were markedly lower than those observed before or after the pulse (Figure 14). In fact, the highest activities observed during any of the three sampling events associated with the pulse (6/19, 6/26, and 7/7/2014) occurred after the flows had returned to normal. The B and E transects on July 7 exhibited enzyme hydrolysis rates approaching 3 µM MUF/hr, and is indicative of extremely P limiting conditions. The rapid increase in enzyme activity one week after the high flow period suggests that algal communities and bacteria that produce enzymes were sustained through the pulse, and responded quickly to changes in P load to the cell. The highest chlorophyll a concentrations were also observed along the B transect on July 7 (10.7 µg/L), and were lower during the flow pulse (Figure 15).

Soluble reactive phosphorus (SRP) concentrations were very low throughout the PSTA Cell during the flow pulse, with detectable levels only along the G transect in the middle of the cell (Figure 16). Dissolved organic phosphorus (DOP) concentrations decreased from 8 to 5 µg/L, with the lowest value of 4 along the G transect. Particulate phosphorus (PP) concentrations decreased from 6 µg/L at the inflow, and B and G transects, to 5 µg/L in the L-transect and at the outflow structure.

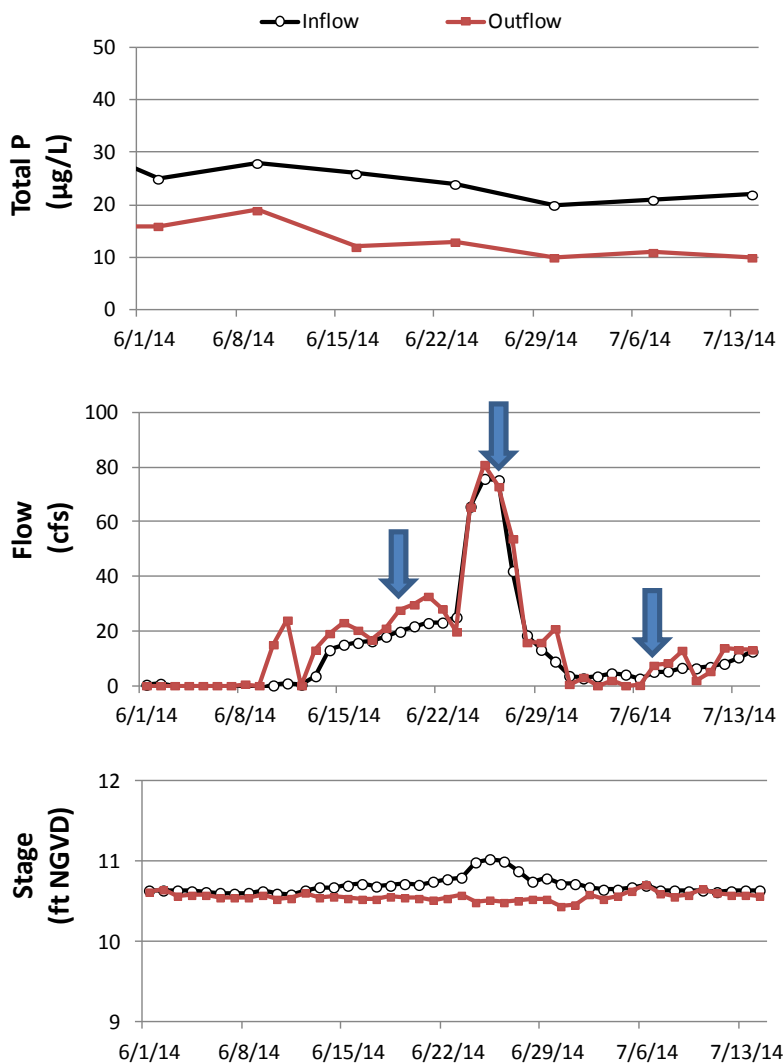


Figure 12. Flow and stage as measured at the PSTA Cell inflow and outflow structures, and the surface water TP concentration at each structure during the period from June 1 – July 14, 2014. The arrows note internal water quality sampling events. Macrophytes were collected July 7, and periphyton samples on slides were collected on June 19 and July 7, 2014, before and after the flow pulse.

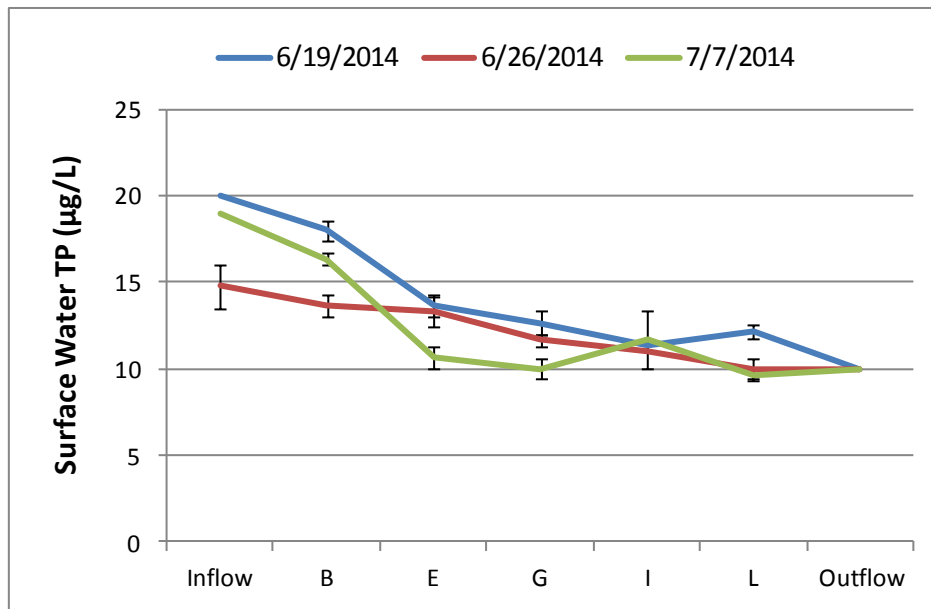


Figure 13. Comparison of total phosphorus concentrations in the surface waters of the PSTA Cell for three sampling dates, before, during and after a period of high flows (flows peaked just prior to 6/26/14). Error bars denote ± 1 SE for three stations along internal transects, or two inflow structures (G390A sampled only on 6/26/14, when the structure was open and flowing).

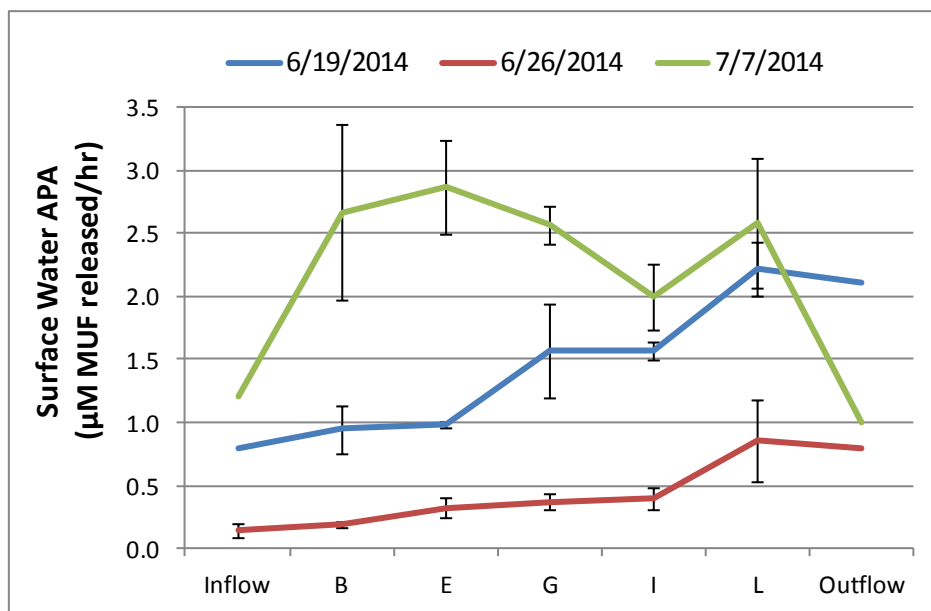


Figure 14. Comparison of alkaline phosphatase activity (APA) in the surface waters of the PSTA Cell for three sampling dates, before, during and after a period of high flows. Error bars denote ± 1 SE for three stations along internal transects, or two inflow structures (G390A was sampled only on 6/26/14, when the structure was open and flowing).

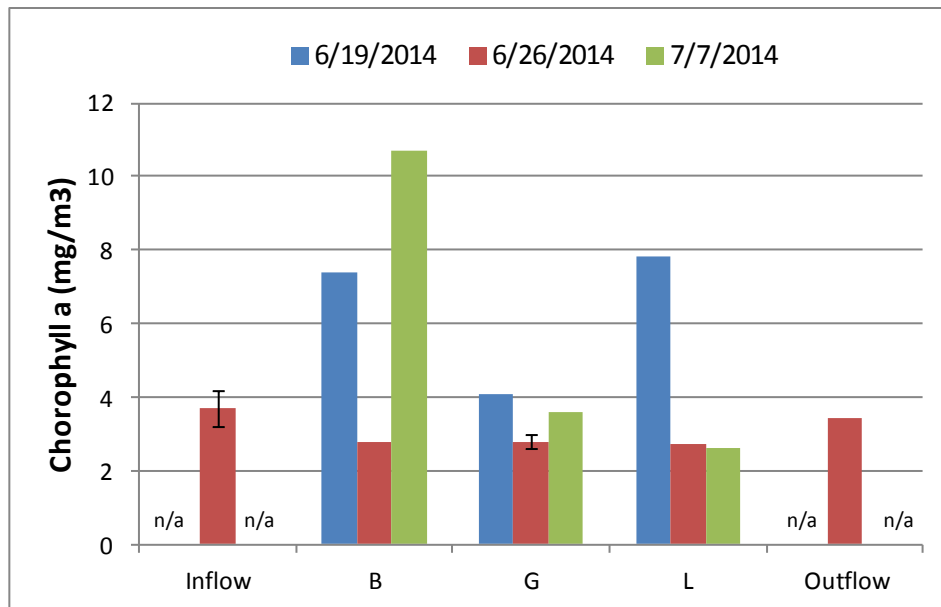


Figure 15. Chlorophyll a concentrations (pheophytin-corrected) in the surface waters of the PSTA Cell for three sampling dates, before, during and after a period of high flows. Error bars denote ± 1 SE for three stations along internal transects, or two inflow structures (G390A sampled only on 6/26/14, when the structure was open and flowing).

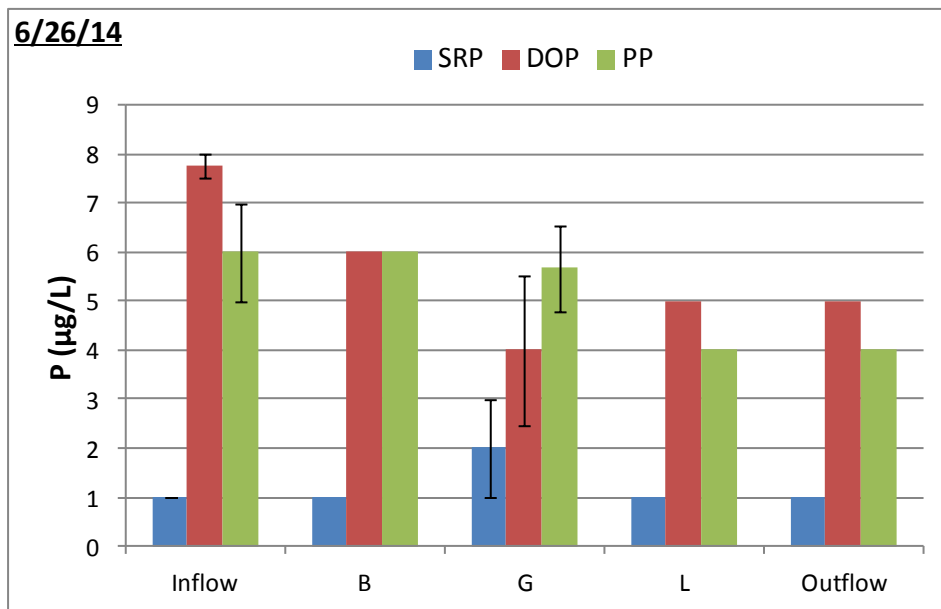


Figure 16. Phosphorus species concentrations in the surface water at inflow and outflow structures, and three internal transects within the cell, on June 26, 2014. Error bars denote the standard error around the mean for duplicate inflow samples, and grab samples at three stations along the middle (G) transect.

Ammonia nitrogen concentrations were low throughout the PSTA Cell, but decreased slightly from inflow (0.052 ± 0.009 mg/L) to outflow (0.036 mg/L). Nitrate + nitrite concentrations were below detectable levels (0.016 mg/L) at all locations, while the Total Kjeldahl N concentrations decreased from 2.0 to 1.6 mg/L between inflow and outflow. Like TP, the decrease in TKN occurred steadily with distance through the cell.

Sulfate concentrations decreased from 55 mg/L at the inflow, to 51 mg/L at the G transect and 47 mg/L at the outflow. DOC also exhibited a minor decrease, from 25 mg/L at the inflow, B, and G transects to 24 mg/L at the L transect and outflow structure. SUVA₂₅₄ showed no change through the cell (3.6 L/mg DOC/m), and the spectral slope, $S_{275-295}$, was only marginally higher at the outflow (0.0179 nm^{-1}) as compared to the inflow (0.0176 nm^{-1}) waters.

3.3.4 Water quality profiles

3.3.4.1 Entire flow path

Total phosphorus concentrations in the PSTA Cell decreased from 15 to 10 $\mu\text{g/L}$ on June 26, 2014, when the hydraulic retention time (HRT) of the cell was approximately 1.2 days (Table 3). Since high flows were sustained for 2-3 days prior to the sampling event (Figure 12), the internal and outflow water samples are reflective of the high-flow conditions. At this time, the inflow waters to the STA-3/4 Central flow way contained only 23 $\mu\text{g/L}$ TP, which is very low for STA inflow waters. However, despite the low inflow P levels, P concentration reductions were observed throughout the flow way (Figure 17). Importantly, P removal continued within the PSTA Cell to reduce TP concentrations below the apparent background concentration identified for well-performing SAV flow ways on muck soils (Juston and DeBusk 2011).

Enzyme activity was low in the surface waters upstream of the PSTA Cell during the flow pulse, with $\leq 0.2 \mu\text{M MUF/hr}$ at each station (Figure 18). Activities of monoesterase (APA) enzymes increased steadily within the PSTA Cell, then rose sharply in the outflow region (L transect) to $0.86 \pm 0.32 \mu\text{M MUF/hr}$. Diesterase activity also increased within the cell, albeit at a slower rate than monoesterase activity.

3.3.4.2 Temporal trends in total phosphorus profiles

The sampling events associated with the pulses described above are among a larger set of 16 internal sampling events performed in the PSTA Cell since May 2012. Total phosphorus concentration profiles in the PSTA Cell for all events (Figure 19) were either flat (when inflow TP was low), or showed steady declines through the treatment area (when inflow TP levels were slightly elevated). With the exception of dry season surveys in May 2012 and April 2013, there was limited evidence of any TP concentration increase within the cell. However, several events indicated that TP in the marsh outflow region (L-transect) was slightly lower than at the outflow structure (G388).

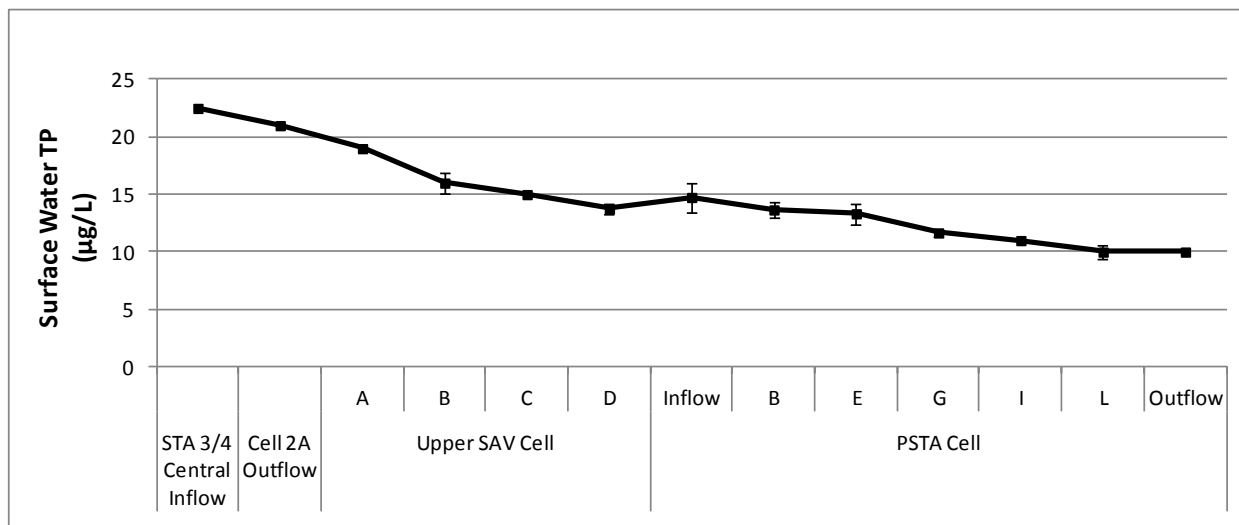


Figure 17. Longitudinal profile of total phosphorus concentrations through the PSTA Cell, as well as the upstream Upper SAV Cell and Cell 2A, in the central flow way of STA-3/4, on June 26, 2014. Error bars denote \pm standard error (SE) around the mean of three stations per transect in the PSTA Cell, or four stations along the B and D transects of the Upper SAV Cell.

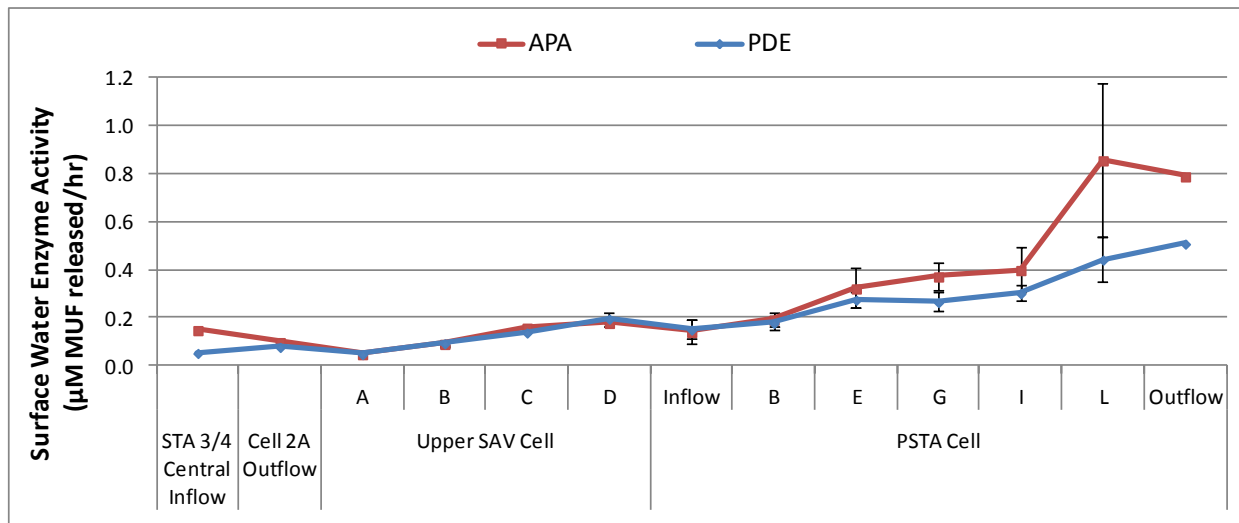


Figure 18. Enzyme activity in the surface waters along internal transects through the PSTA Cell and the upstream Upper SAV Cell, as well as at inflow and outflow structures, on June 26, 2014. Alkaline phosphatase activity (APA) for monoesterase and phosphodiesterase (PDE) were assayed fluorometrically using methylumbelliferyl (MUF)-P substrates, where the release rate of MUF is proportional to the rate of hydrolysis of phosphate from organic P compounds.

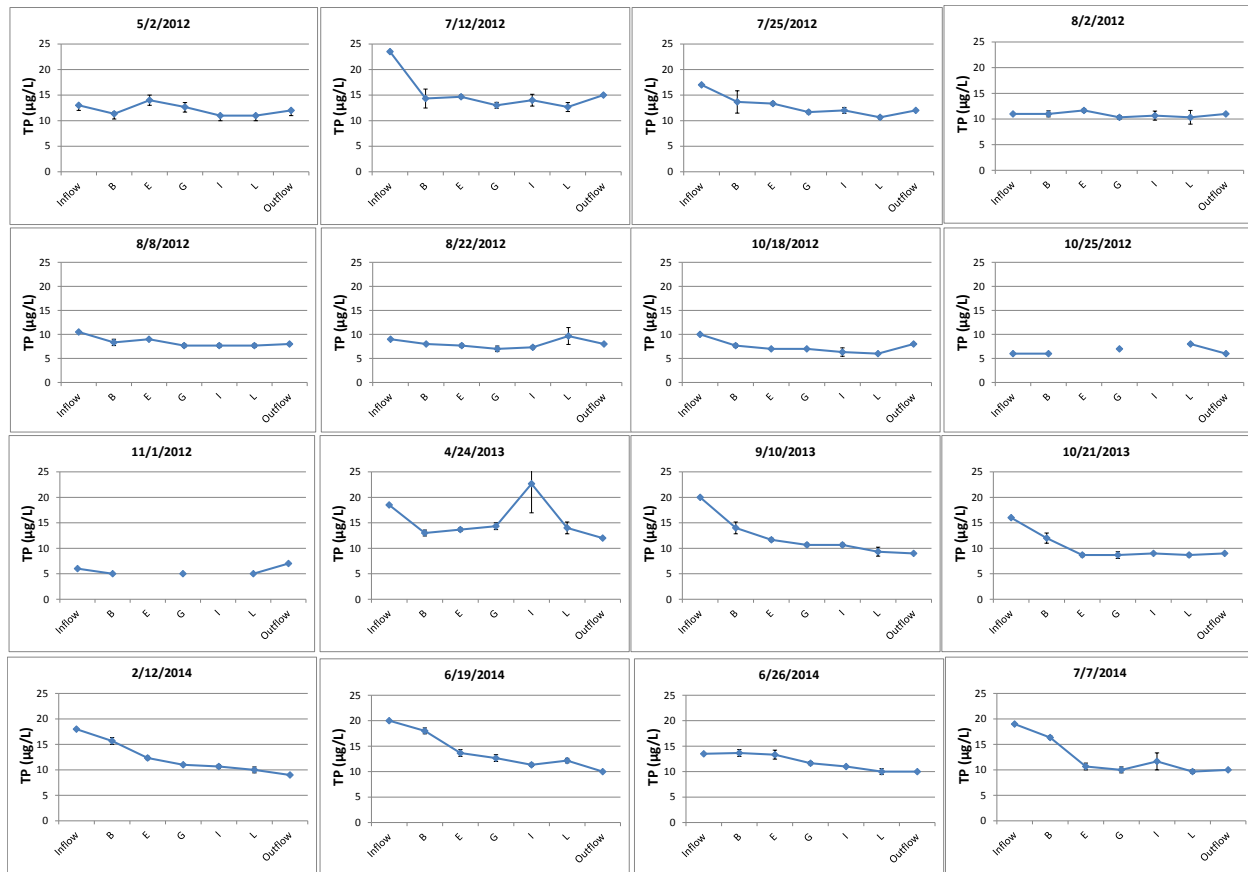


Figure 19. Internal profiles of total phosphorus (TP) for 16 sampling events between May 2012 and July 2014. Values represent the average \pm SE from three stations along each internal transect. Hydrologic conditions for these monitoring events are shown in Table 3..

3.3.4.3 Effects of flow conditions

A comparison of the TP profiles under stagnant (“no flow”) conditions, moderate flows and high flow conditions indicates that flowing conditions provide conditions conducive to lower outflow TP concentrations (Figure 20). Under flowing conditions, enzyme activities increased immediately within the PSTA cell and remained elevated through all internal stations. This trend was observed in 11 water quality surveys during moderate flow conditions (7 – 28 cfs) and 3 surveys during high flow events (mean daily inflow rate > 50 cfs). During stagnant conditions (< 5 cfs) enzyme activities were relatively high, and showed little change between inflow and outflow regions (Figure 20). Additional investigations on the effects of P and hydraulic loading on enzyme activity in the water column, and in PSTA cell periphyton communities, are ongoing.

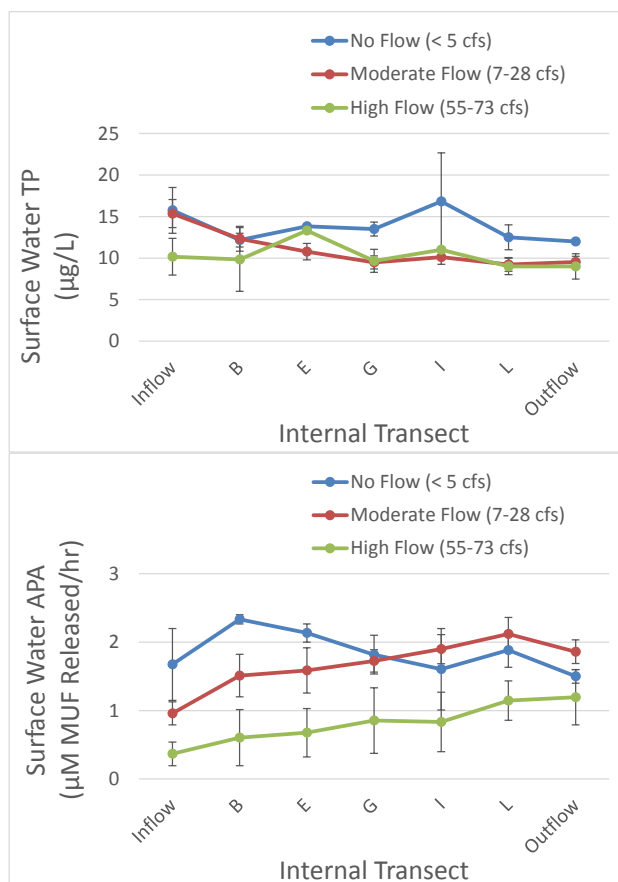


Figure 20. Average (\pm SE) total phosphorus concentrations and alkaline phosphatase activity (APA) in surface waters of the PSTA Cell, based on multiple internal water sampling events under different flow conditions: No flow (N=2), moderate flow (N = 11) and high flow (N=3). Error bars denote the variation across different sampling dates for transect average concentrations, which were derived from 1-3 stations per transect.

3.3.5 Discussion

Internal water sampling provided several important findings related to PSTA Cell performance across a range of flow conditions. The ability of the cell to maintain low internal P concentrations when inflow TP levels are low, and to remove P when inflow TP is in the range of 12-20 $\mu\text{g/L}$, indicates that the P removal capacity of the cell remains intact across a wide range of flow conditions. Total P concentrations of both inflow and outflow waters were lower during high flow events, in part due to the improved performance of the upstream EAV and SAV cells under flowing conditions. The PSTA Cell did not show signs of internal P release into the water column when inflow TP concentrations were very low, except during stagnant conditions. Importantly, the PSTA Cell typically was able to reduce TP concentrations below the apparent background concentration identified for well-performing SAV flow ways on previously-farmed muck soils (Juston and DeBusk 2011).

Under flowing conditions, enzyme activities increased immediately within the PSTA cell (relative to those in upstream cells) and remained elevated through all internal stations (Figure 18). Enzyme activities were depressed during high flow events, due either to a decline in enzyme production by biota or simply due to dilution by the higher volume of inflow waters. Differing responses in enzyme activity were observed between the three pulses for the period following pulsed flows. However, the elevated enzyme activity in the PSTA Cell, as compared to the upstream muck-based Upper SAV cell, demonstrates that a unique biotic environment prevails in this wetland (Figure 18). Recovery of enzyme activity after the recent high flow pulse event suggests resilience in the community responsible for producing these compounds.

3.4 Sediments

3.4.1 Introduction

The STA-3/4 PSTA facility has developed an accrued marl sediment layer on top of the bedrock that was exposed during project construction. This new material is different than the underlying limerock surface upon which the PSTA community was first established, and may affect both water column nutrient exchange and macrophyte and periphyton growth. It is important to understand how the accumulation of new sediment over the original calcium-based substrate can influence outflow TP concentrations and sustainability of P removal performance. As a starting point in addressing these questions, we have begun defining the extent of new sediment accumulation and quantifying its chemical composition.

In most regions within the cell, the muck soils were removed during cell construction (2004), or were used to construct internal berms for vegetated strips. These internal berms are oriented perpendicular to the dominant flow direction. In April 2012, emergent vegetation on selected berms was treated with herbicide. The following month, the dead emergent vegetation was compacted into the soil to reduce hydraulic resistance within the cell. It should be noted that the soil material that originally comprised the internal berms may be susceptible to sloughing into the deeper, adjacent treatment areas. The berms have not been included in sediment sampling described in this report. Rather, the current study characterized the sediments from areas between the internal berms within the PSTA Cell.

To supplement the PSTA cell sediment surveys, the effects of the newly-accrued sediments on water column P dynamics, macrophyte growth and tissue P contents were examined through a series of outdoor experiments using replicated sediment-water cores (batch, 15-cm diameter, 30 cm water depth) and columns (flow-through, 30-cm diameter, 45 cm water depth). These experiments are described in a later section of this report. The sediments used for those studies were collected from the outflow region (L transect) of the PSTA Cell. The following section describes the sediment composition characteristics throughout the PSTA cell.

3.4.2 Methods

Total depth of sediment material above bedrock was determined in situ with a tape measure and tile probe at three stations along each of 13 transects (i.e., within each compartment of the

PSTA cell defined by the vegetated strips) in May 2014 (Figure 21). Intact cores were retrieved to verify the depth of accrued sediment apart from any underlying residual muck layer. Accrued sediments were retained for chemical analysis (Bulk density, TP, TN, TC, TOC, TCa, AFDW, and enzyme activity).

3.4.3 Results and Discussion

3.4.3.1 Sediment accrual in the PSTA Cell

Accrued sediment depths measured along 13 transects within the PSTA Cell ranged from 1 to 15 cm, with a cell-wide average of 7.8 ± 0.5 cm (Figure 22). Standard error around the mean of triplicate measurements made at nine stations ranged from 0.3 to 2.3 cm. Sediments were slightly deeper in the outflow region (10.2 ± 1.2 cm) than middle or inflow region (7.8 ± 1.3 cm and 5.7 ± 0.7 cm, respectively). Total soil depth, including the accrued layer and underlying residual muck soil, ranged from 7 to 49 cm.

3.4.3.2 Accrued sediment chemical composition

The phosphorus content of the accrued layer ranged from 167 - 496 mg/kg (average 257 ± 33 mg/kg), based on our May 2014 sampling effort (Figure 23). This cell-wide survey showed that the PSTA Cell sediments were fairly uniform in P content. Sediment TP content in May 2014 agrees well with an earlier survey of the cell in 2012, when TP ranged from 150-371 mg/kg and averaged 272 ± 24 mg/kg (Andreotta et al., 2014, Figure 5B-34). Additional characteristics of accrued sediments in the outflow region of the PSTA Cell, including bulk density, enzyme activity, C, N, Ca, and organic matter content (total organic carbon (TOC) and ash-free dry weight (AFDW)) are provided in Table 5. Sediment phosphorus monoesterase activity (APA) decreased from inflow to outflow in the PSTA Cell, but phosphorous diesterase (PDE) hydrolysis rates were uniform (Figure 24). Similar rates and trends in APA were observed for PSTA cell accrued sediments collected in 2012 (Andreotta et al., 2014, Figure 5B-36)

3.4.3.3 Sediment P storage

Phosphorus stored in the newly accrued sediment layer averaged 2.3 ± 0.3 g P/m² across the PSTA Cell in May 2014. This mass of stored sediment P exceeds the estimates of historical water column P removal. For the 6-year period including WY2008 through WY2013, an estimated 0.72 g P/m² was removed from the water, based on concentration reduction and inflow volumes reported in Table 5B-15 of Andreotta et al. (2014). It is possible that this “additional” stored P in the sediments was sourced from soils sloughed from the vegetated berms, or from pre-existing muck pockets in the limerock substrate. Excess P stored in newly-acrued sediments, relative to calculated water column P removals, was also reported for STA 2 Cell 3 by Juston et al. (2013), who implicated macrophyte growth and mining of deeper sediment P as a possible mechanism. Changes in storages between this and future soil surveys in the cell should provide greater insight into the observed discrepancy in the mass of P stored vs. mass of P removed by the PSTA cell.

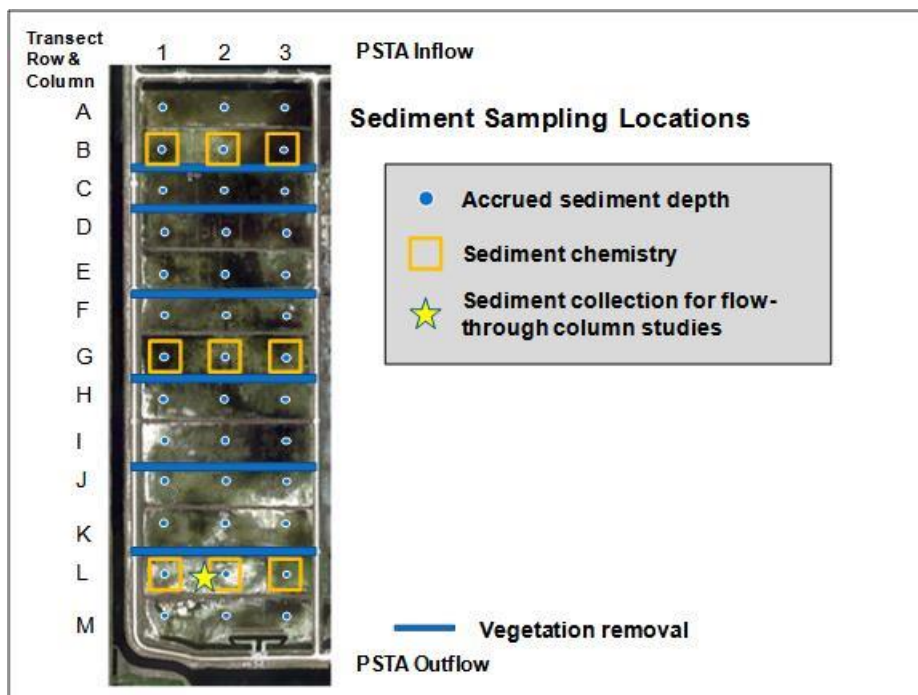


Figure 21. Internal locations within the STA-3/4 PSTA Cell where sediments were assessed for accrual depth, chemistry and P flux studies. For reference, the internal berms where emergent vegetation was removed in 2012 are also shown.

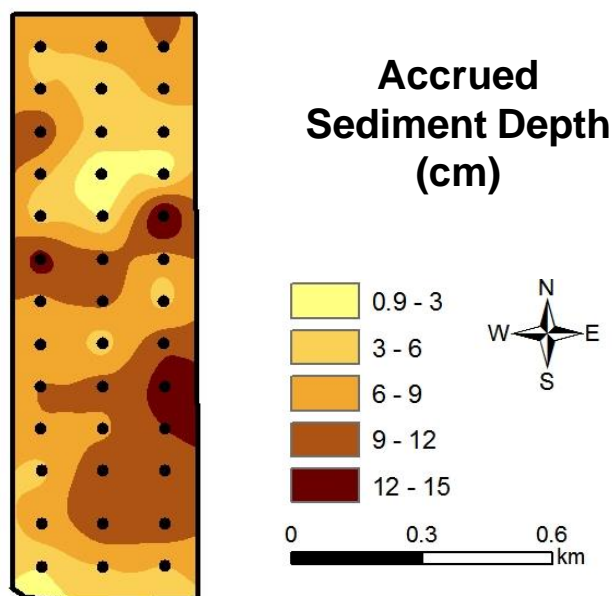


Figure 22. Spatial survey of the depth of the accrued sediment layer in the STA-3/4 PSTA Cell, based on a field survey on May 15, 2014 of 13 internal transects each with three stations where the accrued depth was measured.

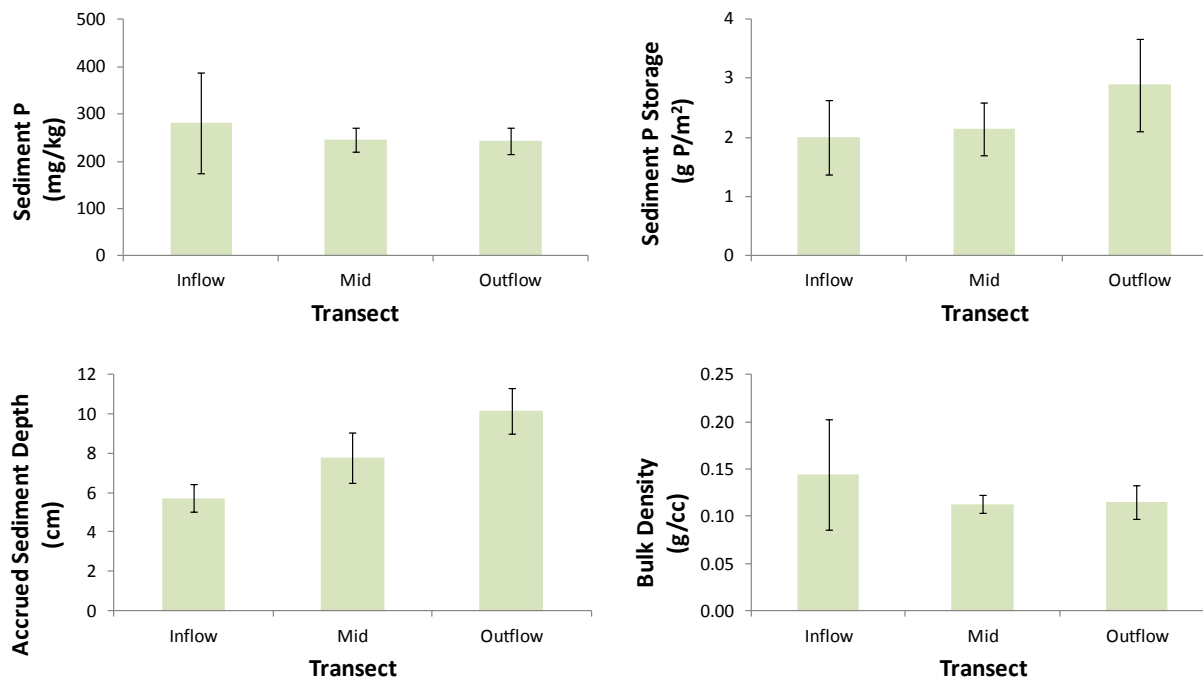


Figure 23. Phosphorus content, depth, bulk density and P storage of the newly accrued sediment layer along three transects within the PSTA Cell, in May 2014. Values represent the average (\pm SE) measurements at three stations per transect.

Table 5. Chemical composition of the accrued sediment layer in the PSTA Cell in May 2014.

Transect	Bulk Density (g/cc)	TP (mg/kg)	TN (%)	TC (%)	TOC (%)	Total Ca (%)	AFDW (%)	APA	PDE	
								$\mu\text{mol MJF released/g soil/hr}$		
Average	Inflow	0.144	282	1.0	18.2	11.0	22.3	22.2	10.6	2.8
	Mid	0.113	246	0.9	18.3	11.0	22.8	22.4	8.1	2.2
	Outflow	0.115	244	0.7	16.9	8.8	28.2	16.8	6.4	2.2
SE	Inflow	0.058	107	0.2	0.8	0.9	2.9	2.6	4.4	1.0
	Mid	0.009	25	0.1	1.2	2.1	3.0	3.6	1.6	0.5
	Outflow	0.018	28	0.1	0.8	1.3	1.3	2.3	1.2	0.9
Whole-Cell Average		0.124	257	0.9	17.8	10.3	24.5	20.5	8.4	2.4
SE		0.018	33	0.1	0.5	0.8	1.6	1.7	1.5	0.4

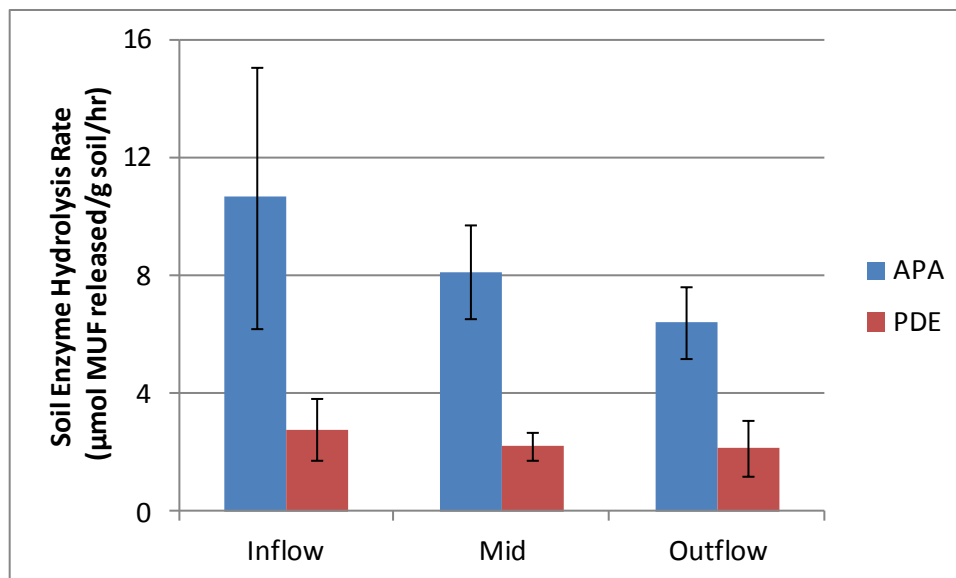


Figure 24. Enzyme activity in the newly-accrued sediment layer along three transects within the PSTA Cell in May 2014. Values denote the mean \pm SE of three stations along each transect. Alkaline phosphatase activity (APA) and phosphodiesterase (PDE) activity rates were normalized to the dry weight of sediments as assayed.

3.5 Macrophytes

3.5.1 Introduction

The community composition and standing biomass of macrophytes and associated periphyton within the PSTA cell may differ from STA flow ways with the organic soil intact, but this has not been investigated in sufficient detail. In shallow lakes, SAV can obtain P exclusively from the sediments when bioavailable-P is low in the water column (Barko and Smart, 1980; Carignan and Kalff 1980). Under such circumstances, the macrophytes act as a nutrient “pump” by using sediment P for tissue growth, then releasing DOP and PP upon senescence. High biomass and/or tissue P contents would suggest that macrophytes were an important source of internally recycled P. Since macrophytes can supply P to epiphytes throughout the year (Burkholder and Wetzel 1990), high P in SAV tissues may also influence the type of periphyton and suppress the production of phosphatases. At present, it is not clear what effects organic soil removal may have on macrophyte biomass and tissue P contents.

Preliminary monitoring and start-up operations for the STA-3/4 PSTA Project began in WY2006, and a vegetation survey during 2007 revealed that SAV had become established throughout the PSTA project (Pietro et al., 2008). The spatial distribution of SAV species in the PSTA Cell was further quantified in August 2008 and February 2009, and indicated dominance by *Chara* sp., with moderate coverage by *Najas guadalupensis*, and lesser amounts of *N. marina*, *Potamogeton* sp., *Hydrilla*, and *Ludwigia repens* also present (Pietro et al., 2010). *Chara* and *N.*

guadalupensis are common to STA flow ways with muck soils, and isolated patches of *N. marina* and *Potamogeton* sp. have also been reported (Andreotta et al., 2014). However, little information exists on the biomass density SAV beds, or to what extent the macrophyte community acts as a natural substrate for periphytic growth in either muck- or calcitic- substrate wetlands.

To understand the role of macrophytes in PSTA systems, we posed two initial questions. Does macrophyte biomass differ between the PSTA Cell and other muck-based STA areas? Are macrophyte growth rates and nutrient contents affected by sediment type?

3.5.2 Methods

Macrophyte species composition and distribution were monitored during 11 semi-quantitative surveys in the PSTA Cell between July 2011 and June 2015. The first SAV survey occurred July 21, 2011, 2.5 weeks after stages returned to normal following a relatively severe drydown event (Figure 25). Selected surveys, such as the one performed in July 2014, also included assessments of both SAV and EAV cover, in the PSTA cell along with the upstream “Head Cell”, also known as the Upper SAV Cell.

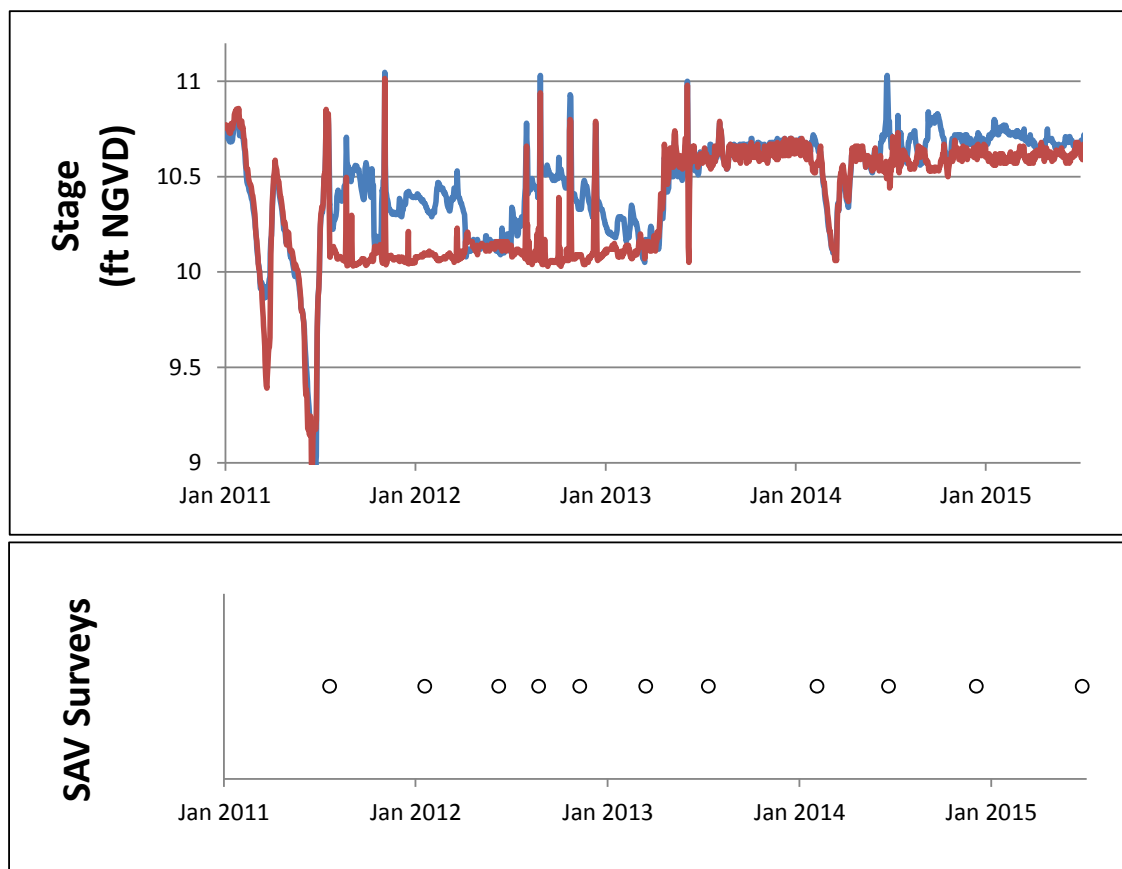


Figure 25. Stages in the STA-3/4 PSTA Cell during the period from May 1, 2010 through August 1, 2015, and dates of 11 SAV surveys within the cell during that time.

The vegetation monitoring scheme used to determine the relative density and coverage of periphyton, emergent vegetation, and SAV species, was based on an approach developed by DBE for SAV-dominated STA cells. Relative density was assessed at 39 stations within the PSTA cell (Figure 7). The presence or absence of common macrophyte species was recorded, along with a density or cover ranking on a scale from 0 to 5. The percent of available substrate area covered by periphyton at each station was also assigned a density score, on the same scale.

Spatial maps of the SAV species distribution were constructed using Arc GISv9 Spatial Analyst (Environmental Systems Research Institute, Redlands, CA). Previous surveys conducted in WY2013 were provided in Chapter 5B of the 2014 South Florida Environment Report (Andreotta et al., 2014).

On three occasions (August 2012, January 2014 and July 2014), macrophyte biomass density was determined by collecting aboveground SAV biomass from within a 0.5 m x 0.5 m sampling frame. This approach was taken on a coarser spatial scale than the visual surveys. Macrophyte samples were collected from three stations within each of three regions of the PSTA Cell: the inflow (B-transect), middle (G-transect) and outflow (L-transect). Triplicate quadrat throws were performed at each station and wet biomass was recorded in the field, unless total sample weight was < 0.1 kg. In this instance, low-weight samples were retained in their entirety for later weight determination. Otherwise, a grab subsample of the dominant SAV was retained from each station to determine dry:wet ratio and nutrient contents of the tissues. Dry weight of SAV biomass from within the sampled area (0.25 m²) was used to calculate standing crop biomass. The dried tissue was then ground and analyzed for tissue N, P, C and Ca concentrations. Biomass P storage was calculated from the standing crop estimate (g dry mass per m²) and tissue P content (mg P/kg tissue dry mass).

In order to determine the relative proportion of periphyton biomass to macrophyte biomass, the two fractions were separated, dried, weighed and analyzed for nutrient contents. On several occasions, the periphyton growing on macrophytes in the PSTA Cell were sampled as epiphyton on “natural substrates”, which provided a point of comparison to periphyton grown on artificial substrates. Additional detail on periphyton collection efforts, processing and analyses are presented in a later section of this report.

3.5.3 Results

3.5.3.1 Macrophyte cover surveys

Across multiple survey dates, the distribution of the three most abundant SAV species in the PSTA cell has remained stable. *Chara* dominated the overall SAV community on all dates (Figure 26), while *Potamogeton* and *Najas guadalupensis* have exhibited a consistent presence on the inflow region (Figures 27 and 28). During recent surveys, *Potamogeton* has become established in the outflow region as well. When only the areas supporting moderately dense vegetation or greater are considered, the temporal trajectory of SAV coverage shows that *Chara*

and *Potamogeton* have been fairly stable during all surveys performed by DBE since 2011, while *Najas guadalupensis* may be increasing in recent years (Figure 29).

The results of a recent semi-quantitative vegetation survey on June 19, 2014, are shown in Figures 30, 31, and 32. *Chara* was again the dominant SAV taxa in the PSTA Cell during that wet-season survey (Figure 30). *Chara* was less common in the upstream Upper SAV Cell, where *Najas marina* was most prevalent. Other SAV species observed in the PSTA Cell include the vascular rooted macrophytes *Najas guadalupensis* and *Potamogeton illinoensis*, both of which are found in the inflow region of the PSTA Cell, and the outflow region of the Upper SAV Cell. *Utricularia foliosa* was moderately dense in the middle region of the PSTA Cell, just downstream of an area colonized by *Eleocharis cellulosa* (Figures 31 and 32). *Sagittaria lancifolia* and *Panicum* grasses were also observed at low densities in the PSTA Cell and Upper SAV Cell, while *Typha* was restricted to the Upper SAV Cell. Note that the surveys did not consider vegetation on the muck berms within the PSTA cell.

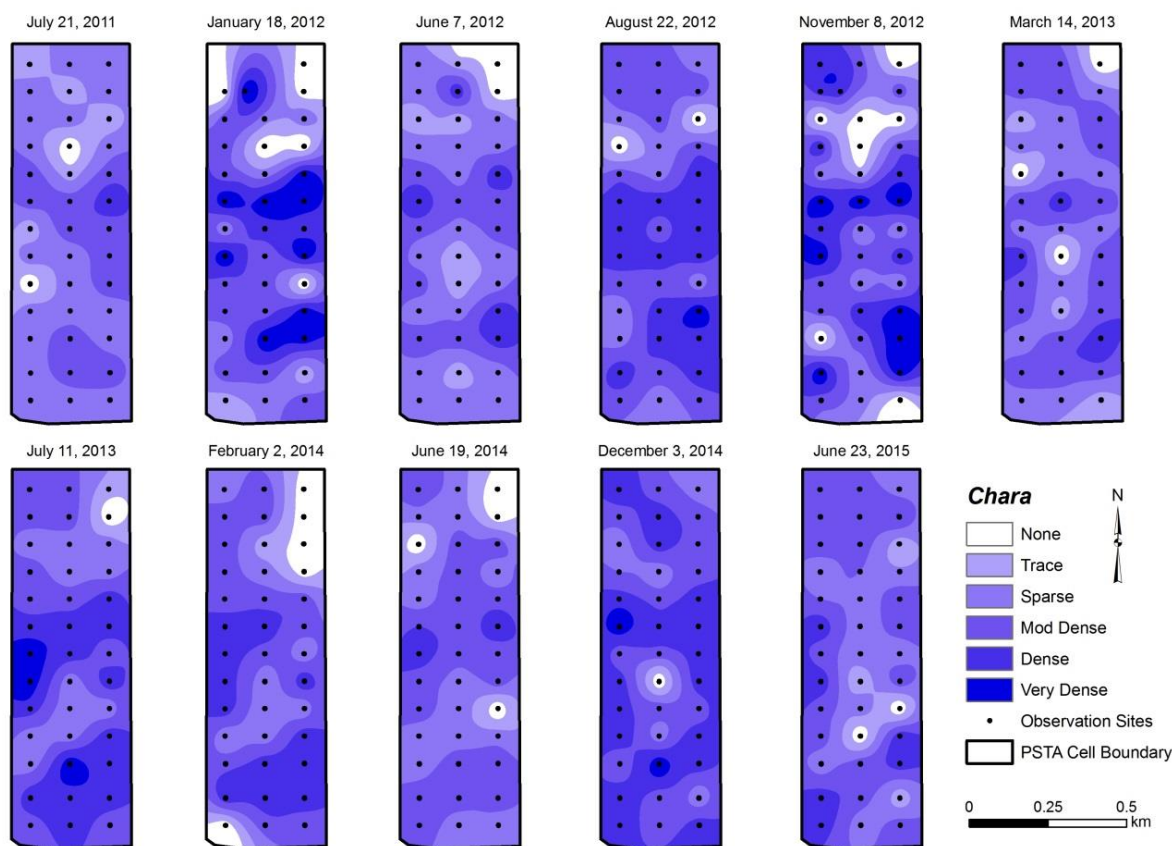


Figure 26. Relative density and distribution of *Chara* in the PSTA Cell for each of 111 semi-quantitative vegetation surveys between July 2011 and June 2015.

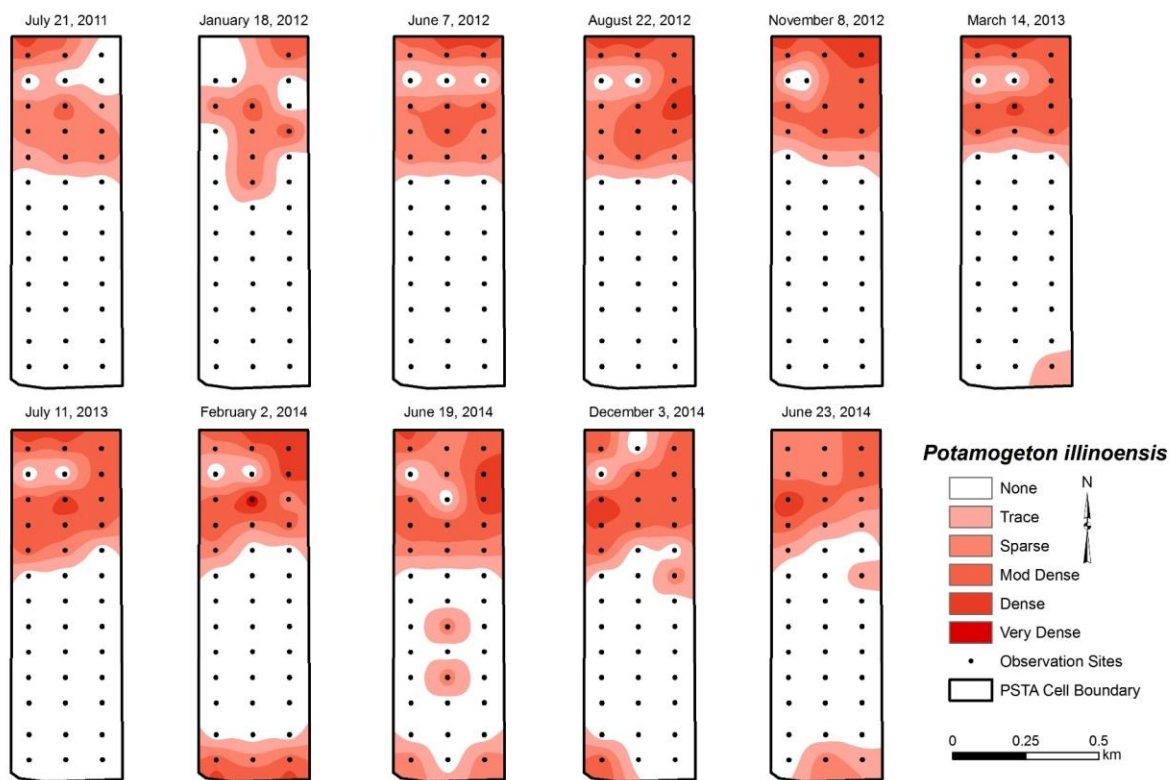


Figure 27. Relative density and distribution of *Potamogeton* in the PSTA Cell for each of 11 semi-quantitative vegetation surveys between July 2011 and June 2015.

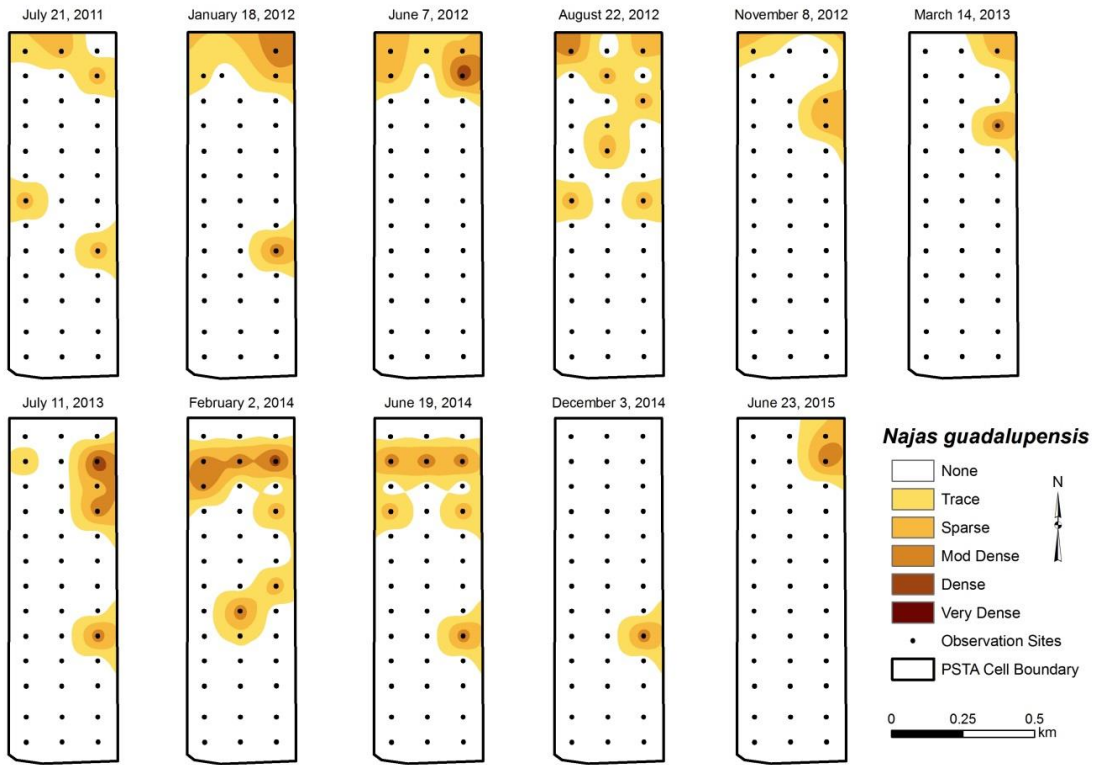


Figure 28. Relative density and distribution of *Najas guadalupensis* in the PSTA Cell for each of 11 semi-quantitative vegetation surveys between July 2011 and June 2015.

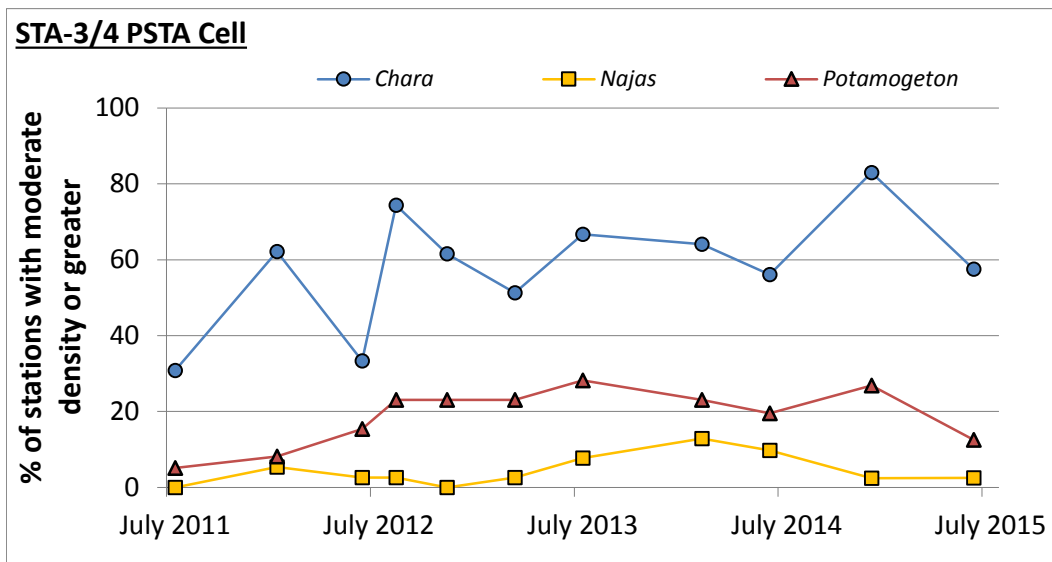


Figure 29. Percent cover of three SAV species (under moderately dense conditions, or greater) in the STA-3/4 PSTA Cell over time.

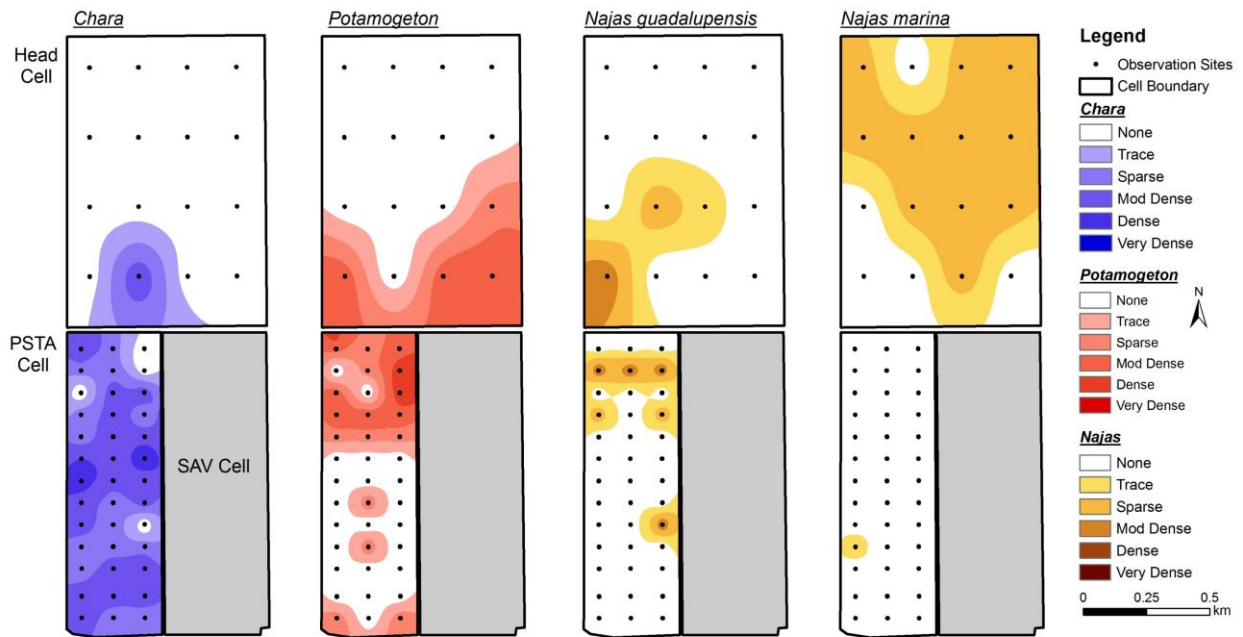


Figure 30. Density and distribution of submerged macrophyte species in the PSTA Cell and Upper SAV Cell (“Head Cell”) during a survey on June 19, 2014.

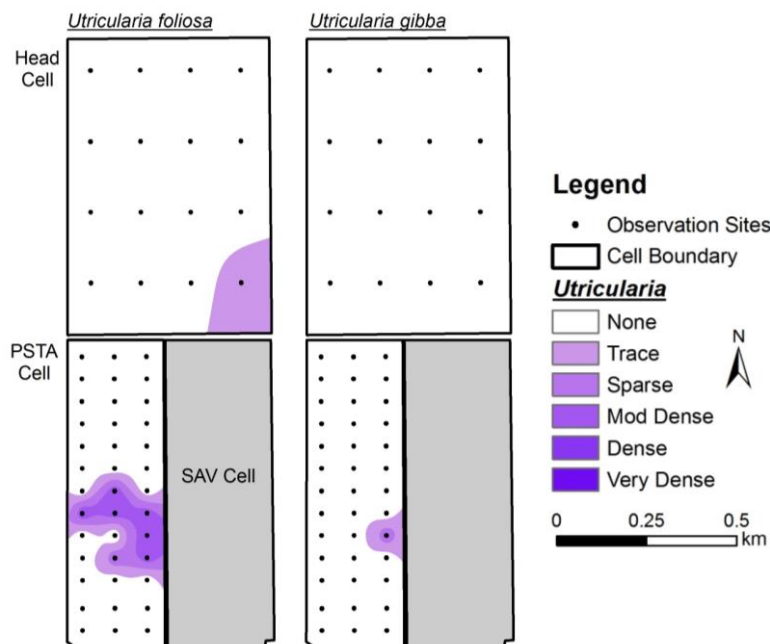


Figure 31. Density and distribution of *Utricularia* species in the PSTA Cell and Upper SAV Cell (“Head Cell”) during a survey on June 19, 2014.

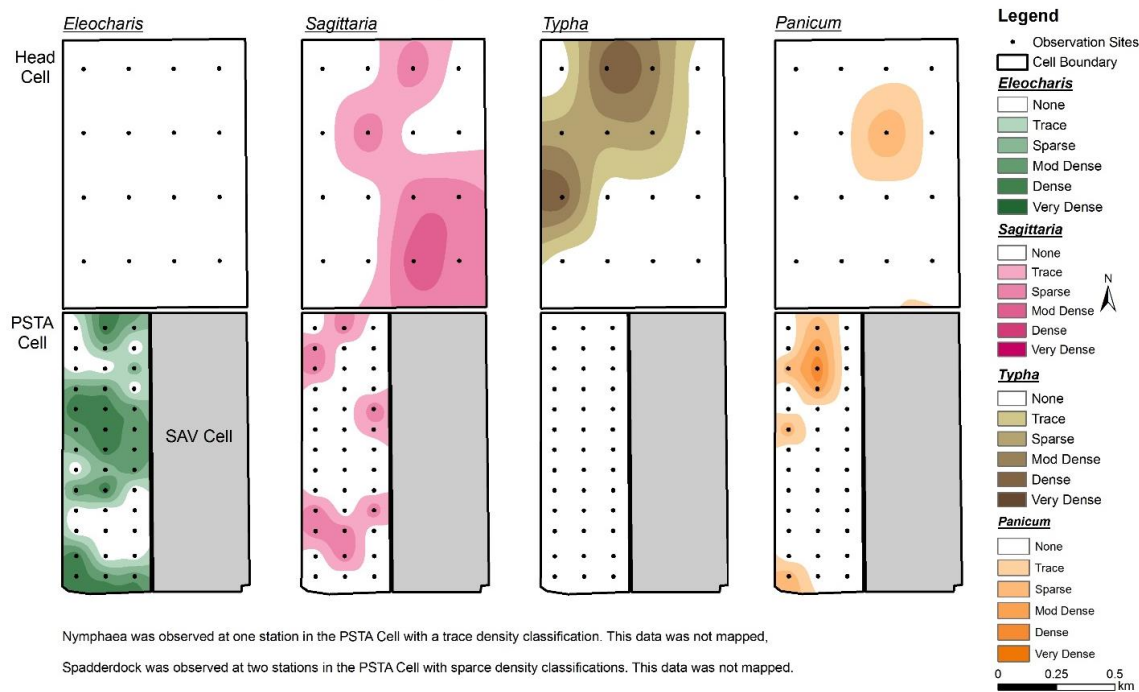


Figure 32. Density and distribution of emergent macrophyte species in the PSTA Cell and Upper SAV Cell (“Head Cell”) during a survey on June 19, 2014.

3.5.3.2 Macrophyte standing crop

Macrophyte standing crop biomass in the PSTA Cell ranged from 146-787 g dry wt./m² in July 2014, and 499 – 2119 g dry wt./m² in January 2014 (Table 6). These values are comparable to estimates of SAV biomass in the outflow region of STA-2 Cell 3, a muck based cell. In September 2005, SAV biomass in Cell 3 was 712 – 1325 g dry wt./m², and in January 2010 was 103 – 638 g dry wt./m², (DBE unpublished data). In STA -1W, average SAV biomass was between 53 and 636 g dry wt./m² (DBE 2002, Table 7). There was no trend observed in SAV biomass from inflow to outflow within the PSTA Cell (Figure 33).

3.5.3.3 Tissue P content

The macrophyte tissue P contents from PSTA Cell inflow, mid and outflow transect sampling on July 7, 2014, averaged 238 ± 54 mg/kg, 175 ± 14 mg/kg, and 243 ± 63 mg/kg, respectively. These P concentrations result in an estimated 0.04 – 0.20 g P/m², and a cell-wide average P storage of 0.11 g P/m² in the macrophyte tissues. These values were on the lower end of what has been observed during the prior two sampling events in the PSTA cell (Figure 34), or for the SAV beds in the outflow region of STA-1W Cells 3 and 4 (Table 7). Rather than P-enrichment over time, it appears that P contents of PSTA Cell SAV tissues are stable or even in decline (in the inflow region), relative to earlier surveys (Figure 35).

Table 6. Macrophyte standing crop estimated from replicate throws of a sampling frame (0.5 m x 0.5 m) at three stations along internal transects in the PSTA Cell, on July 7, 2014. Phosphorus (P) mass storage, total P and calcium concentrations, ash-free dry weight and % dry weight values are also shown.

	Station	Standing Crop Biomass	P Storage	TP	AFDW	Calcium	% Dry Wt
Average		g dry wt./m ²	g P/m ²	mg/kg	%	%	%
Inflow	B transect	146	0.04	238	44	20	9.0
Mid	G transect	787	0.20	175	36	23	9.8
Outflow	L transect	392	0.08	243	41	21	8.4

SE

Inflow	B transect	62	0.02	54	6	2.1	0.6
Mid	G transect	467	0.13	14	1	0.4	0.3
Outflow	L transect	258	0.05	63	5	1.7	0.5

Whole cell average		441	0.11	219	40	21	9.0
	SE	181	0.04	29	2.8	1.0	0.3

Table 7. Standing crop biomass and nutrient content of back-end SAV communities from a previous study in STA-1W (DBE 2002).

			Standing Crop Biomass		Tissue P		Tissue N	
			g/m ²		mg/kg		%	
			Avg	SE	Avg	SE	Avg	SE
STA 1W Cell 4 outflow	Winter 2002	Najas	636	146	1750	160	2.06	0.47
STA 1W Cell 4 outflow	Summer 2002	Najas	270	53	1180	160	2.21	0.2
STA 1W Cell 3 outflow	Winter 2002	Najas	53	20	1470	180	2.85	0.16
STA 1W Cell 3 outflow	Summer 2002	Najas	114	42	1180	130	1.90	0.17
STA 1W Cell 3 outflow	Winter 2002	Ceratophyllum	366	40	2660	240	2.11	0.35
STA 1W Cell 3 outflow	Summer 2002	Ceratophyllum	477	66	1050	150	1.40	0.17

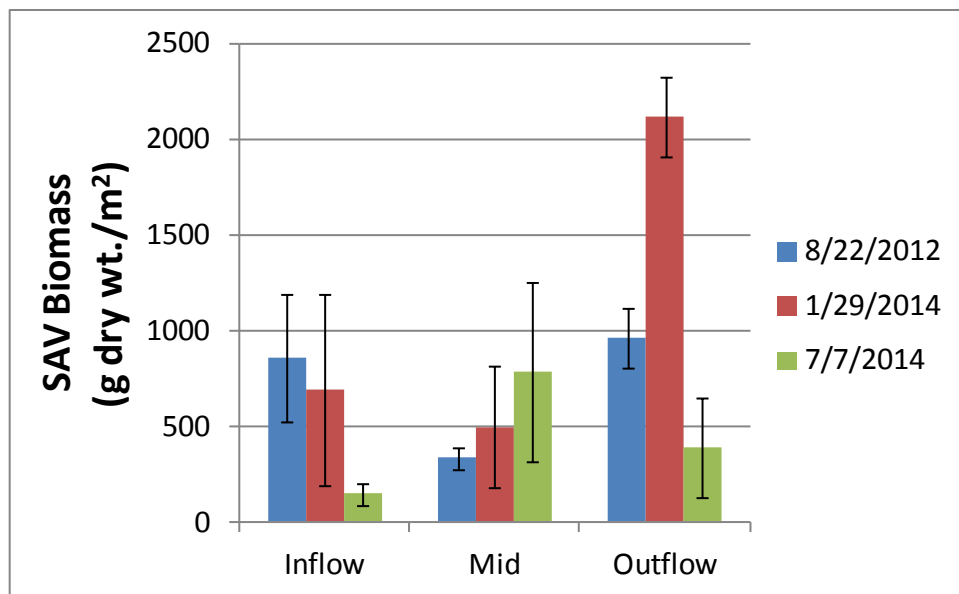


Figure 33. Comparison of SAV biomass along inflow, mid, and outflow transects through the PSTA Cell on 3 dates. Values represent the average of 3 stations per transect, and 3 samples per station. Error bars denote variability (\pm SE) among stations along each transect.

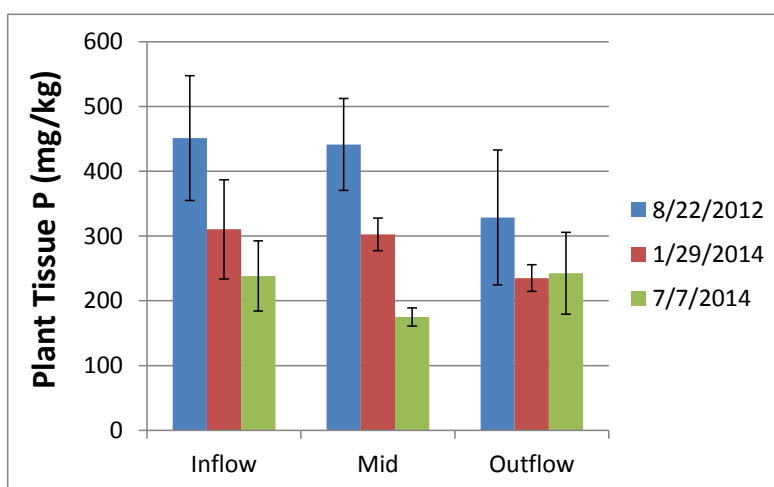


Figure 34. Changes in tissue P content over time along internal transects within the PSTA cell.

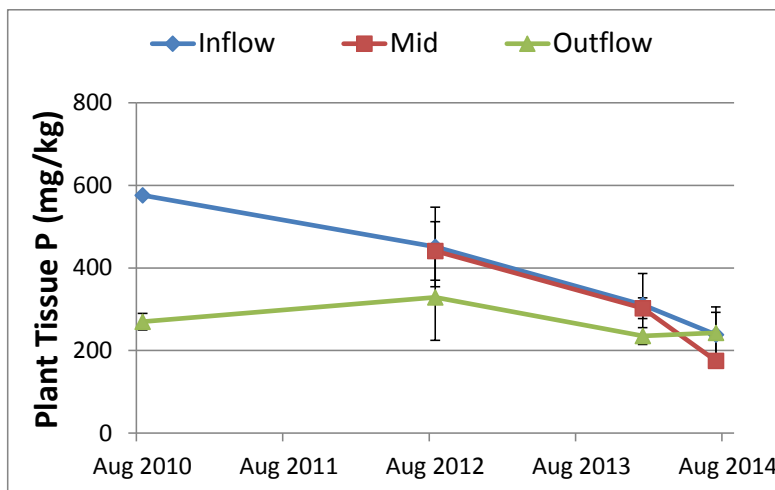


Figure 35. Recent plant tissue P concentrations are shown relative to an earlier sampling event in August 2010.

3.5.4 Discussion

The macrophyte species distribution in the STA-3/4 PSTA Cell appears stable over the period of record (POR), with *Chara* dominant but *Potamogeton* and *Najas* persistent. Standing crop biomass for the PSTA cell is within the range found for muck-based STA flow ways. However, SAV tissue P content in the PSTA Cell is low compared to muck-based cells. This can have important implications for nutrient cycling through the macrophyte vegetation and into the water column. Phosphorus can be acquired by macrophytes from either the water column or sediments, and continues in excess of nutritional requirements as “luxury” uptake so long as P is available. The low P contents observed for PSTA macrophytes indicate that P supply is strongly limited in this cell. A similar situation is apparent for nitrogen supply to SAV tissues. PSTA SAV tissues sampled in January 2014 averaged 1.07 ± 0.05 % N (data not shown), while N contents of SAV beds in STA-1W were 1.4 – 2.8 % N (Table 7).

A comparison of PSTA tissue P contents to SAV tissues from selected muck-based STA flow ways strongly suggests that muck soils increase P supply available to plants, which results in elevated SAV tissue P. Upon senescence, these SAV tissue likely decompose rapidly, potentially providing a source of P to the water column. SAV tissues are also important sources of nutrients to epiphytic algae and periphyton growth. Growth of P-sensitive periphyton communities may be constrained on P-enriched macrophytes. The macrophyte surveys described in this study did not identify turnover rates of SAV tissues in the PSTA Cell. However, our small-scale experiments (described later) examined growth rates and tissue P changes for *Chara* and *Potamogeton* exposed to PSTA sediments and muck soils from STA-2 Cell 3.

3.6 Periphyton

3.6.1 Introduction

Selected periphyton communities may enhance enzyme hydrolysis of DOP, and benefit from the high light environment in a shallow PSTA system with an inorganic, low-P substrate. In this section, we present recent findings on periphyton distribution, biomass, taxonomy, and P contents from the PSTA Cell. In a later section of this report, we describe an on-going experiment to better quantify the relationships between water depth, periphyton development, and P removal performance.

3.6.1.1 **Periphyton standing crop estimates in the Everglades**

Mean biomass in periphyton-dominated areas of the southern Everglades was 1517 g AFDW/m², with a mean total P content of 137 mg/kg, and N:P ratio of 192:1 (Iwaneic et al., 2006). Across the Everglades landscape, periphyton biomass can be as high as 2500 g AFDW/m² (Wood and Maynard 1974, Browder et al. 1982, as cited in McCormick and Scinto 1998). Periphyton mats comprise >50% of organic biomass in some areas of the Everglades (Wood and Maynard, 1974; Gaiser et al., 2006, as cited in Iwaneic et al., 2006). In these low-P areas of the Everglades, periphyton (specifically calcareous periphyton) is clearly an important component of the biological community. However, less is known of the community that develops in a full-scale PSTA system periodically exposed to pulsed flows containing TP concentrations in the 20 - 35 µg/L range. It has been previously reported that periphyton biomass decreases with P additions (e.g., Craft et al., 1995; McCormick et al., 2001). It therefore is important to understand whether healthy stands of calcareous periphyton can be sustained in PSTA treatment systems, which typically would be situated at the outflow of a STA muck-based SAV cell.

3.6.1.2 **Periphyton Communities in the STA-3/4 PSTA Cell**

Periphyton has been found in the STA-3/4 PSTA cell on a variety of substrates other than the sediment surface, including both SAV (*Chara*, *Potamogeton*; Figure 36) and emergent vegetation (*Eleocharis*, *Sagittaria lancifolia*, *Panicum* sp.). Artificial substrates also have been utilized to support direct comparisons between inflow, middle and outflow regions of the PSTA Cell.

3.6.2 Periphyton on Natural Substrates

3.6.2.1 **Methods**

On five occasions between August 2013 and February 2015, during both wet and dry seasons, samples of periphyton growing on naturally occurring substrates (e.g., macrophyte tissues) were collected at inflow, middle and outflow stations in the PSTA cell and analyzed for nutrient contents. On three occasions (August 2013, January 2014 and June 2015), the areal biomass was determined by scraping the periphyton from a known area of the host plant tissue, then drying the recovered material to a constant weight. In order to normalize potential effects of host plant, we focused on periphyton growing on *Chara*, the dominant macrophyte in the PSTA Cell. However, on several other dates, periphyton was collected from a variety of macrophytes to evaluate potential influence of host plant on periphyton P contents.

Wet season sampling of the periphyton on macrophyte hosts was conducted in July 2014, in conjunction with the SAV standing crop biomass determinations. Macrophyte and periphyton tissues were analyzed separately. During the dry season sampling (January 2, 2014), both the scraped periphyton and the host tissue-periphyton complex were analyzed for nutrient contents (TP, TN, TC, TOC, TCa, and Ash-free dry-weight). Samples from the previous wet season sampling event (August 8, 2013) were analyzed as the scraped periphyton only.



Figure 36. Periphyton growth on *Chara* in the PSTA Cell.

3.6.2.2 Results

On August 8, 2013, the wet season biomass of periphyton on *Chara* tissues in the PSTA Cell ranged from 7.5 to 31 mg/cm², much lower than 106 - 170 mg/cm² observed on January 2, 2014 during the dry season (Figure 37). Differences in tissue nutrient (TP and TN) contents of the periphyton between these two periods were not as marked (Figures 38 and 39).

Across all substrates sampled in January 2014, TP in periphyton ranged from 97 - 195 mg/kg (Table 8). Periphyton N content (0.65 - 1.34 %) and TOC content (9.0 - 22.3 %) also varied ~two-fold across available substrates. The variation in organic matter content of the periphyton (as estimated by either TOC or AFDW) was largely determined by the degree of calcium-enrichment of the periphyton matrix ($r^2 = 0.82$ for TOC; $r^2 = 0.56$ for AFDW).

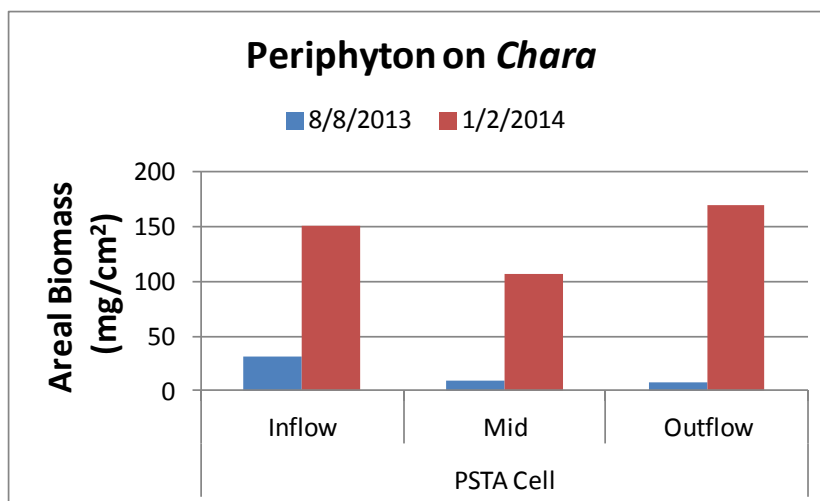


Figure 37. Areal biomass of epiphytes growing on *Chara* tissues in the PSTA Cell, on two sampling dates.

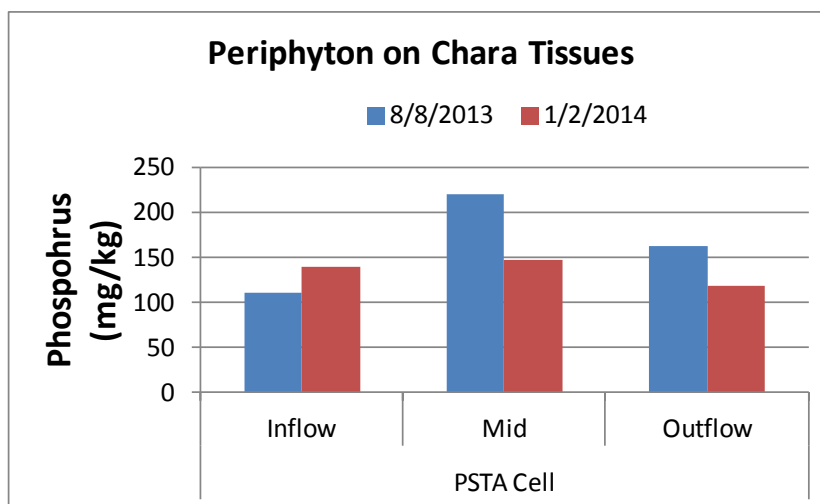


Figure 38. Phosphorus content of periphyton growing on *Chara* tissues in the PSTA Cell, on two sampling dates. Values represent individual grab samples.

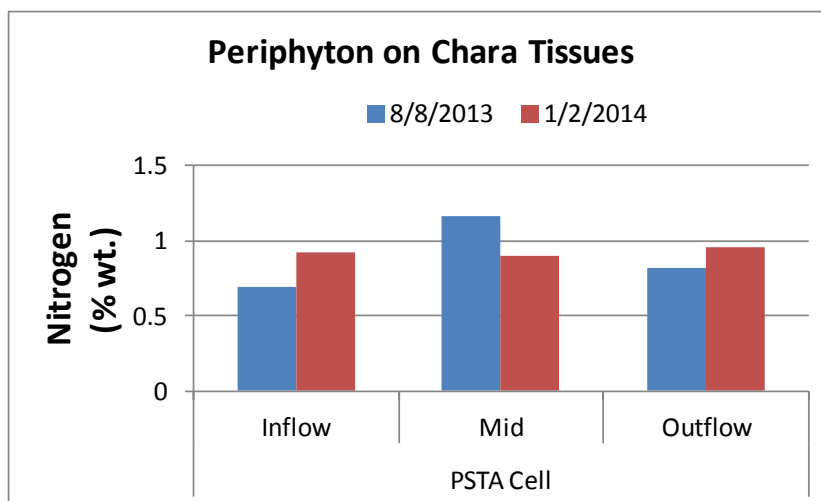


Figure 39. Nitrogen content of periphyton growing on *Chara* tissues in the PSTA Cell, on two sampling dates. Values represent individual grab samples.

Table 8. Chemical composition of periphyton grown on naturally-occurring substrates in the PSTA Cell on two dates. n.d = not determined.

	Station	Substrate	TP (mg/kg)	TN %	TC %	TOC %	AFDW %	Total Ca %	Areal Biomass (mg/cm ²)
Wet Season August 8, 2013	PSTA A-2	Potamogeton	98	0.58	17.4	7.9	16.1	29.3	13
	PSTA B-2	Chara	111	0.70	17.2	8.1	18.6	28.6	31
		Eleocharis	95	0.85	20.1	11.5	26.6	26.1	25
	PSTAG-2	Chara	219	1.16	20.0	12.7	29.4	22.0	10
		Eleocharis	182	1.23	21.8	14.7	34.1	22.0	12
	PSTA H-1	Chara	98	0.76	18.7	10.0	22.6	27.0	41
		Eleocharis	145	1.09	21.9	14.0	32.1	24.0	4.5
	PSTA L-2	Chara	162	0.83	19.6	11.3	25.3	26.0	7.5
		Sagittaria	247	1.26	21.5	14.4	34.0	22.0	4.4
	Dry Season January 2, 2014	PSTA B-2	Chara	139	0.92	19.8	11.4	28.5	24.7
Eleocharis			132	0.98	22.9	15.7	35.3	21.0	8.8
Floating			184	1.16	20.2	12.1	28.1	25.4	n.d.
Panicum			126	0.96	20.3	15.9	30.3	24.3	21
Potamogeton			97	0.65	18.0	9.0	22.1	28.2	15
Sagittaria			127	0.92	23.0	15.3	34.5	21.3	9.6
PSTAG-2		Chara	147	0.90	20.0	11.8	29.1	24.0	106
		Eleocharis	195	1.28	24.1	17.8	35.1	n.d.	7.9
		Floating	118	0.81	20.1	11.6	28.2	25.6	n.d.
		Sagittaria	168	1.07	21.7	14.2	39.6	22.1	9.7
PSTA L-2		Chara	118	0.96	21.1	13.5	32.0	24.0	170
		Eleocharis	124	1.34	27.4	22.3	32.8	18.0	27
		Floating	121	0.80	20.2	11.6	28.3	25.8	n.d.
		Floating	110	0.87	21.6	14.3	33.7	24.1	48

In our most recent (June 2015) periphyton sampling effort, loosely attached, or “easily-dislodged” epiphyte biomass comprised between 15 and 58% of the total weight of macrophyte + periphyton matrix at the nine sites surveyed. The epiphytic periphyton tissue P content was between 242 and 694 mg/kg, with an average of 412 mg/kg. Together, these values provide an estimate of 64 ± 14 mg P/m² in the easily dislodged periphyton biomass.

The periphyton tissues were P-enriched, relative to the host macrophyte tissues in June 2015 (Figure 40). This pattern was also observed in a previous sampling event in July 2014 (Figure 40). In contrast to that earlier event, however, there was a marked gradient in the P content of both periphyton and plant tissue P contents in June 2015, from inflow to outflow within the PSTA Cell. This may reflect the relatively high P content of the *Potamogeton* and *Najas* tissues sampled in the inflow region but not along either the middle or outflow transects in June 2015, due to the presence of *Chara* at these latter sites. It may also reflect the fact that an inflow-to-outflow gradient in tissue P is finally becoming established in the PSTA cell, following 7 years of operation.

Calcium and organic carbon contents of macrophyte tissues were inversely related (Figure 41). Nitrogen contents of the two rooted SAV species were higher than *Chara* (a rootless macroalgae)

or *Utricularia*, suggesting a link between soil N availability and tissue nutrients. By contrast, the emergent rush, *Eleocharis cellulosa*, was low in P, N and especially Ca contents, compared to other rooted macrophytes, and higher in organic carbon (Figure 41).

Epiphytes associated with these macrophyte taxa exhibited composition differences, ostensibly related to the host macrophyte. The epiphytes associated with *Najas* had elevated N and P contents relative to epiphytes on other host plants (Figure 42). *Potamogeton* epiphytes contained comparably high calcium contents to the epiphytes on *Chara*, despite the latter having ~2.5 times the calcium associated with the host plant tissues.

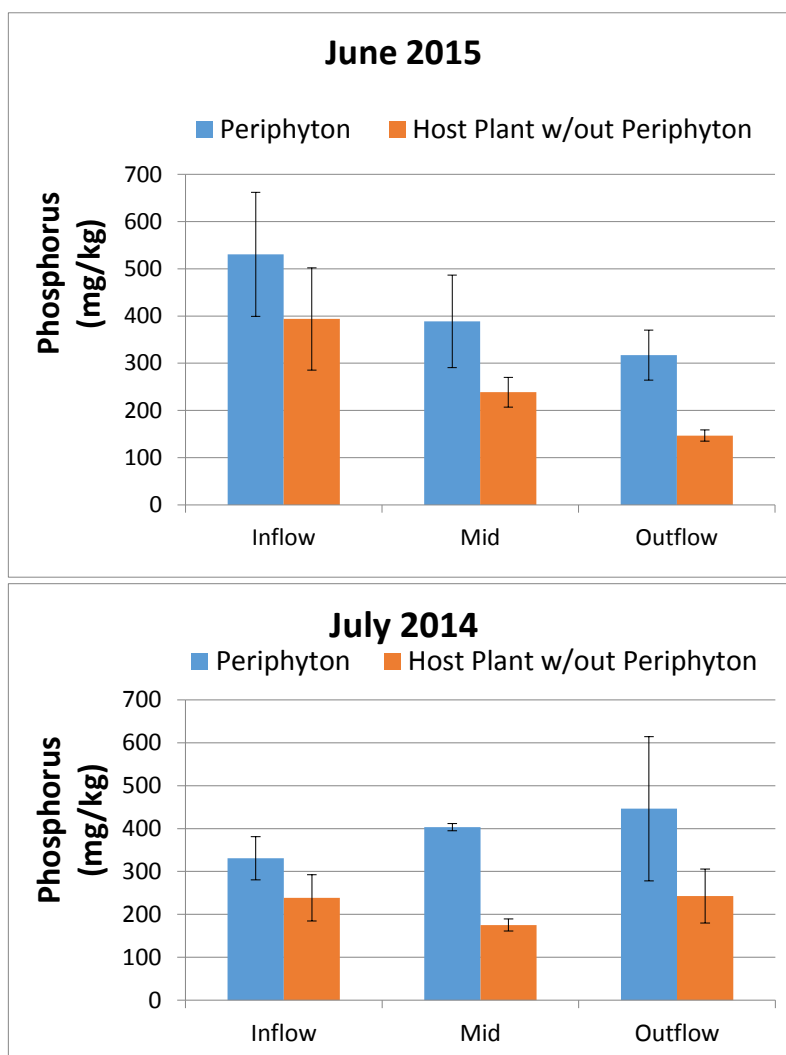


Figure 40. Phosphorus content of periphyton and its associated host macrophyte, along three internal transects within the PSTA Cell, in 2015 (top) and 2015 (bottom).

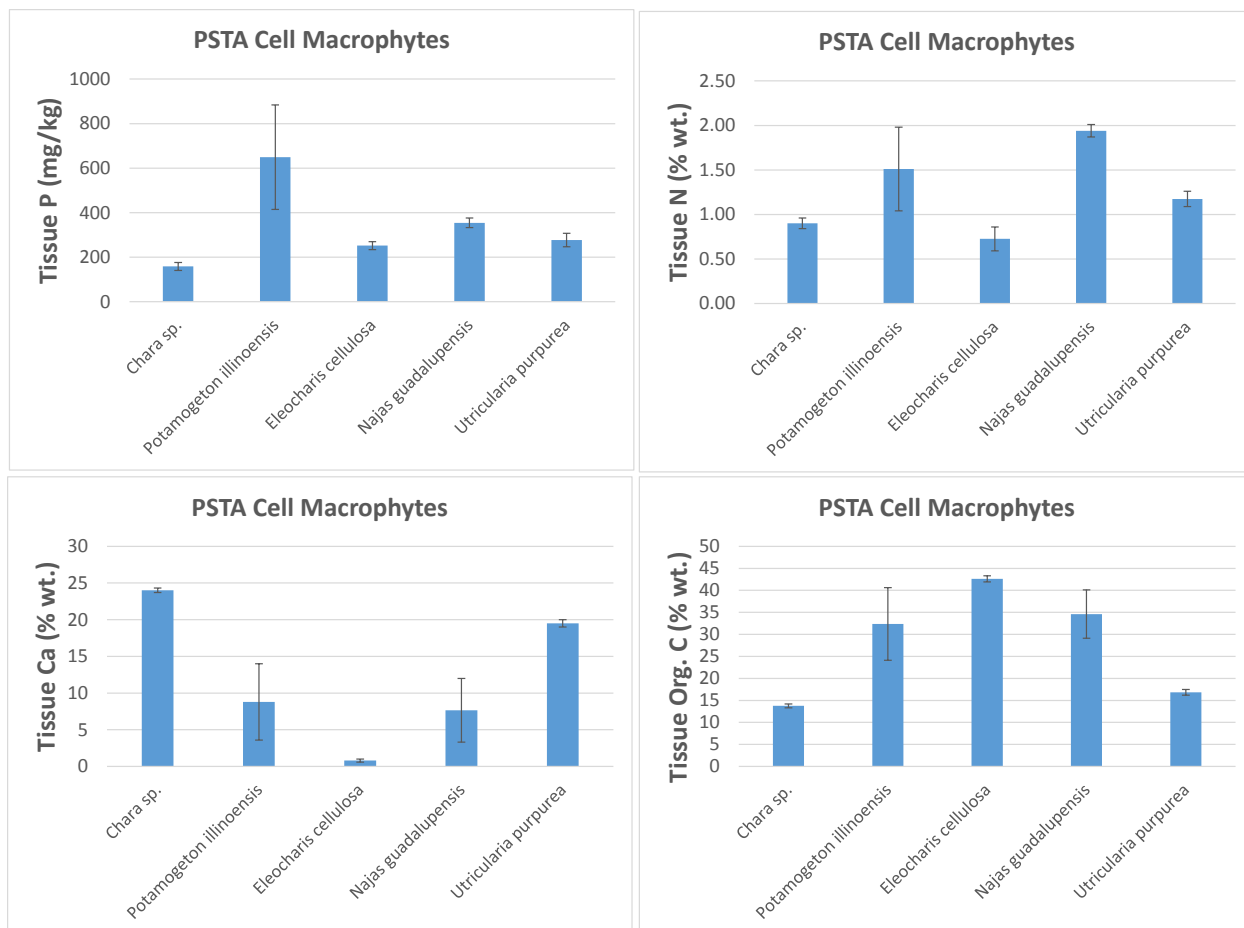


Figure 41. Comparison of tissue composition of five macrophyte species found within the PSTA Cell on June 24, 2015. Error bars denote the standard error around the mean value for 2-7 samples per species.

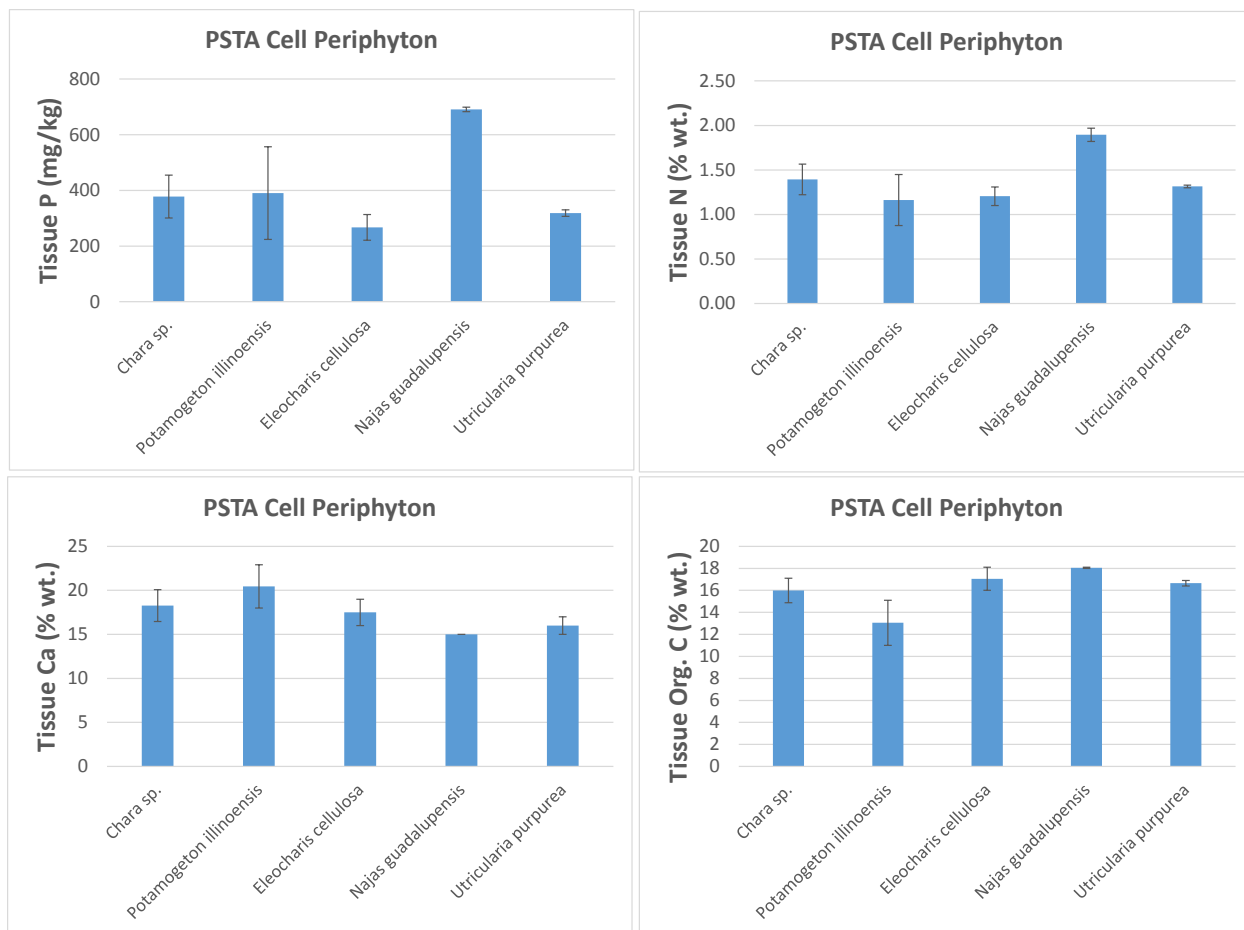


Figure 42. Comparison of the nutrient composition of periphyton tissues associated with five macrophyte species found within the PSTA Cell on June 24, 2015. Error bars denote the standard error around the mean value for 2-7 samples per species.

As noted above, differences in host plant tissue chemistry and morphology may influence the nutrient status of periphyton growing on the plant surfaces. To provide a common basis for comparison, the phosphorus contents of periphyton on *Chara* within the PSTA Cell were assessed for five sampling dates (Figure 43). Results of the most recent three dates represent the average of 2-3 samples of periphyton on *Chara* per transect, while the results from earlier surveys represent a single grab sample along each of the three transects. These data show high variability in P content of the periphyton associated with *Chara* in the PSTA Cell, with higher values in July 2014 and June 2015 than the other three dates (Figure 43). These data also suggest that the periphyton may be becoming gradually enriched over time, particularly in the inflow and mid region of the PSTA cell. Additional epiphytic periphyton sampling therefore will be performed in FY 2016 to better characterize this temporal trend.

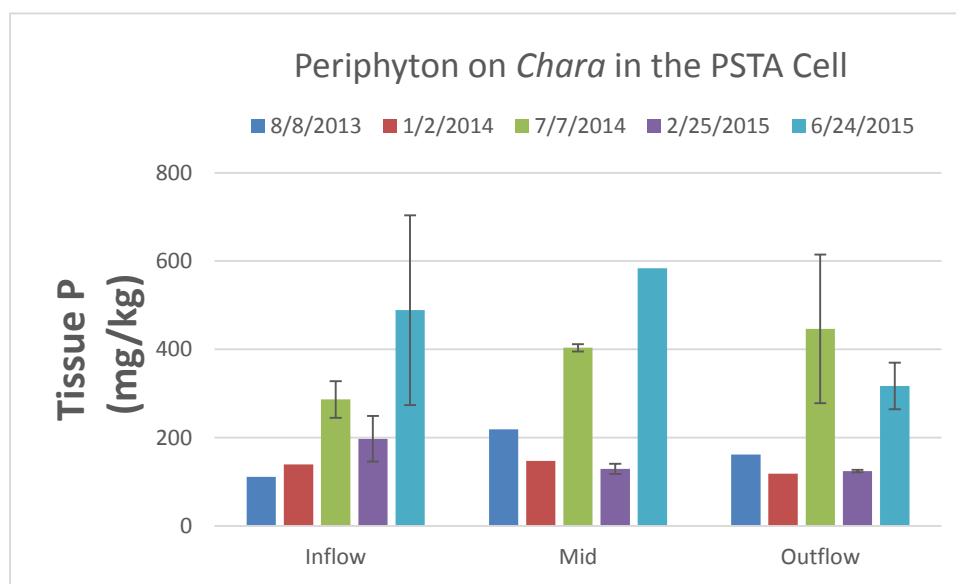


Figure 43. Phosphorus concentrations of periphyton associated with *Chara* along inflow, mid and outflow transects within the PSTA Cell, on five dates between August 2013 and June 2015.

3.6.3 Periphyton on Artificial Substrates: Glass Slide Periphytometers

3.6.3.1 Methods

Periphyton samples were also collected from artificial substrates (i.e., glass slides in periphytometers) deployed in the PSTA Cell. At each station and sampling interval, replicate slide pairs were sampled for areal biomass and nutrient content (TP, TN, TC, TOC, TCa, ash-free dry-weight). Deployments typically were six weeks long, with subsamples collected at two-week intervals. Additional slides were composited, homogenized, then split for Chlorophyll a, enzyme activity, and taxonomic analyses. Data are presented for three periods: August 2013 (wet season), January 2014 (dry season) and summer 2014 (flow pulse). The wet and dry season deployments are compared in terms of areal biomass growth and nutrient contents. For the flow pulse, periphytometers were deployed May 20, 2014, and then slide periphyton samples were collected before and after a 3-day pulsed flow event in the PSTA cell, about 30 days after deployment.

The duration of exposure can influence results when periphytometers are used to estimate biomass growth. Low nutrient environments such as the PSTA cell can require lengthy deployments to allow biofilm development, but sloughing, herbivory and disturbance from wildlife are all more likely to occur during extended deployments. Glass slide periphytometers have been used previously in Everglades research (McCormick et al. 1996). Using an 8-week exposure period, that study identified the diatom, *Mastogloia smithii*, as a key indicator of the oligotrophic conditions found within the interior of WCA2A, where surface water TP concentrations averaged between 8 and 11 $\mu\text{g}/\text{L}$. Another periphytometer study used Plexiglas slides and a 2-month deployment period to determine periphyton response to P dosing with *in situ* channels in WCA 2A (Katovsky et al. 2008). In our study, repeated sampling at each station provided an assessment of biomass accrual and nutrient accumulation over time, although the biofilm development after 2 and 4 weeks was minimal in some cases, especially in the winter (dry season) sampling period (January 2014).

It should be noted that our initial approach to periphyton monitoring with artificial substrates entailed placement of slides and attached periphyton biofilms into site water for transport to the lab. This approach has been used in previous work with Everglades periphyton, though this detail is not provided for all studies in the literature. After review of the tissue nutrient data for deployments in the summer of 2013 and winter of 2014, it became apparent that the low algal biomass grown on slides, together with high dissolved solids content of the surface waters, could potentially bias results of periphyton samples placed in site water for transport to the lab. Our approach was modified so that slides were dedicated to samples and assigned to dry weight and nutrient analysis (transported in DI water) or enzyme assays, chlorophyll a determination and taxonomic identifications (transported in site water), starting with the summer 2014 (pulse event) deployment.

3.6.3.2 Results

3.6.3.2.1 Areal biomass and growth rates

Periphyton development on glass slides in the PSTA cell resulted in standing crops as high as 3.83 mg dry weight/cm². This high biomass was observed August 8, 2013, at site G-2 at the end of a 6-week deployment (Figures 44 and 45). A comparison of the range of standing crop values from this study to work in other ultra-low P environments is provided in Table 9. Areal standing crop biomass values for the glass slide periphytometers in the present study were greater than reported for 8-week deployments in the Everglades National Park, but lower than values reported on natural substrates in both this study and others (Table 9). The peak standing crop noted above (for our 6-week deployment) is equivalent to a periphyton growth rate of 0.91 g dry matter/m²/day. By contrast, periphyton growth during January 2014 was low, between 0.04 and 0.12 g/m²/day. Extrapolation of these observed algal growth rates on periphytometer slides to the entire treatment area in the PSTA cell may now be possible, using the standing biomass estimates of potential substrates, spatial coverage estimates, and periphyton growth per host tissue area and weight. However, this extension of the current analysis will be performed in the near future, and provided in a later report.



Figure 44. Periphytometers retrieved on August 8, 2013, from the middle of the PSTA Cell (Station G-2) after a 6-week deployment.

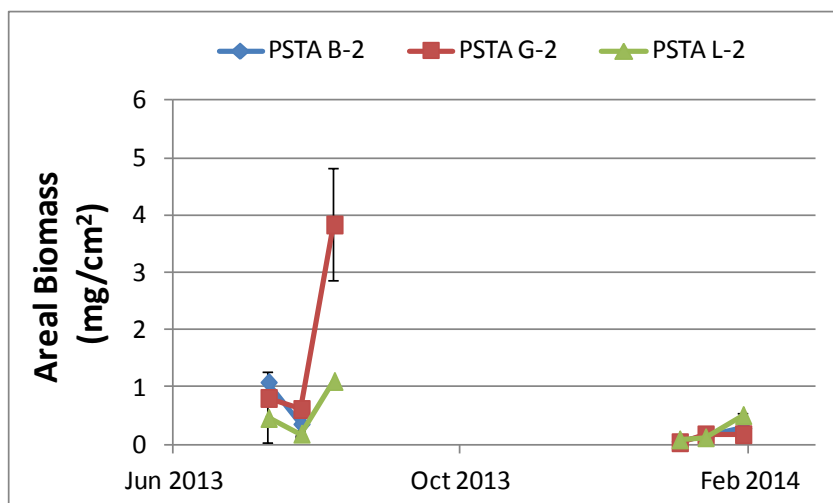


Figure 45. Areal biomass of slide periphyton after 2, 4, and 6 weeks of exposure to *in situ* conditions at three locations in the STA-3/4 PSTA Cell. Each data point is the average of 1-3 replicate measurements per date.

Table 9. Periphyton areal biomass estimates from this study and two similar studies conducted in the Everglades National Park (ENP) and Water Conservation Area (WCA) 2A.

Location	Areal Biomass (mg/cm²)	Sampling Method	Source
PSTA	0.17 - 3.8	Glass slides after 6 weeks	This Study
	4.4 - 170	Natural substrates	
ENP	0.13 - 0.15	Glass slides after 8 weeks	Childers et al. 2002
	20-30	Benthic mat	
un-enriched WCA 2A	5.8-11.8	Natural substrates	Vymazal and Richardson 1995

3.6.3.2.2 Nutrient Content of Slide Periphyton

Total phosphorus concentrations in periphyton from glass slides at the end of 6 weeks ranged from 117 - 376 mg/kg (Figure 46). This compared favorably with our measured nutrient contents for periphyton from natural substrates (Table 10). Gottlieb et al. (2006) found periphyton in short and long-hydroperiod marshes of Shark River Slough to contain on average, 172 and 107 mg P/kg, respectively. Our measured periphyton P contents were similar to the low end of the range reported for the interior of WCA 2A (Table 10). Nitrogen contents were lower in our study than those from WCA-2A, an oligotrophic wetland on muck substrates. Nutrient ratios for the slide periphyton samples showed consistent trends during the dry season

sampling with slightly higher ratios in periphyton from the outflow than the inflow region (Figure 47).

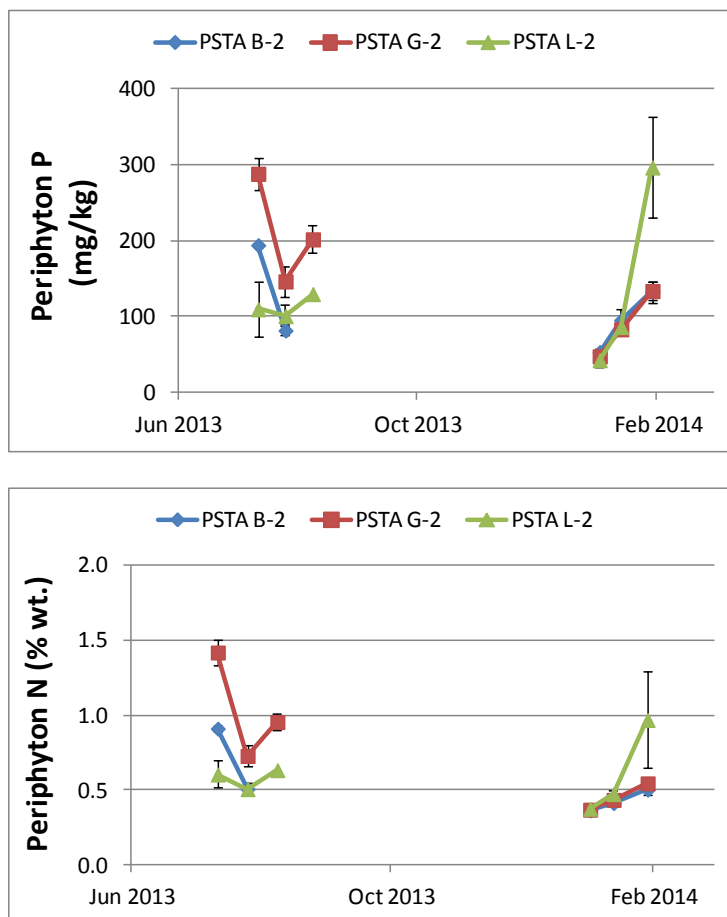


Figure 46. Change in nutrient content of periphyton growing on glass slides, during two 6-week deployment periods in summer 2013 and winter 2014. Error bars denote the standard error around the mean of triplicate samples at each sampling interval.

Table 10. A comparison of periphyton phosphorus and nitrogen contents from slides and natural substrates in this study, with estimates from the interior region of Water Conservation Area 2A.

Location	Phosphorus (mg/kg)	Nitrogen (% wt)	Source
PSTA	26 - 376	0.34 - 1.62	This Study, periphytometers
	95 - 247	0.65 - 1.34	This Study, grab samples
Interior WCA 2A	30 - 454	1.23 - 2.72	Vymazal and Richardson 1995
	60 - 490	1.12 - 3.01	Swift 1981, 1984
	100 - 940	0.99 - 3.57	Swift and Nicholas 1987
	104 - 289	1.1 - 2.3	Scinto and Reddy 2003

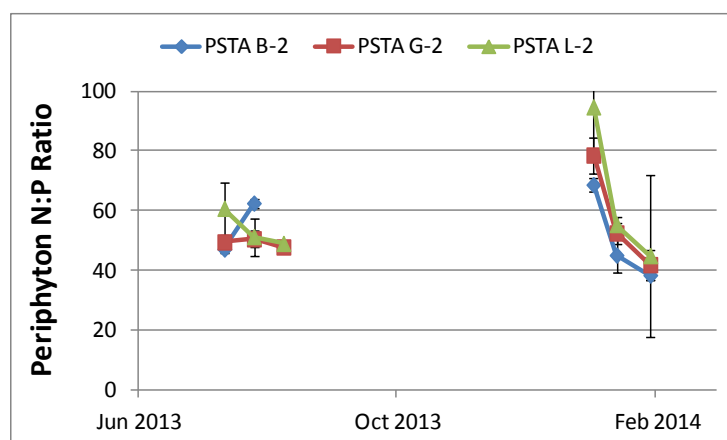


Figure 47. Nutrient ratios in the periphyton grown on glass slides in the PSTA cell.

3.6.3.2.3 Effect of flow pulsing on periphyton

Slide periphyton was sampled before and after the period of high flows (described earlier in this report) to examine P uptake potential by the periphyton community, as well as potential effects of the flow pulse on enzyme activity. In contrast to expectations, P contents were lower following the flow pulse, as compared to tissue levels prior to the pulse (Figure 48). Areal biomass of periphyton on glass slides was lowest in the middle region of the PSTA Cell on both dates, with little change between dates (Figure 49). A similar trend was found for chlorophyll a (Figure 50). The enzyme activity of periphyton scraped from the slides was high for all sites on both dates, with a slight increase in activity per unit dry weight in the outflow region, relative to inflow and middle regions of the PSTA Cell (Figure 51).

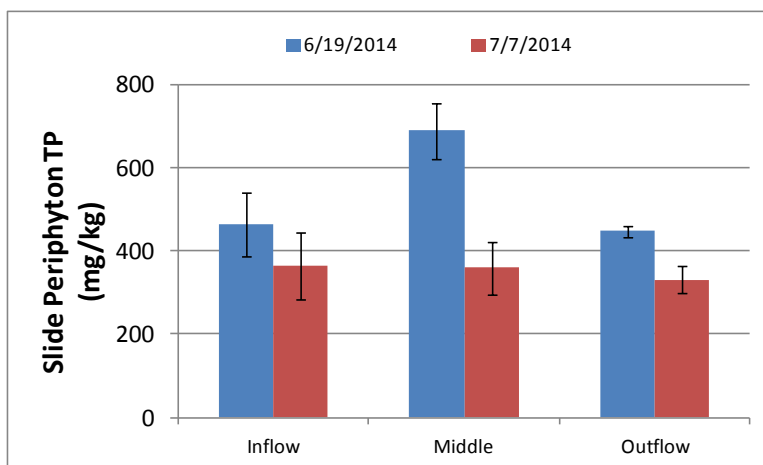


Figure 48. Tissue phosphorus contents in periphyton growing on glass slides, collected along internal transects within the PSTA Cell, on two dates before and after a flow pulse.

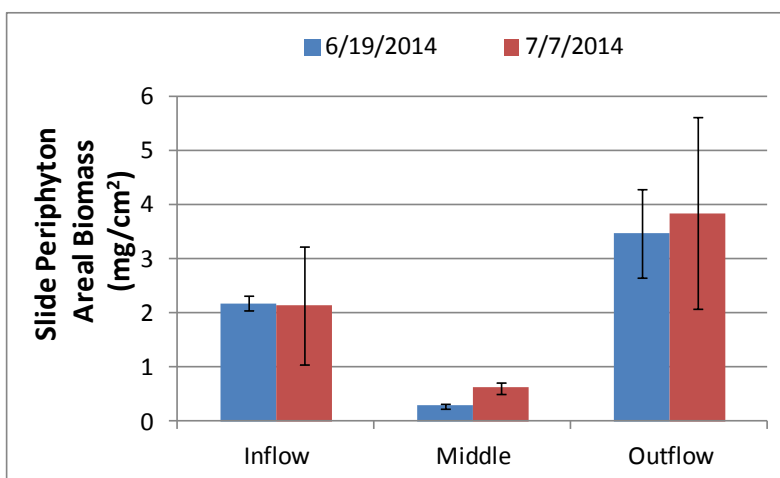


Figure 49. Areal biomass of periphyton grown on glass slides along transects internal to the PSTA Cell, before and after a flow pulse.

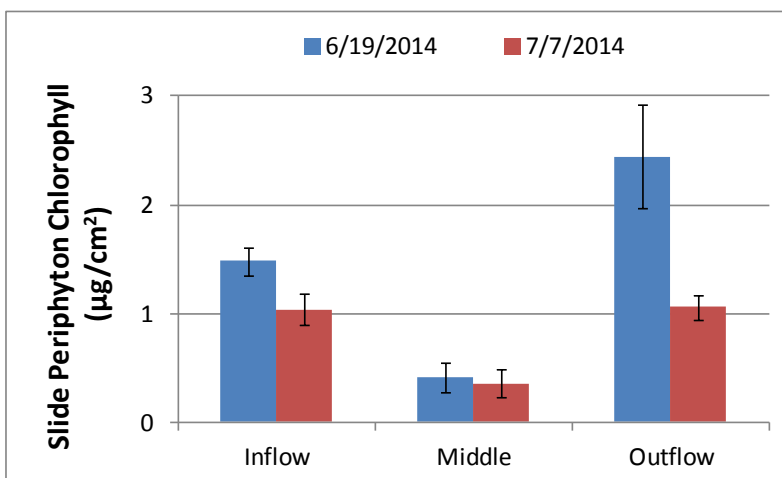


Figure 50. Chlorophyll a contents for periphyton grown on glass slides along transects internal to the PSTA Cell, before and after a flow pulse.

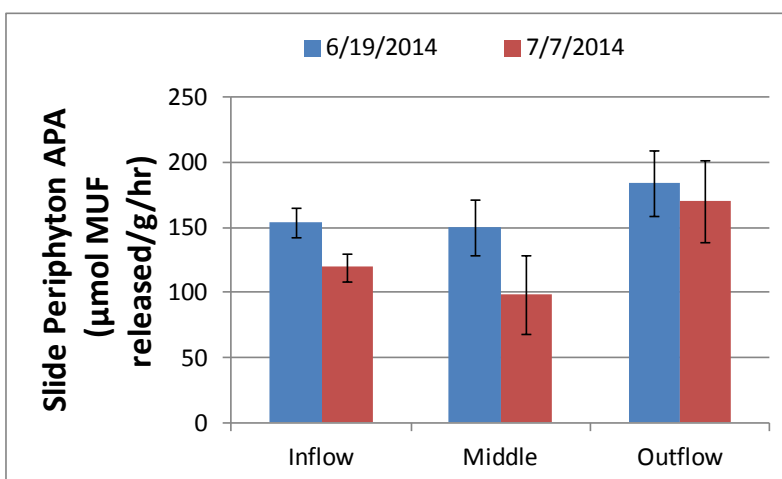


Figure 51. Monoesterase alkaline phosphatase activity (APA) of periphyton along transects internal to the PSTA Cell, before and after a flow pulse.

3.6.3.2.4 Enzyme Activity Associated with Periphyton

A variety of units are used to present both enzyme activity and periphyton growth. Slide periphyton chlorophyll levels were low at all three locations in the PSTA Cell (Figure 52). Areal biomass on a dry weight was similar across sites, while AFDW biomass suggested higher periphyton biomass in the inflow region, as compared to the outflow region. Enzyme activity was higher in assays of the inflow periphyton than outflow periphyton, when normalized to units of chlorophyll in the same sample.

Relative to epiphyte dry weight, enzyme activity in the dry season (January 2014) slide periphyton was higher at inflow and outflow stations than in the middle portion of the cell (Figure 52). This trend was also evident in periphyton on *Chara* sampled the same month (Figure 53). When the comparison between inflow, middle, and outflow regions of the cell is broadened to include all available periphyton substrates, enzyme activities per epiphyte dry weight showed a slight increase with distance through the cell, for both APA and PDE enzyme classes (Figure 54).

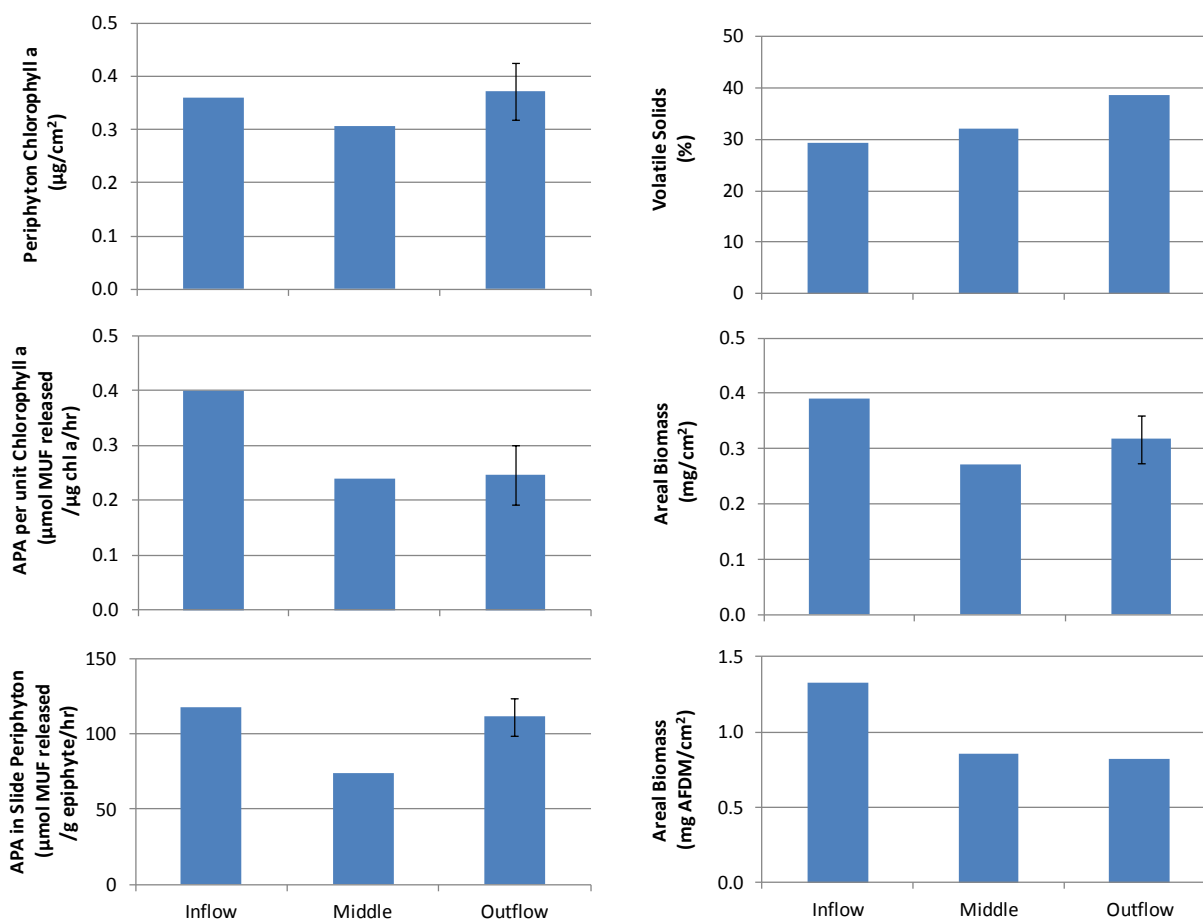


Figure 52. Alkaline phosphatase (monoesterase) activity (APA) associated with periphyton growing on glass slides on January 29, 2014. The error bars for the outflow station (L-2) denote \pm one standard error around the mean of three field replicates. All other values represent values from field composited samples.

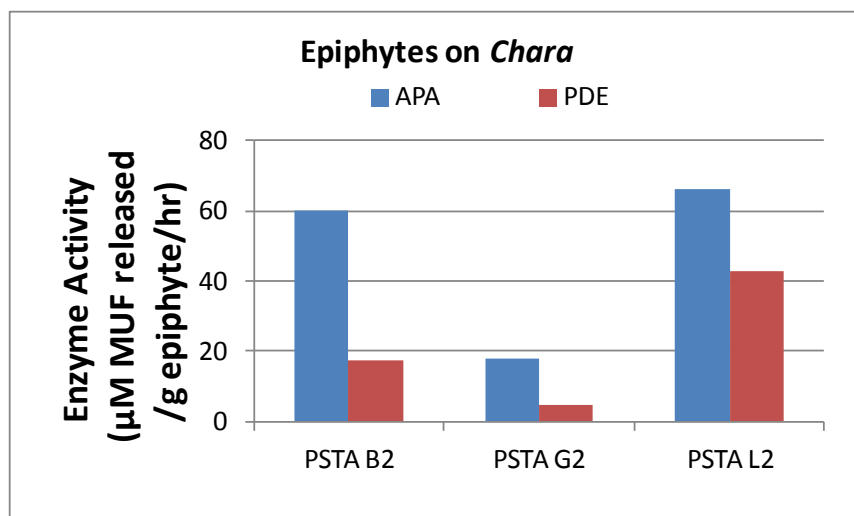


Figure 53. Enzyme activity associated with periphyton growing on *Chara* tissues on January 2, 2014. Values represent individual grab samples.

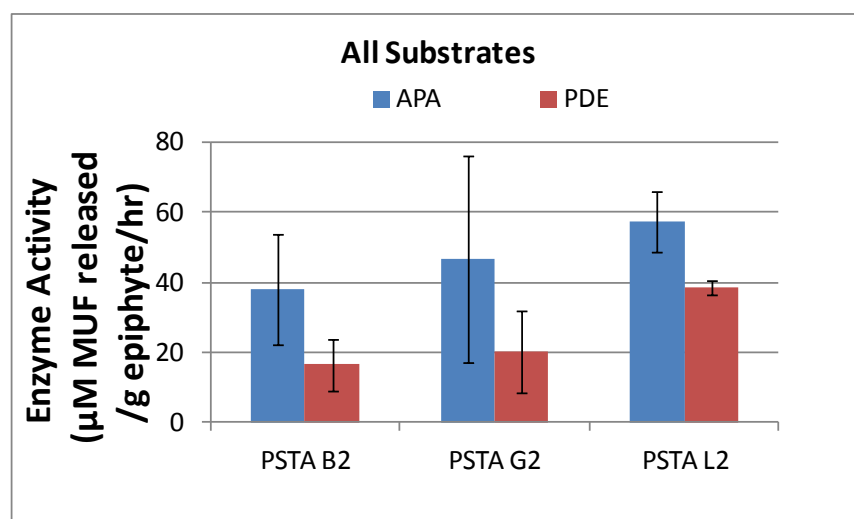


Figure 54. Enzyme activity of periphyton growing on a variety of naturally-occurring substrates in the PSTA Cell, on January 2, 2014. See Table 8 for substrate type and periphyton chemistry. Values represent the mean \pm SE from 3-5 grab samples per station.

3.6.4 Periphyton Taxonomy

Periphyton communities vary across the Everglades landscape, and have been previously reviewed by Browder, Gleason and Swift (1994) and more recently by Gaiser et al. (2011) and Hagerthey et al. (2011). In an STA setting, less is known about the species composition of periphyton. This is especially difficult to determine during short-term mesocosm studies, as diatom and bluegreen algae communities continue to mature over several months to years (Vymazal 2003). Thus, the long-term operation of the STA-3/4 PSTA Cell provides a unique opportunity to understand the periphyton community as it evolves in a constructed system. The effects of removing muck soils as an internal nutrient source may include the development of specific periphyton communities in the PSTA Cell, relative to other muck-based systems.

Based on previous work with Everglades periphyton, low-P communities are dominated by diatoms and blue green algae, with P-sensitive species such as *Cymbella minuta* and *Mastogloia smithii* present (See table 3-2 in McCormick et al., 2000). Assessment techniques using periphyton are not standardized, but artificial substrates allow for direct comparisons between different locations, or over time. A drawback to artificial substrates is that the periphyton communities are not fully represented on these substrates during short-term deployments. For this reason, periphyton samples in Porta-PSTA systems were collected from the mesocosm walls (CH2M-Hill 2003). However, there is still valuable insight to be gained by examining the diatom communities and other taxa that colonize uniform substrates (such as glass slides), during a known period of development. A combination of artificial substrates and grab samples of natural substrates is required to gain a complete representation of the communities present in the PSTA Cell. Community characteristics (species composition and relative biovolume) were determined for the PSTA Cell on several occasions to provide a basis for comparison with communities that develop in mesocosm-scale experiments, and with natural communities in low-P areas of the WCAs.

3.6.4.1 Methods

3.6.4.1.1 January 2014 (Dry Season)

On January 29, 2014, three grab samples of periphyton associated with macrophytes at stations B-2, G-2, and L-2 in the PSTA cell were examined for taxonomic characteristics (Figure 55). These were examined together with five samples from the periphytometer slides collected the same day: one composite each from stations B-2 and G-2, and triplicate composite samples from L-2. Glass slides had been deployed in periphytometers for 42 days.

3.6.4.1.2 June 19, 2014 (Wet Season)

Triplicate samples were obtained from the PSTA Cell at B-2, G-2, and L-2, using glass slide periphytometers deployed 30 days prior (May 20, 2014). This was slightly shorter than the dry season incubation period, because slides needed to be retrieved in advance of a managed flow pulse through the PSTA Cell during the end of June 2014.

Representative samples were preserved with formalin for later analysis. Periphyton community composition was classified by Klara Rehakova (Laboratory of Phytoplankton Ecology, Biological Centre of the Academy of Sciences of the Czech Republic). Each sample was examined to determine dominant species by biovolume. Relative dominance within the two major groups (diatoms and cyanobacteria) was also calculated separately. On a split sample, APA, chlorophyll a, areal biomass and AFDW were determined in conjunction with all periphyton taxonomic efforts.

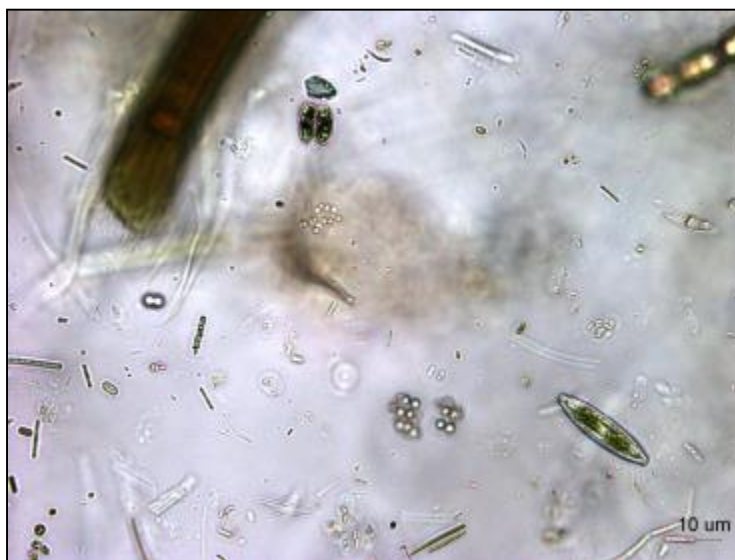


Figure 55. Periphyton assemblage from the STA-3/4 PSTA cell. Photo by Michael Hein (400X).

3.6.4.2 Results and Discussion

3.6.4.2.1 Dry Season (January 2014)

Diatoms and cyanobacteria made up 99% of the total periphyton biovolume, while chlorophytes and charophytes made up < 1% of the total biovolume for all samples.

Altogether, 62 individual taxa were identified across all dry season periphyton samples. The most abundant taxon was *Nitzschia linearis* (AG.) W.SMITH, a large diatom that was found in samples from the inflow and outflow stations, but absent from the middle portion of the cell, in both slide samples and grab samples (Figures 56 through 59). In the central portion of the cell, where senescent and living *Eleocharis* was prevalent, the dominant taxa were another diatom, *Amphora coffaeformis* (AG.) KUTZ, again found on both grab samples and glass slides. This species was found to respond negatively when TP concentrations were increased above the background in WCA2A P-dosing channels (Kastovsky et al., 2008). *Nitzschia linearis*, by contrast,

was shown in that study to reach greatest abundance at water TP concentrations between 10 and 30 $\mu\text{g/L}$.

Greater diversity was observed in grab samples (32 – 36 taxa/sample) than in slide periphyton (11-13 taxa/sample in middle and outflow-region samples; 22 taxa in the inflow slide composite sample). Among species found only in grab samples, *Scytonema* sp. 22 was an important cyanobacteria taxa reported to disappear or be substantially reduced in abundance by surface water TP concentrations > 10 $\mu\text{g/L}$ (Kastovsky et al., 2008). We observed this species in grab samples from the middle and outflow region of the cell, while another *Scytonema* (sp. 28) was found in the inflow region. Increased relative proportions of the cyanobacterium, *Chroococcus mipitanensis* (WOLOSZYNSKA) GEITLER (up to 23% of the total biovolume identified) was observed in the slide sample from the middle region of the PSTA Cell, where stems of senescent *Eleocharis* serve as the dominant naturally-occurring substrate (Table 11, Figure 56). In general, there was strong agreement between the replicate samples collected from the PSTA cell outflow region, with respect to relative abundance and community composition (Figures 56 and 57).

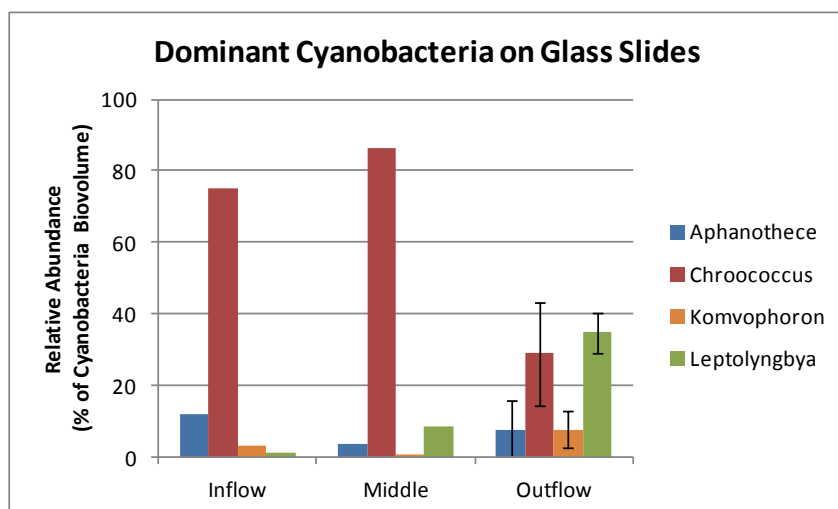


Figure 56. Relative abundance of the most dominant Cyanobacteria genera observed on glass slides retrieved January 29, 2014, after 6 weeks of deployment in the STA-3/4 PSTA Cell. Values represent composite samples from inflow and middle stations or mean \pm SE of three field replicate composites from the outflow region. Only genera with > 5% of the total cyanobacteria biovolume within a sample are shown.

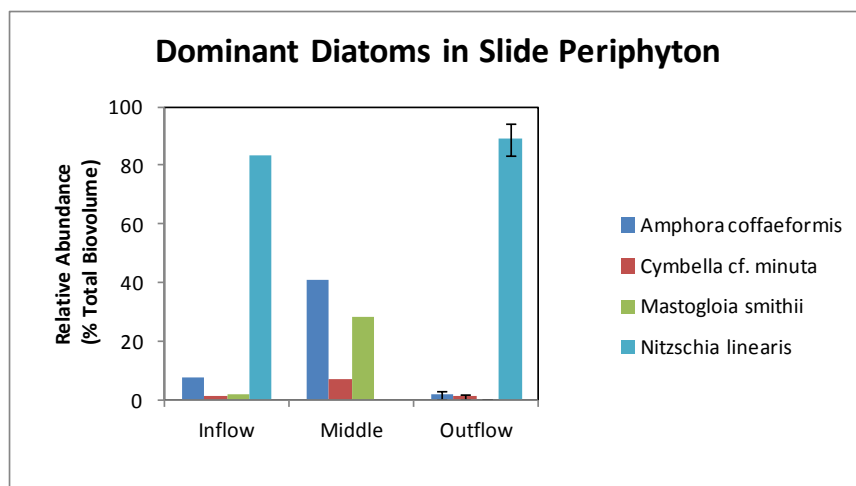


Figure 57. Relative abundance of dominant diatom species observed on glass slides retrieved January 29, 2014, after 6 weeks of deployment in the STA-3/4 PSTA Cell. Values represent composite samples from inflow and middle stations or mean \pm SE of three field replicate composites from the outflow region. Only taxa with $>$ 5% of the total biovolume within a sample are shown.

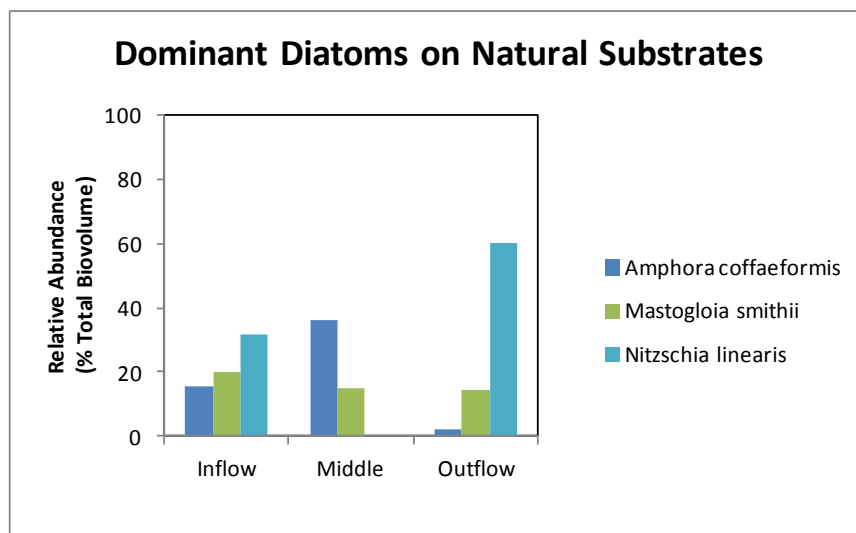


Figure 58. Relative dominance of three diatom species found in periphyton grown on natural substrates (*Chara* and *Eleocharis*), at three locations within the PSTA Cell. The values represent grab samples collected on January 29, 2014. Only diatom taxa with $>$ 5% of the total biovolume within a sample are shown.

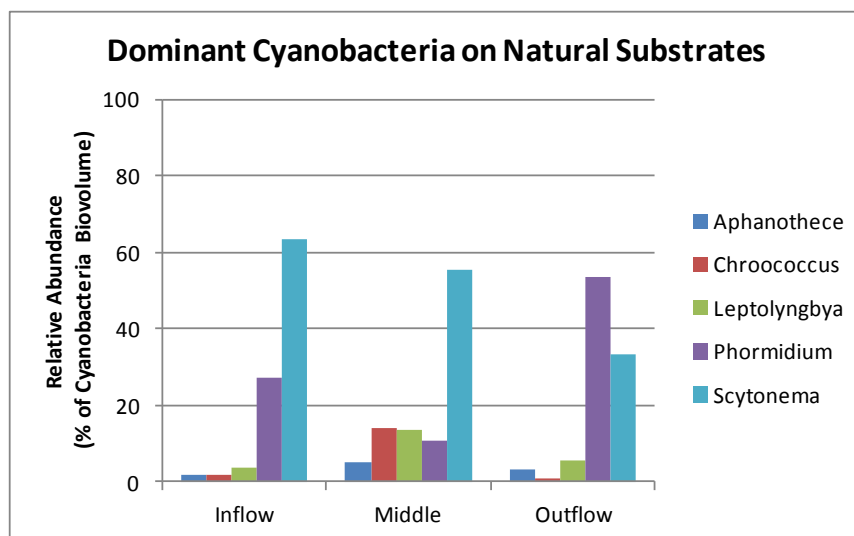


Figure 59. Relative dominance of cyanobacteria genera found in periphyton grown on natural substrates (*Chara* and *Eleocharis*), at three locations within the PSTA Cell. The values represent grab samples collected on January 29, 2014. Only genera with > 5% of the total cyanobacteria biovolume within a sample are shown.

Table 11. Relative dominance (%) of taxonomic groups in slide periphyton samples. Dominant groups within periphyton communities were determined from samples collected from glass slides after 6 weeks of deployment in the PSTA Cell.

	Inflow	Middle	Outflow
Slide Periphyton			
Diatoms	98.8	76.1	98.5
Charophyta	< 0.1	< 0.1	0.1
Chlorophyta	< 0.1	0.3	0.2
Cyanobacteria	1.2	23.5	1.2
Natural Substrates			
Diatoms	88.8	94.1	93.5
Charophyta	< 0.1	0.6	0.1
Chlorophyta	0.3	0.8	0.2
Cyanobacteria	10.9	4.5	6.2

3.6.4.2.2 Wet Season (June 2014)

Periphyton growing on glass slide periphytometers along inflow, middle and outflow transects were retrieved June 19, 2014 and analyzed for species composition, biovolume, and presence of indicator taxa. Between 11 and 26 taxa were identified in each sample, including 5-17 Cyanobacteria taxa and 3-9 diatom species per sample. Other groups represented in the samples were Charophytes (including the desmid *Cosmarium* sp.), Chlorophytes (e.g., the filamentous green algae, *Oedogonium* sp.), and the Dinoflagellate *Peridinium* sp.

Diatoms were the dominant group across all stations (92-95% by biovolume). *Mastogloia smithii* and *Cymbella minuta*, two diatom species that can indicate oligotrophic conditions (See table 3-2 in McCormick et al., 2000, McCormick et al., 1996), were found in 7 of 9 and 9 of 9 samples, respectively, and at all three stations in June 2014. *Nitzschia linearis* was also observed in all samples, and comprised 48 - 77 % of the total biovolume identified in the slide samples (Figure 60).

Cyanobacteria accounted for the second largest group, with 2.9 - 5.5% by biovolume. Among this group, *Aphanothece*, *Chroococcus*, and *Komvophoron* were found in all samples in June (Figure 61). Conspicuously absent from the species identified from glass slide samples in June was *Scytonema*, a cyanobacteria taxon that is known to dominate calcareous periphyton mats in oligotrophic regions of the Everglades. This taxon was identified in grab samples of periphyton mats in the PSTA Cell collected in January 2014, when *Scytonema* was as much as 47% of the total biovolume. However, slide samples collected at that time also did not contain *Scytonema*. Therefore, this potentially important taxon is apparently not well represented by glass slide periphytometer sampling.

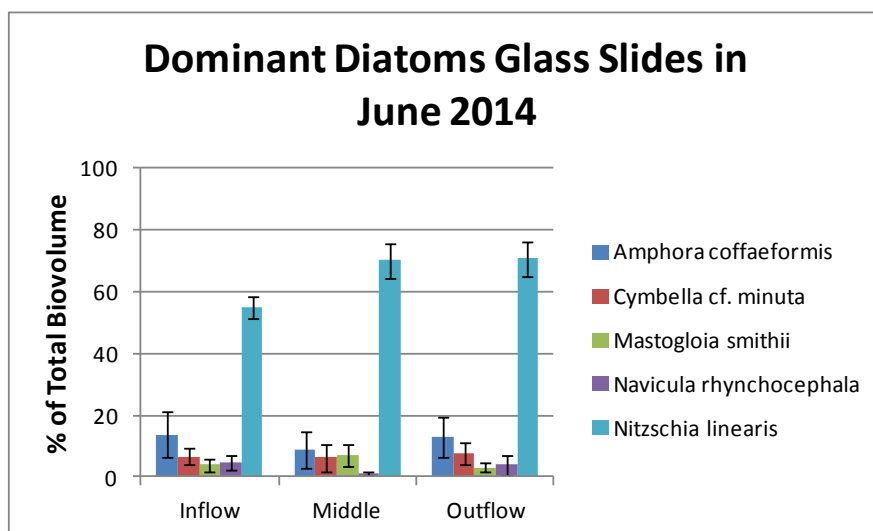


Figure 60. Relative dominance of diatoms in the slide periphyton samples collected June 19, 2014 from inflow, middle and outflow transects within the PSTA Cell. Values represent the mean (\pm SE) from triplicate samples along each transect, as a percent of total biovolume of all species.

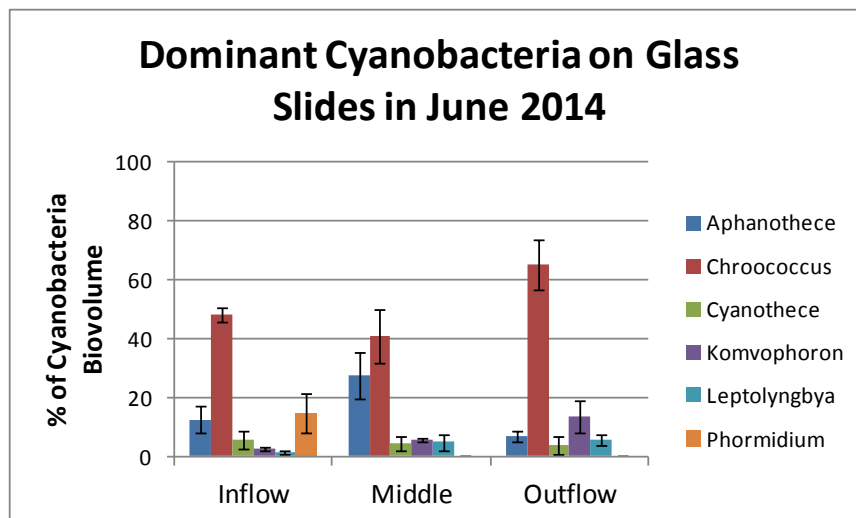


Figure 61. Relative dominance of cyanobacteria in the slide periphyton samples collected June 19, 2014 from inflow, middle and outflow transects within the PSTA Cell. Values represent the mean (\pm SE) from triplicate samples along each transect, as a percent of biovolume of all cyanobacteria species.

3.6.5 Discussion

Periphyton is abundant throughout the PSTA Cell, with P-sensitive diatoms and cyanobacteria dominating the assemblage. Periphyton nutrient concentrations were found to be typical of other south Florida ultra-low P marsh environments, whereas the areal periphyton biomass values measured in the outflow region of the PSTA cell are at the upper end of values reported in other studies. Surface water trends through the PSTA Cell in both P and ancillary parameters such as phosphatase enzyme activity suggest active and continuous processing of dissolved organic matter within the PSTA Cell footprint. The low-level P reductions evident in the PSTA Cell may be a result of several factors, including lack of an organic soil substrate, shallow depths, and abundant periphyton with associated enzymatic activity. On-going research using replicated mesocosms will provide additional insights into the effects of factors such as depth and P loading on periphyton assemblages, and on mechanisms that enable the STA-3/4 PSTA Cell to provide lower outflow TP levels muck-based STA flow ways.

4 Mesocosm and Microcosm Studies

4.1 Quantifying Operational Boundaries: Water Depth Effects on Water Column Phosphorus and Vegetation Communities

4.1.1 Introduction

There are potential benefits to shallow water depths in PSTA systems, including increased light penetration to the benthic surface. However, because shallow water depths may be difficult to establish and maintain in full-scale STA flow paths, particularly under pulse loading conditions, the effects of water depth on PSTA performance must be better defined. Prior research with PSTA systems operated at 30 or 60 cm water depths showed no difference in P removal performance, although static depth treatments outperformed variable depth treatments (CH2M-Hill 2003). The best performing experimental PSTA platforms were operated at 30 cm (STA-1W 0.2 ha test cells and mesocosms) and 9 cm (STA-1W mesocosm raceways, DeBusk et al. 2004). The STA-3/4 PSTA Cell typically has operated at a depth of 30-45 cm, with high flow events increasing average water depths to just over 60 cm.

The ability of these prior PSTA research efforts to define suitable water depth ranges has been limited in some cases by a lack of replication, and in other instances by the inability to produce ultra-low outflow TP concentrations. To overcome these limitations and provide insights into the effects of water depth on surface water TP concentrations, periphyton communities and P removal mechanisms in PSTA systems, we currently are operating a replicated outdoor mesocosm study using periphyton and macrophytes from the STA-3/4 PSTA Cell.

The current report focuses on the biological response to fluctuations in water depth and along nutrient gradients. The relative densities of macrophytes and periphyton were measured and the enzyme activity of the benthic periphyton layer was assayed as part of this evaluation. Phosphorus removal performance, TP concentrations and other water quality characteristics of these PSTA mesocosms were previously described in a recent report (DBE 2015). Nutrient contents of the macrophyte and periphyton tissues are currently being determined; those results will be presented in a future report.

4.1.2 Methods

4.1.2.1 Experimental Design

Operational “boundaries” of PSTA systems are being investigated in mesocosms at an experimental facility near the outflow of STA-1W. Triplicate flow ways with a local limerock substrate were established under each of four water depth treatments. The first two treatments are static in depth. Shallow treatments (23 cm) and deeper treatments (46 cm) consist of 4 tanks (each 1.8 m²) plumbed in series. These tanks were initially established in September 2013, under constant flows that provide a hydraulic retention time (HRT) of 5 and 10 days for the shallow (23 cm) and deep (46 cm) flow ways, respectively. Delivery of a constant flow rate to both

shallow and deep tanks insures equal P mass loading rate (PLR) to those treatments on an area basis.

In January 2014, additional mesocosms were established to test PSTA performance at greater water depths. Six new flow ways were constructed using larger tanks (2.8 m² per tank) plumbed two in series (Figures 62 and 63). These systems were initially established at 46 cm depth, and flows are being delivered to provide equivalent HRT and PLR conditions to the existing mesocosms operating with 4 tanks-in-series at 46 cm depth. The first tanks in series of the new flow ways receive an equivalent PLR to the first half (first 2 tanks) of the 4-in-series systems. This approach enables a comparison of “midpoint” and “outflow” positions with equivalent HLR and P loading across static and variable-depth treatments. Key operational parameters of these systems are outlined in Table 12.



Figure 62. Mesocosms were established at a range of water depths to explore the effects of operating conditions on P removal effectiveness and biological community response. The shorter tanks (to the lower left) were plumbed 4 in-series at water depths of 23 or 46 cm. The larger mesocosms were plumbed 2 in-series and were also established at 46 cm, before transitioning to 69 cm or 92 cm water depths.

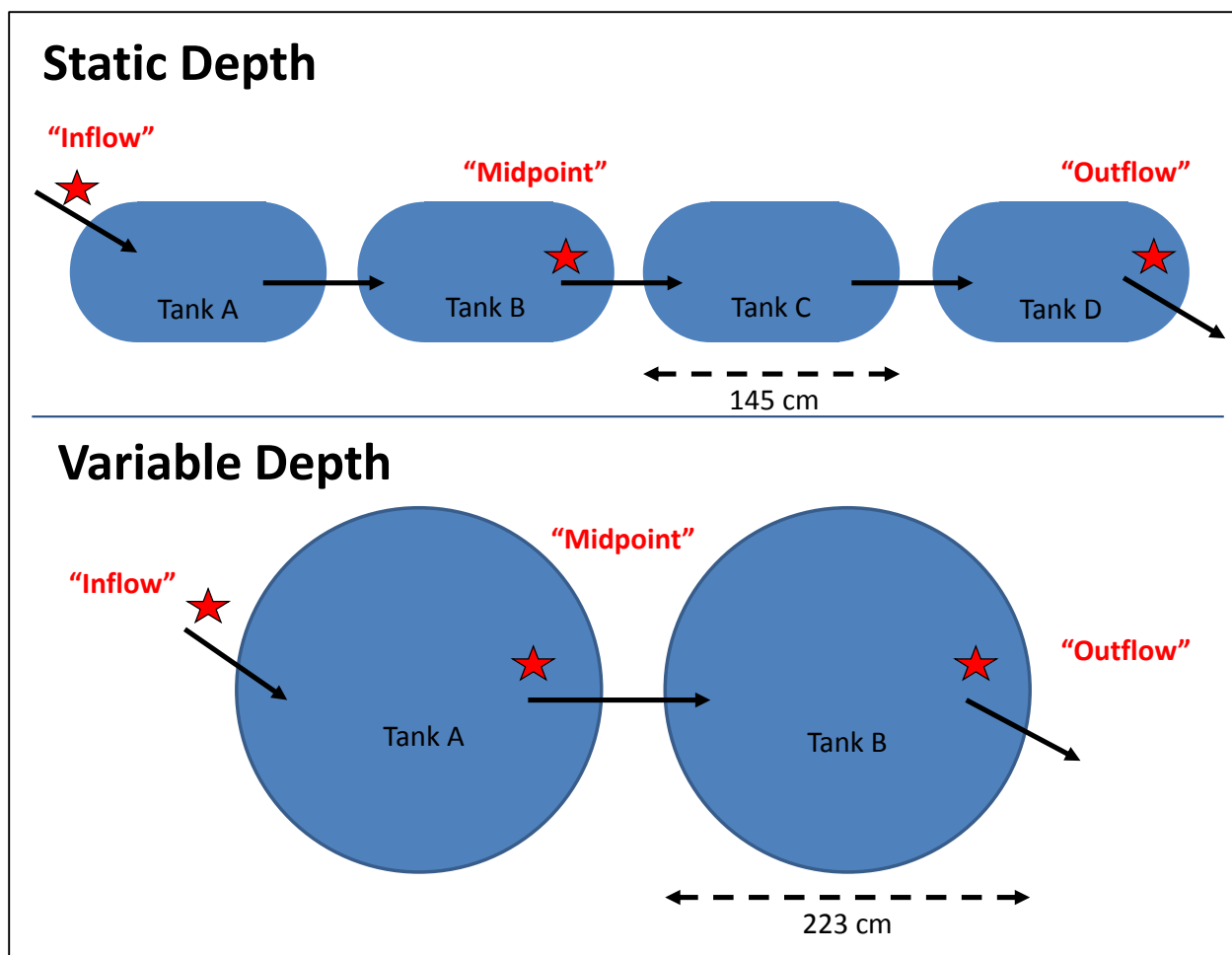


Figure 63. Process train configuration for static depth and variable depth mesocosms. Also shown are the surface water sampling locations along each flow way. Benthic samples were collected throughout the tanks to avoid resampling areas affected by earlier sampling efforts.

After an initial phase of comparable operations, the newer mesocosms were assigned to two new variable water depth treatments (46-69 cm and 46-92 cm). The transition to deeper conditions began after the water sampling on 5/29/2014 (Figure 64). On 9/15/2014, water depths were lowered back to 46 cm in the variable depth treatments, and the “shallow” conditions continued until January 15, 2015. Since January, water depths have been maintained at 69 and 92 cm in the respective variable-depth treatments to examine the P removal performance and periphyton community response to longer-duration deep water conditions.

Table 12. Operational targets for experimental flow ways assigned to one of four depth treatments.

Static Depth Treatments				
	Tank			
	A	B	C	D
HLR (m/day)	0.182	0.091	0.061	0.046
PLR at 20 ppb (g P/m ² /yr)	1.33	0.67	0.44	0.33
Water Depth	HRT (days)			
23 cm	1.3	2.5	3.8	5.0
46 cm	2.5	5.0	7.5	10.0
Variable Depth Treatments				
	First Tank	Last Tank		
HLR (m/day)	0.091	0.046		
PLR at 20 ppb (g P/m ² /yr)	0.67	0.33		
Water Depth	HRT (days)			
46 cm	5	10		
69 cm	7.5	15		
92 cm	10	20		



Figure 64. Water depth schedules for each of four depth treatments during the monitoring period (December 12, 2013 – April 1, 2015).

4.1.2.2 Water Quality Monitoring

Inflow and outflow surface water quality sampling began December 18, 2013 with weekly TP and enzyme activity, pH and temperature measurements. From March 5 to May 28, 2014 additional samples were collected on a bi-weekly basis from the midpoint and outflows of each flow way (Figure 63), and analyzed for P species (TSP, SRP). On a monthly basis beginning in February 2014, nitrogen species (TKN, NO_x, NH₄), DOC and UV absorbance properties were evaluated in inflow, midpoint and outflow samples from each flow way. In July 2014, surface water sampling frequency for TP and enzyme activity was reduced to twice per month. The analytical methods and detection limits for each parameter are provided in Table 13.

The data presented in this report are limited to water quality from the period between December 18, 2013 and April 1, 2015. The chemical measurements described above examined the response in PSTA performance to differences in water depth. However, it will also be important to determine the mechanisms causing such performance differences. Periphyton and macrophyte sampling was also performed, and will be presented in a future report.

Table 13. Analytical methods and method detection limits (MDLs) for inflow and outflow waters collected from the mesocosms.

Parameter	Method	MDL
Total Phosphorus	SM4500-P F	3 µg/L
Total Soluble Phosphorus	SM4500-P F	3 µg/L
Soluble Reactive Phosphorus	SM4500-P F	2 µg/L
Alkaline Phosphatase Activity	DBE SOP	0.01 µM/hr
Ammonia	EPA 350.1 (1978)/ SM4500-NH3 (18 th ed.)	0.020 mg/L
Nitrate + Nitrite (NO _x)	SM4500NO3 H-2000	0.016 mg/L
Total Kjeldahl Nitrogen	EPA 351.2	0.033 mg/L
Dissolved Organic Carbon	SM 5310B	1.0 mg/L
S ₂₇₅₋₂₉₅	Helms et al. 2008	n/a
UV ₂₅₄	SM5910B	0.005 cm ⁻¹

4.1.2.3 Measurement of Light at the Benthic Surface

Algal growth is strongly controlled by the amount of light available for photosynthesis. The intensity of photosynthetically-active radiation (PAR) at the benthic surface was determined by placing a spherical underwater quantum sensor (LiCOR, Lincoln, NE) in a recess within the outflow region of each process train, so that the sensor was even with the benthic surface (Figure 65). The PAR available at the benthic surface was determined as a percent of ambient levels, as measured above each tank. Measurements were made twice monthly from March 20, 2014 through June 18, 2014, then once monthly beginning in July 2014. The period of record in this report includes all measurements through May 27, 2015 (N = 18 events).



Figure 65. Periphyton in mesocosms has developed on the benthic surface, as well as tank walls, plant surfaces, and in some areas, benthic mats have separated to form floating mats (left image). The middle image shows a sampling collar used to define the area for benthic periphyton sampling, and a recess for measuring photosynthetically active radiation (PAR) at the benthic surface. The benthic periphyton mat shown in the right image was removed from the outflow region of a mesocosm on May 29, 2014.

4.1.2.4 Benthic periphyton sampling in outdoor mesocosms

Following initiation of water flows, benthic periphyton mats developed readily on the limerock mesocosm substrates. In order to compare biomass growth across depth treatments, we measured areal biomass (dry mass of periphyton per unit area of benthic surface) on three sampling dates: May 29, 2014 (prior to first deep phase); September 16, 2014 (end of 1st deep phase); and January 15, 2015 (prior to 2nd deep phase). Benthic samples were collected from each tank on each of the three sampling dates, with the following exception: static depth “B” and “C” tanks were only sampled from one replicate in May 2014.

A clean plastic bucket was submerged into the mesocosm water column next to the target sampling area. A sampling collar (14.6 cm inside diameter) was inserted into the limerock substrate. Periphyton was carefully transferred from the benthic surface by hand into the submerged bucket. Limerock gravel was also transferred, as necessary, to ensure that all periphyton was included in the sample. For each location, two grab samples were collected and composited into one sample representing a total benthic surface area of 335 cm². In contrast to water sampling efforts (see Figure 63), benthic samples were collected throughout the tanks to avoid resampling areas affected by earlier sampling efforts.

4.1.2.5 Periphyton Processing

In the laboratory, excess site water from each settled sample was decanted. Gravel was rinsed free of periphyton, using DI water as rinsate in a large beaker. The sample was stirred so that periphyton fragments suspended, while the gravel settled to the bottom of the beaker. Then, the suspension was transferred into the mixer (leaving the gravel behind in the beaker). Once the gravel was isolated from the bulk of the algal material, DI was added to the beaker and swirled to dislodge any remaining algal material from the gravel. While the algae was in suspension, the liquid and algae was poured off while holding back the gravel. The gravel was inspected for

any remaining periphyton fragments, and then discarded. Once the gravel was removed, the algal suspension was settled and the overlying water decanted, taking care to retain all particles.

The sample was gently stirred with a metal spoon, then “unhomogenized” samples (i.e., not blended) were transferred into 2 clean scintillation vials. The samples were then thoroughly homogenized in a food mixer. The homogenized slurry was again sub-sampled for enzyme assay (20 mL) and “homogenized” taxonomy samples (2 vials, each 20 mL). Another subsample of the remaining slurry (150 mL) was transferred into a pre-weighed plastic cup and dried to constant weight at 65°C. The remaining sample was transferred to a graduated cylinder to record the remaining volume. Periphyton samples were preserved in 4% formalin buffered with sodium borate for taxonomic identification and biovolume determination.

4.1.2.6 Enzyme Assay

Periphyton samples were diluted by dispensing a known volume of the enzyme subsample into a pre-weighed centrifuge tube, and adding DI as necessary, to achieve appropriate hydrolysis rates for the assays. The remainder of the diluted sample, once the enzyme assay was complete, was then dried to constant weight to calculate the enzyme assay bulk density. Results of the assay were normalized to dry weight of periphyton in the slurry as assayed.

Benthic periphyton enzyme activity was converted to $\mu\text{mol MUF released}/\text{cm}^2/\text{hr}$, using the APA per unit weight, and the dry weight biomass of periphyton per unit area (“areal biomass”). Taxonomic samples were archived and will be prioritized for identification at the conclusion of the study.

4.1.2.7 Relative Density and Species Composition of Macrophytes and Periphyton Communities in Outdoor Mesocosms

The relative density of SAV species (*Chara* and *Potamogeton*) was recorded on a 0-5 scale, with 5 indicating very dense macrophyte beds. This method was developed for use in the full-scale STA flow ways, and was adapted for mesocosm research to avoid the disturbances associated with sampling biomass from these small systems. A similar density score was also recorded for benthic, floating, and epiphytic periphyton in each mesocosm. These scores were recorded each month to document changes in the species composition and relative density of macrophytes and periphyton during the establishment of flow-through PSTA mesocosms. Relative density values were averaged for the 8-9 locations within each tank, on each sampling date (Figure 66). These values were compared across replicates under each treatment to calculate a standard error for each treatment.

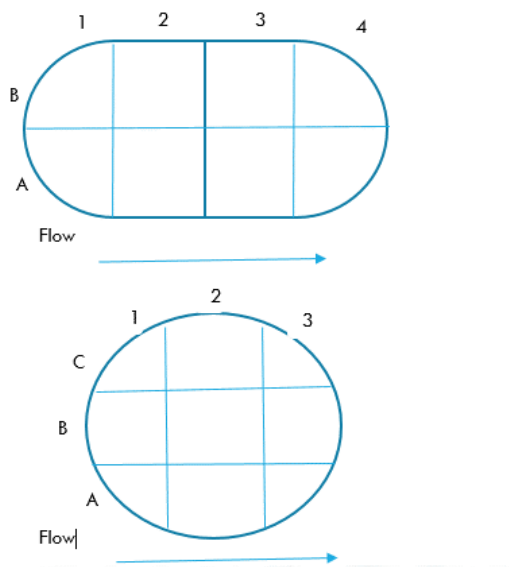


Figure 66. Sampling grid used for relative macrophyte density evaluations.

4.1.3 Water Quality

4.1.3.1 Results

During the initial phase (December 12, 2013 to April 1, 2015) of this on-going study, the PLR to these systems varied with inflow P concentration and ranged from 0.15 to 0.62 g P/m²/yr, with an average 0.36 ± 0.02 g P/m²/yr for the period (Figure 67). Inflow TP concentrations averaged 21 ± 1 µg/L. These loading rates and inflow concentrations fall within the range of annual values for the STA-3/4 PSTA Cell.

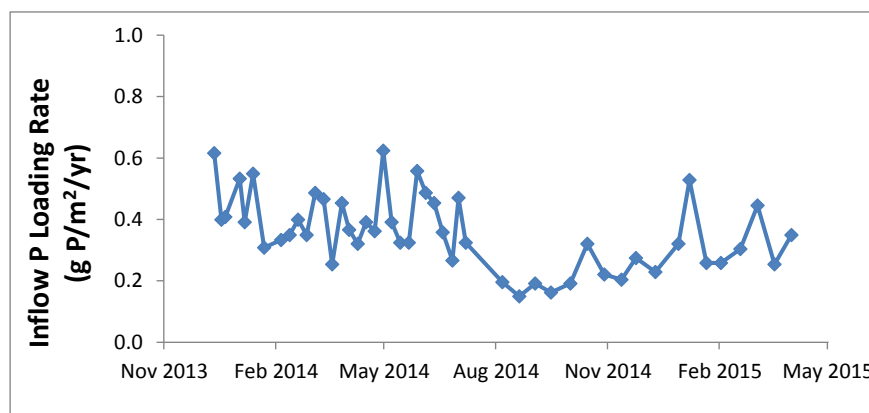


Figure 67. Inflow phosphorus (P) loading rate to each flow way during the period of record (December 18, 2013 – April 1, 2015).

4.1.3.1.1 Effect of shallow depth on TP removal performance

Total phosphorus concentrations were similar in the outflow waters of 23 cm and 46 cm static water depth conditions (Figure 68). Mean inflow concentrations of $21 \pm 1 \mu\text{g/L}$ were reduced to $8 \pm 0 \mu\text{g/L}$ in both 23 cm and 46 cm treatments over the period from December 12, 2013 through April 1, 2015. After July 2014, the inflow TP concentrations became very low for several weeks. However, P export was not observed from any of these periphyton-dominated mesocosms on a limerock substrate.

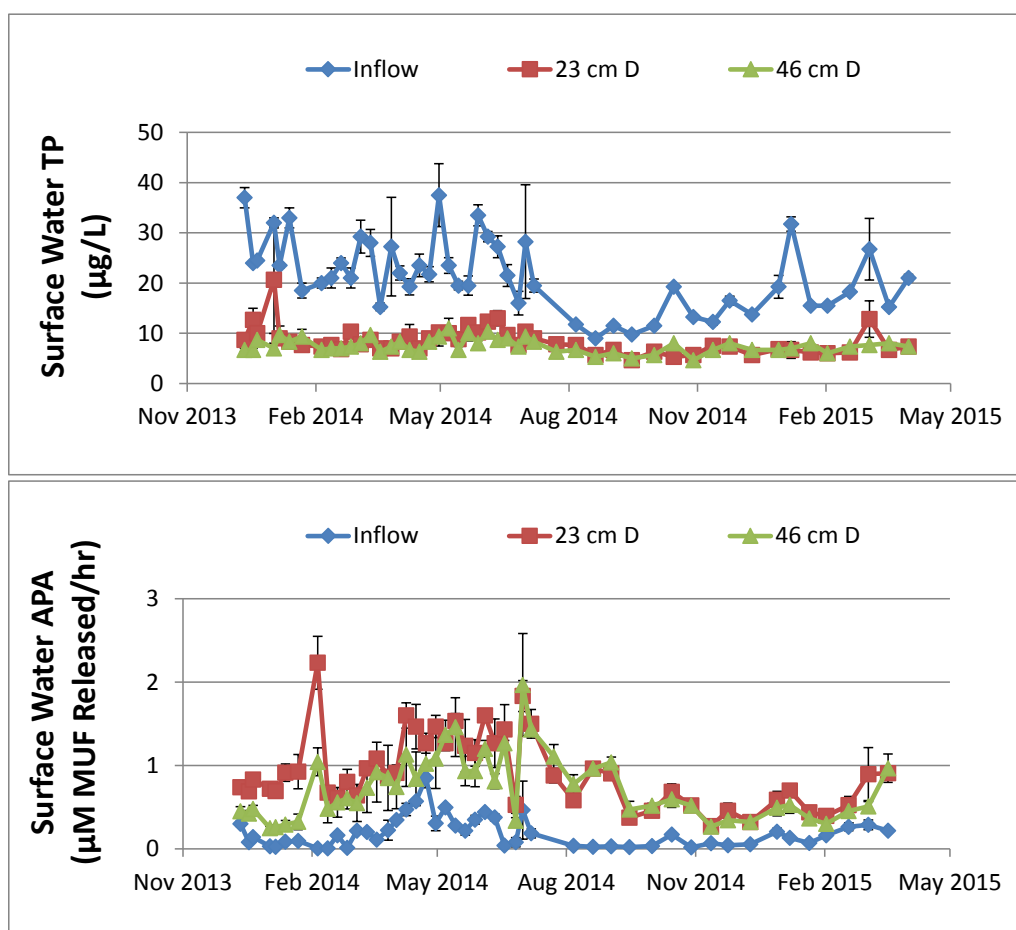


Figure 68. Surface water total phosphorus (TP) concentrations and alkaline phosphatase activity (APA) for inflow and outflow waters (D = fourth tank in series) from mesocosms operated at static depths of 23 and 46 cm.

Enzyme activity was typically low in the inflow water ($0.20 \pm 0.01 \mu\text{M MUF released/hr}$), with the highest values ($0.85 \mu\text{M/hr}$) measured on April 23, 2014 (Figure 68). Activity in the outflow waters was always higher than the inflow waters, with period of record average values of $0.92 \pm$

0.03 $\mu\text{M/hr}$ and $0.73 \pm 0.11 \mu\text{M/hr}$, for the 23 cm and 46 cm depth treatments, respectively. The shallow (23 cm) mesocosms exhibited the greatest activity during the period up to July 2014. After that time, there was no difference between 23 cm and 46 cm treatments at the outflow.

Nitrogen compounds in the inflow waters were dominated by the organic fraction, with 1-3 mg/L (mean concentrations: $2.11 \pm 0.03 \text{ mg TN/L}$; $1.82 \pm 0.024 \text{ mg Org-N/L}$), compared to maximum NO_x and ammonia-N concentrations of 0.085 mg/L and 0.72 mg/L, respectively (Figure 69). Inorganic N forms were routinely removed to near the limits of detection (0.020 mg/L for ammonia, and 0.016 mg/L for NO_x) (Figure 69).

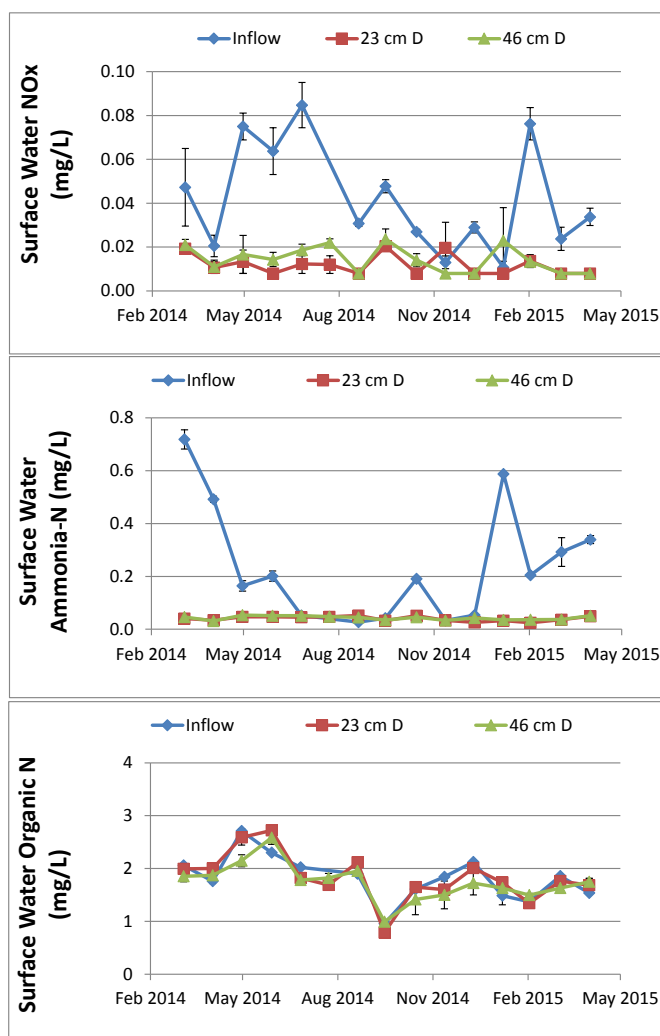


Figure 69. Concentrations of three forms of nitrogen in the inflow and outflow waters from mesocosms operated at static water depths of 23 cm and 46 cm. Error bars denote the standard error around the mean from triplicate process trains under each depth condition.

A further examination of the organic matter in the water column revealed temporal changes in inflow quality and, at times, some reduction in DOC from inflow to outflow. Inflow DOC concentrations ranged from 16.0 to 41.5 mg/L (mean 28.9 ± 0.0 mg/L) over the period from February 19, 2014 through April 1, 2015. Outflow concentrations from the 23 and 46 cm treatments averaged 28.3 and 26.9 mg/L, respectively, indicating slightly greater DOC removal in the deeper treatment. No DOC removal has been observed in the last several months (since January 2014) for either 23 cm or 46 cm treatments. The period of greatest DOC concentration reductions by the 46 cm treatment (October – December 2014) was coincident with org-N removal, low enzyme activity and low concentrations of TP and inorganic N in the inflow waters (Figures 69 and 70). It appears from these data that the longer residence time of water in the deeper mesocosms (46 cm depth) may have been a more important factor for breaking down organic compounds than either shallow water depths or high enzyme activity.

The absorbance characteristics showed more consistent effects of water depth throughout the monitoring period. UV_{254} , a measure of absorbance of ultraviolet light (at a wavelength of 254 nm) by the dissolved constituents of the surface waters, showed lower values in the outflows from flow ways at 46 cm depth than at 23 cm depth. Spectral slope ($S_{275-295}$) and $SUVA_{254}$ are two parameters that describe the relative size and recalcitrance of the dissolved organic matter pool. These metrics showed greater changes from inflow to outflow in the 46 cm treatments, as compared to the shallower 23 cm deep flow ways. These metrics (UV_{254} , $SUVA_{254}$, and $S_{275-295}$) also continued to show consistent differences between treatments during the recent months of little to no change in DOC concentration.

4.1.3.1.2 *Effect of variable water depth*

Mesocosms operated at variable water depths (up to 92 cm) showed higher TP concentrations at the first half (“midpoint”) sampling location than the mesocosms operated at a static depth of 46 cm over the entire period of record (Figures 71 and 72). At the outflow, however, mean TP concentrations were similar between static and variable depth treatments. Phosphorus removal performance by the midpoint of the variable depth treatments appeared to diverge from that of the static depth treatments during the first deep water phase that began in June 2014. Midpoint TP concentrations of the variable depth treatments remained elevated for several months, as compared to the static depth treatment, even after the depths returned to 46 cm in the variable depth tanks.

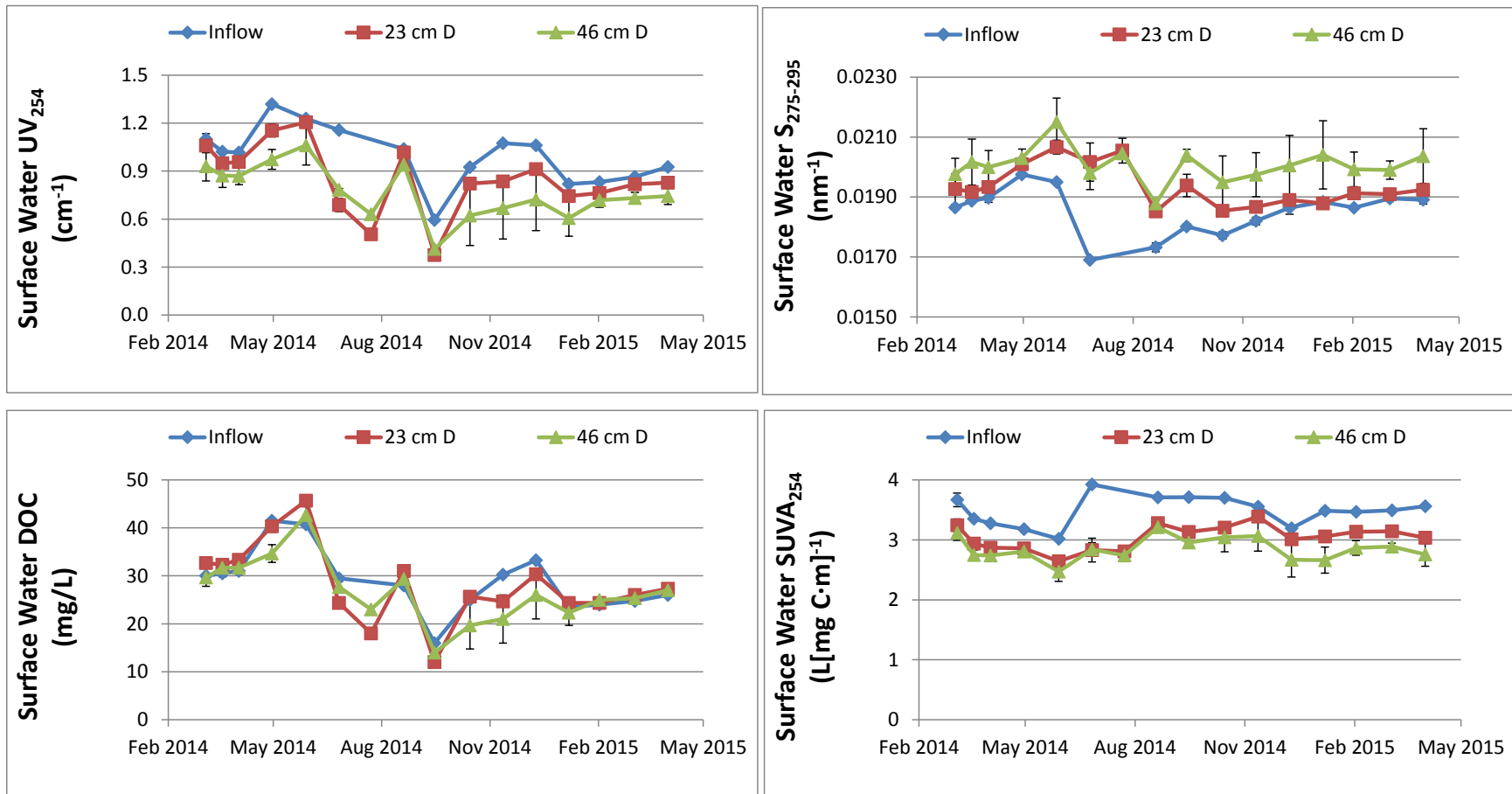


Figure 70. Dissolved organic matter characterization of the outflow waters from mesocosms operated at 23 cm and 46 cm water depths.

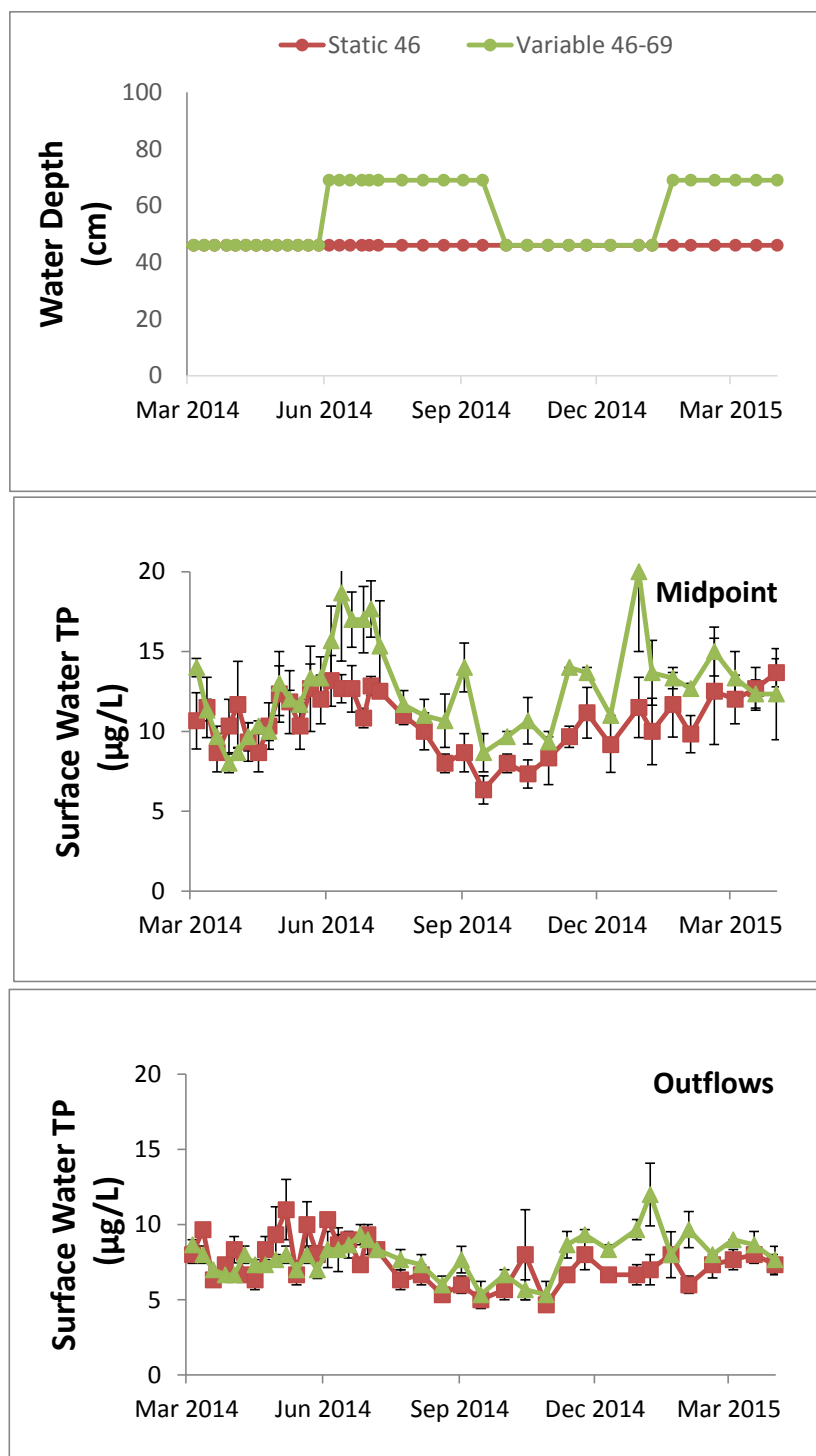


Figure 71. Response of surface water TP concentrations to increased water depths, measured at the midpoint and outflows from mesocosms operated at depths between 46 and 69 cm. The concentrations are also shown for mesocosms operated at a static depth of 46 cm throughout the study. Error bars denote \pm one standard error around the mean value from triplicate flow ways under each treatment.

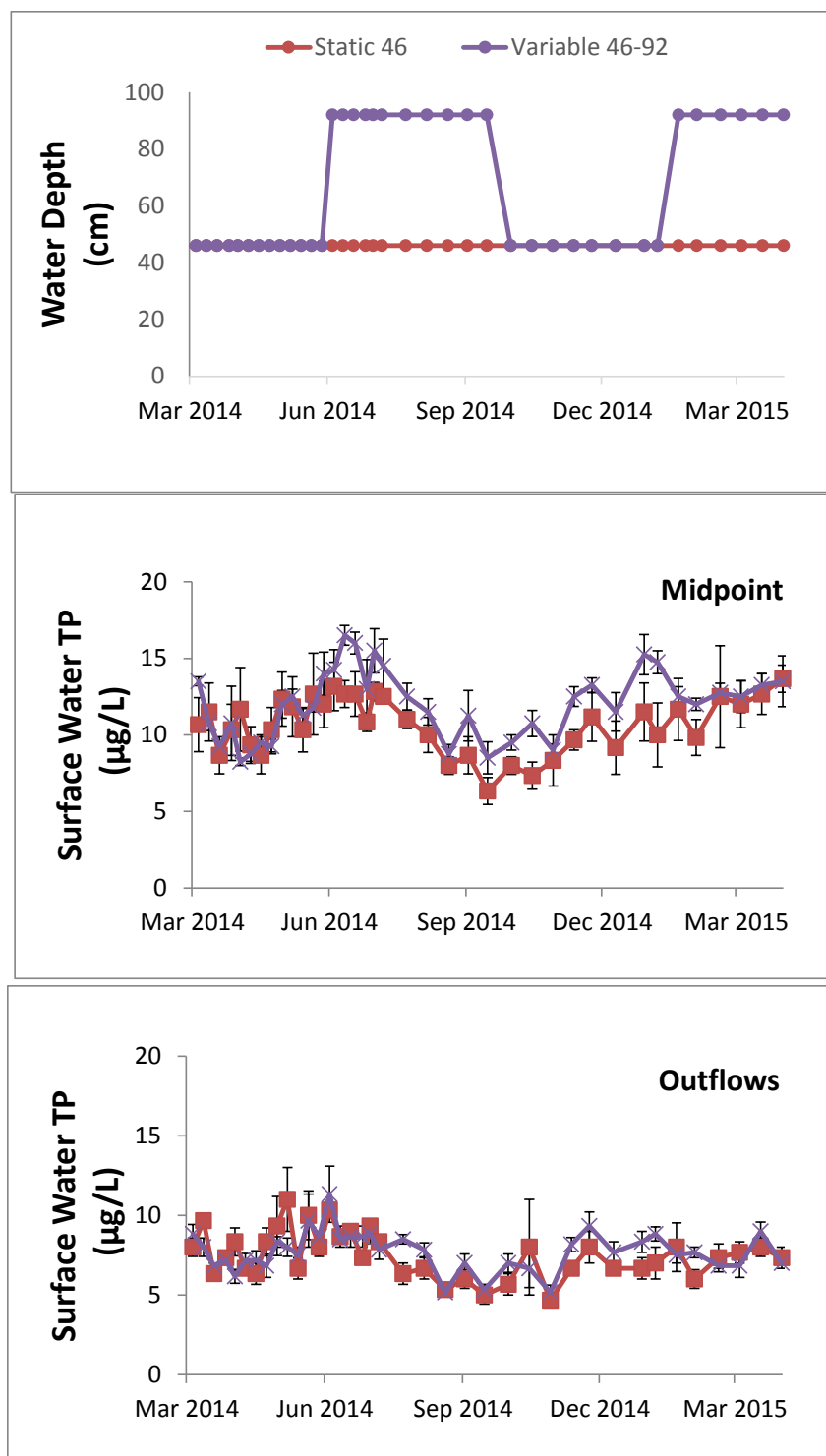


Figure 72. Response of surface water TP concentrations to increased water depths, measured at the midpoint and outflows from mesocosms operated at depths between 46 and 92 cm. The concentrations are also shown for mesocosms operated at a static depth of 46 cm throughout the study. Error bars denote \pm one standard error around the mean value from triplicate flow ways under each treatment.

A summary of the TP concentrations in inflow and outflow waters during the initial establishment “shallow” phase, and subsequent phases of deep and shallow conditions, are shown in Figure 73. Characteristics of the dissolved organic matter and nitrogen concentrations are shown in Figures 74 and 75. Dissolved organic carbon concentrations were typically stable between inflow and outflow, though slight reductions were seen in both static depth and variable depth treatments during the second shallow period (October 2014 – January 2015). Absorbance of UV radiation by the DOM pool indicated smaller, more labile compounds were associated with the static depth treatment than the variable depth treatments during second shallow period. This trend was less pronounced during the subsequent deep period. Statistical analysis of these treatment effects will be conducted at the conclusion of the study.

The light available at the sediment surface was measured in the outflow region of the last tank in each series, and indicates that light conditions are similar between the two variable depth treatments when both were operated at 46 cm depth (see Figure 83 in section 4.1.4.1.1).

For the entire period of record, TP concentrations at the midpoint locations were lowest for the two static depth treatments (11 µg/L), and higher in the variable depth treatments (12-13 µg/L). At the outflow locations, however, no effect of depth treatment could be observed from the TP concentration data (Figure 76). The differences in TP concentration between treatments at the midpoint were the result of higher PP concentrations in the variable depth mesocosms (Figure 77).

□ Inflow ■ Static 46 cm ■ Variable 46-69 cm ■ Variable 46-92 cm

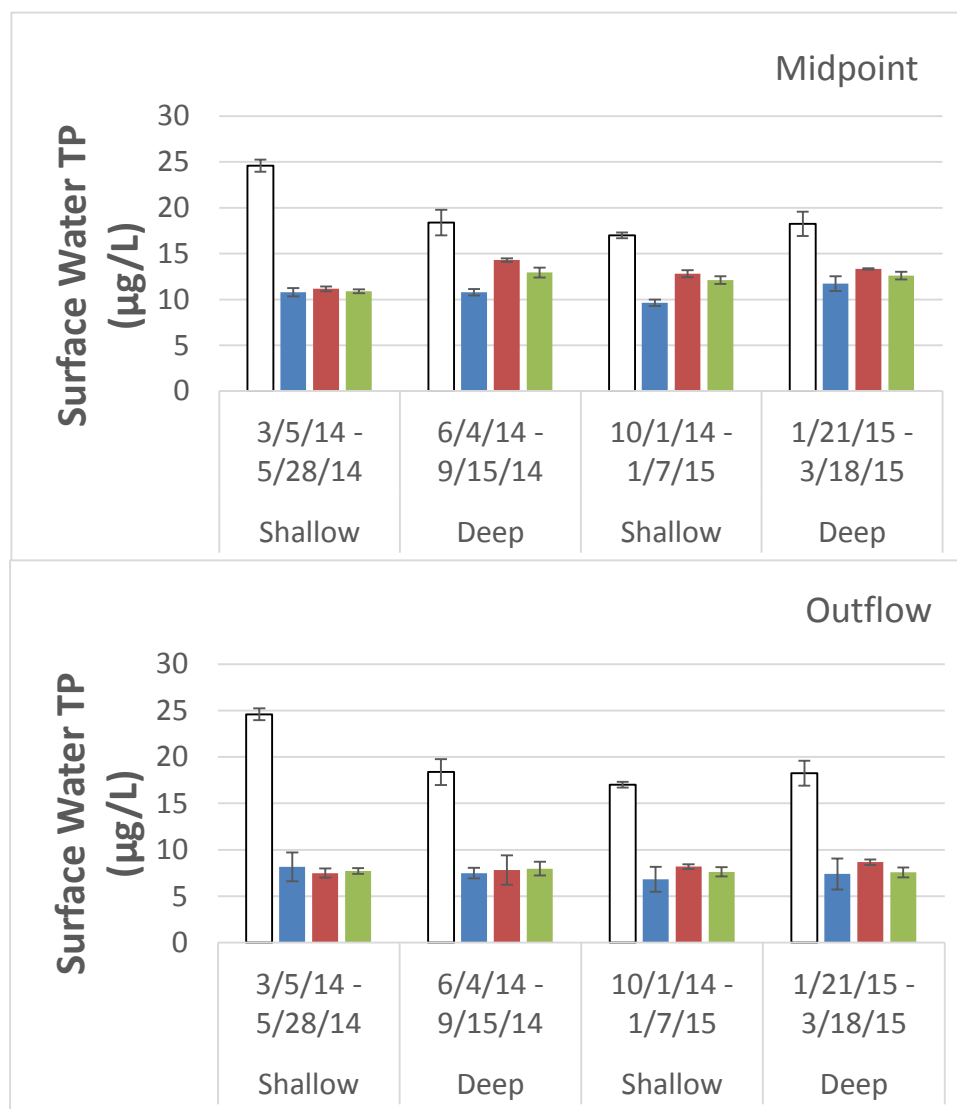


Figure 73. Average (\pm SE) inflow and midpoint surface water total phosphorus (TP) concentrations (top panel) and outflow concentrations (lower panel) from process trains operated at static depth (46 cm) or variable depths during the period between March 2014 and January 2015. Variable-depth treatments were changed from a water depth of 46 cm to either 69 cm or 92 cm after sampling on May 28, 2014. Water depths in variable-depth treatments were returned to 46 cm after sampling on September 15, 2014, then increased again on January 15, 2015. Error bars denote \pm 1 SE around the mean of triplicate process trains under each treatment.

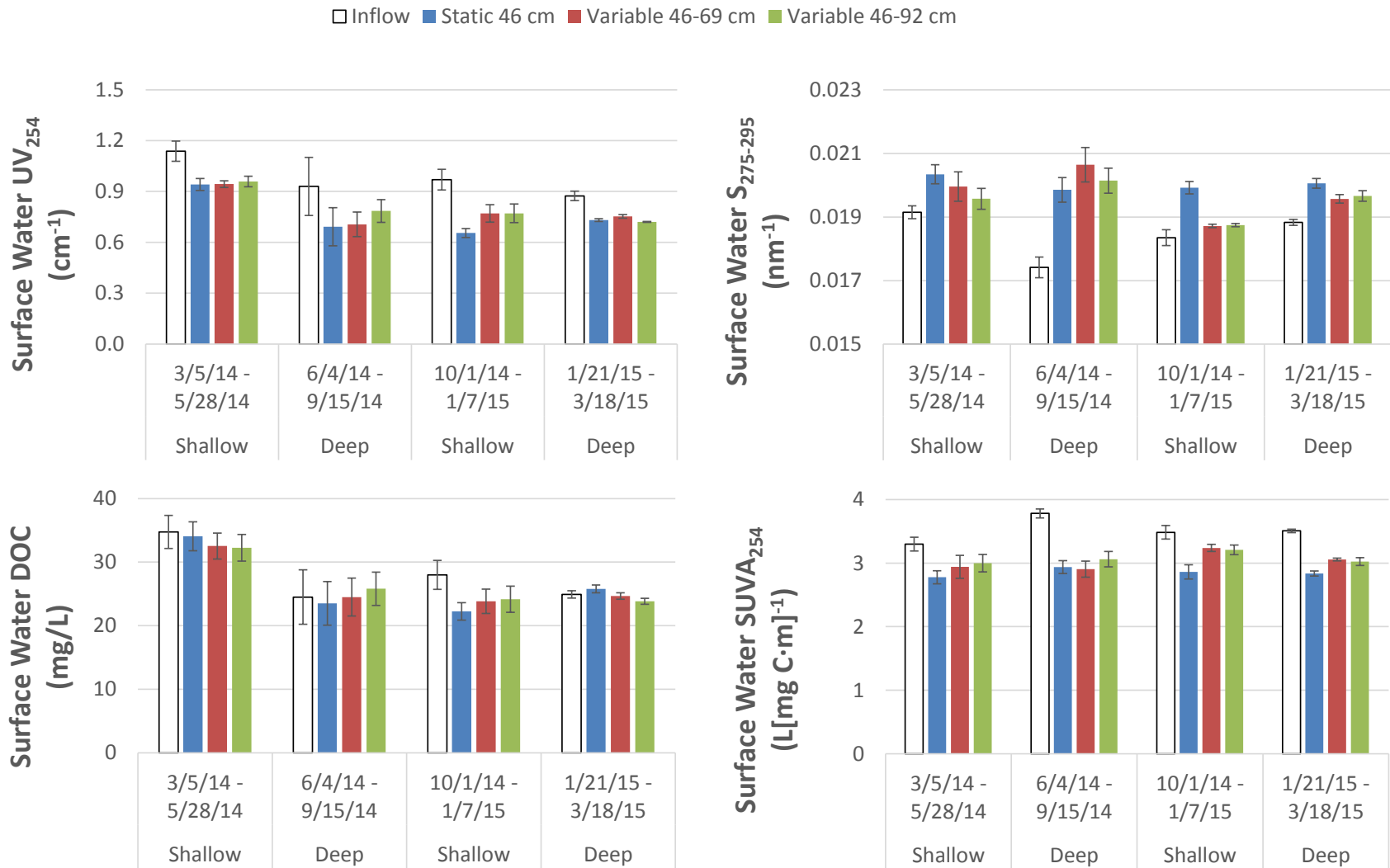


Figure 74. Characteristics of the dissolved organic matter in inflow and outflow waters from mesocosms operated at static or variable depths. Values reflect the average \pm SE across triplicate flow ways under each treatment for four periods of time where variable depth treatments were either “shallow” (46 cm) or “deep” (69 or 92 cm).

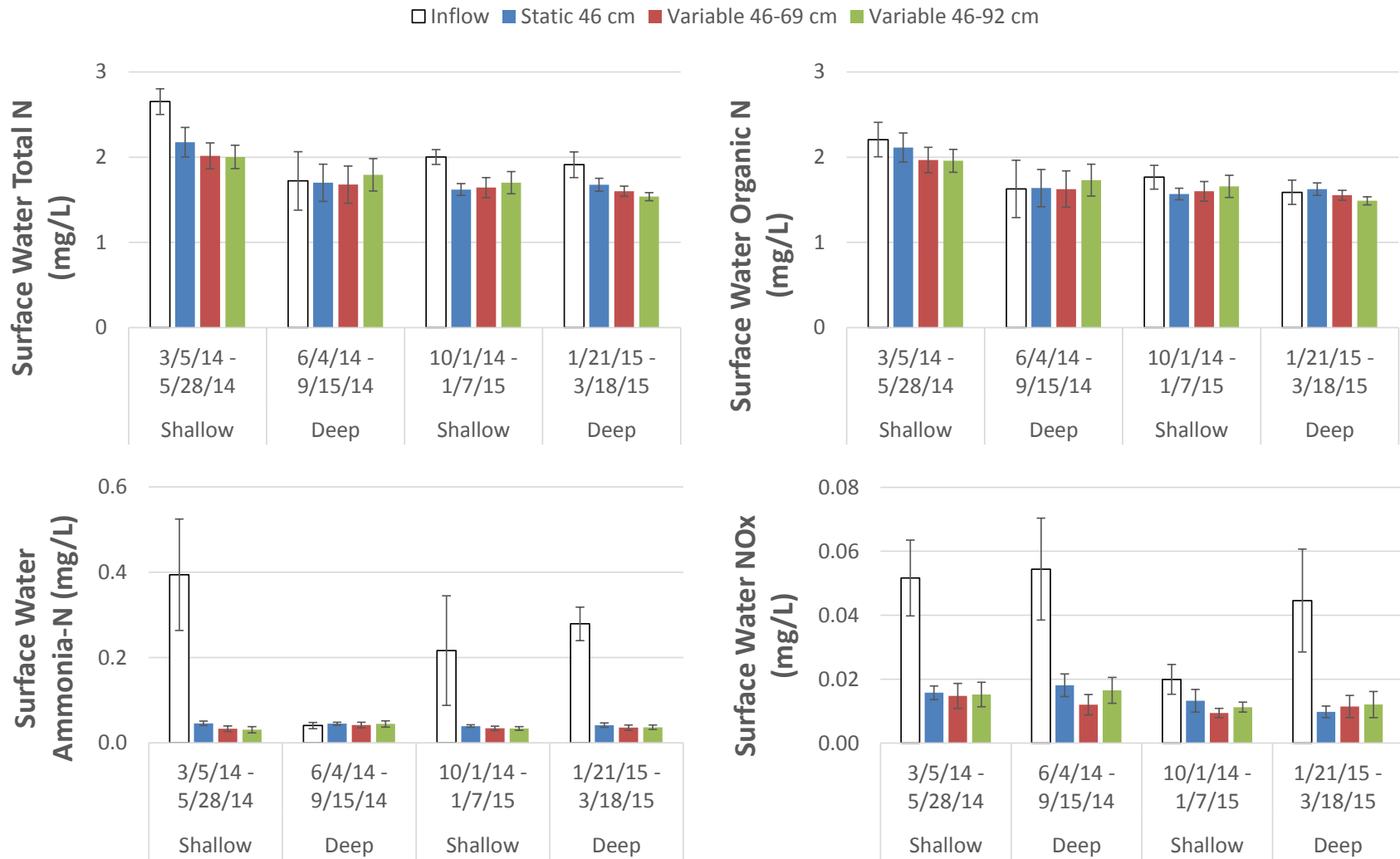


Figure 75. Nitrogen concentrations in inflow and outflow waters from mesocosms operated at static or variable depths. Values reflect the average \pm SE across triplicate flow ways under each treatment for four periods of time where variable depth treatments were either “shallow” (46 cm) or “deep” (69 or 92 cm).

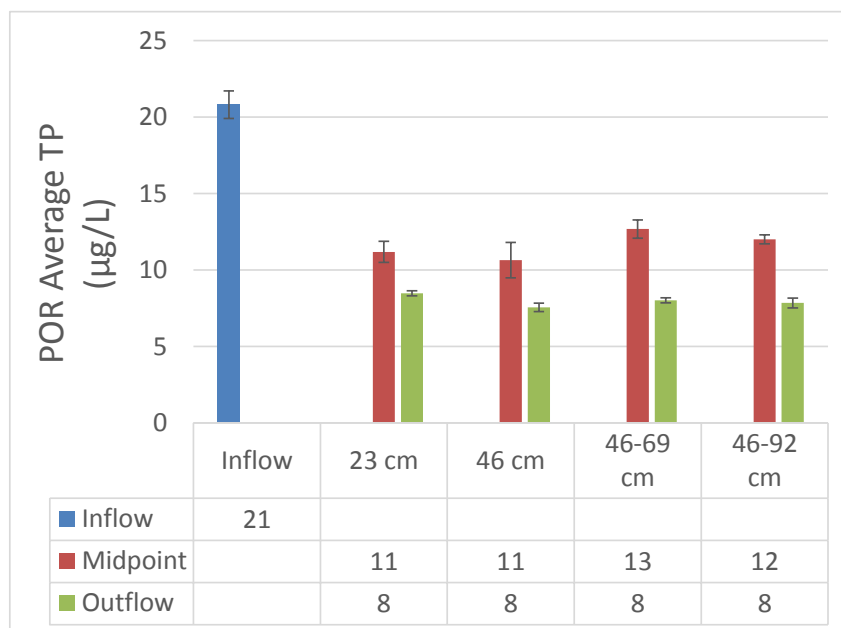


Figure 76. Inflow, midpoint and outflow concentrations of total phosphorus (TP) for mesocosm flow ways operated at either static depths (23 cm or 46 cm) or variable depths (46-69 cm or 46-92 cm). Values represent the average \pm standard error for triplicate flow ways under each depth treatment, for the period of record (December 2013 – April 2015).

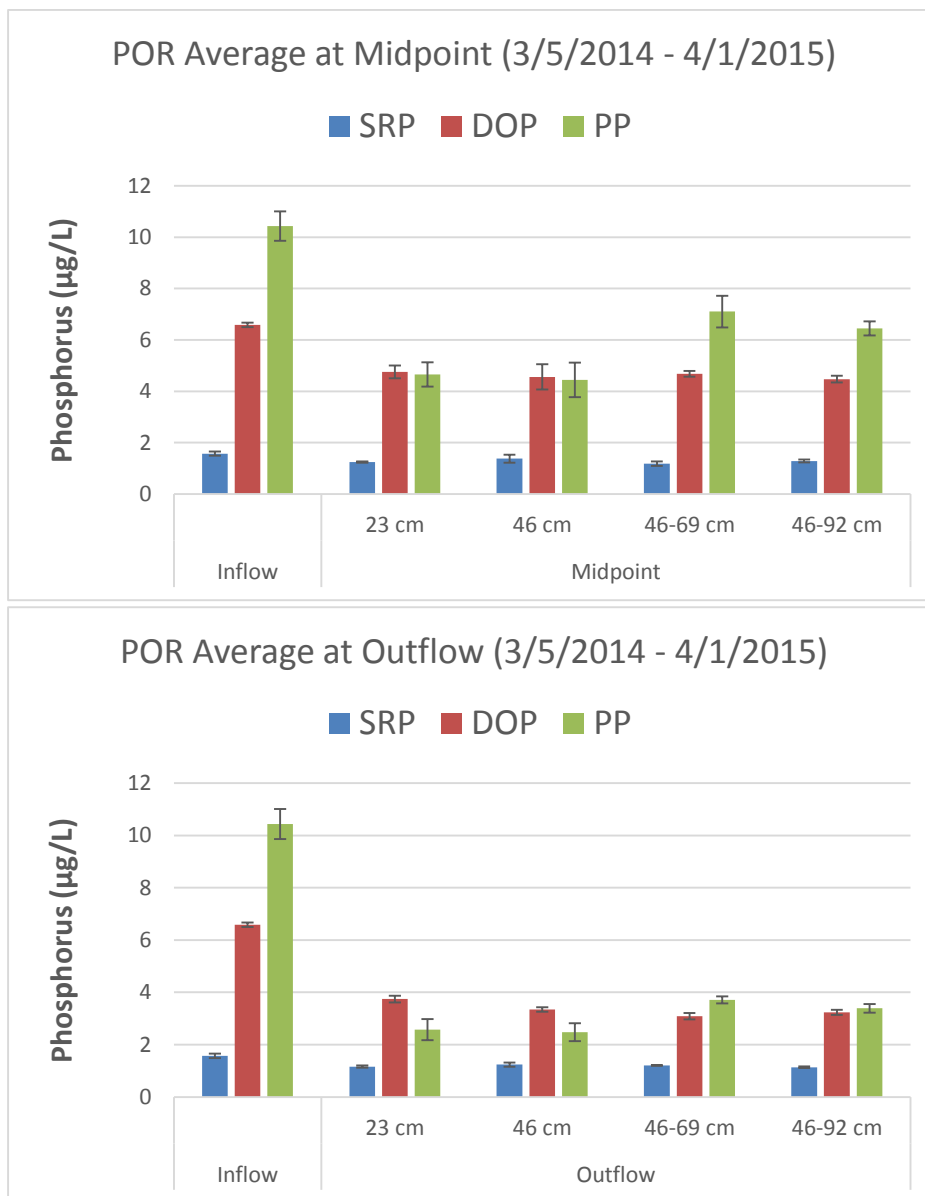


Figure 77. Inflow concentrations of phosphorus species are compared to midpoint concentrations (upper panel) and outflow concentrations (lower panel) for mesocosm flow ways operated at either static depths (23 cm or 46 cm) or variable depths (46-69 cm or 46-92 cm). Values represent the average \pm standard error for triplicate flow ways under each depth treatment, for the period of record (March 2014 - April 2015).

4.1.3.1.3 Phosphorus and enzyme gradients

Phosphorus gradients became established in all four treatments during the initial monitoring phase, with steadily declining TP concentrations from inflow to outflow (Figures 78 and 79). These gradients indicate the greatest removals occurred in the first tank in series, but decreases in surface water TP concentrations continued to ultra-low levels ($< 10 \mu\text{g/L}$). Enzyme activities were highest in the variable depth mesocosms, especially during the deep water phase between June and September 2014 (Figure 80). Activities were elevated in both midpoint and outflow samples during that time. In fact, APA was frequently higher at the midpoint location than in the outflow waters. There are several reasons why this could be occurring, including differences in periphyton communities or a limitation on enzyme production, such as nitrogen or a micronutrient.

Dissolved organic phosphorus was consistently reduced by the midpoint under all treatments, with further reductions in the second half of each flow way (Figure 81). Particulate phosphorus was also reduced between inflow and outflow in all treatments, but the midpoint PP concentrations indicated some increases occurred in the first tanks in series under of variable depth conditions (Figure 82). The back half of those flow ways was able to maintain low PP concentrations regardless of depth variation.

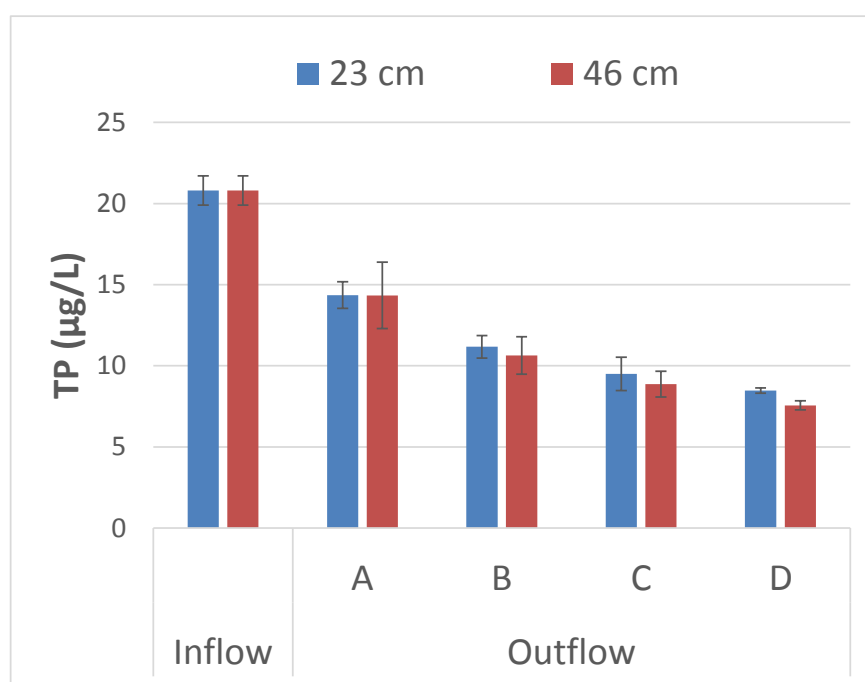


Figure 78. Average total phosphorus concentrations in the inflow waters and outflow-region surface waters of flow ways operated at either 23 cm or 46 cm depths, for the period December 2013 – April 1, 2015. Each flow way was comprised of four tanks in series (A, B, C, D). Error bars denote the standard error from triplicate flow ways under each depth treatment.

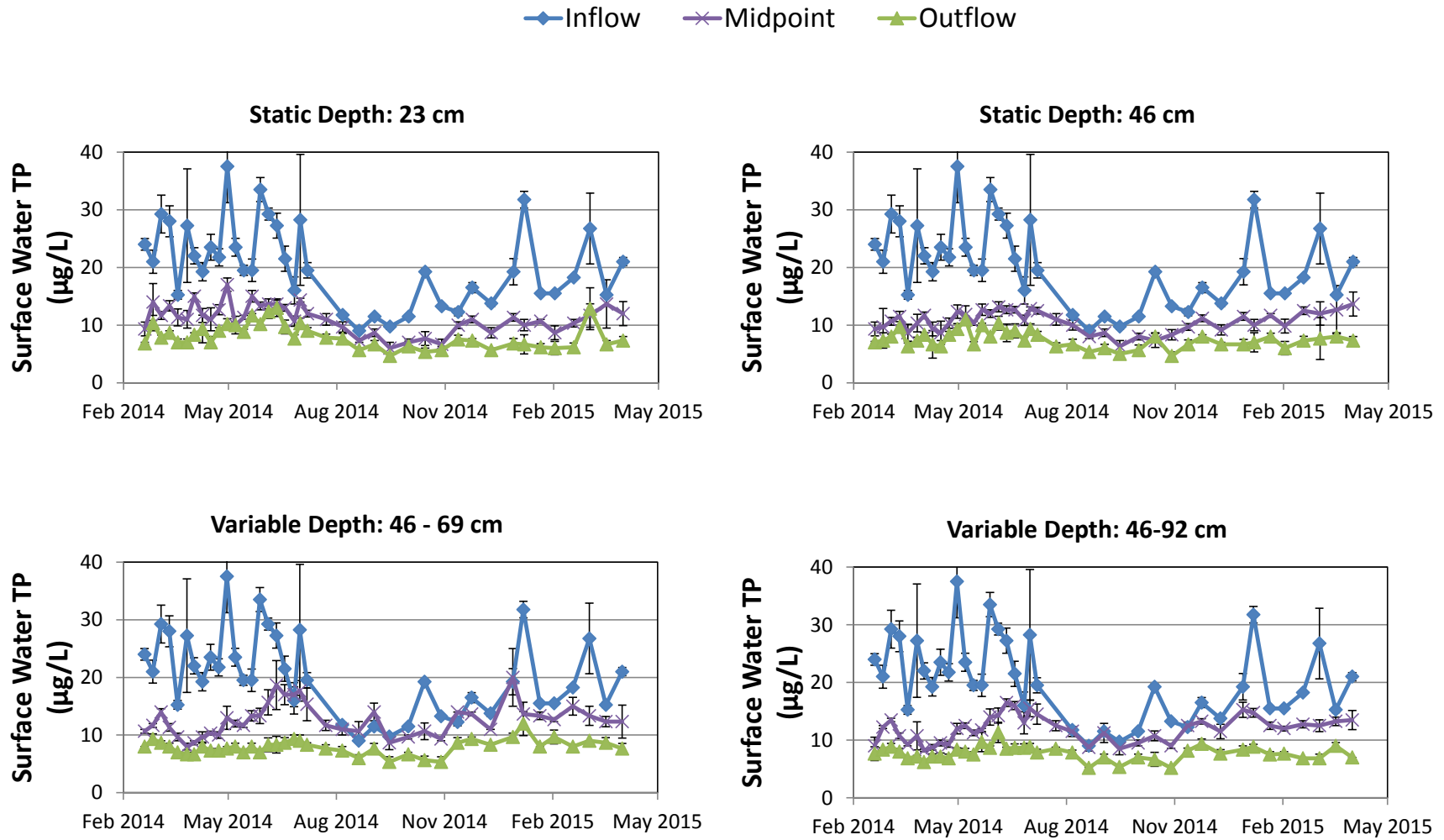


Figure 79. A comparison of total phosphorus concentrations in the inflow, midpoint, and outflows from the four treatments.

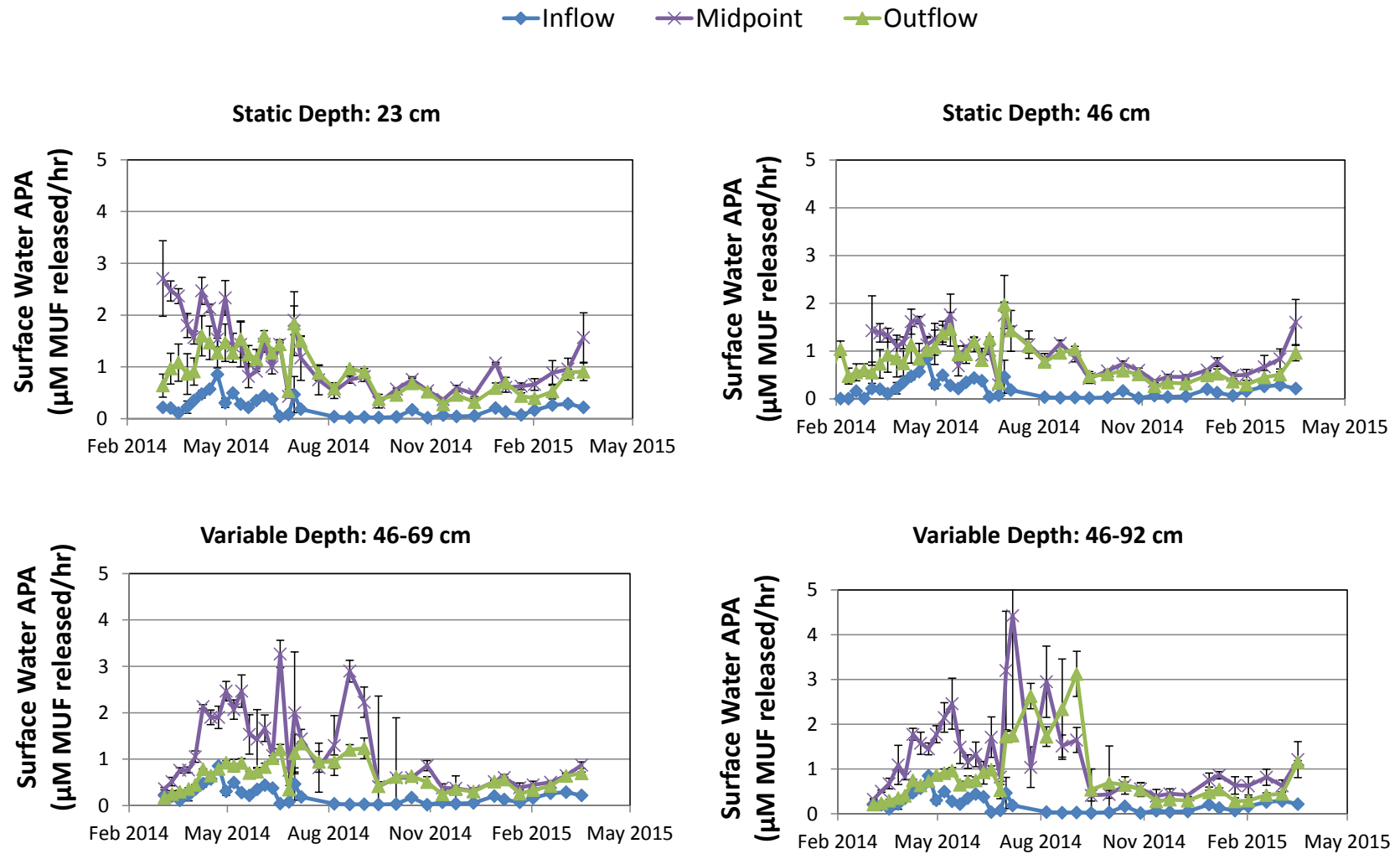


Figure 80. Alkaline phosphatase activity (APA) in the surface waters of inflow, midpoint and outflow waters during the period of record between February 2014 and April 2015.

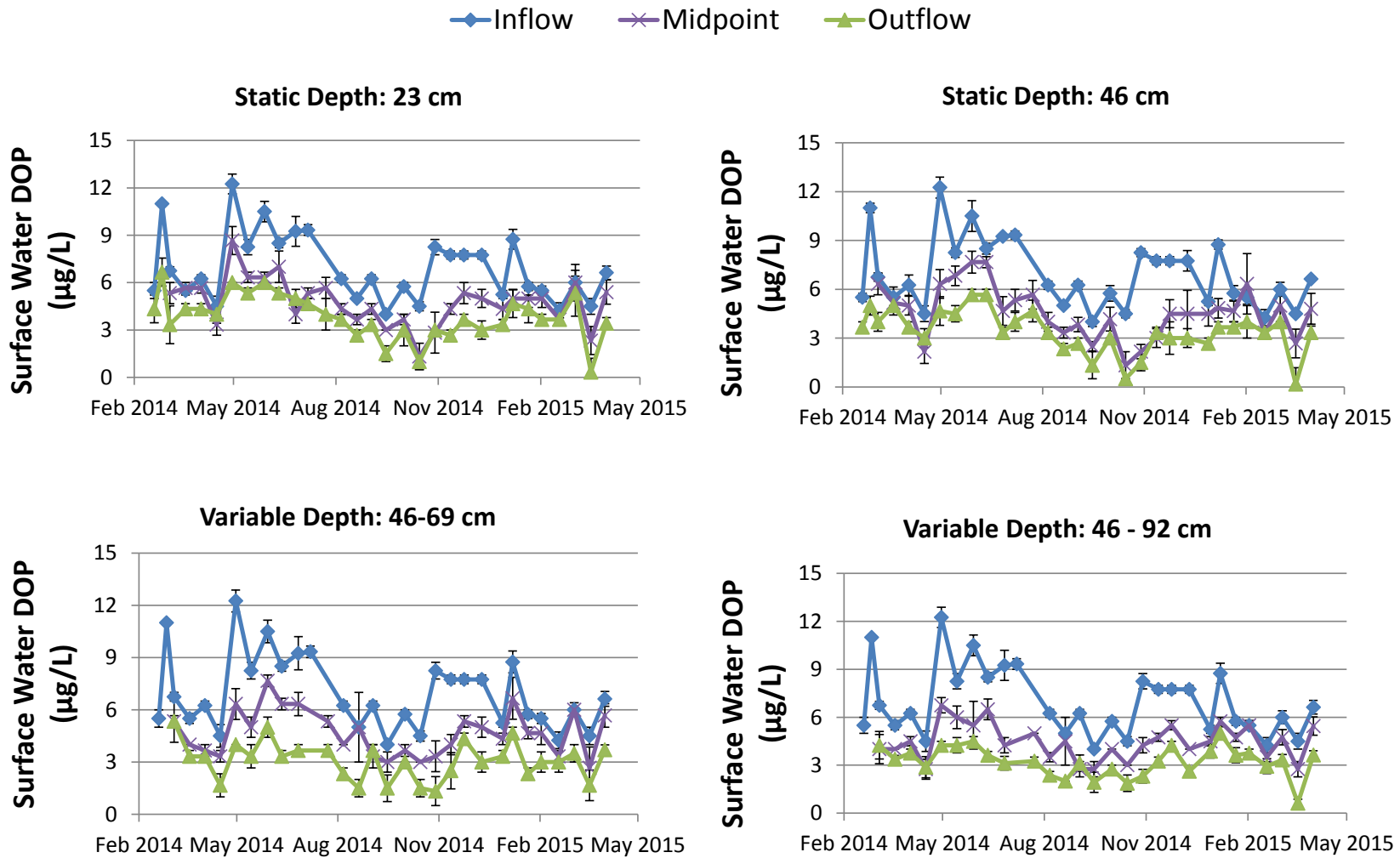


Figure 81. A comparison of dissolved organic phosphorus (DOP) concentrations in the inflow and outflows from the four treatments.

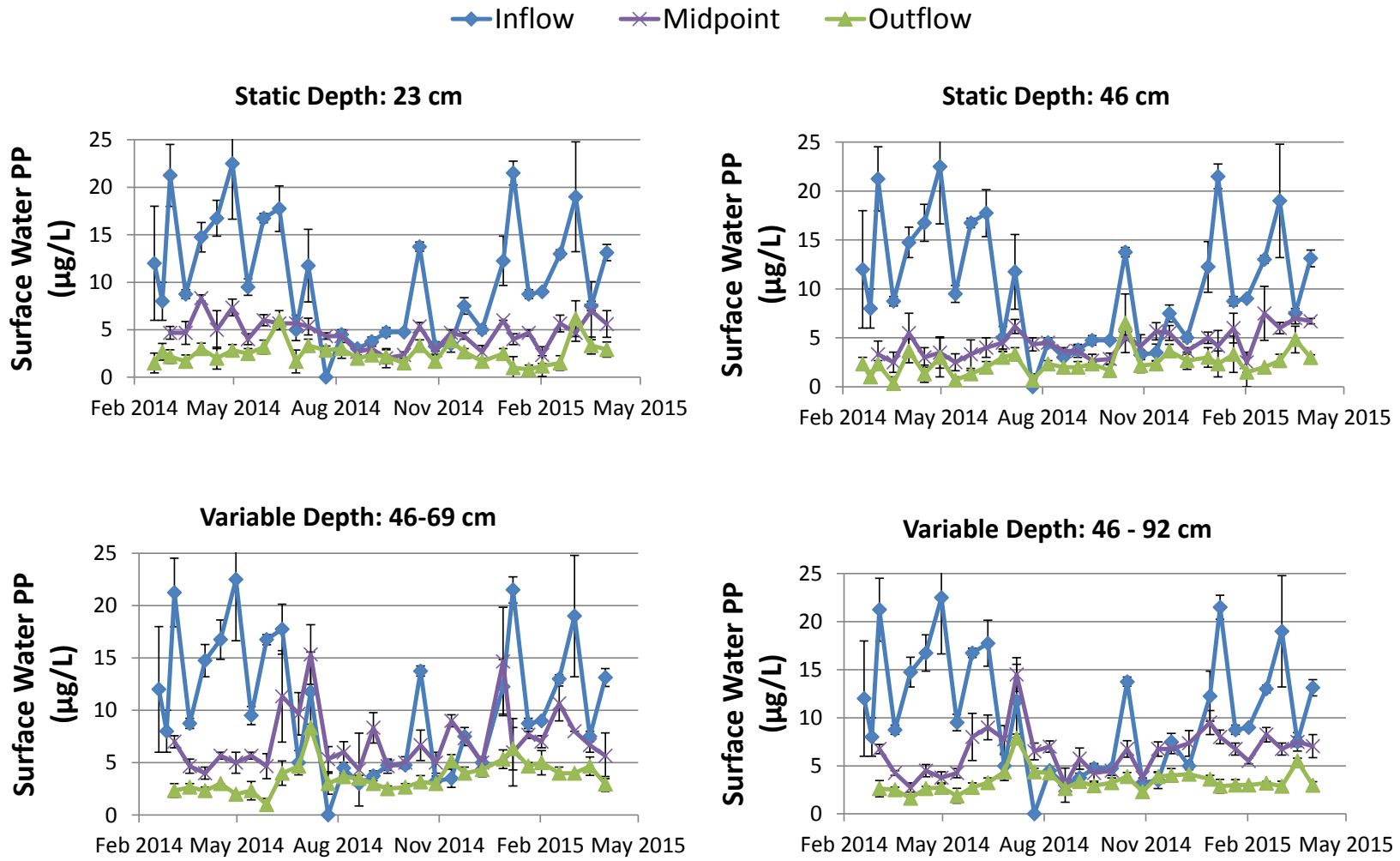


Figure 82. A comparison of particulate phosphorus (PP) concentrations in the inflow and outflows from the four treatments.

4.1.3.2 Discussion

To facilitate our ability to quantify key PSTA design and operational factors, we established a mesocosm PSTA facility in September 2013. This facility is designed to assess effects of static (at 23 and 46 cm) and variable water depths (46 to 69 cm and 46 to 92 cm) on outflow water quality and health of macrophyte and periphyton communities. Additionally, we also are evaluating P loading effects. From December 2013 - April 2015, all of the water depth treatments have provided comparable performance, reducing inflows of 21 $\mu\text{g/L}$ TP to 8 $\mu\text{g/L}$ TP, at a PLR of 0.33 $\text{gP/m}^2\text{-yr}$. Note that this comparable outflow performance has occurred despite widely differing HRTs among treatments. With the variable depth treatments operating at maximum depth, the HRTs for the 23, 46, 69 and 92 cm depth treatments are 5, 10, 15 and 20 days, respectively. At the two greatest water depths, we do see some slight reduction in performance (12-13 $\mu\text{g/L}$) at the midpoint of the process train, versus the midpoint at the shallower depth treatments (11 $\mu\text{g/L}$). These initial findings suggest robust, sustainable performance at depths of 23 and 46 cm, and only a modest penalty, if any, to TP removal performance for depth increases up to 69 and 92 cm. The water depth evaluation trials are continuing.

This mesocosm study also has provided insight into appropriate loading rates. Both the 23cm and 46 cm water depth treatments consist of four tanks in series. The first tank in series has reduced the average 21 $\mu\text{g/L}$ TP levels to a mean of 14 $\mu\text{g/L}$, at a PLR of 1.3 $\text{gP/m}^2\text{-yr}$. Respective TP outflows from the 2nd, 3rd and 4th tanks in series collectively averaged 11, 9 and 8 $\mu\text{g/L}$, at PLRs of 0.7, 0.4, 0.3 $\text{gP/m}^2\text{-yr}$.

4.1.4 Biological Response

4.1.4.1 Results

Comparisons of biological response variables were made between the static depth treatments at 23 and 46 cm for each position down the four-in-series flow ways. Then, as a separate comparison, our variable depth treatments were compared for periods of shallow and deep operations. These comparisons across depth treatments were made for both the first tanks and final tanks in series.

4.1.4.1.1 *Light conditions as a function of depth*

The available PAR at the benthic surface was highest in the shallow treatments, and lowest in the depth-variable treatments (Figure 83). During shallow-phase operations, PAR levels were similar between the two variable depth treatments operating at 46 cm, while under deep-phased operations, the increased water depth in the 46-92 cm water depth treatment reduced PAR to 33% of incident levels, as compared to 65-70% in the shallow 23 cm treatment.

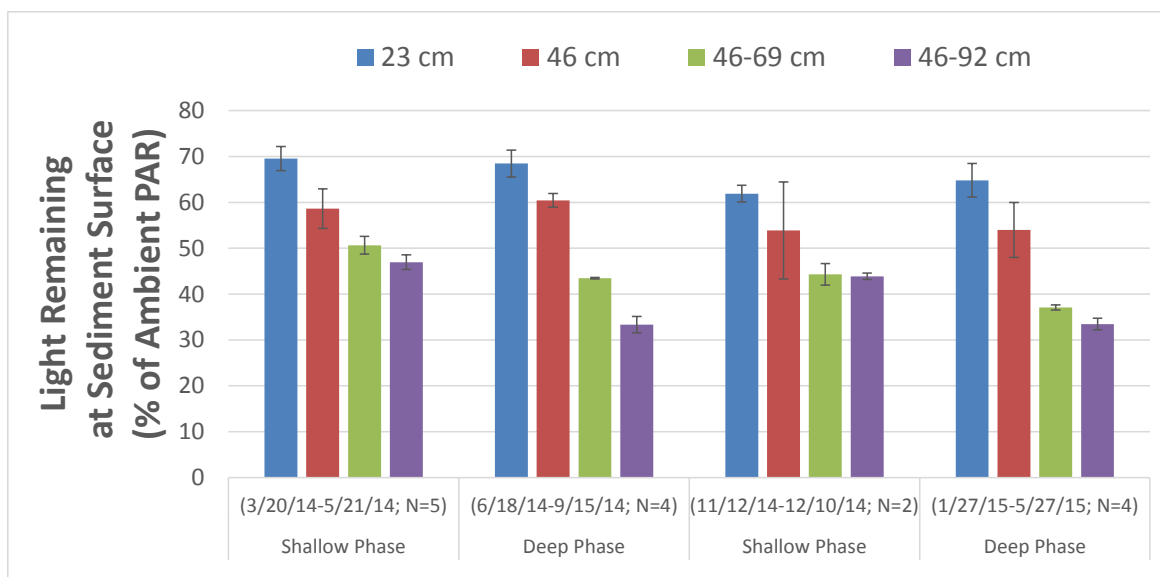


Figure 83. Light remaining at the sediment surface, as a fraction of the ambient light available above the water column, in the outflow region of mesocosms operated under four depth treatments. Error bars denote \pm SE around period averages for triplicate flow ways under each treatment. Light was measured in the photosynthetically-active range (400-700 nm) during midday.

4.1.4.1.2 Areal Biomass of Benthic Periphyton

On May 29, 2014, the static depth mesocosms had been in flow-through operations for 9 months. Biomass of benthic periphyton remained low in the inflow region of mesocosms (1.3 ± 0.4 g/m²) at both 23 cm and 46 cm. However, downstream tanks supported higher levels, especially at 23 cm depth (Figure 84). Repeated sampling of these communities in September 2014 and January 2015 showed increasing biomass over time for a given position along the gradient. One exception was the second tank in series for the shallow (23 cm depth) treatment, which showed no change or a slight decline in biomass over time. The trend of increasing biomass over time was also apparent in the variable depth mesocosms (Figure 85). Gains in biomass were greater in the outflow region than midpoint. It is noteworthy that benthic periphyton did increase in the outflow region between May and September 2014, when the variable depth mesocosms were operated at water depths of either 69 or 92 cm. By contrast, the midpoint sampling indicated that low biomass conditions persisted through this period in those treatments. During the subsequent shallow period (September 2014 – January 2015) areal biomass values increased in the midpoint of variable depth treatments, but to a much smaller degree than the biomass gains over the same period in the outflow region.

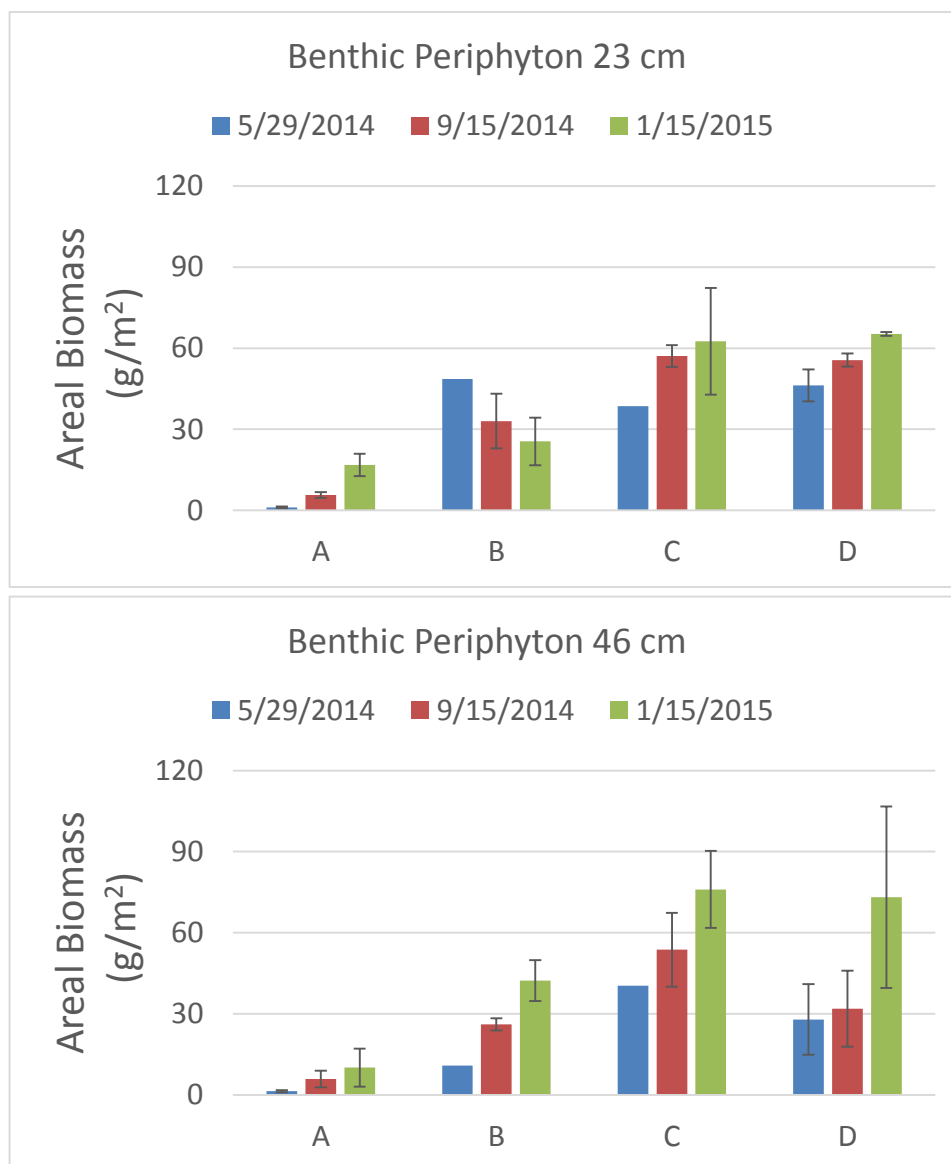


Figure 84. Areal biomass development on the benthic surface of mesocosms operated at either 23 cm or 46 cm water depths. The process trains consisted of four tanks in series, with inflow into “A” tanks and outflow from “D” tanks. The error bars denote the standard error around the mean values from triplicate process trains under each depth treatment.

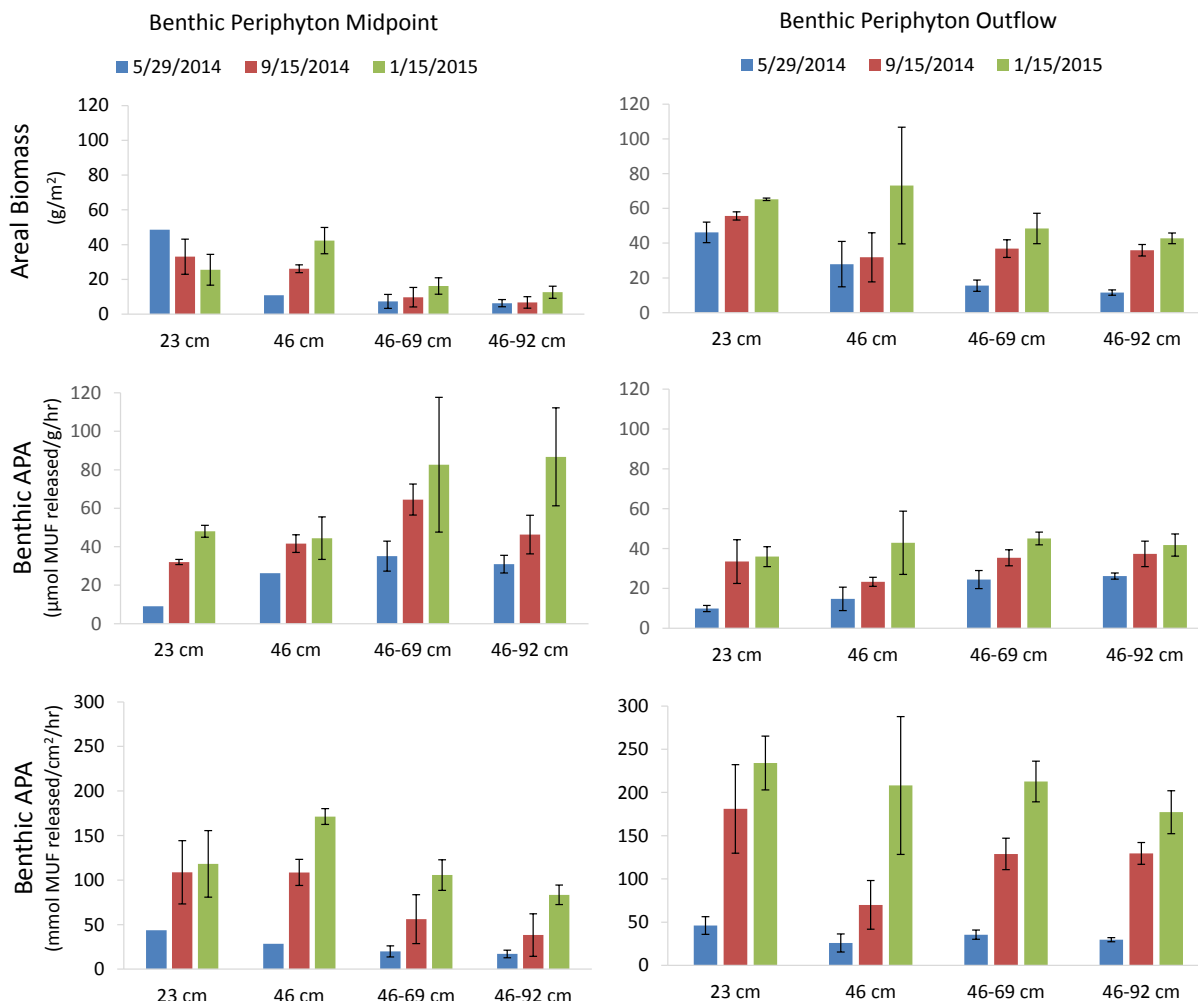


Figure 85. Areal biomass of benthic periphyton grown in mesocosms operated at either static water depth (23 or 46 cm) or variable water depth, on three sampling dates (Top panels). The midpoint and outflow of each flow way was sampled. Benthic periphyton was assayed for alkaline phosphatase activity (APA) and normalized to the dry weight of the periphyton (middle panels) and the benthic surface area supporting periphyton growth (bottom panels). The error bars denote standard error around the mean of values from three replicates under each treatment.

4.1.4.1.3 Biological community development over time

The benthic periphyton mat became established within a few months in the outflow region of the 23 cm deep flow ways (Figure 86). The benthic periphyton in upstream tanks were slower to colonize, and the first tank in series (A) never developed dense mats. *Chara* and *Potamogeton* also did not develop into dense stands, with relative density scores typically less than 3 (Figures 87 and 88).

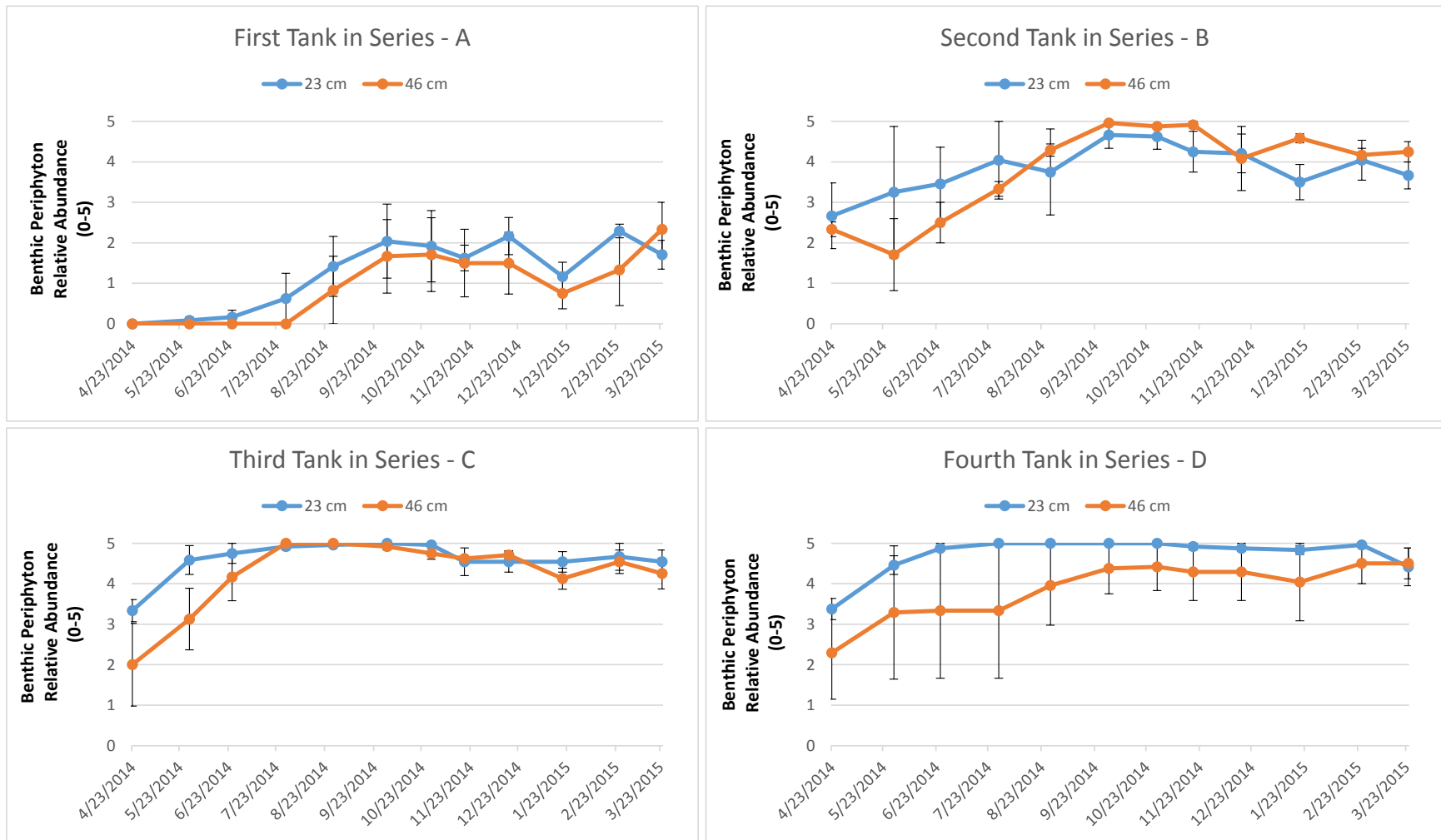


Figure 86. Relative density of benthic periphyton in each of four tanks in series of process trains operated at static water depths of either 23 cm or 46 cm. Values represent the average (\pm SE) of triplicate mesocosms under each depth treatment, and 8 measurements within each tank for each date.

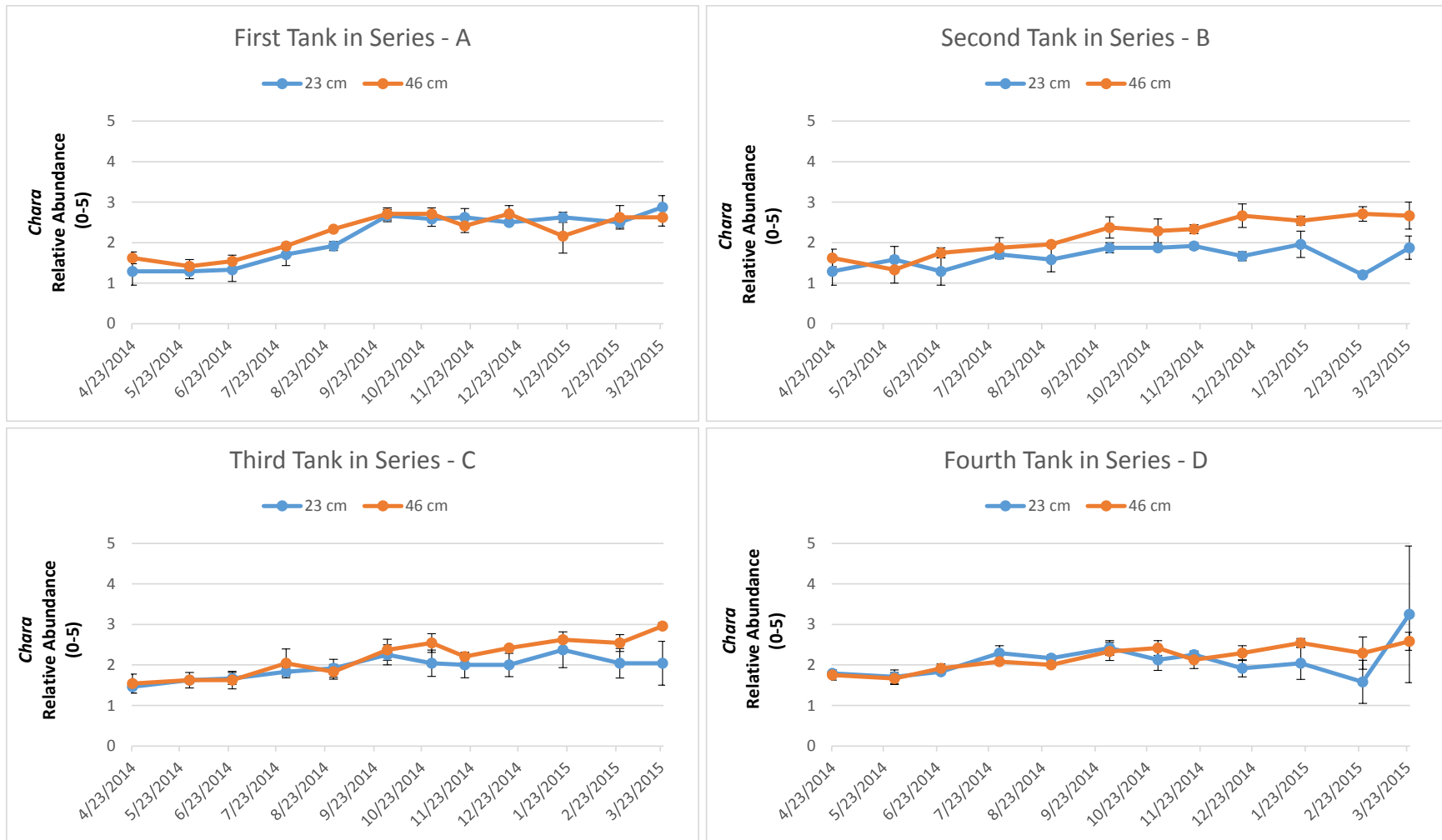


Figure 87. Relative density of *Chara* in each of four tanks in series of process trains operated at static water depths of either 23 cm or 46 cm. Values represent the average (\pm SE) of triplicate mesocosms under each depth treatment, and 8 measurements within each tank for each date.

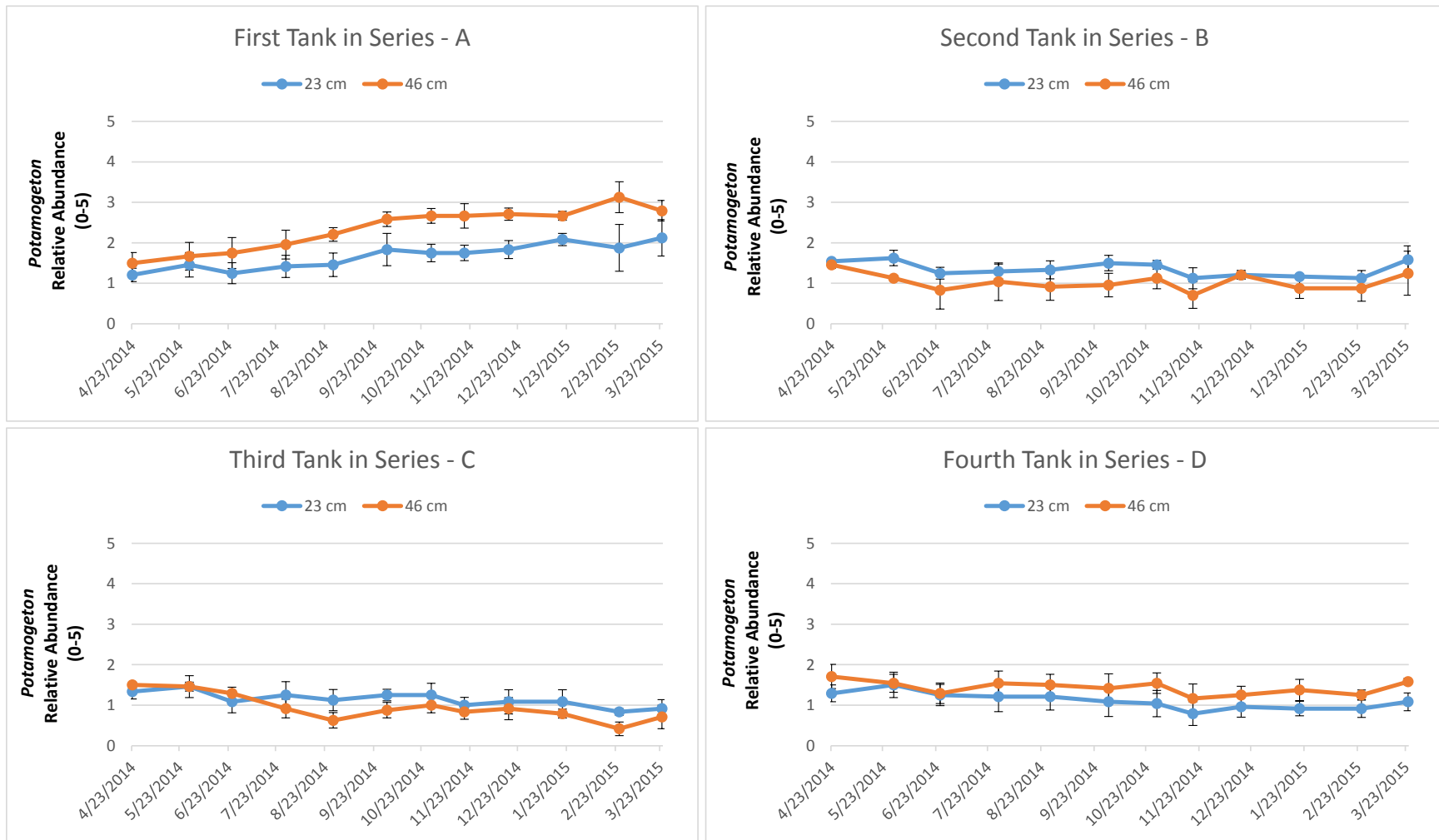


Figure 88. Relative density of *Potamogeton* in each of four tanks in series of process trains operated at static water depths of either 23 cm or 46 cm. Values represent the average (\pm SE) of triplicate mesocosms under each depth treatment, and 8 measurements within each tank for each date.

4.1.4.1.4 *Macrophyte and periphyton responses to water depths*

Effects of water depth on benthic periphyton and macrophytes are shown in Figures 89 - 91. *Chara* density in the B tanks was higher at 46 cm than 23 cm late in the period of record, but little effect of depth was evident for *Chara* at other positions in the flow way (tanks A, C, or D). Relative density of the benthic periphyton generally was not negatively affected by deeper (46 cm) water depths, with the exception of the first few months for the B, C, and D tanks. The last tank in series in the shallowest treatment maintained a very dense benthic mat, while the average density of the last tank in series for the 46 cm treatment was somewhat lower. *Potamogeton* density was consistently higher at 46 cm than 23 cm in the first tank in series. This relationship, however, was not observed consistently at other positions further down the gradient.

4.1.4.2 Discussion

Biofilm development occurred sooner after startup, and closer to the inflow, in mesocosms with shallow water depths (23 cm). Benthic mat relative density was strongly affected by the deep water conditions that occurred in variable-depth treatments between May and September 2014, but this effect was evident only in the upstream tanks. At the beginning of the second deep-water period (January - April 2015), no such effect was observed.

Periphyton enzyme activity on a relative weight basis was higher at the midpoint than at the outflow. Periphyton biomass per unit area of the benthic surface was greatest near the outflow, however, which resulted in the highest enzyme activity per unit benthic surface area in the outflow region.

Potamogeton and *Chara* were able to persist across a range of water depths (23-92 cm), but did not achieve high relative biomass density values in these mesocosms. *Chara* density was similar across each of the four tanks in series of static depth treatments, while *Potamogeton* exhibited higher biomass in the inflow region, as compared to the outflow region, suggesting nutrient limitation to plant growth on the low-nutrient rock substrates.

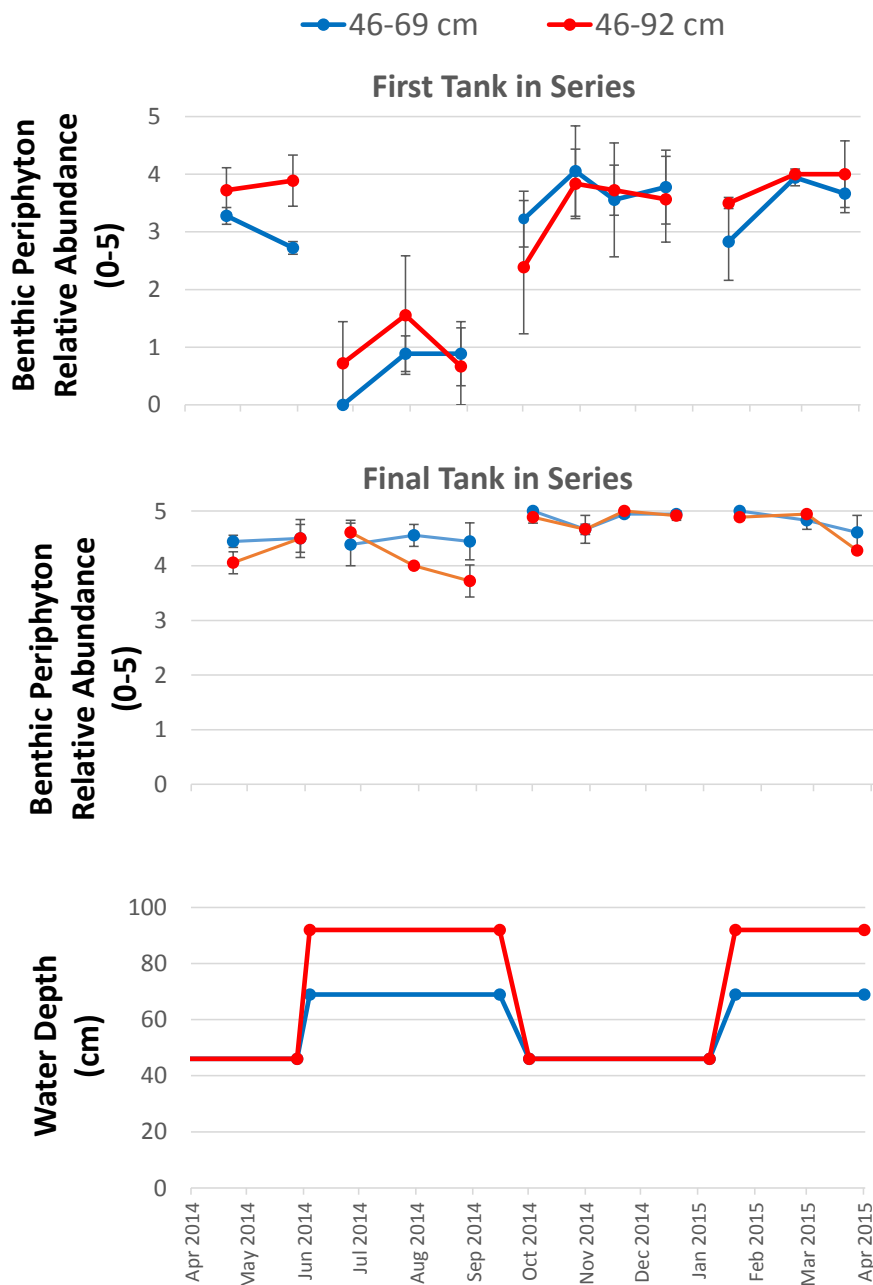


Figure 89. Relative density of benthic periphyton in the first tank in series (top panel) of process trains operated at variable water depths of either 46-69 cm or 46-92 cm. (bottom panel). Values represent the average (\pm SE) of triplicate mesocosms under each depth treatment, and 9 measurements within each tank for each date.

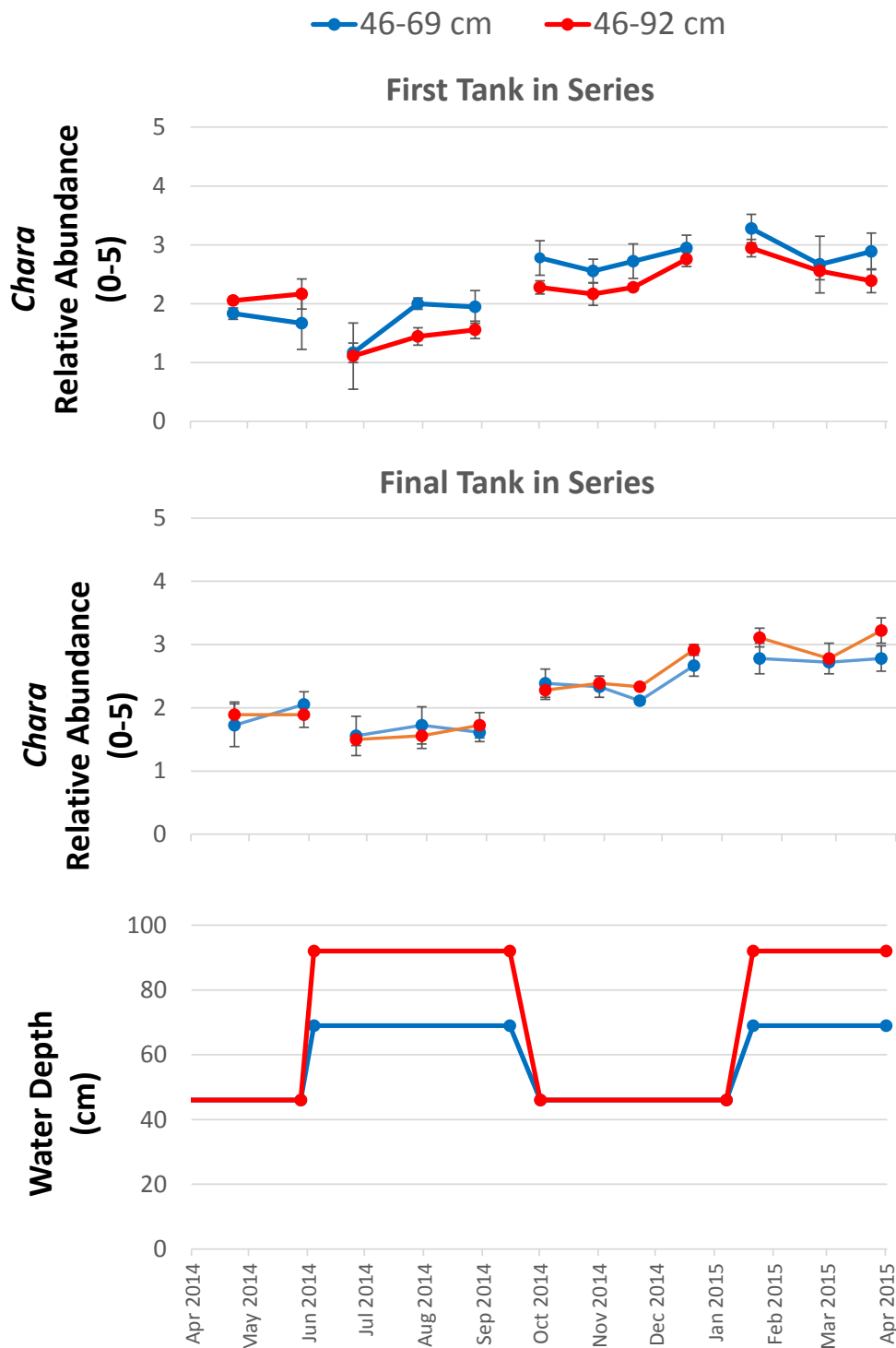


Figure 90. Relative density of *Chara* in the first tank in series (top panel) of process trains operated at variable water depths of either 46-69 cm or 46-92 cm. (bottom panel). Values represent the average (\pm SE) of triplicate mesocosms under each depth treatment, and 9 measurements within each tank for each date.

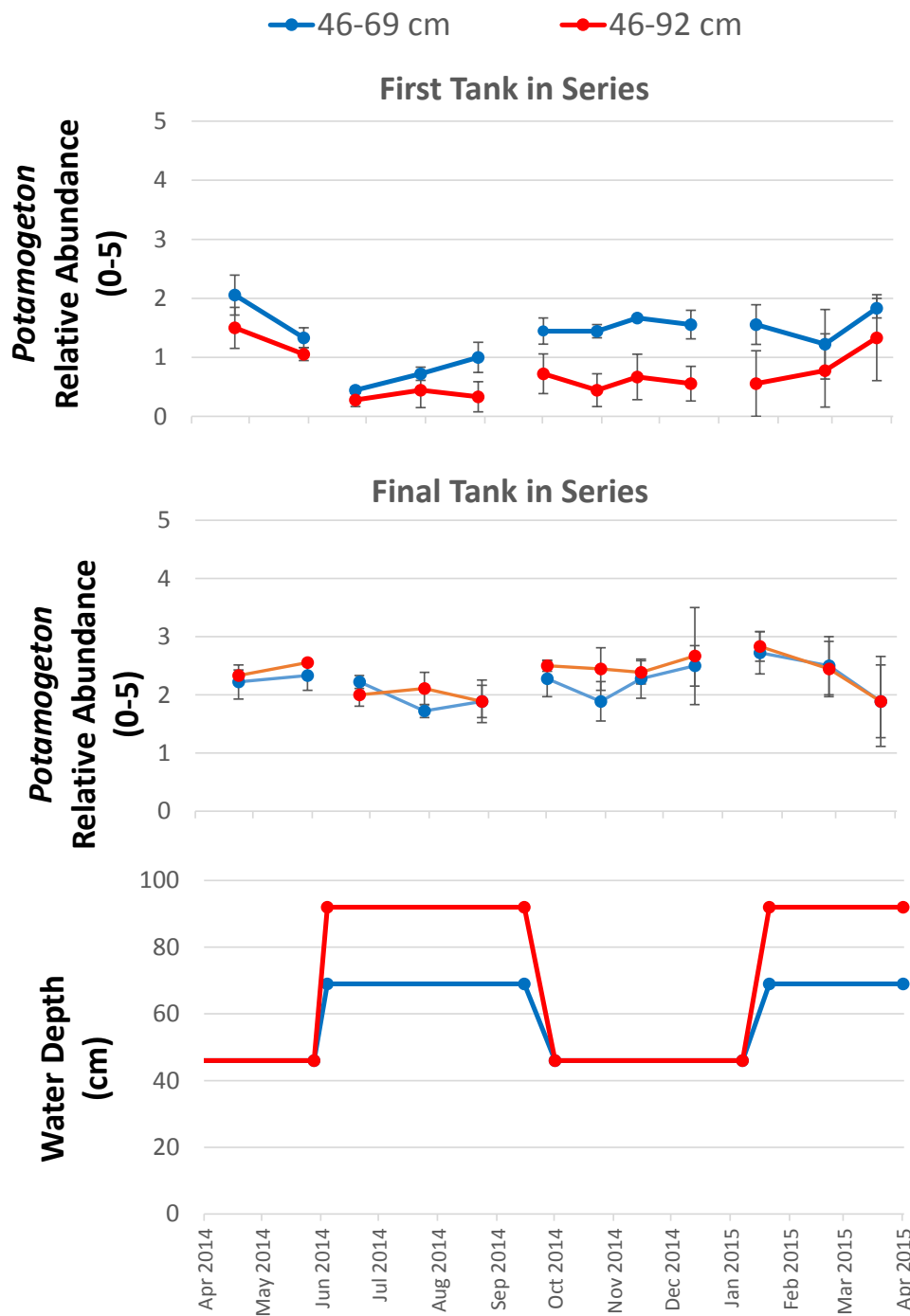


Figure 91. Relative density of *Potamogeton illinoensis* in the first tank in series (top panel) of process trains operated at variable water depths of either 46-69 cm or 46-92 cm. (bottom panel). Values represent the average (\pm SE) of triplicate mesocosms under each depth treatment, and 9 measurements within each tank for each date.

4.2 PSTA Substrate Effects on Vegetation and Water Column Chemistry

4.2.1 Introduction

While phosphorus removal performance of the STA-3/4 PSTA cell has remained relatively consistent over time, it is important to determine whether the accumulating marl material ultimately may impair P removal effectiveness. In order to better define the relationship between substrate type/conditions and P removal performance, a soil-water “column” study was performed under controlled conditions, using replicated experimental units.

In the initial phase of this two-phase column study, we addressed two questions: 1) Does the accrual of sediment in the PSTA cell increase water column P concentrations (presumably by increasing soil-P flux), relative to the original limerock substrate?, and 2) Does removal of the accrued layer and/or upper muck soil layer in a conventional “muck-based” wetland affect water column P (presumably by decreasing soil P flux)? In the second phase of the study, we incorporated a treatment to evaluate P removal from waters overlying an intact core (complete with accrued sediments and associated biota) collected from a well-performing muck-based wetland.

4.2.2 Methods

Outdoor soil-water columns were constructed with one of four substrate types (Figure 92). To address the first question (above), two substrates (a bare limerock substrate, and limerock covered with accrued-layer marl sediments from the PSTA cell) were established. These substrate materials were collected from near the outflow of the PSTA cell. To address the second question, intact muck soil cores were collected from the flow way adjacent to the PSTA cell (i.e., the Lower SAV Cell) where, in contrast to the PSTA Cell, muck sediments were not removed during STA construction. The accrued sediment layer was removed from one set of intact soil cores to expose the upper muck soil layer (hereafter referred to as the “Upper” treatment). To another set of cores, both the accrued sediment layer and the upper 10 cm of muck soils were removed to expose a lower muck layer (hereafter, “Lower”).

At the time of intact muck soil core collection, three additional cores were collected and sectioned in the field to characterize P contents of the accrued sediment layer and muck soils in the 0-10, 10-20 and 20-30 cm depth layers. Approximate total depth of the muck soil at the collection location (outflow region of the Lower SAV Cell) was 46 ± 2 cm, with an accrued layer 5 ± 1 cm thick.

After the initial phase, a second phase of the study was conducted to evaluate an additional question: Does a bare limerock surface result in lower water TP concentrations than a muck soil with an intact surficial sediment layer from a well-performing STA flow way? To evaluate this question, fresh limerock and PSTA sediments were collected from the PSTA Cell to re-establish columns under the limerock (LR) and PSTA sediment treatments from Phase I. A new treatment, “Muck (3B)” was established using muck soils collected from STA-3/4 Cell 3B

outflow region. The western flow way in STA-3/4 (which consists of cells 3A and 3B, in series) was considered a better representation of a well-performing, muck-based flow way than the Lower SAV Cell.

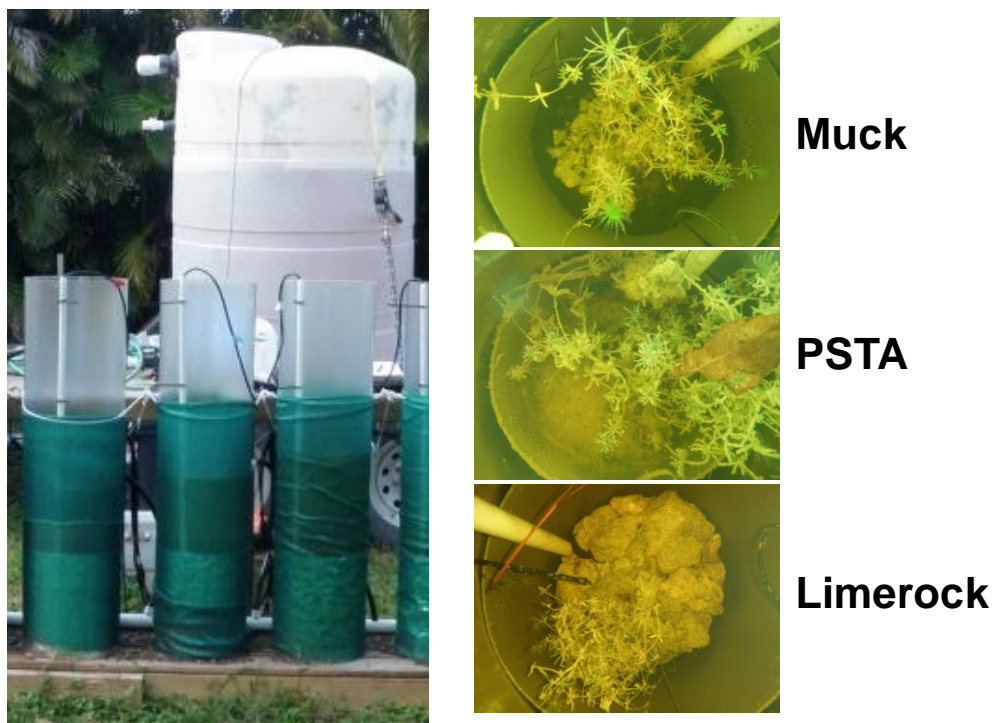


Figure 92. Photo of the experimental soil-water columns, and inflow water reservoir (left). Photos on the right depict the mixture of macrophytes (*Chara*) and algae in three of the treatments.

We elected to maintain the “Upper” and Lower” treatments from Phase I through the Phase II monitoring period to allow for a longer-term evaluation of the consequences of partial muck removal.

Soil/substrate depths in the columns were 10-13 cm, and water depths were maintained at 45 cm. At the time of setup, each column was inoculated with an aliquot of *Chara* and calcareous periphyton. Inflow waters to the column study were collected from the outflow of STA-2 Cell 3. This water was fed continuously to the columns at a hydraulic loading rate of 5 cm/day.

4.2.2.1 Water sampling and analyses

Water samples were collected as follows. An initial unfiltered grab sample was used for TP and enzyme assays. Temperature and pH were also measured. Subsequent grabs were used for the remaining analytes (TSP, SRP). Water samples were collected weekly for TP, pH and temperature determination. On a bi-weekly basis, SRP, TSP and enzyme activity was also

measured. Flow rates were maintained through periodic measurements at each column, and bi-weekly cleaning of the inflow lines.

4.2.2.2 Characterization of periphyton growth and composition

During conduct of the study, periphyton biofilms colonized the submerged walls of the columns. This periphyton was quantitatively sampled in June 2013 to provide a measure of standing crop development, which presumably would be associated with concentrations of bioavailable nutrients in the water column. Enzyme (alkaline phosphatase and phosphodiesterase) activities of the harvested biofilm materials also were measured.

Upon conclusion of Phase II of the study, the plant tissues were harvested from each column and analyzed for dry weight biomass and tissue P contents.

4.2.2.3 Sediment sampling and analyses

Upon conclusion of the Phase II study, sediments were sampled with a 7-cm diameter acrylic core, and the upper 5 cm layer was retained for analysis. Duplicate sediment samples were collected from two columns. Large fragments of macrophytes or benthic algae were removed from all sediment samples. The “sediments” collected from the exposed limerock treatments were comprised of recently settled material and contained benthic algae that could not be isolated or removed from sediment. This resulted in its inclusion in the sediment sample.

Enzyme assays were performed at the laboratory on September 12 and 13, 2013. Sediments were sub-sampled to prepare a diluted solution for assay and dry weight analysis. A second aliquot of sediment was dried for bulk density, then ground and analyzed for TP, TN, TC, TOC, and TCa.

4.2.3 Results

4.2.3.1 Phosphorus content of column substrates

PSTA sediments used in the column experiment contained 264 ± 33 mg P/kg prior to Phase I (measured in May 2012) and 195 ± 17 mg P/kg prior to Phase II (measured in March 2013). TP contents in the Lower SAV Cell were 527 – 773 mg/kg and 291 – 487 mg/kg for the accrued and muck layers, respectively (Figure 93). Cell 3B soils contained 634-760 mg P/kg in the accrued layer prior to the experiment.

Nitrogen content was 2.5-2.9 % dry wt. in the accrued and muck soil layers from the outflow region of the Lower SAV Cell, while PSTA accrued sediment and underlying muck were lower, with 0.9 % and 1.2 % N, respectively (Figure 93). In contrast with N contents, P contents decreased with depth in the muck soil profile within the Lower SAV Cell muck soils that were selected for the partial muck removal treatments (Figure 93).

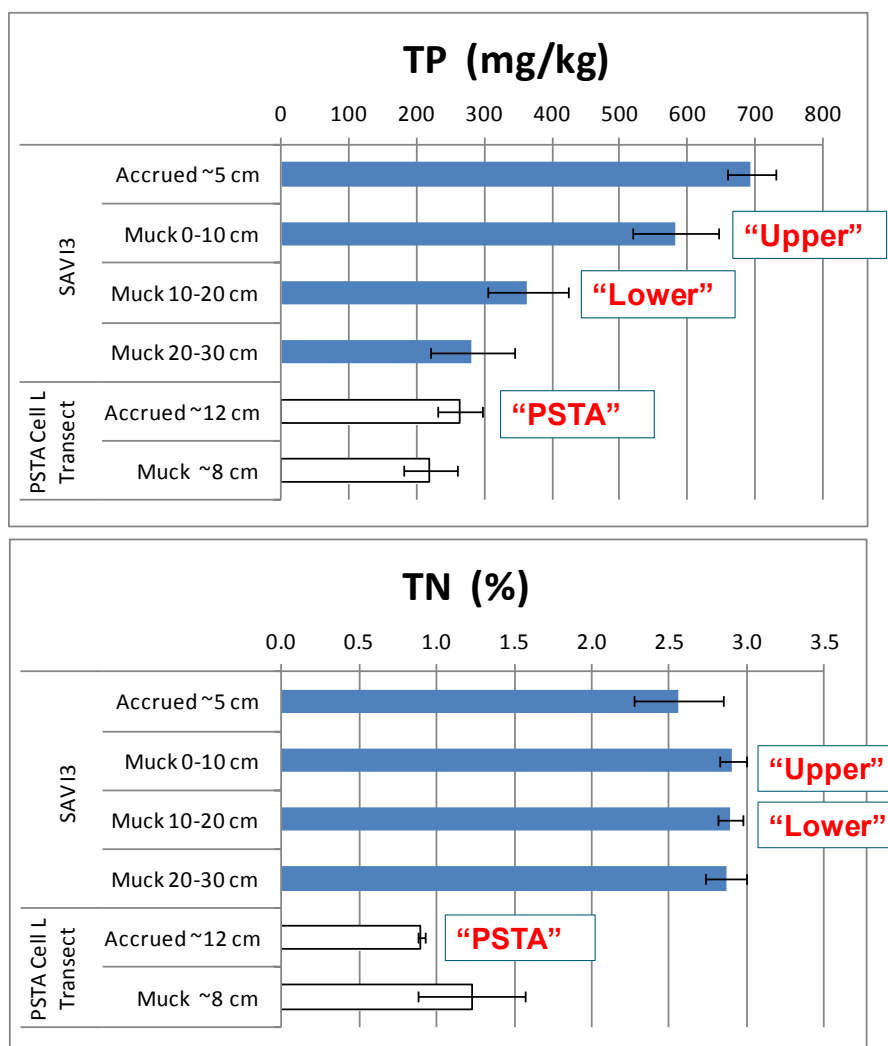


Figure 93. Total phosphorus (TP) and total nitrogen (TN) contents of sediments collected May 31 and August 22, 2012 from the outflow regions of the PSTA Cell and Lower SAV Cell, respectively. Error bars denote ± 1 SE around the average of 3 replicates.

4.2.3.2 Water Column Phosphorus and Enzyme Activity

During Phase I, water column TP concentrations were reduced from 19 $\mu\text{g/L}$ in the inflow waters to 16 ± 1 $\mu\text{g/L}$ in the PSTA sediment treatment, and to 11 ± 0 $\mu\text{g/L}$ in the LR treatment (Figure 94). During Phase II, by contrast, LR and PSTA treatments performed similarly, with outflows from both treatments (12 ± 2 and 13 ± 1 $\mu\text{g/L}$) markedly lower than the 18 $\mu\text{g/L}$ inflow TP concentration. Upper and Lower treatments reduced TP concentrations to 15 and 16 $\mu\text{g/L}$ in Phase I and 17 and 15 $\mu\text{g/L}$ in Phase II (Figure 95). Outflow P concentration reductions were dominated by particulate P in Phase I and DOP in Phase II, regardless of treatment (Figures 96 through 99). Enzyme activity was elevated in inflow waters and PSTA columns, relative to

levels observed in waters above LR, Upper or Lower treatments during both phases (Figure 100 and Figure 101).

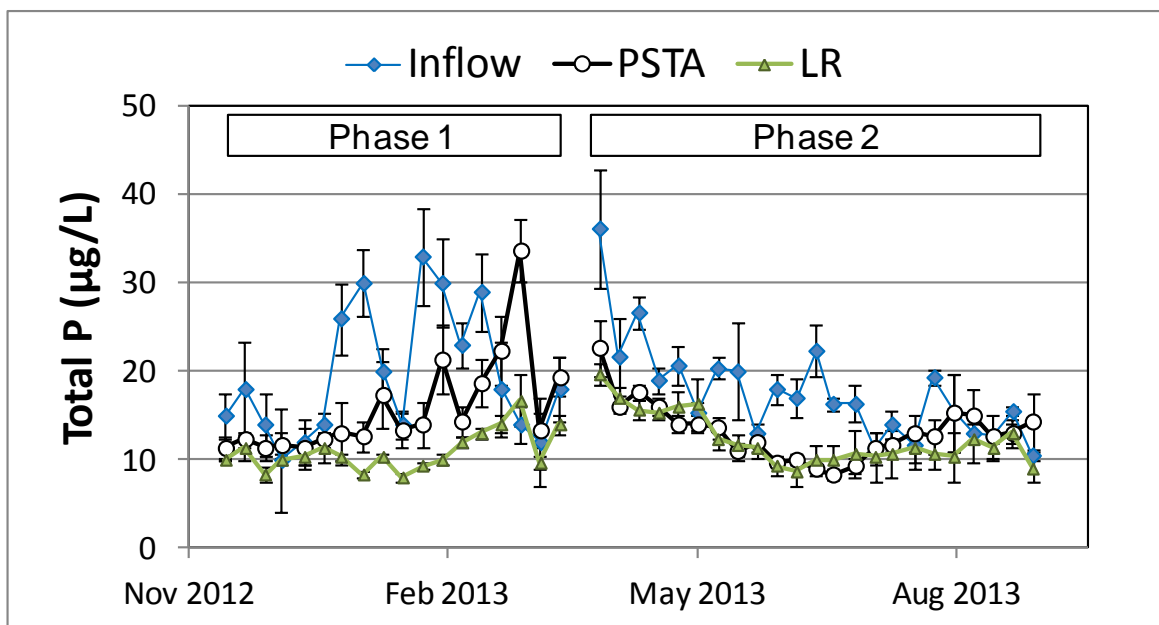


Figure 94. Total phosphorus (TP) concentrations in the inflow waters to experimental columns and in the surface waters above PSTA sediment and exposed limerock (LR) substrate treatments, during the period of record (November 28, 2012 - September 11, 2013). Error bars denote standard error around three replicates.

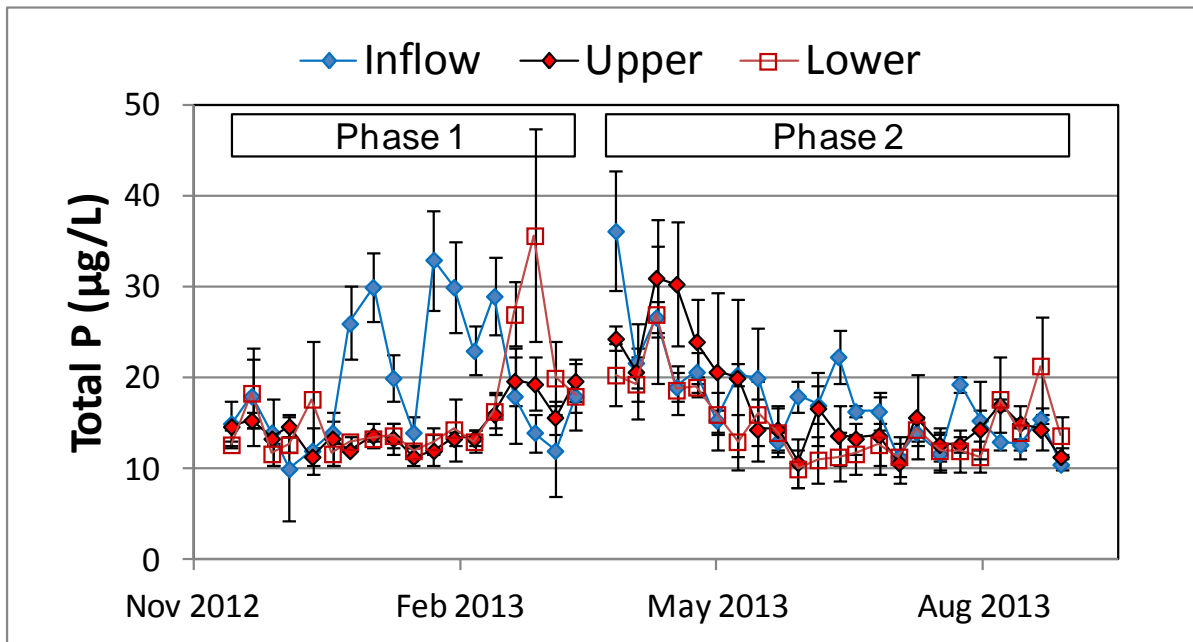


Figure 95. Total phosphorus (TP) concentrations in the inflow waters to experimental columns and the surface waters above two substrate treatments, during the period of record (November 28, 2012 – September 11, 2013). Error bars denote standard error around three replicates.

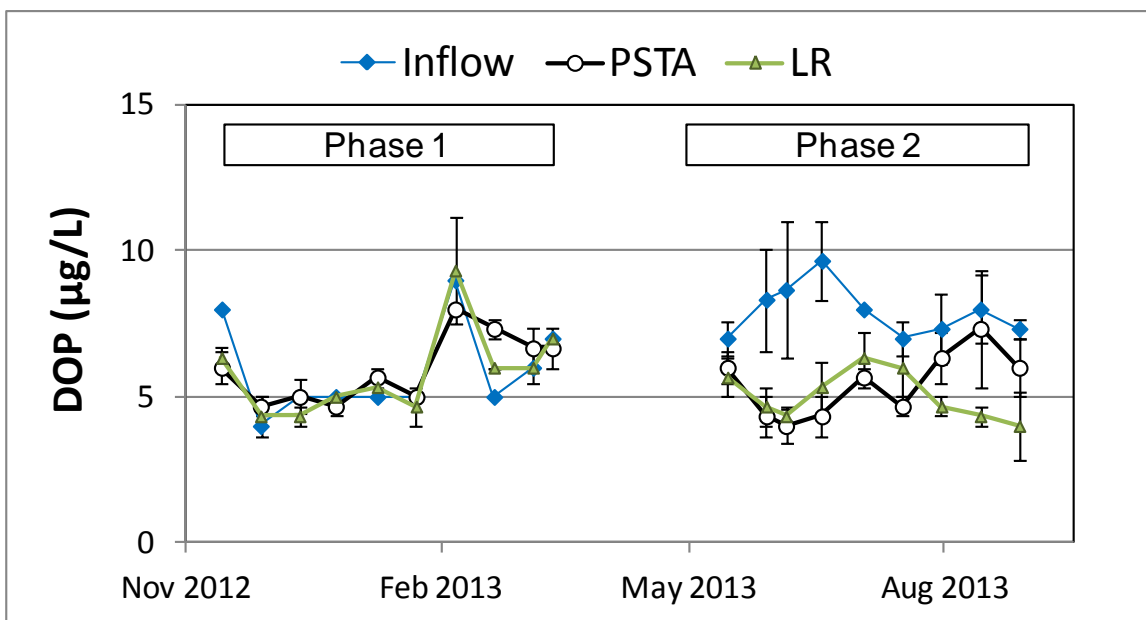


Figure 96. Dissolved organic phosphorus (DOP) concentrations in the inflow waters to experimental columns and in the surface waters above PSTA sediment and exposed limerock (LR) substrate treatments, during the period of record (November 28, 2012 – September 11, 2013). Error bars denote standard error around three replicates.

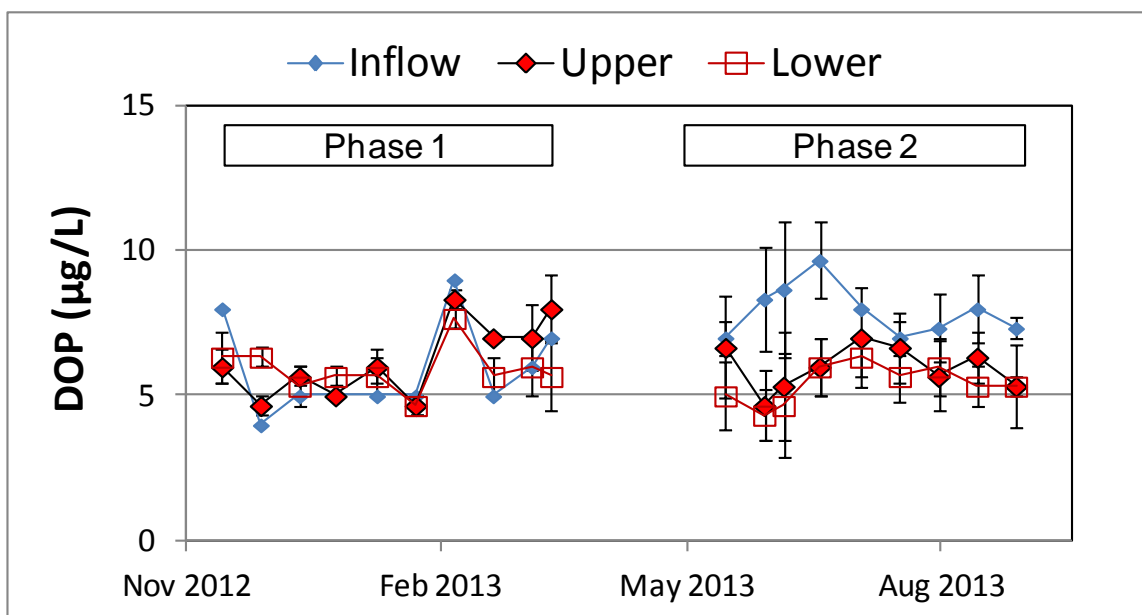


Figure 97. Dissolved organic phosphorus (DOP) concentrations in the inflow waters to experimental columns and in the surface waters above two muck substrate treatments, during the period of record (November 28, 2012 – September 11, 2013). Error bars denote standard error around three replicates.

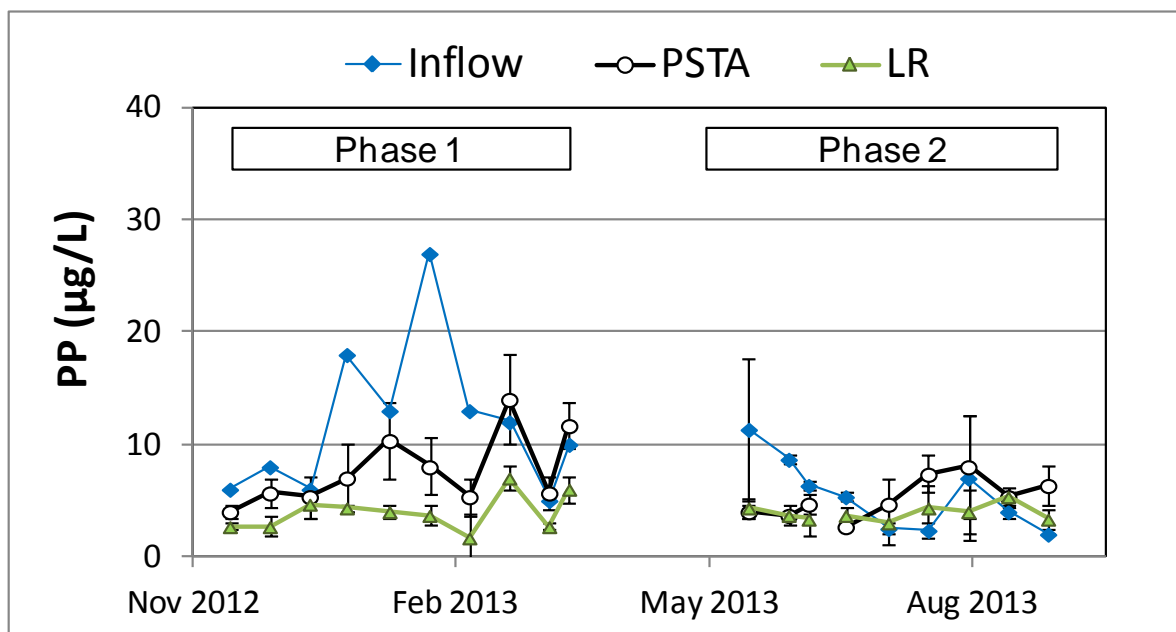


Figure 98. Particulate phosphorus (PP) concentrations in the inflow waters to experimental columns and in the surface waters above PSTA sediment and exposed limerock (LR) substrate treatments, during the period of record (November 28, 2012 – September 11, 2013). Error bars denote \pm SE around the mean of three replicates under each treatment.

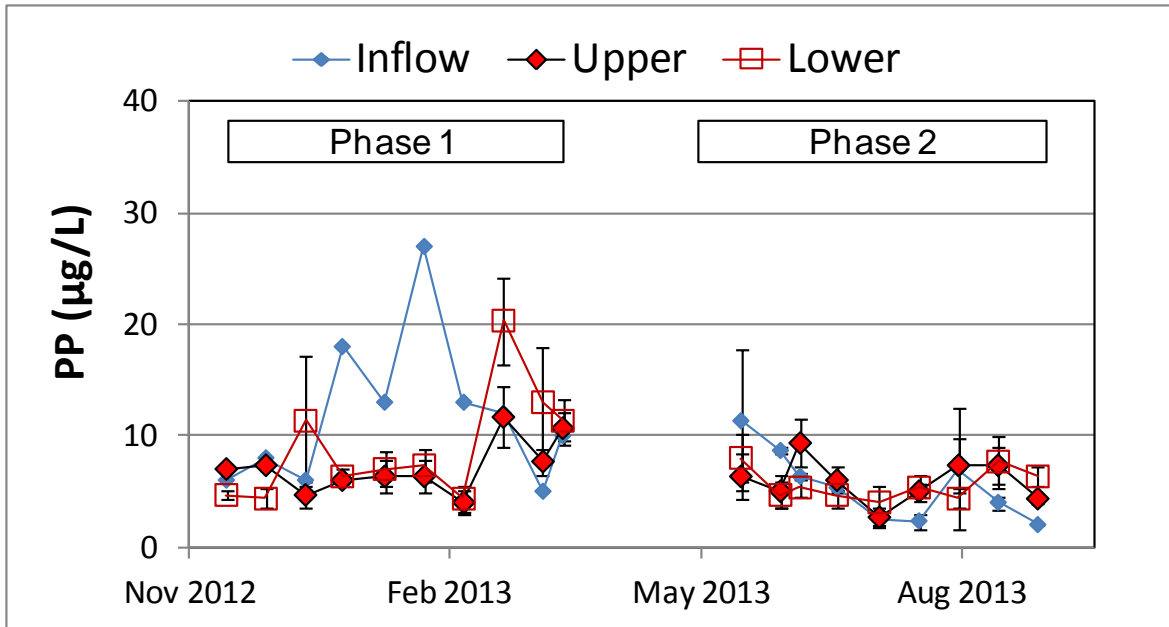


Figure 99. Particulate phosphorus (PP) concentrations in the inflow waters to experimental columns and in the surface waters above two muck substrate treatments, during the period of record (November 28, 2012 – September 11, 2013). Error bars denote \pm SE around the mean of three replicates under each treatment.

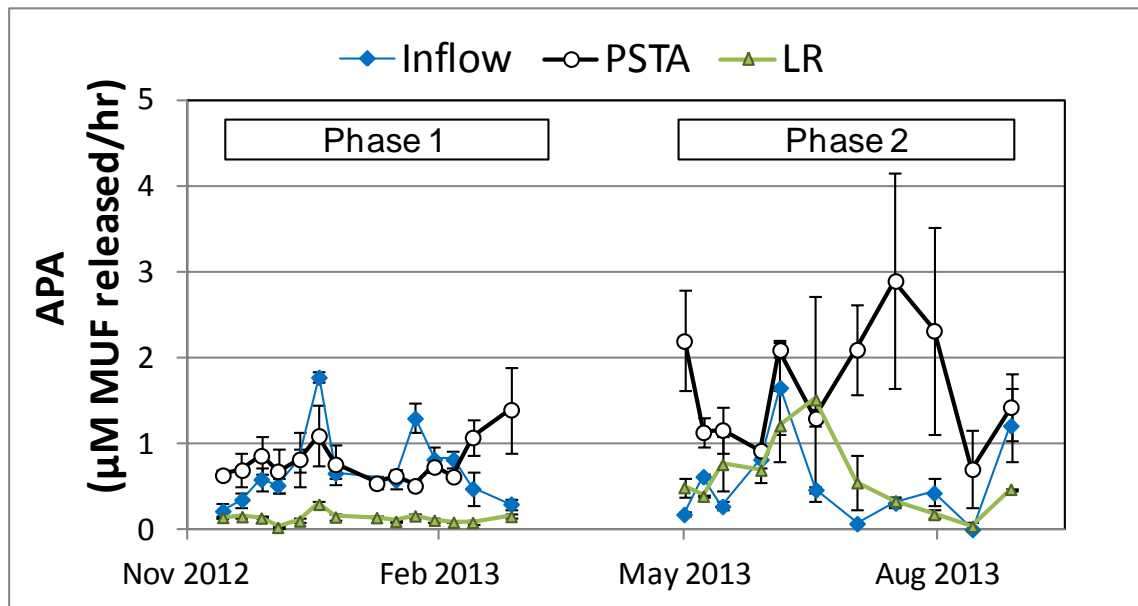


Figure 100. Alkaline phosphatase activity (APA) in the surface waters above PSTA sediment and exposed limerock (LR) substrate treatments, during the period of record (November 28, 2012 – September 11, 2013). Error bars denote standard error around three replicates.

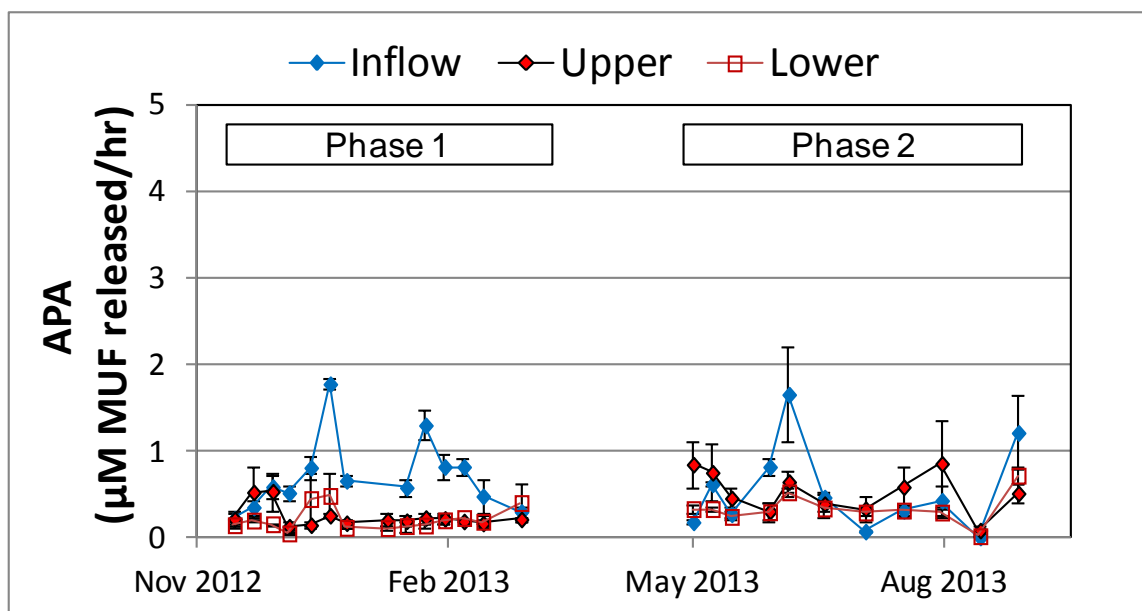


Figure 101. Alkaline phosphatase activity (APA) in the inflow waters to experimental columns and the surface waters above two substrate treatments, during the period of record (November 28, 2012 – September 11, 2013). Error bars denote standard error around three replicates.

4.2.3.3 Effects of exposed_limerock, accrued PSTA sediments and intact muck soils on water column P and enzyme concentrations

A comparison of outflow TP concentrations between LR, PSTA and intact muck substrates showed that the newly accrued PSTA sediment provided equal P removal performance to the exposed LR, while P removal performance by muck soil from Cell 3B was substantially less effective (Figures 102 and 103). On average the APA and PDE hydrolysis rates in the overlying water were elevated in the PSTA-sediment treatment, as compared to the LR and muck-soil treatments or the column inflow water (Figure 104).

The effects of substrate type on periphyton growth and enzyme activity indicated higher growth in PSTA sediment and intact Cell 3B muck soils treatments than in the exposed LR treatment (Figure 105). On a dry weight basis, this periphyton exhibited the highest enzyme activity (APA) within the columns established on PSTA sediments (Figure 106), which agreed with the observed differences between treatments in long-term average surface water enzyme activity. When soil enzyme activity was assayed at the conclusion of Phase II, LR “sediment” contained the highest enzyme activity, though the sample consisted largely of recently settled periphyton and macrophyte tissues. PSTA sediment exhibited higher activity than did the intact muck soil from Cell 3B (Figure 107).

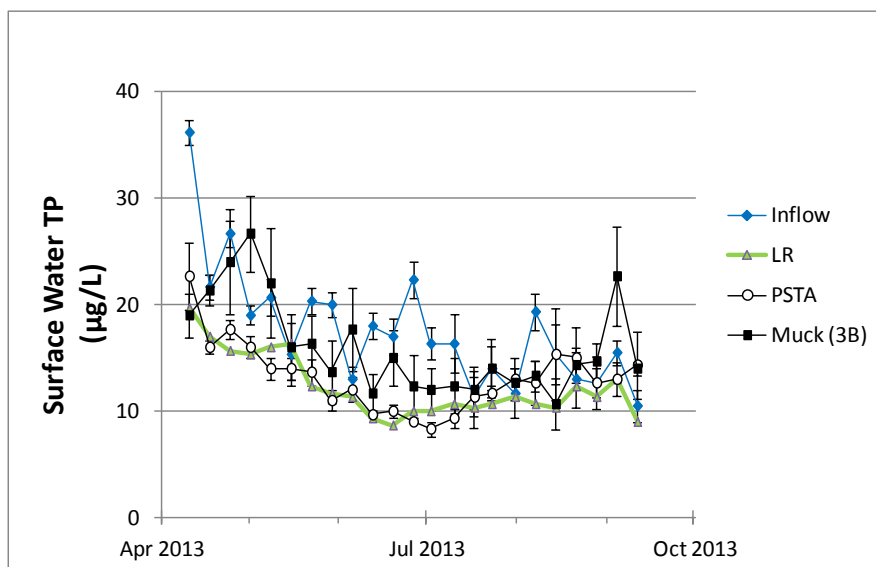


Figure 102. A comparison of water column TP concentrations in flow-through columns established on PSTA sediments and muck soils from Cell 3B of STA-3/4, during the period from April 10 – September 11, 2013.

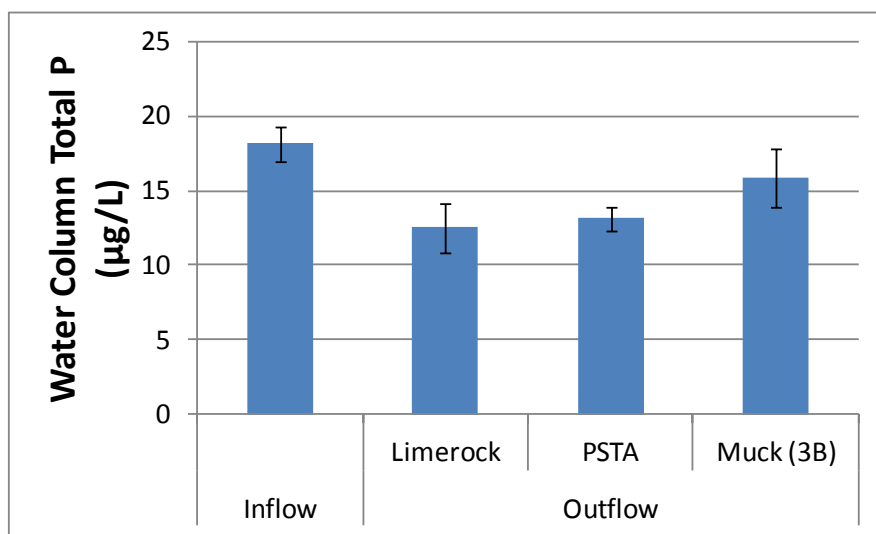


Figure 103. Average (\pm SE) inflow or water column total phosphorus (TP) concentrations in triplicate columns established on limerock (LR), muck sediments (STA-3/4 Cell 3B), or PSTA sediments, for the period April 10 – September 11, 2013 (N=23).

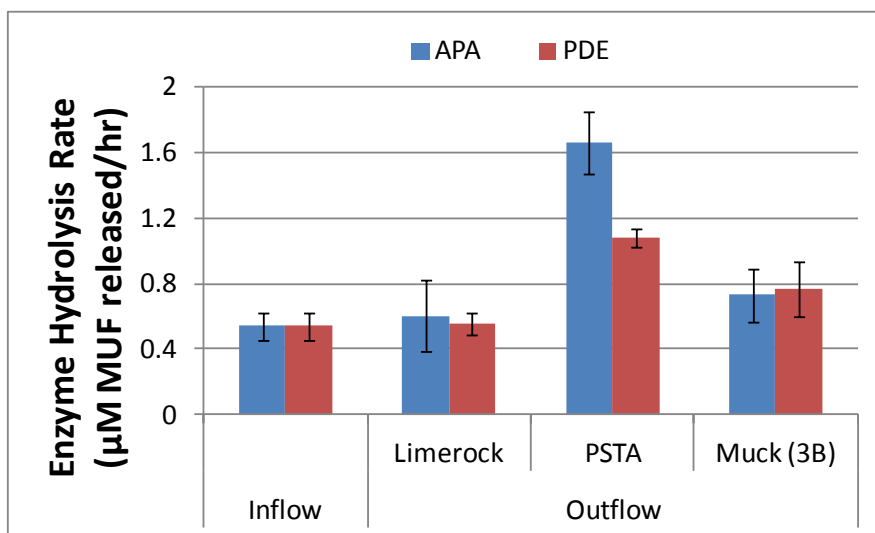


Figure 104. Enzyme hydrolysis rate of inflow and outflow waters in columns established on 3 substrate types, over the period of record (May 15, 2013 - September 11, 2013; N= 11 bi-weekly sampling events). Error bars denote \pm SE around the mean from triplicate columns on each substrate.

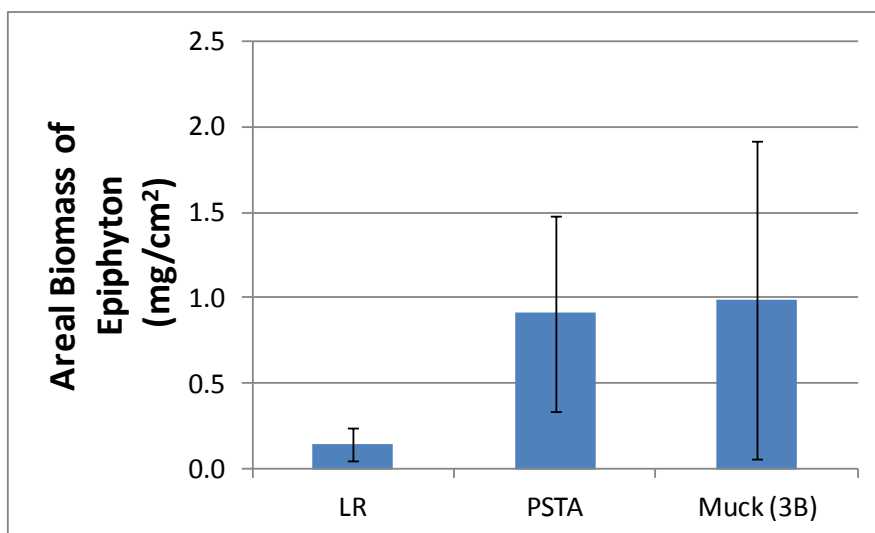


Figure 105. Areal biomass of periphyton growing on the walls of experimental columns established on three substrates: exposed limerock (LR), PSTA sediment, and muck sediments from STA-3/4 Cell 3B. Error bars denote \pm SE around the mean from triplicate columns under each substrate.

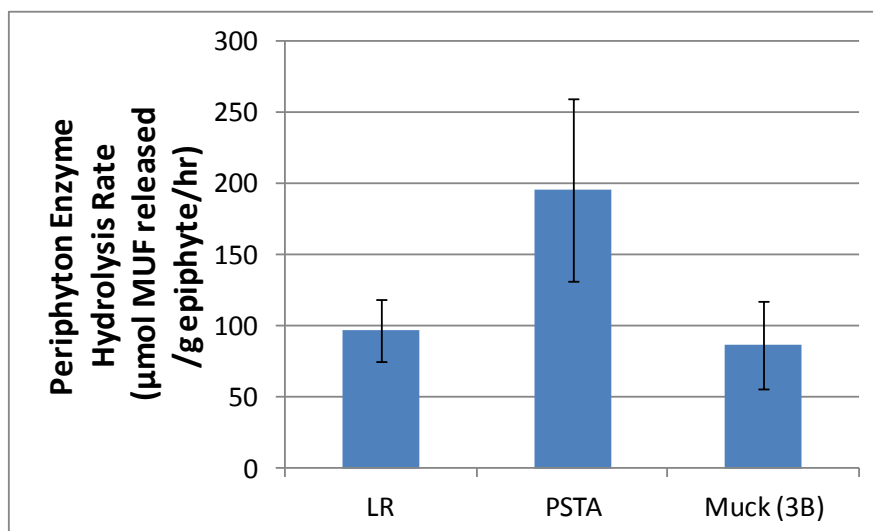


Figure 106. Enzyme (monoesterase) activity in periphyton (June 2013) collected from the fiberglass walls of experimental columns established on three substrates: exposed limerock (LR), PSTA sediments, and muck soils from STA-3/4 Cell 3B. Enzyme hydrolysis rates were normalized to the dry weight of the periphyton as assayed. Error bars denote \pm SE around the mean from triplicate columns for each treatment.

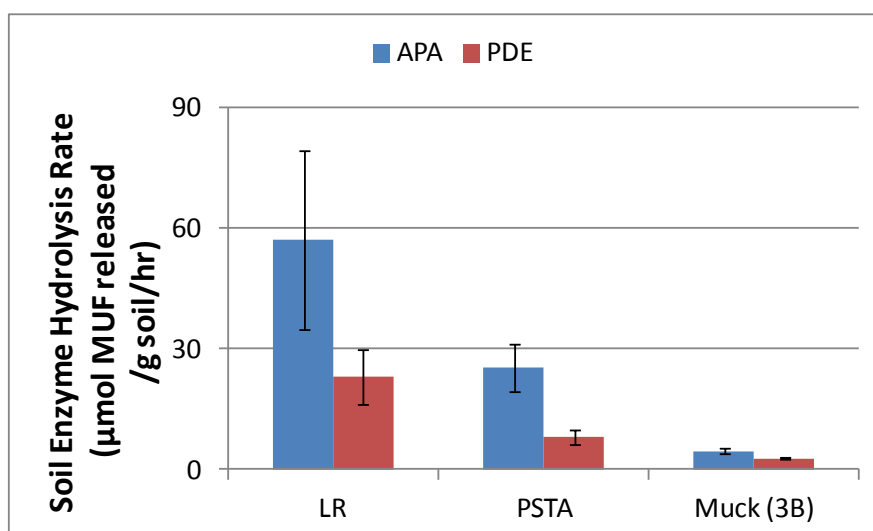


Figure 107. Soil enzyme activity at the end of the study period (September 2013) in the upper 5 cm soil layer in experimental columns under three substrate treatments: exposed limerock (LR), PSTA sediments, and muck soils from STA-3/4 Cell 3B. Monoesterase (APA) and diesterase (PDE) activity was normalized to the dry weight of the soil as assayed. Error bars denote \pm SE around the mean from triplicate columns for each treatment.

4.2.4 Discussion

During Phase I of this study, the LR treatment outperformed both the PSTA sediments, and the two muck strata, with respect to water column P removal. It should be noted that the PSTA sediments used in Phase I contained 264 ± 33 mg P/kg, and that these were replaced, prior to the initiation of Phase II, with “freshly collected” PSTA sediments, which later analyses revealed to have a P content of 195 ± 17 mg P/kg. Subsequent P removal performance of the PSTA treatment during Phase II was quite good, with this accrued material providing comparable outflow P levels to those of the limerock treatment. By contrast, the various muck treatments generally provided only a slight reduction in TP levels below those of the inflow waters. We intend to perform additional review of field sediment collection notes for this study, as well as statistical analyses, to characterize potential spatial differences in sediment chemistry near the outflow region of the PSTA cell, and to determine whether this could account for observed differences in P removal in the column study (Figure 108).

At the conclusion of Phase II of the experiment, P contents of surficial sediments (0-5 cm depth, which included “accrued material”) were similar between LR and PSTA treatments (226 and 232 mg/kg, respectively), while the selected muck strata treatments contained moderate surficial sediment P levels (424 and 455 mg/kg for Upper and Lower treatments, respectively). Surficial sediments from Cell 3B contained the highest P content (734 mg/kg) among treatments (Figure 108).

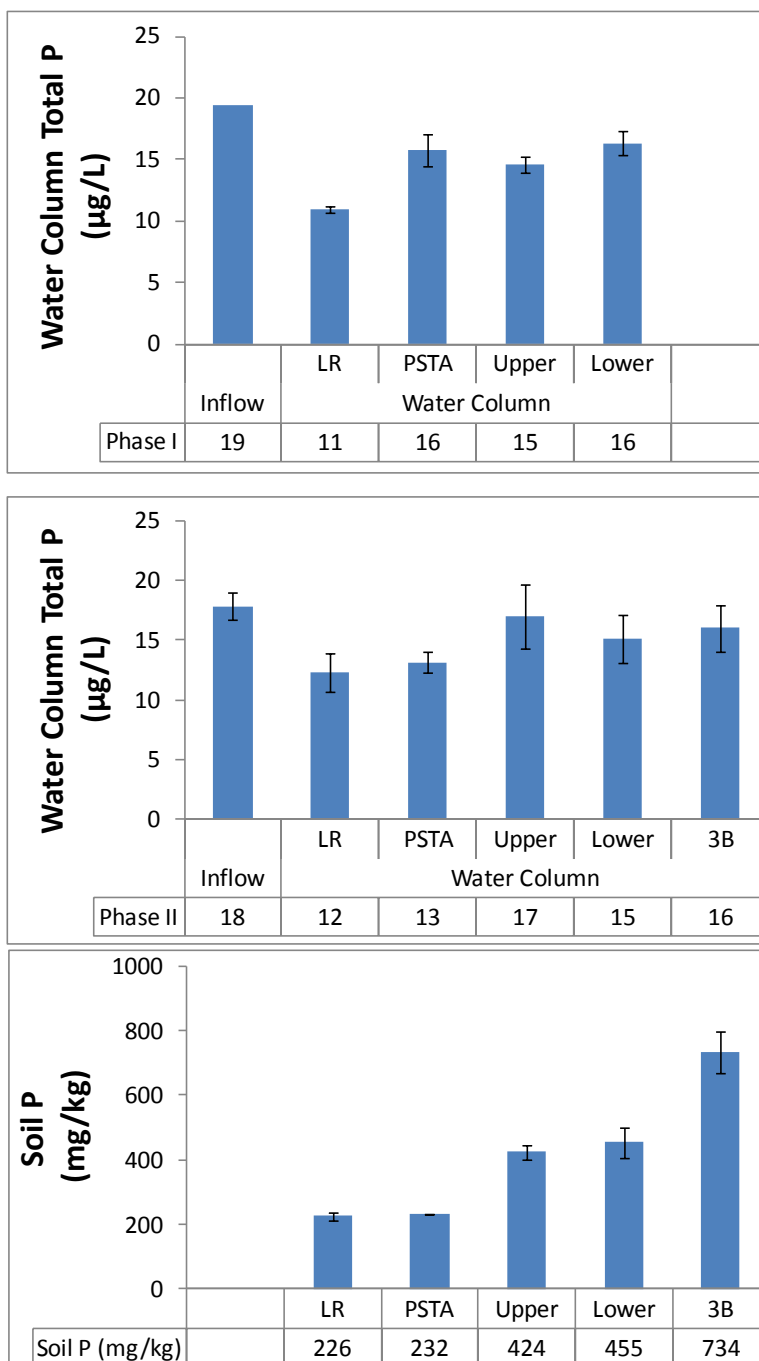


Figure 108. Average total phosphorus (TP) concentrations in the inflow water to experimental columns and the surface water above substrate treatments, during two consecutive phases of operation. Also shown is the P content as measured in the upper 5 cm of the soil at the conclusion of Phase II. Error bars denote \pm SE around the mean from triplicate columns under each treatment.

4.3 Substrate and Macrophyte Interactions

4.3.1 Introduction

Our SAV surveys in the PSTA Cell indicate that macrophyte species composition and relative density may not differ substantially from muck-based STA flow ways, but that PSTA Cell macrophyte tissues exhibit a low P content relative to plants collected from muck-based STA flow ways. Because of their more nutrient deficient conditions, macrophytes in the PSTA cell may exhibit a lower turnover relative to those in muck cells. In the following section, we further evaluate macrophyte responses to substrate conditions.

For the current study, sediments collected from the PSTA Cell were utilized to represent a “long-term” substrate condition. We also utilized bare limerock, to represent initial (startup) PSTA Cell conditions, and we utilized intact marl/muck cores from the outflow region a well performing SAV cell (STA-2 Cell 3). The two SAV species most common to the PSTA cell, *Potamogeton illinoensis* and *Chara* sp., were used for this evaluation. It should be noted that the former is a vascular plant, with true roots, whereas the latter is a non-vascular macro-algae, with holdfasts, rather than true roots. Because of these morphological differences, the soil nutrient “mining” potential of *Potamogeton* may theoretically be greater than that of *Chara*.

4.3.2 Methods

The core incubation study was established using *Potamogeton*, *Chara*, and unvegetated controls as “plant” treatments and exposed limerock, PSTA sediment or STA-2 Cell 3 intact marl/muck cores as “substrate” treatments. The 3 x 3 factorial design was conducted as a batch study in 15-cm diameter cores, outdoors in a water bath and under partial shade (to moderate temperature fluctuations). In “PSTA” treatments, the sediment depth was 10 cm of limerock, covered by an additional 10 cm of accrued sediment from the outflow region of the PSTA Cell. For “Muck” treatments, intact cores were collected from STA2 Cell 3 to a depth of 26 ± 1 cm, from an area where *Potamogeton* was the dominant SAV (*Najas guadalupensis* was also present). The accrued soil layer in these cores was a greyish marl typical of SAV-dominated STAs, and averaged 11.4 ± 0.4 cm. Plants were carefully removed from all cores, leaving the accrued sediment layer intact. A 30-cm water column was established above the sediment surface in triplicate cores under each treatment. Plants were added as 20 g wet weight per core, which consisted of several *Chara* strands or three *Potamogeton* plants with both new root growth and healthy apical leaf tips. Water (originating from the PSTA cell) in the cores was sampled weekly for TP concentrations, and exchanged every 2 weeks with care to avoid physical disturbance to plants and sediments. Six water exchanges were performed over 84 days, after which the plant responses were evaluated.

Soil P content was determined from cores collected and sectioned in the field into the accrued layer (both sites), and underlying muck layers (0-10 cm and 10-20 cm layers) in STA 2 Cell 3. Plant chemistry was measured at the beginning (initial inoculum) and end of the study.

4.3.3 Results

4.3.3.1 Water column phosphorus dynamics

During the initial cycle, surface water TP concentrations in the core reflood water, collected from the PSTA Cell outflow (G388), were quite low (14-15 µg/L). The core study water source subsequently was changed from the PSTA cell outflow to the inflow (G390B structure) for the subsequent 5 water exchanges, to provide more moderate inflow TP levels (17-26 µg/L). During the batch incubations, the limerock-based cores were able to maintain very low TP concentrations throughout the study, regardless of vegetation presence or type (Figure 109). On muck soils, TP concentrations increased over 5 of the 6 cycles for the unvegetated controls. *Chara* provided lower water column TP levels than did *Potamogeton*, with greater vegetation treatment differences observed on muck substrates toward the end of the study.

On PSTA sediments, the differences in water TP levels between *Chara* and *Potamogeton* treatments were smaller than for muck treatments, but showed the same overall trend. Within each plant treatment, PSTA sediments provided lower water TP concentrations overall than muck, but higher than for the limerock substrate treatments (Figure 109).

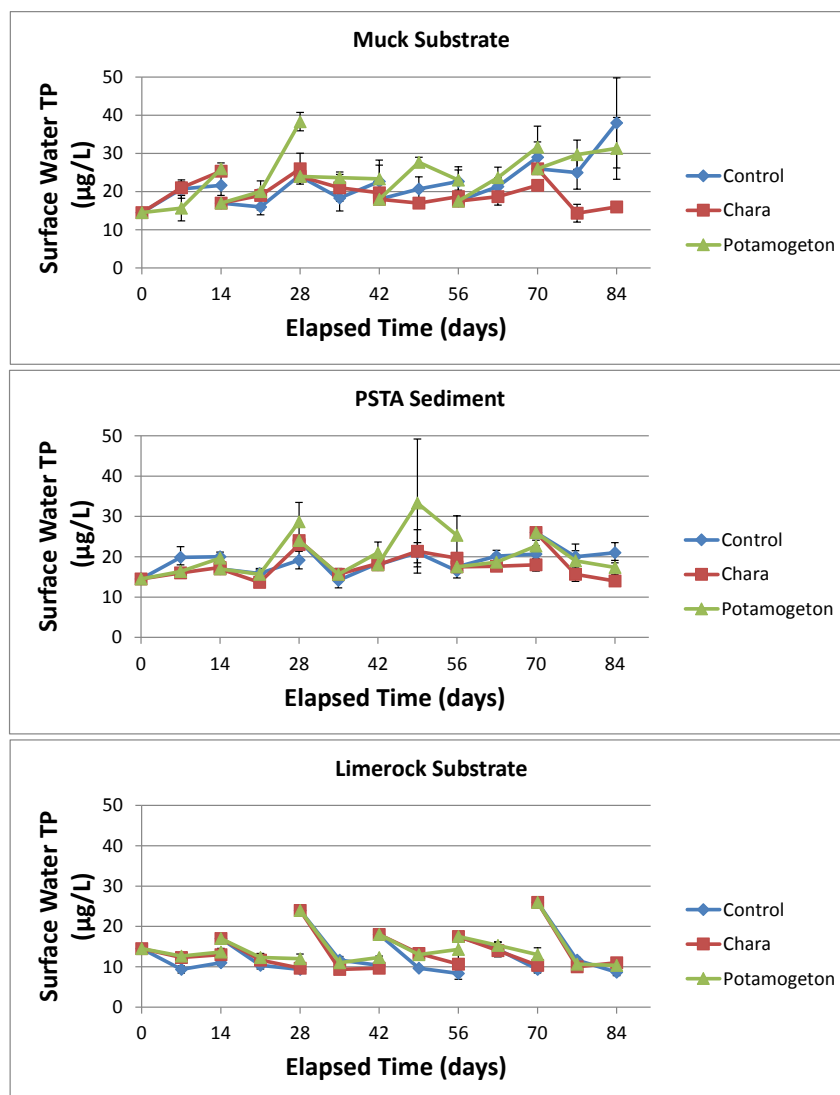


Figure 109. Surface water Total P concentrations in cores incubated outdoors with one of three substrates (limerock (LR), PSTA sediment, or muck), and one of three vegetation treatments, during a 12-week study period. The control cores were unvegetated.

4.3.3.2 Vegetation response to sediment conditions

Analyses of the soils revealed significantly higher TP levels for the muck than for the PSTA sediments (Figure 110). Slightly lower P was found at depth in the muck soils. It should be noted that P in this deeper soil was potentially available to *Potamogeton*, which was seen to extend new root tissues into the soil below the accrued layer.

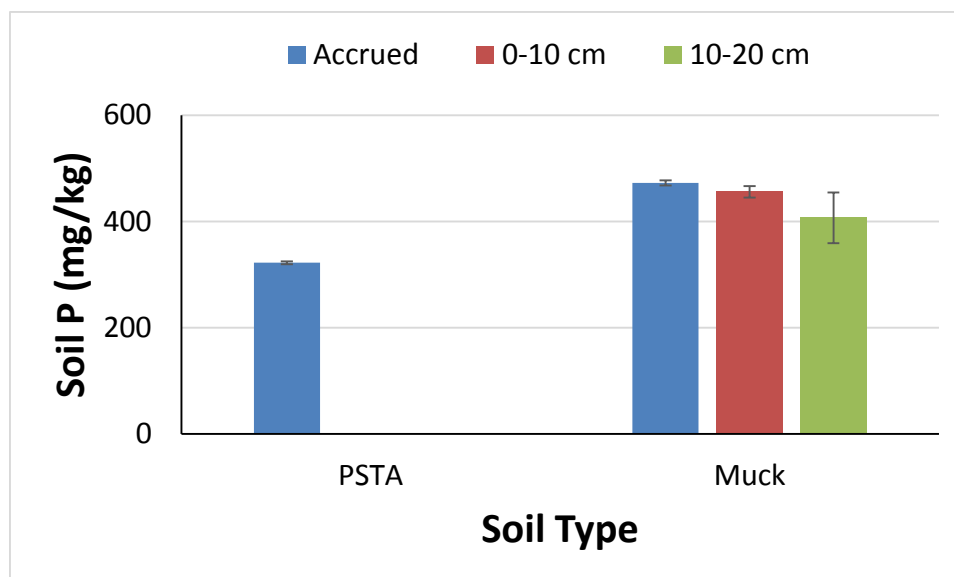


Figure 110. Total phosphorus content in soils from the PSTA Cell and the outflow region of STA 2 Cell 3 (Muck). Error bars denote the standard error around the mean of triplicate samples.

At the end of the 84-day study, *Chara* and *Potamogeton* tissue P contents were elevated in muck treatments, as compared to the tissue P levels of the originally stocked plant materials (**Figure 111**). No such increase was noted for macrophytes grown on limerock, indicating that the muck sediment, rather than the reflood water, was the principal source of the P that accumulated in the plant tissues. PSTA sediment treatments were intermediate with respect to P content of macrophyte tissues. The dry weight biomass of *Chara* increased in the muck treatment, but decreased in the limerock treatment. *Potamogeton* on muck also increased in biomass, but decreased over time in the limerock and PSTA sediment treatments.

On all soils, the calcium contents of the plants changed little during the study, so the changes observed in dry weight biomass were likely the result of growth or senescence, rather than gain or loss of calcium carbonate encrustations commonly associated with macrophytes in alkaline waters. *Potamogeton* tissue on PSTA sediment showed the greatest change in calcium contents, increasing from 5.5 ± 0.2 % Ca to 8.0 ± 0.6 % Ca over the course of the study. The Ca content of *Chara* tissues were higher initially (23%), then decreased slightly to 21% on all substrates (**Figure 111**).

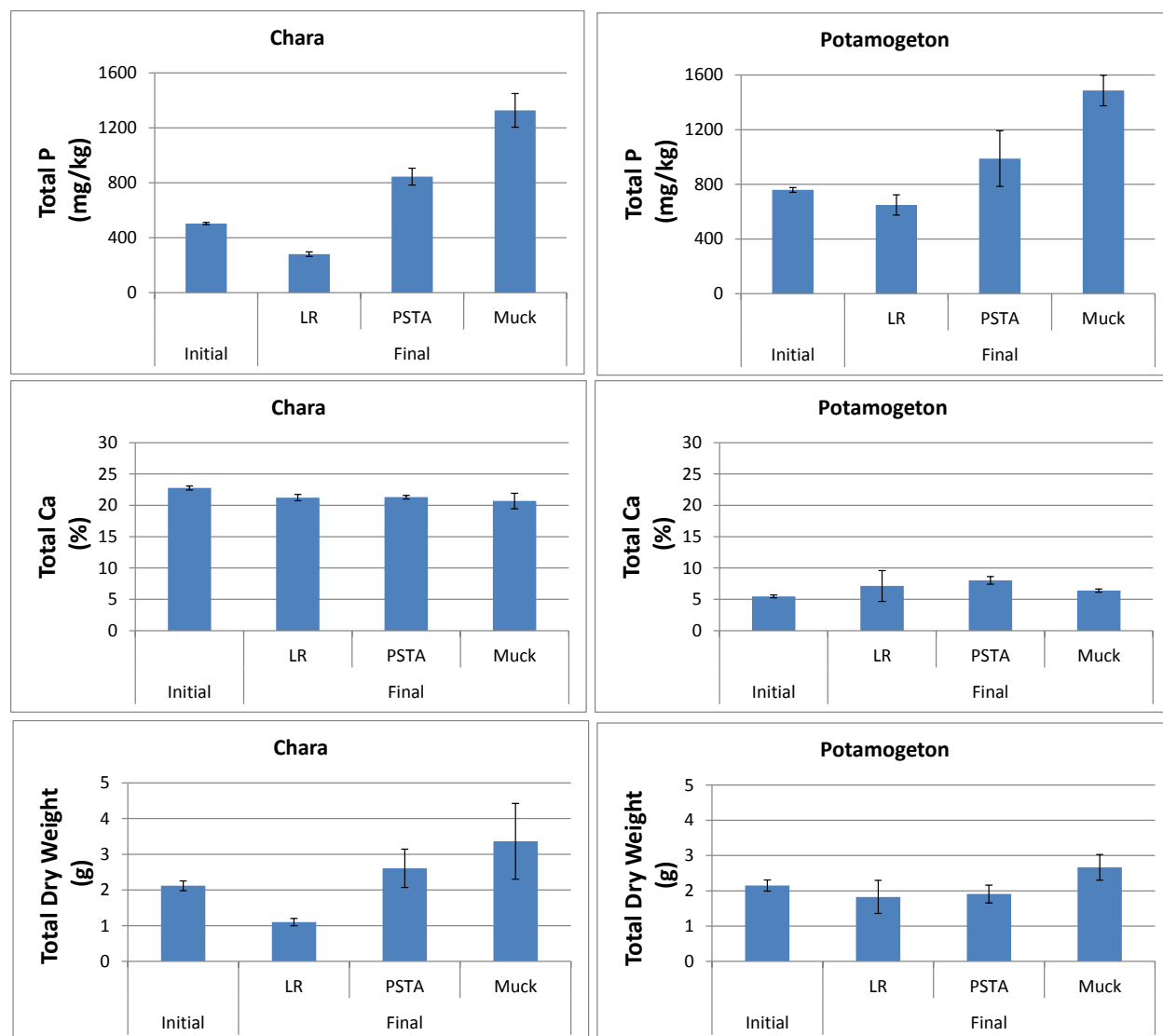


Figure 111. Chemical composition and dry weights of *Chara*, and *Potamogeton* tissues in cores incubated outdoors for 84 days, compared to the initial conditions of the inoculum, as a function of sediment type.

4.3.4 Discussion

As noted previously in the section on macrophyte growth in the PSTA Cell, macrophytes can act as a nutrient “pump” in low nutrient environments by using sediment P for tissue growth, then releasing P species upon senescence. High standing crop biomass and/or high tissue P contents would suggest that macrophytes can be an important source of internally recycled P. Since macrophytes can supply P to epiphytes throughout the year (Burkholder and Wetzel 1990), high P in SAV tissues may also influence the type of periphyton present, and potentially suppress the production of phosphatase enzymes.

Chara and *Potamogeton* exhibited biomass increases on muck soils, while no change was seen on PSTA sediments. Macrophytes also exhibited the least growth on the exposed limerock, compared to PSTA or muck soils. Tissue P contents were also affected by substrate type, indicating that low P substrates are important for maintaining low P conditions in macrophyte tissues. On both PSTA sediment and muck soils, *Chara* demonstrated better P removal performance than did *Potamogeton* or unvegetated controls, while on limerock there was no effect of vegetated treatment.

These findings have important implications for the sustainability of effective P removal by PSTA systems. As sediments accrue in a PSTA wetland, the growth rate and nutrient content of macrophytes potentially can increase, relative to initial conditions on “raw” calcitic substrates. This in turn could impair the cell’s ability to achieve ultra-low outflow P concentrations. Since its inception, the STA-3/4 PSTA Cell has produced sediment, despite being low in P, that appears capable of supporting higher macrophyte growth rates and tissue P contents than would be expected on the original, bare limerock substrate. However, the macrophyte growth and P enrichment of the accumulating PSTA sediments is not as great as that observed on intact marl/muck cores collected from well-performing SAV cells. Further research is needed to confirm the substrate and vegetation (macrophyte/periphyton) relationships in the STA-3/4 PSTA cell, but to date, the accumulating PSTA sediments appear reasonably well suited for limiting the effects of P export from the substrate.

4.4 Investigations with Low-P Muck Soils and a Limerock Cap

4.4.1 Introduction

Due to past exceptional P removal performance of STA-2 Cell 1, it recently has been assumed that “unfarmed” muck soils exhibit chemical or physical attributes that minimize P flux, or in some other fashion contribute to low P levels in the overlying waters. We therefore established a mesocosm study, using muck soils obtained from an unfarmed parcel of land adjacent to STA-1W (beneath the FPL power lines), to investigate this phenomenon. As a second treatment, we employed a “cap” of limerock over this same muck, to assess whether the presence of CaCO₃ or some other constituent would enhance development of a desirable benthic community, which in turn would lead to reduced outflow P levels. This approach is similar to the concepts investigated in the pilot-scale PSTA trials performed previously in the STA-1E eastern flow path, in which three separate types of calcitic substrates were deployed. The results from the STA-1E investigation were inconclusive.

4.4.2 Methods

The outdoor mesocosm study was established in April 2011. Limerock “gravel” (6 - 10 mm diameter nominal size, #89 stone from SFWMD Lake Okeechobee Division) was applied as a 3-cm thick “cap” over 15 cm muck soils in triplicate mesocosms, while three mesocosms with un-amended muck soils served as controls (Figure 112).



Figure 112. Mesocosms were established on unfarmed low-phosphorus muck soils with and without a “cap” of limerock gravel placed onto the sediment surface prior to flooding.

The mesocosms were operated with water from the discharge canal of STA-1W, with additional pre-treatment as necessary during periods when the STA performance was not adequate to provide inflow water TP levels < 40 µg/L. A water column was maintained at constant depth of 45 cm, and the hydraulic loading rate of 9 cm/day resulted in a 5-day nominal hydraulic retention time within each mesocosm.

The initial period of operation was characterized by ultra-low inflow TP concentrations. On January 29, 2013, the pre-treatment system was bypassed, which enabled us to deliver higher P water to the study. During a 2-week transition period, hydraulic loads were also increased, which mimicked a large prolonged flow pulse. On February 13, 2013, flows were returned to normal and a nominal 5-day HRT was resumed.

After water, vegetation and soil sampling was completed on April 9, 2014 the mesocosms were subjected to a draw-down of water levels. The surface waters were drained to within a few cm of the sediment surface. This exposed the remaining SAV to drying out above the sediment. On May 22, 2014, inflow water was reintroduced to the mesocosms, ending the 43 day dry down period.

This updated interim report presents the data for the entire period of record (April 2011 – February 2015), including an 8-month period after the dryout/reflood event.

4.4.2.1 Water sampling and analyses

Routine water monitoring consisted of biweekly sampling for TP from April 2011 through April 2014. Beginning in November 2011, samples were collected bi-weekly for analyses of TSP, SRP, dissolved Ca, DOC and UV absorbance. Calcium monitoring was discontinued on January 17, 2012. DOC and UV absorbance monitoring was reduced to monthly from September 2012 through July 2013, then discontinued. Enzyme activity in the surface water was measured monthly from July 2013 through April 2014.

After the dryout/reflood period, surface water sampling resumed on a biweekly basis for P species and enzyme activities until the conclusion of the monitoring period on February 2, 2015.

4.4.2.2 Vegetation sampling and analyses

Aliquots of the originally stocked macrophyte vegetation were analyzed for TP and TCa contents. Plant tissue grab samples were collected April 27, 2012, May 2, 2013, April 9, 2014, and February 2, 2015, and analyzed for TP, TN, TC, TOC, and Total Ca. Biomass standing crop was sampled April 9, 2014, by harvesting all the SAV biomass from a 0.5m x 0.5 m quadrat placed generally in the center of each tank. At the conclusion of the study, plants from the entire tank were collected (aboveground biomass only) and separated by genera (*Potamogeton* or *Chara*). A wet weight was obtained in the field, and the entire sample was retained for analysis. Total dry weights of the biomass were determined at the lab to estimate standing crop biomass as plant dry weight per unit area. Observations on SAV species and periphyton coverage within each mesocosm were recorded periodically throughout the study.

4.4.2.3 Sediment sampling and analyses

Sediments were collected with a 2-inch diameter push corer in October 2013 and sectioned into an accrued layer (when present), 0-5 cm, 5-10 cm, and 10-15 cm layers. All layers were analyzed for bulk density, TP, TN, TC, TOC. Enzyme activity and pH were determined on the accrued and 0-5 cm layers.

Sediments were again collected on April 9, prior to the initiation of the drawdown. These cores were sectioned into accrued layer, 0-5, 5-10, and 10-15 cm depths. Bulk density, TP and pH were analyzed on all samples.

4.4.2.4 Additional Monitoring during the Dryout/Reflood Period

Distance from the sediment surface to a fixed benchmark in each mesocosm was used to monitor the change in soil thickness during desiccation. Sediment redox was measured *in situ* (5 cm below surface) several times prior to and subsequent to reflooding.

Reflooding of each mesocosm was initiated at same hydraulic loading rate used prior to the dryout. (9 cm/day, 5 day HRT @ 40 cm depth). Surface waters and porewaters were sampled during reflooding (~24 hours after flows turned on), when ~ 2 inches surface water had accumulated above the sediment surface. Porewaters were collected from each mesocosm using

a sipper that targeted 5 cm depth into soil profile. Samples were retained for dissolved Ca, DOC, TSP and SRP.

Surface waters were sampled again once the water column was re-established at 40 cm deep (nominal operational depth during the experiment). The above surface water samples were analyzed for temp and pH in the field, and preserved as appropriate for TP, TSP, SRP, and dissolved Ca analyses.

4.4.3 Results

4.4.3.1 Water column constituents

Surface water (outflow) TP concentrations ranged from 6-20 $\mu\text{g/L}$ during the POR, while inflow waters ranged from 6-35 $\mu\text{g/L}$ (Figure 113). Long-term outflow TP concentrations in the LR Cap and Muck treatments were identical for both the low-P period ($9 \pm 0.3 \mu\text{g/L}$) and the high-P period ($13 \pm 0.3 \mu\text{g/L}$). Mean inflow TP concentrations for the two periods were 11 and 21 $\mu\text{g/L}$, respectively (Figure 114).

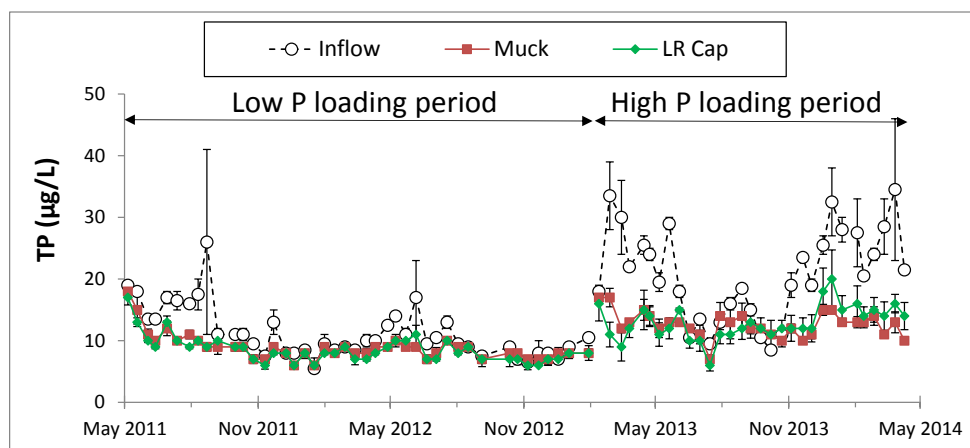


Figure 113. Mean total phosphorus (TP) concentrations in the inflow waters and outflow waters of triplicate mesocosms established with or without limerock added as a cap over muck soils, for the period of operation prior to draw-down (May 2011 – April 2014).

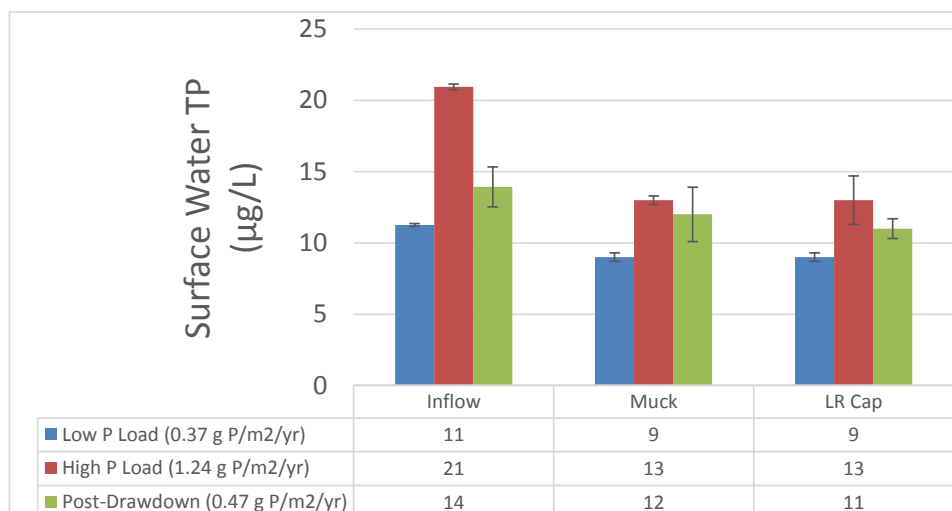


Figure 114. Long-term mean total phosphorus (TP) concentrations from mesocosms for three periods of operation: an initial period of low P loading (May 2011 – January 2013), higher P loading (February 2013 – April 2014), and a post-drawdown period (June 2014 – February 2015). The error bars denote the standard error between triplicates of each treatment, or duplicate measures of the inflow.

Similar to TP concentrations, there was no difference in the long-term average SRP (data not shown), or DOP and PP concentrations between Muck soil and LR Cap treatments (Figure 115). The observed reductions in the inflow TP were the result of slight decreases in both DOP and PP fractions.

Enzyme hydrolysis rates were elevated under both treatments (Muck and LR Cap), compared to the inflow waters (Figure 116). Long-term (period of record) average monoesterase hydrolysis rates increased from 0.12 ± 0.01 μM MUF released/hr in the inflow, to 0.34 ± 0.16 $\mu\text{M/hr}$ and 0.42 ± 0.22 $\mu\text{M/hr}$ for the outflows from Muck and LR Cap treatments, respectively. Diesterase rates increased as well, from an inflow average of 0.09 ± 0.00 $\mu\text{M/hr}$, to 0.26 ± 0.08 $\mu\text{M/hr}$ and 0.24 ± 0.05 $\mu\text{M/hr}$ in the Muck and LR Cap treatment outflows, respectively.

Dissolved organic carbon (DOC) concentrations were conservative through both substrate treatments, with an average concentration of 29 mg/L in both inflow and outflow waters, for the period November 2011 through July 2013 (Figure 117). Spectral slopes were lower, on average, in inflow waters than in surface waters within either treatment (Data not shown).

Dissolved calcium content in the surface water was, on average, 59 ± 0.3 mg/L and 58 ± 2.0 mg/L for the Muck and LR Cap treatments, respectively. These concentrations were slightly lower than the long-term average concentration (62 ± 0.3 mg/L) in the inflow waters (Figure 118).

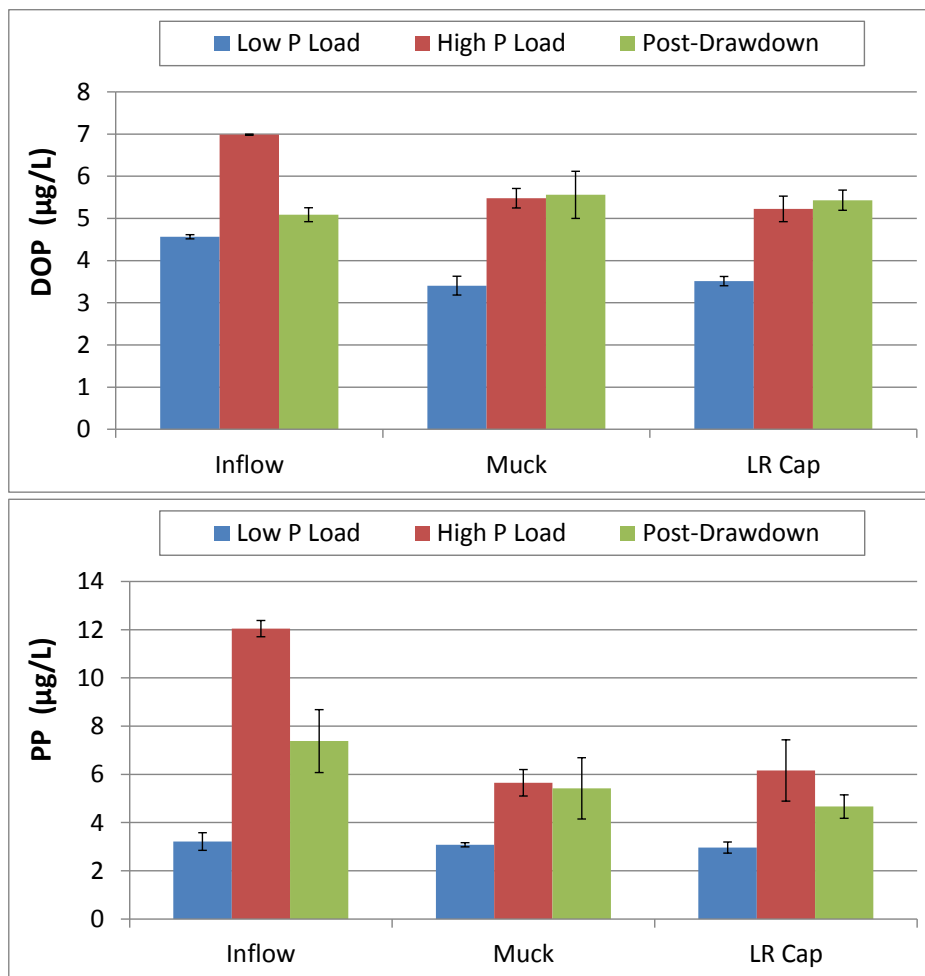


Figure 115. Mean surface water outflow dissolved organic phosphorus (DOP) and particulate phosphorus (PP) concentration for mesocosms established with limerock added as a cap to muck soils.

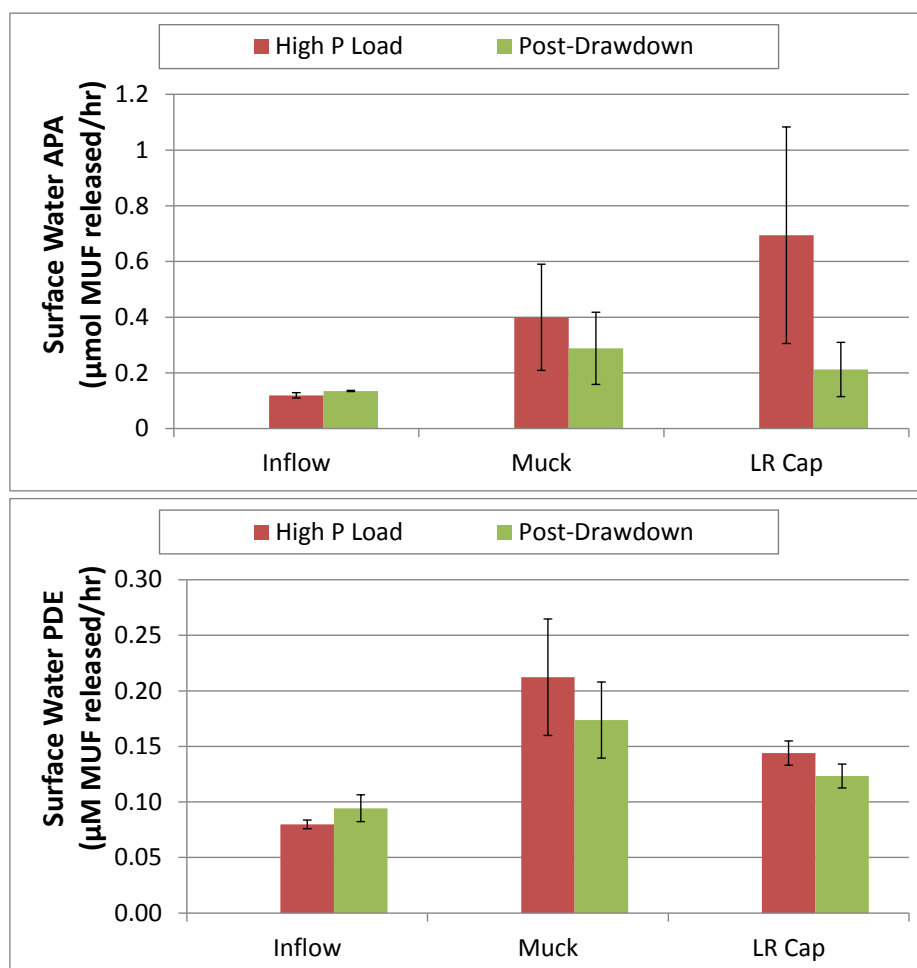


Figure 116. Average enzyme hydrolysis rates for monoesterase (APA) and diesterase (PDE) in the inflow and outflow waters of mesocosms with or without limerock added as a cap over muck soils. Error bars denote \pm SE around the average of long-term means for triplicate mesocosms under each soil treatment, or for two inflow monitoring locations.

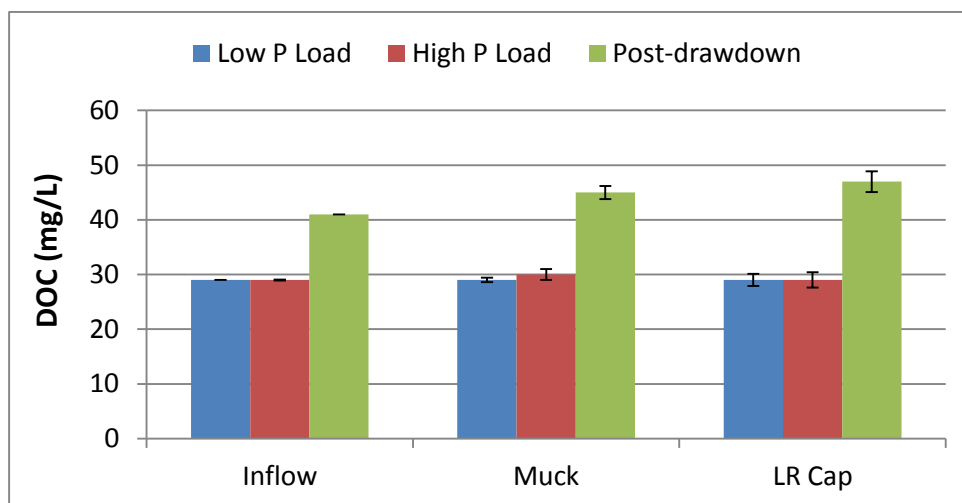


Figure 117. Average dissolved organic carbon (DOC) concentrations in the inflow and outflow waters of mesocosms with or without limerock added as a cap over muck soils. Error bars denote \pm SE around the average of long-term means for triplicate mesocosms under each soil treatment, or for two inflow monitoring locations. The period of record represents November 2011 through July 2013.

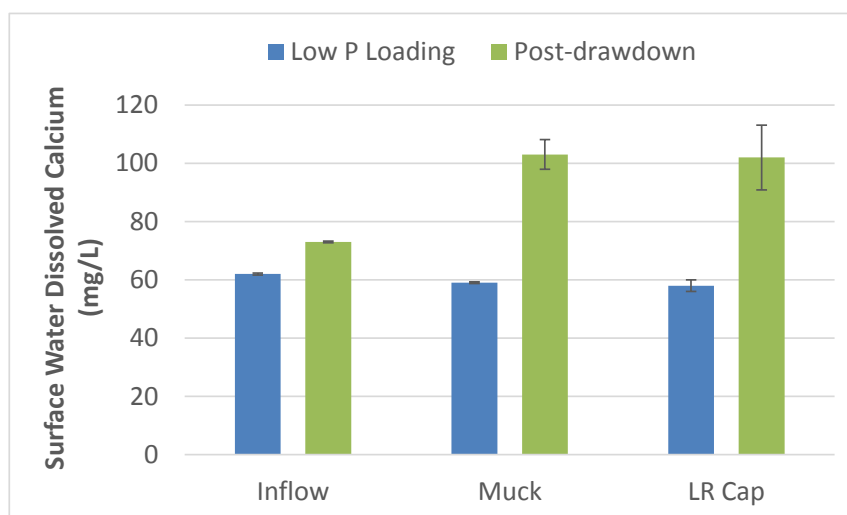


Figure 118. Average dissolved calcium concentrations in the inflow and outflow waters of mesocosms with or without limerock added as a cap over muck soils. Error bars denote \pm SE around the average of long-term means for triplicate mesocosms under each soil treatment, or two inflow monitoring locations. The period of record for calcium was 11/10/2011 through 1/17/2012 (N = 6 bi-weekly sampling events) under the low P loading conditions, and 5/22/14-5/29/2014 (N = 3 events during the first week after reflooding).

4.4.3.2 Effect of Drawdown and Reflooding on water column P

The break in the time series in Figure 119 indicates a drawdown period that temporarily suspended water sampling. Higher than average concentrations of both DOP and PP were observed immediately following the reflooding of mesocosms. Senescent plant tissues and desiccated soils likely both contributed to the release of stored nutrients during this period. What is remarkable is the short duration of the effect of the draw down. Within weeks, the concentrations of TP and P species returned to pre-drawdown levels. For the nine-month period following reflooding, as well as the prior periods of low and high P loading, the LR cap did not affect DOP or PP removal rates (Figure 115).

Enzyme activities in unfiltered surface water samples were variable in the LR-added treatment (Figure 116). The high APA rates observed in one replicate were coincident with a benthic periphyton mat that developed during the first year and then subsequently was replaced by macrophytes. APA levels declined after the transition to macrophyte dominance in that LR-capped tank. Overall, the average APA in LR Cap and muck treatments were similar, and higher than in inflow waters. After the drawdown/reflood event, the increase in enzyme activity from inflow to outflow was reduced, with no difference between mesocosms with or without the added LR.

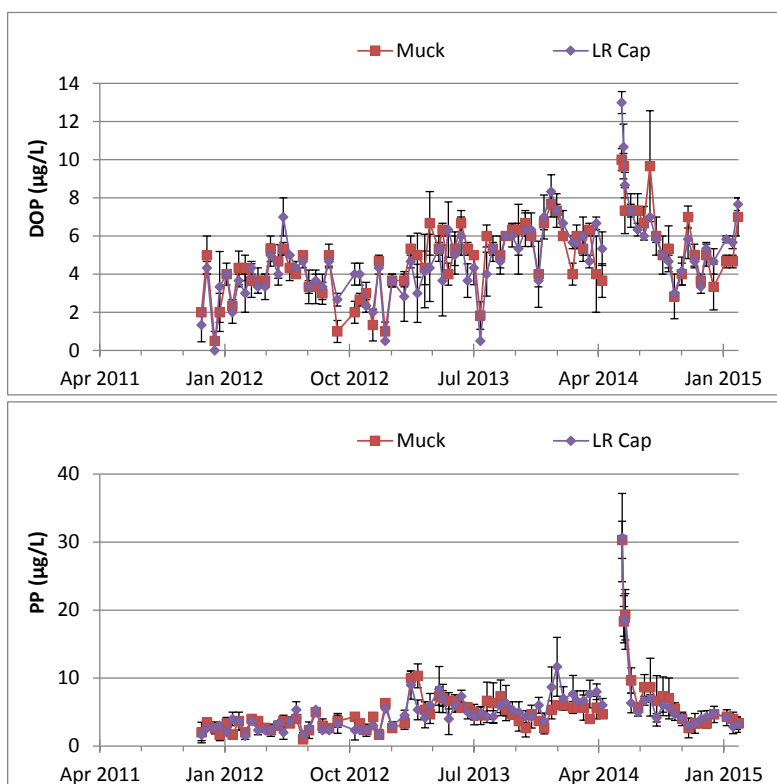


Figure 119. Dissolved organic phosphorus (DOP) and particulate phosphorus (PP) concentrations in the surface waters of muck-based mesocosms with or without a limerock cap, during a 3.8-year period of operations.

DOC concentrations were temporally variable, averaging between 20 and 38 mg/L among inflow samples collected between November 2011 and July 2013. Average concentrations were unchanged between inflow and outflow during the pre-drawdown periods, thus monitoring was suspended until after the reflood event. An increase in DOC was observed during post-drawdown monitoring, for both the muck and LR Cap treatments 45 ± 1 and 47 ± 2 mg/L, respectively, despite higher than normal inflow concentrations (41 ± 0 mg/L) during and immediately following mesocosm reflooding (Figure 117). It should be noted, however, that DOC monitoring occurred only the day of reflooding (5/22/2014) and four days later (5/26/2014).

4.4.3.3 Soil Characteristics

Soil characteristics in October 2013 were similar for both Muck and LR Cap treatments (Figure 120). Total P concentrations were elevated in the newly-accrued sediment layer (266 and 360 ± 60 mg/kg, for Muck and LR Cap treatments, respectively), as compared to the muck soil layers (134 - 180 mg/kg) from either treatment (Figure 120). Calcium enrichment of the newly-accrued layer (23 and 22 % for Muck and LR Cap, respectively), relative to underlying muck soil layers (2 - 5 % Ca), was evident in both muck and LR Cap treatments. Calcium enrichment can effectively dilute the P content of soils, but in the present study calcium contents in the accrued layer were similar between treatments and may have provided additional P sorption capacity to this new soil material. Total N and organic C contents were reduced in the accrued sediment layer, likely the result of dilution by Ca enrichment of that surficial layer.

Enzyme activity in the sediment was enriched in the accrued layer, relative to the upper (0-5 cm) muck layer. Muck-based mesocosms without limerock exhibited consistently higher potential for both APA and PDE than did the LR Cap soils within respective soil layers (Figure 121). Soil pH, by contrast, was similar between treatments and between accrued and 0-5 cm muck layers.

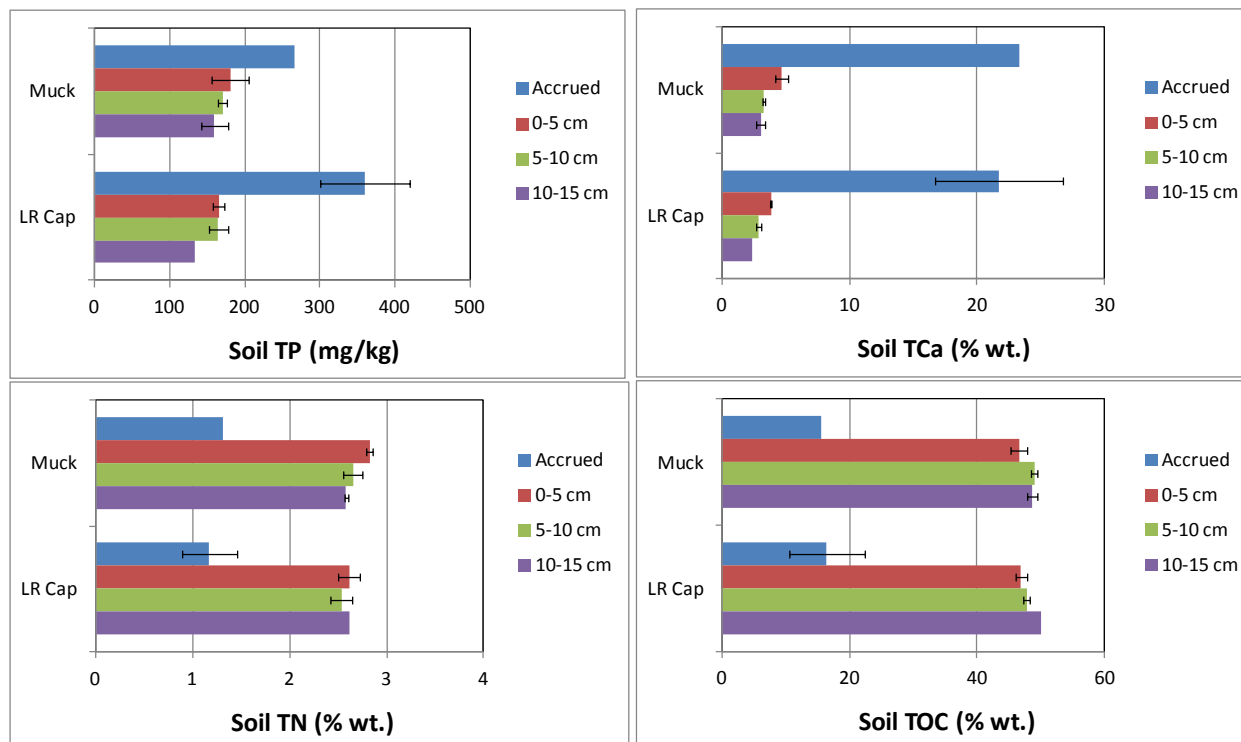


Figure 120. Soil characteristics in the accrued layer and at discrete depth intervals for cores collected on October 22, 2013, from mesocosms where the P removal performance of un-amended muck soils is compared to treatments with a limerock (LR) cap. Error bars denote \pm SE around the mean value from triplicate mesocosms for each soil treatment.

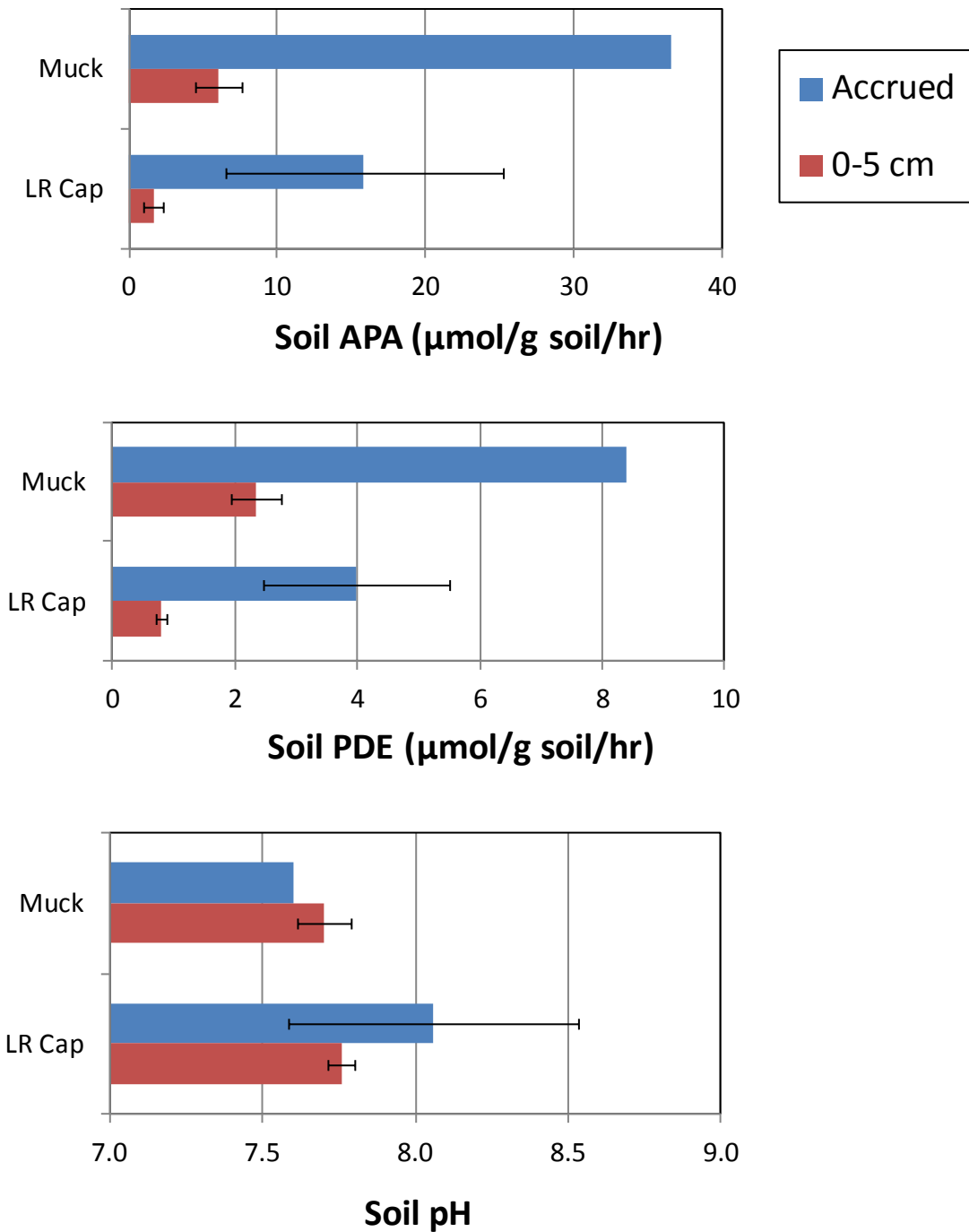


Figure 121. Alkaline phosphatase activity (APA), phosphodiesterase (PDE) activity and pH measured in the newly-accrued sediments and underlying muck soils collected from outdoor mesocosms on October 22, 2013, after 2.5 years of flow through operations. Drawdown Effects on Sediment Consolidation and P Stability

During the 42-day drawdown period, soil consolidation occurred in both limerock capped and unamended treatments. However, changes in soil thickness were small, < 2 cm from an original muck soil layer of 15 cm, or about 10% loss of soil volume. No difference was observed between LR cap and Muck treatments during the drawdown period. During rehydration of the soils, however, the muck treatments returned to near the original soil thickness, whereas limerock-capped muck soils maintained the consolidated soil depths achieved during the drawdown (Figure 122).

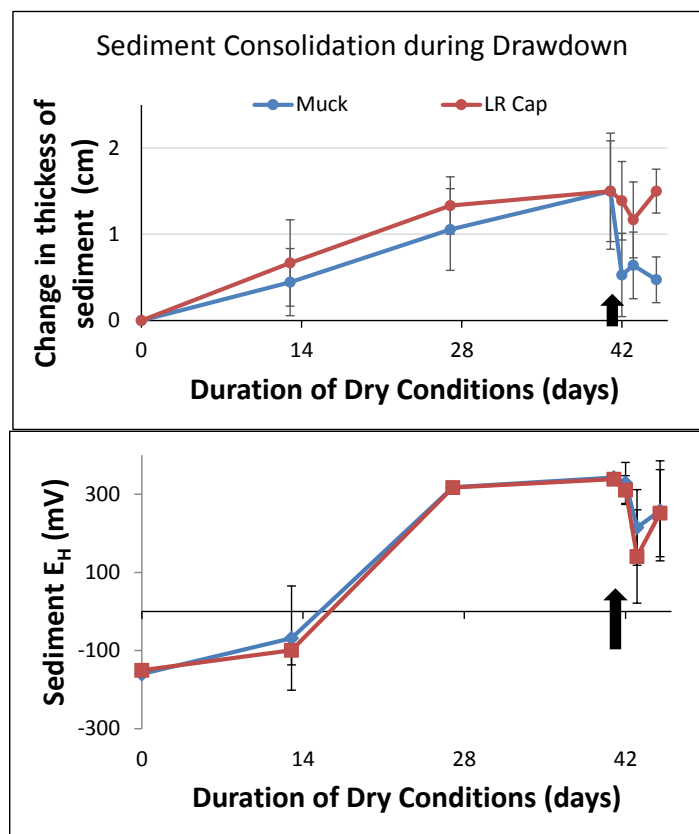


Figure 122. Change (amount of reduction) in sediment thickness (top panel) and sediment oxidation-reduction potential during a 42-day drawdown period. The arrow denotes when reflooding was initiated on May 22, 2014 (Day 42).

4.4.3.4 Porewater during reflooding

Porewater concentrations of SRP and DOP were slightly higher in the LR Cap treatments than Muck treatments immediately upon reflooding (Table 14). However, neither treatment showed high P levels that might be expected to contribute to large P releases. DOC concentrations were slightly higher in the porewater after reflooding than the average surface water concentrations during the rest of the study. However, the concentrations in the reflow waters were also

elevated (41 mg/L), indicating little to no additional DOC contribution from the soil porewater was expected. By contrast, porewater calcium concentrations were high in both LR-capped and uncapped muck treatments, relative to inflow concentrations after drydown (Figure 118). Surface water calcium concentrations during reflooding were similar or slightly higher than porewater calcium concentrations, indicating the Ca enrichment of the surface water may have occurred from the porewater, but also may reflect Ca release from desiccated SAV tissues.

Table 14. Porewater constituents on May 23, 2014, one day after initial reflooding of the dried soils in mesocosms containing low-P soils with or without a limerock cap. Also shown are the surface water concentrations for each treatment, as measured during reflooding on May 22, 2014. Values represent the mean \pm SE of triplicate mesocosms under each treatment.

Parameter	Units	Porewater		Surface Water	
		Muck	LR Cap	Muck	LR Cap
SRP	$\mu\text{g/L}$	11 \pm 2	15 \pm 5	5 \pm 1	7 \pm 2
DOP	$\mu\text{g/L}$	17 \pm 1	20 \pm 3	10 \pm 1	13 \pm 1
DOC	mg/L	43 \pm 1	45 \pm 1	45 \pm 2	48 \pm 2
Dissolved Ca	mg/L	127 \pm 7	121 \pm 17	134 \pm 5	115 \pm 10

4.4.3.5 Water Column P Response to Drawdown-Reflood Event

Immediately following the reflooding of mesocosms the TP concentrations increased in both treatments to levels higher than the inflow waters (Figure 123). However, this phenomenon was temporary, and outflow TP concentrations returned to very low levels within a few weeks of reflooding. During the post-drawdown monitoring period, outflow TP concentrations remained low in both treatments, averaging 11 and 12 $\mu\text{g/L}$ in mesocosms with and without a limerock cap, respectively (Figure 114). Inflow TP was also quite low (14 \pm 1 $\mu\text{g/L}$) over the same period, but net P removal was maintained by these recently dried systems.

Phosphorus forms in the post-drawdown period were similar between treatments, with greater particulate P release immediately after reflooding (Figure 119). Outflow concentrations of DOP immediately after reflooding were only slightly elevated from pre-drawdown levels. Average outflow DOP concentrations were equivalent during the post-drawdown and high loading periods and lowest during the low loading period at the beginning of the study (Figure 115). Particulate P concentrations in the mesocosm outflow waters were also lowest during the low loading periods and higher during the high load and post-drawdown periods. No difference in P species was observed between treatments (with or without the limerock cap) for any of the three evaluation periods.

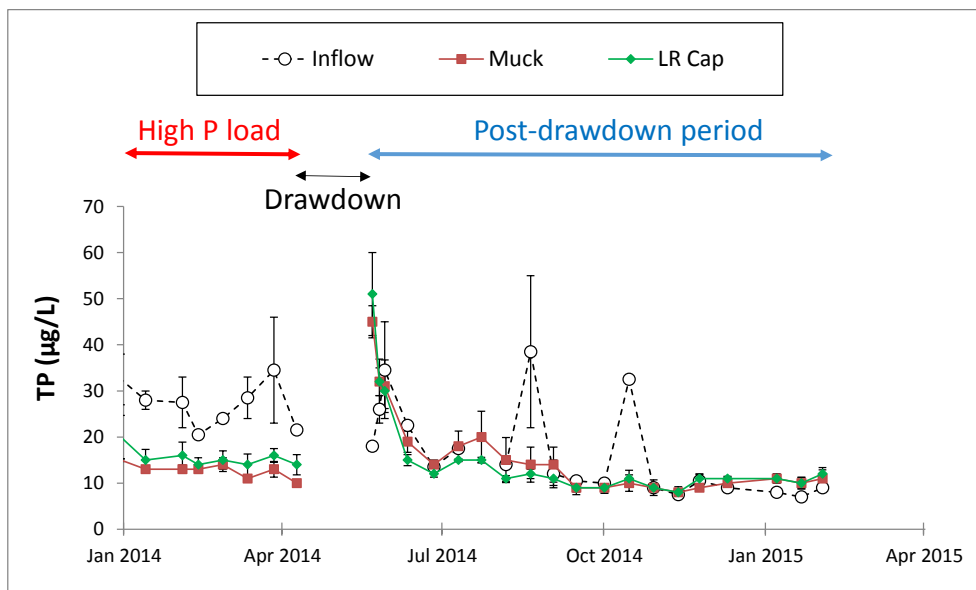


Figure 123. Average total phosphorus (TP) concentrations in the inflow and outflow waters of mesocosms established on low-P muck soils with and without a limerock cap, for the period prior to and following a drawdown of water levels in each mesocosm. Error bars denote the standard error around values for triplicate mesocosms under each soil treatment.

Enzyme activity was generally higher in the outflow waters than inflow waters for both the high loading period and the post-drawdown period (Figure 116). Differences between treatments were not apparent in the monoesterase activity (APA), in part due to large variability in the LR capped treatments during the high loading phase. Phosphodiesterase (PDE) activity showed higher levels in the muck treatments than LR cap treatments for both the high loading period and the post-drawdown period. Diesters are common within organic P compounds derived from soil organic matter. The levels of PDE observed in the outflow waters were low compared to APA, but high enough to suggest that the LR cap may have limited the supply of soil-derived DOP compounds to the water column.

Surface water Ca and DOC levels in the post-drawdown period were higher than previously observed in this study (Figure 117 and Figure 118). However, the monitoring period for these parameters was limited to the first week following reflooding of the mesocosms. The elevated concentrations were likely the result of DOC and Ca released from both desiccated soils and macrophyte biomass. Again, no difference was observed in DOC or calcium between treatments.

4.4.3.6 Vegetation Characteristics

Initial plant stocking materials were added in equal portions to all mesocosms, and contained 440, 841, and 1812 mg P/kg dry weight, for *Potamogeton*, *Chara* and *Najas* tissues, respectively. After one year of operation under low P-loading conditions, the macrophyte biomass was low in the LR Cap treatments, which precluded grab sampling for tissue nutrient analysis without

compromising the potential for new growth. In the muck treatment, tissue P content was very low (200 ± 30 mg/kg), indicating a lack of available P for uptake. *Chara* and *Potamogeton* were co-dominants while *Najas* biomass declined during the first year, based on visual observations.

Over the next two years, P contents remained low in the macrophytes growing in both muck and LR Cap treatments (Figure 124). The N contents of macrophytes growing on muck increased slightly over time, from 0.70 ± 0.08 % N in April 2012 to 0.94 ± 0.01 % N in April 2014. Macrophytes in the LR-capped mesocosms were 1.00 ± 0.17 % N and 0.92 ± 0.10 % N, after 2 and 3 years of operation, respectively. Tissue C contents of macrophytes were lower in Muck treatments than LR Cap treatments for May 2013 and April 2014. This was likely due to greater calcification of tissues in the muck treatments, as compared to the LR cap treatment (Figure 124).

Throughout the study period, macrophyte biomass appeared lower in the LR Cap treatment than in Muck treatments (Figure 125). After 3 years of operations, measurements of the standing crop in April 2014, and again 9 months after a drawdown/reflood cycle (February 2015), confirmed this observation (Figure 126). Macrophyte biomass was largely *Chara* in both treatments, but a larger percentage of the total biomass was *Potamogeton* in the LR capped treatment ($25 \pm 10\%$) than in the unamended muck treatment ($5 \pm 3\%$)(Figure 127). Phosphorus contents were slightly higher in *Potamogeton* than in *Chara* tissues in February 2015 (Figure 128). This result was consistent with increased P supply from the soil to the rooted vascular species (*Potamogeton*) than to the rootless macroalga (*Chara*). Assays of epiphyte enzyme activity showed higher APA rates were associated with the *Chara* than with *Potamogeton*, supporting the notion that soil P supply to rooted SAV may become available to epiphytes and reduce the production of enzymes needed in P limited environments (Figure 129). However, there was no difference in the PDE rates between treatments or species at the end of the mesocosm study (Figure 129). This class of enzymes may be influenced more by soil-derived diesters of organic P than SAV or epiphyte-derived organic P.

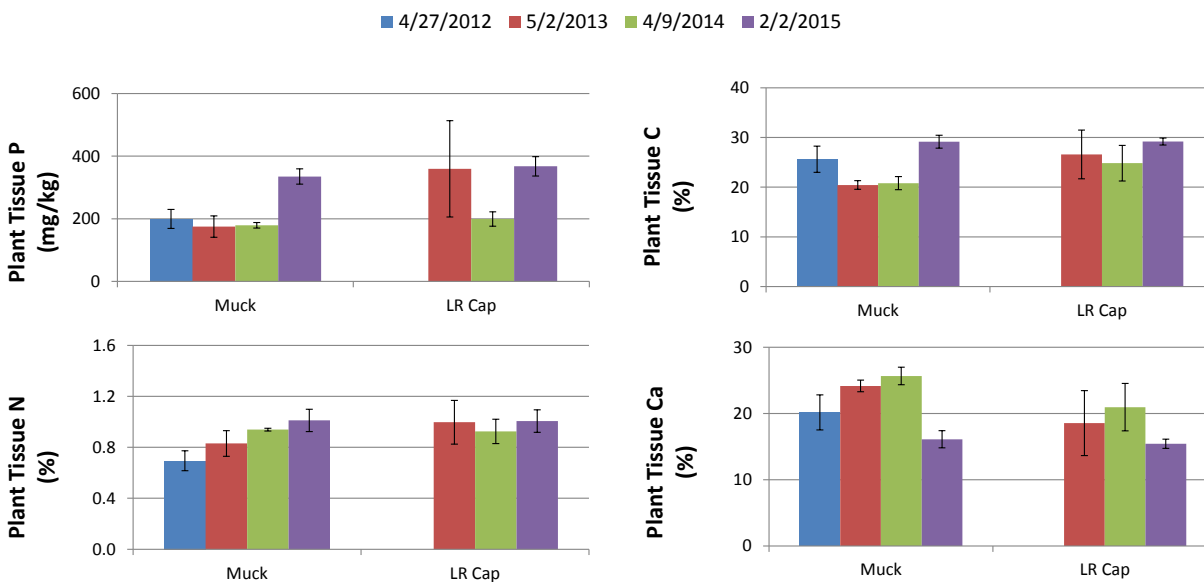


Figure 124. Plant tissue characteristics on three sampling dates. Values represent the average (\pm SE) of grab samples from triplicate mesocosms under each treatment. Macrophyte biomass in the LR Cap treatments was low during the April 2012 sampling, which precluded sampling tissues for nutrient analysis on that date.



Figure 125. Macrophyte biomass in muck-based mesocosms with and without a limerock cap, on April 7 2014, just prior to vegetation sampling and drawdown.

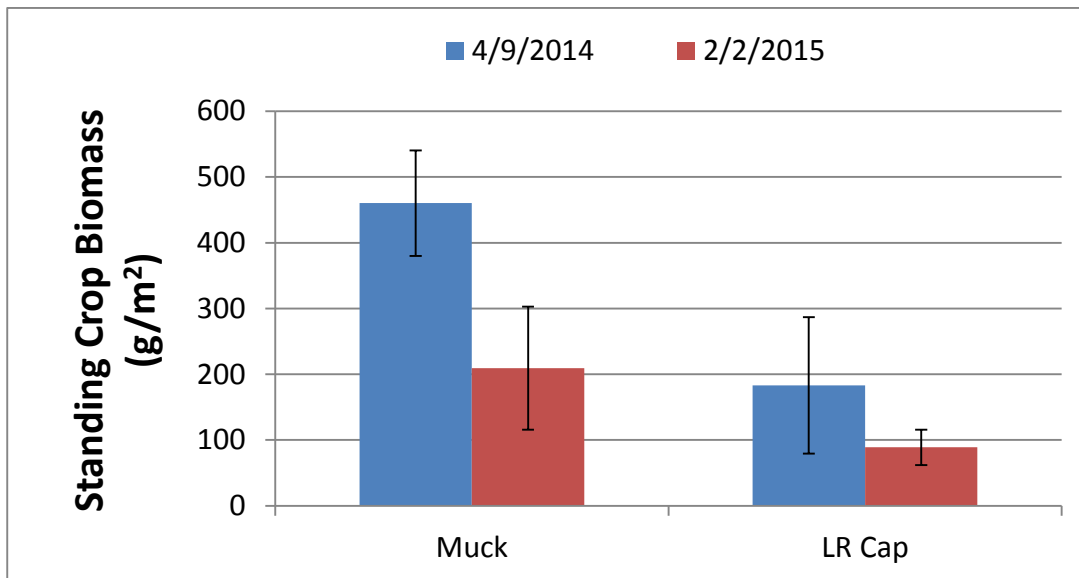


Figure 126. Average (\pm SE) standing crop biomass of submerged aquatic vegetation (primarily *Chara* and *Potamogeton*) in triplicate mesocosms with or without a limerock (LR) cap above muck soils, as determined April 9, 2014 after three years of flow-through operations.

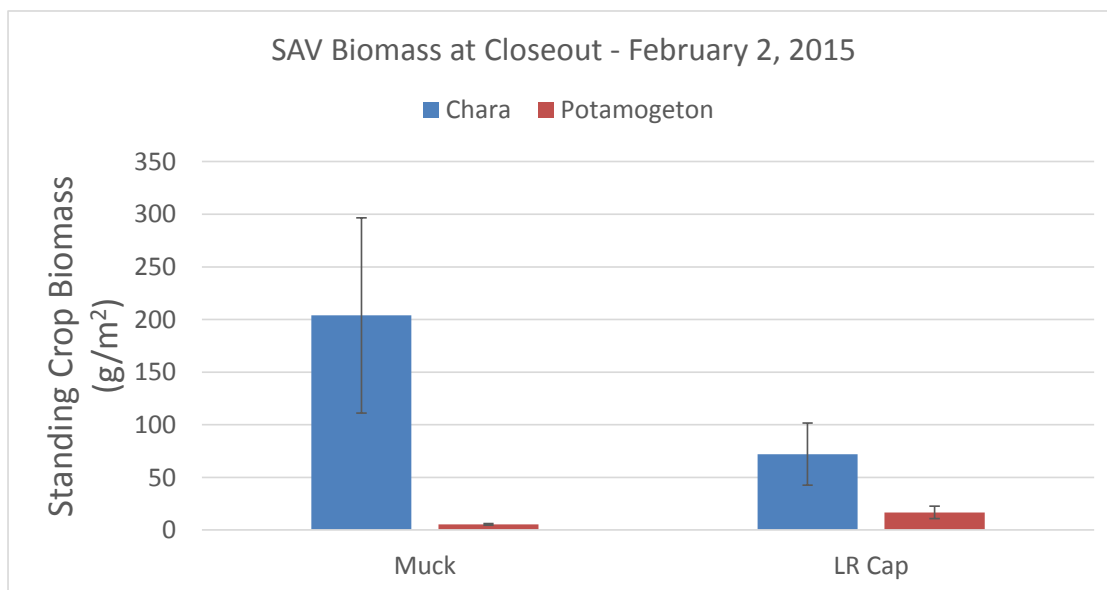


Figure 127. Standing crop biomass of the two dominant SAV species at the conclusion of the study on February 2, 2015. Error bars denote the standard error from triplicate mesocosms under each treatment.

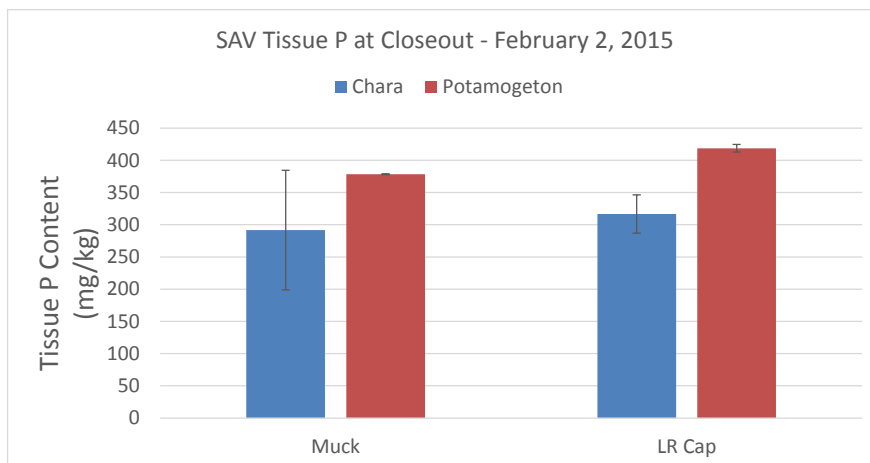


Figure 128. Standing crop biomass and total phosphorus content of submerged aquatic vegetation (SAV) tissues on February 2, 2015, at the end of the period of operations. Error bars denote \pm SE around the mean value from triplicate mesocosms.

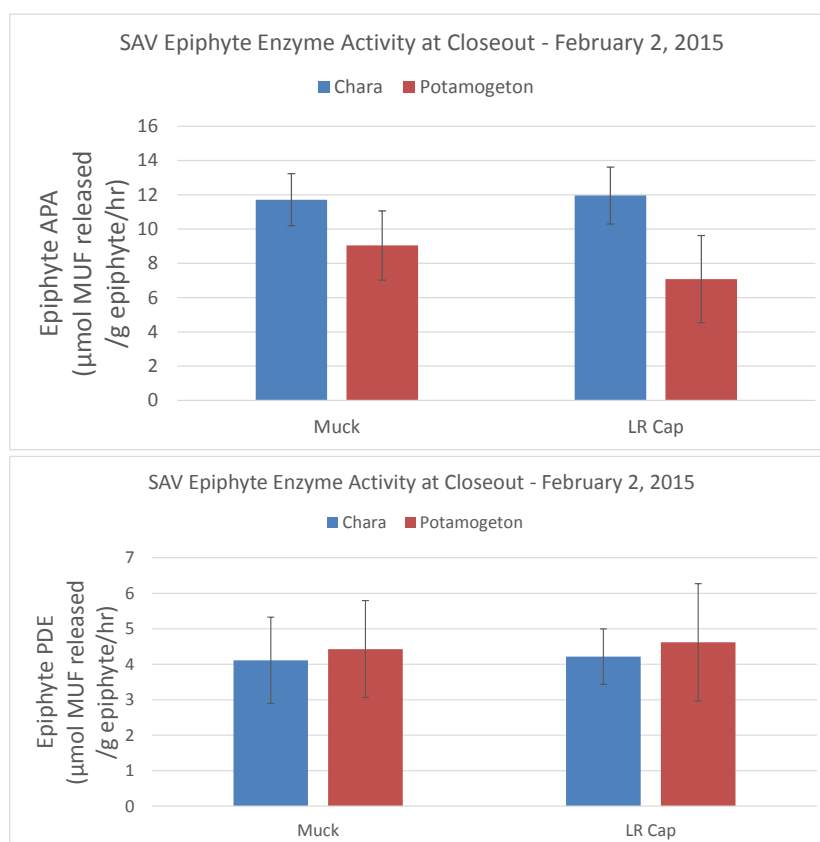


Figure 129. Enzyme activity of epiphytic algae on *Chara* and *Potamogeton* grown in outdoor mesocosms established on a low-phosphorus muck soil with or without a limerock (LR) cap. Alkaline phosphatase activity (APA) and phosphodiesterase (PDE) hydrolysis rates are shown in the top and bottom panels, respectively.

4.4.4 Discussion

Long-term outflow TP concentrations from mesocosms operated with low-P muck with and without a limerock cap were identical between treatments for both the low-P period (9 ± 0.3 $\mu\text{g/L}$) and the high-P period (13 ± 0.3 $\mu\text{g/L}$). Mean inflow TP concentrations for the two periods were 11 and 21 $\mu\text{g/L}$, respectively.

Drawdown in a long-term (3.8 years), replicated outdoor mesocosm study resulted only in a short-term (a few weeks) period of elevated TP concentrations. Most of the released P was measured in PP form, likely indicating phytoplankton growth was occurring before macrophyte biomass recovered. No effect on long-term P removal performance was observed for either substrate; outflow TP concentrations were near 10 $\mu\text{g/L}$ within several months of reflooding.

SAV biomass rebounded after reflooding within several months on the low-P muck soils with or without a LR cap. However, throughout the study, the LR cap maintained lower SAV biomass than muck soils without the cap.

4.5 Use of Limerock Cap to Reduce Flux from High P Soils

4.5.1 Background

In order to achieve strict outflow P concentration targets, internal P loading in the outflow region of STAs should be minimized. Internal loading in wetlands can be direct, through advective and diffusive transfers of nutrients from soil porewater to the overlying water, or indirect, through plant uptake and senescence. One approach to limiting internal loads is to remove soils with moderate or high P release potential. Another approach is to add soil amendments that stabilize nutrients and provide a low-P substrate to limit flux into the water column. Either of these approaches could potentially be applied to outflow regions of existing STAs or to areas where farmed soils will be flooded to expand treatment areas.

The present study examined P flux from high-P muck soils to overlying water, and the effect of a limerock layer above muck soil, under unvegetated conditions.

4.5.2 Methods

On January 14, 2015, intact soil cores were collected from Roth Farm near STA-1W (hereafter, "Farm Muck") and the Lower SAV Cell in STA-3/4 (hereafter, "STA Muck"). The Farm muck was collected after removing vegetation from the soil surface. From the STA muck cores, the accrued layer was removed to expose the underlying muck soil. Target soil depth in each core was 10-15 cm. Cores with > 15 cm soil, large rocks or large roots were discarded and additional cores were collected until 12 uniform cores were obtained from each site.

The day after soil collection, the walls of each core were wiped clean. For each of the two muck soil types, a layer of limerock was placed above the muck soil in replicate cores. Limerock-amended treatments consisted of 5, 10, or 15 cm of added limerock above the soil (Figure 130). Phosphorus flux rates to the overlying water from the muck soils with these calcareous

amendments were compared to P flux from controls (no LR added) of each muck soil type, and to P flux from calcareous PSTA sediments (Figure 131). The PSTA sediment was collected from the back end of the PSTA Cell near station L1, where calcium content of the sediment was ~28% (Section 4.4).

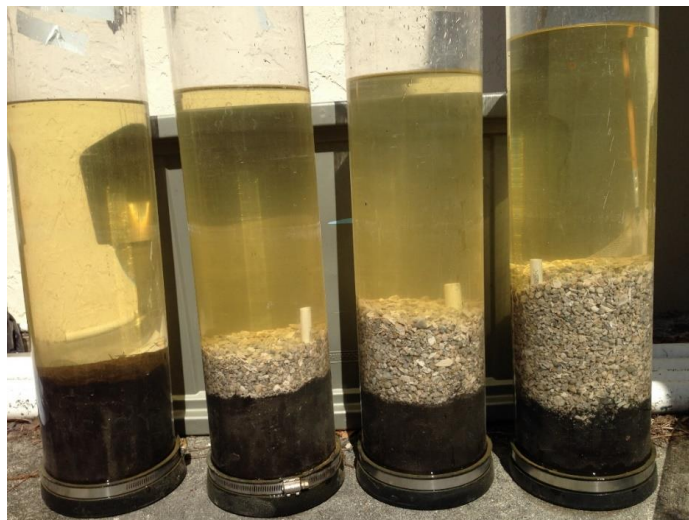


Figure 130. Four limerock treatments were applied to the muck soils: 0, +5, +10, +15 cm limerock gravel amendments.

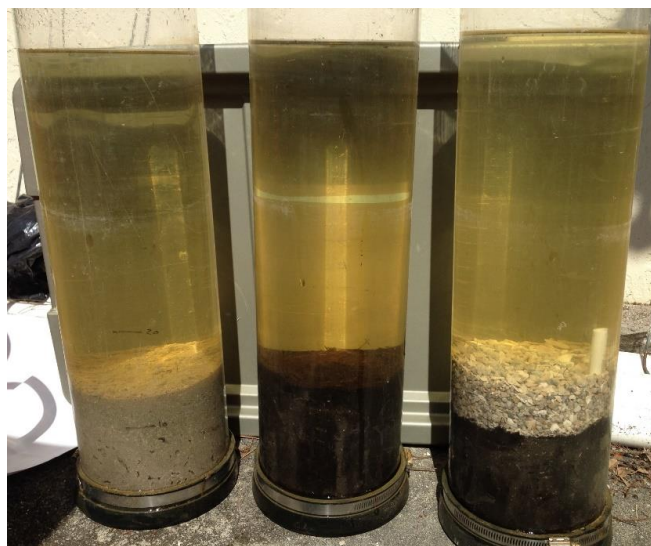


Figure 131. Soil incubation treatments (from left to right): PSTA sediments, STA muck soil without limerock, and STA soil with a 5-cm limerock cap.

In each core designated for limerock amendment, a sampling well (clean 3/8" diam. rigid tubing) was installed. Each well was sealed at the bottom, but perforated just above the muck soil surface to allow water to be drained from the limerock layer during water exchanges. For +15 cm treatments, the sampling well also had holes drilled 7-8 cm above the muck, at the midpoint of the limerock layer.

4.5.2.1 Reflood Water

Outflow water from the PSTA Cell was used to reflood each core. Two samples of the reflood water were collected during each water exchange and measured for SRP, TP, and Ca. Reflood water was added to saturate the soil in Roth Farm treatments, while STA soils from the Lower SAV Cell and PSTA Cell were already saturated. The overlying water was drained from these later cores immediately prior to reflooding with fresh water at the start of the incubation. A total of 5 L was added to each core to establish a water column above the substrate. The cores remained unplanted, and stored in a dark water bath.

Aeration was provided to maintain aerobic conditions in all treatments during the first four of six cycles in the study. Dissolved oxygen was measured twice weekly and a minimum amount of bubbling was used to achieve DO concentrations of ~3-8 mg/L. Bubbles were released into the middle of the water column, ~15 cm above the sediment surface. Disturbance of surficial sediments was negligible. At the beginning of cycle 5, aeration was discontinued and the top of each core was sealed to minimize re-oxygenation of the water column. During the final cycle, nitrogen gas was sparged into each core to induce hypoxic conditions (DO < 0.5 mg/L).

4.5.2.2 Monitoring P flux

On a weekly basis, surface water SRP concentrations were measured, and pH and temperature were recorded during each sampling. Water was exchanged every two weeks. Before each water exchange, DO was also measured. In the control (no LR added) cores and +15 cm LR treatments, dissolved calcium was also sampled in the surface water.

In the +15 cm LR treatments, porewater was also sampled for SRP, dCa, pH and temperature measurements at the middle of the LR layer (7-8 cm above the muck surface). This was accomplished by using a syringe and sample tubing placed within the sampling well.

This experiment was conducted over a 12 week period.

4.5.3 Results

4.5.3.1 Experimental conditions

Mean soil TP content of the farm muck was 971 ± 12 mg/kg, over twice the content of STA muck (456 ± 10 mg/kg) and three times higher than PSTA sediment (275 ± 7 mg/kg; Figure 132). During the incubation, DO concentrations were initially high (> 4 mg/L), but were lower in the final water exchange as a result of the nitrogen gas sparge of the water column (Figure 133). No difference in DO concentration was observed between control cores and LR-amended treatments.

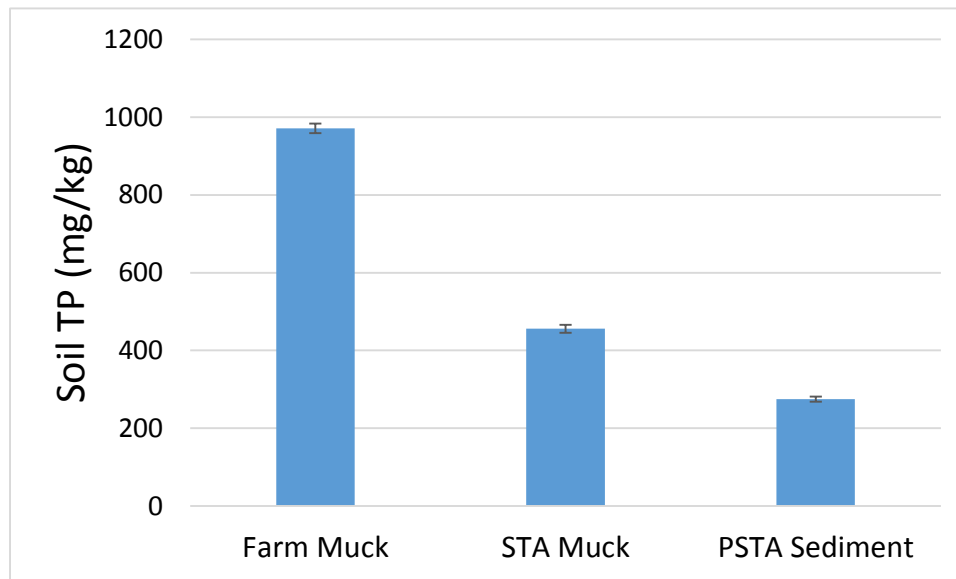


Figure 132. Mean soil total phosphorus (TP) content of three soils used in the incubation.

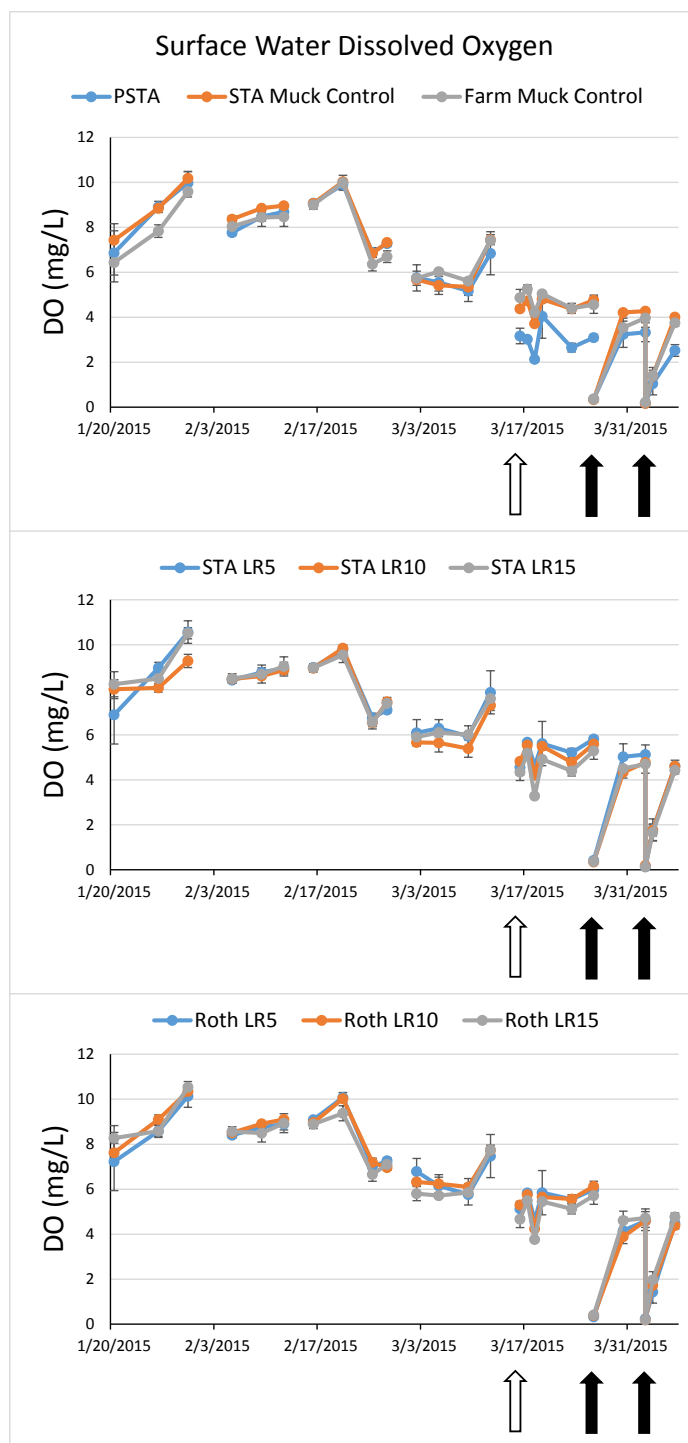


Figure 133. Mean dissolved oxygen (DO) concentrations in control cores containing muck soils or PSTA accrued sediments during the 12-week study. Breaks in the lines denote water exchanges between each of six cycles. The open arrow at the beginning of cycle 5 denotes when aeration ceased and the top of each core was sealed to minimize reaeration. Solid arrows denote N₂ sparge to DO < 0.5 mg/L on two occasions during the final cycle.

4.5.3.2 P Concentrations in the Water Column

Concentrations of SRP in the water column increased during each cycle for the cores with farm muck (without limerock), while STA muck (without limerock) and PSTA sediment treatments both showed a decrease in SRP concentrations to the limits of detection during the first cycle, and then sustained concentrations at the limits of detection during subsequent cycles (Figure 134). After the end of the first 14 days of incubation, the farm muck cores had SRP concentrations of $126 \pm 21 \mu\text{g/L}$ in the overlying water. Subsequent cycles showed lower TP concentration increases ($< 50 \mu\text{g/L}$), until the 5th and 6th cycles. Elevated P accumulation in the water column above farm muck during the last cycle was likely due to the temporarily hypoxic conditions that resulted from the sparging with N_2 gas.

The same hypoxic conditions that affected the farm soils had no influence on P stability in the STA muck soils. The STA soils would have been exposed to anoxic conditions under flooded conditions typical of STA soils. Therefore, phosphorus forms that become unstable under anoxic conditions (such as Fe-hydroxide associated P compounds) were likely not a substantial part of the soil P in the STA muck soil or PSTA sediments, but may have been more prevalent in the farm muck soil.

While the presence of a limerock layer clearly had an effect on SRP in the water column, relative to controls without LR added, the thickness of the limerock layer showed little effect for either soil type (Figures 135 and 136).

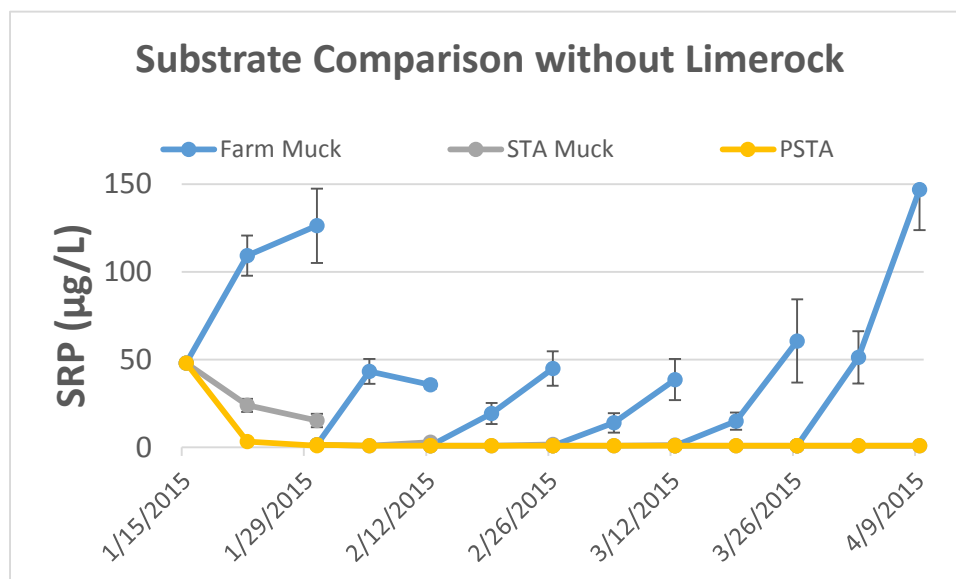


Figure 134. Soluble reactive phosphorus (SRP) concentrations in the overlying water above three soil types. Error bars denote the standard error around the mean of triplicate cores under each treatment.

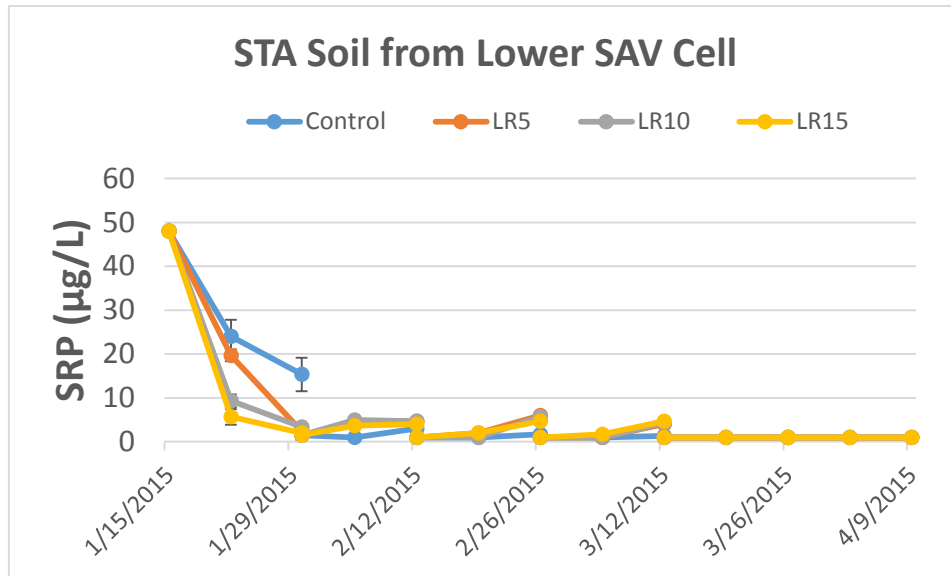


Figure 135. Soluble reactive phosphorus concentrations in the surface waters overlying STA muck soils during six consecutive batch cycles of 14 days each. Error bars denote the standard error around triplicate soil cores assigned to each of four limerock cap treatments (0 cm (“control”) or 5, 10 or 15 cm of limerock added).

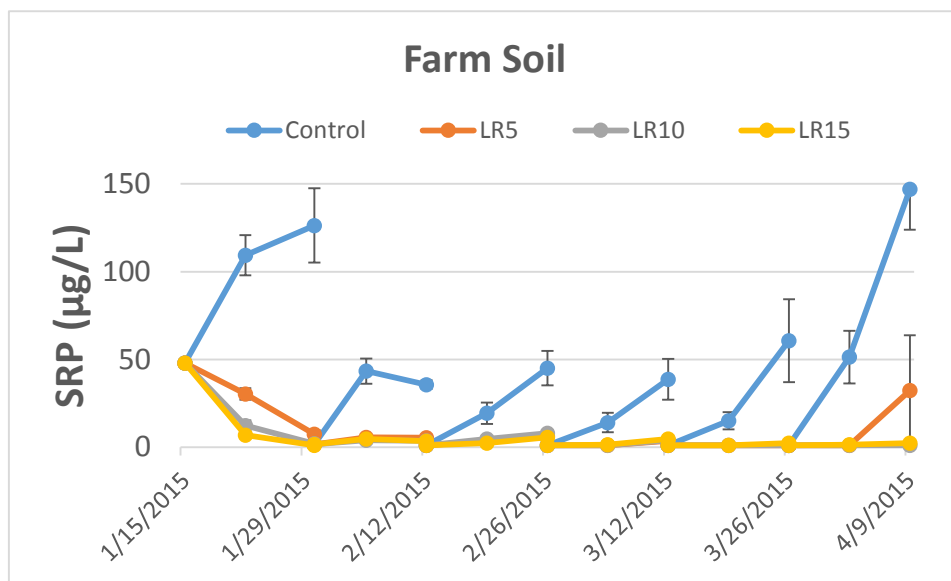


Figure 136. Soluble reactive phosphorus concentrations in the surface waters overlying Farm Muck soils during 6 consecutive batch cycles of 14 days each. Error bars denote the standard error around triplicate soil cores assigned to each of four limerock cap treatments (0 cm (“control”) or 5, 10 or 15 cm of limerock added).

4.5.3.3 Porewater chemistry

The porewater well sampling from within the limerock layer indicated that high SRP concentrations began to accumulate above the Farm muck during the 2nd cycle and remained elevated through the remainder of the study (Figure 137). By contrast, the limerock layer above the STA muck soil showed little evidence of P enrichment. Porewater calcium concentrations were similar between treatments at the end of the first cycle, with 71 ± 3 mg/L and 63 ± 3 mg/L. In subsequent cycles, however, porewater above the farm soil showed increased concentrations of calcium and lower pH levels, as compared to porewater in the LR cap above STA muck soils (Figures 138 and 139). Partial dissolution of the limerock cap by organic acids from the farm muck may have contributed to the changes observed in both parameters.

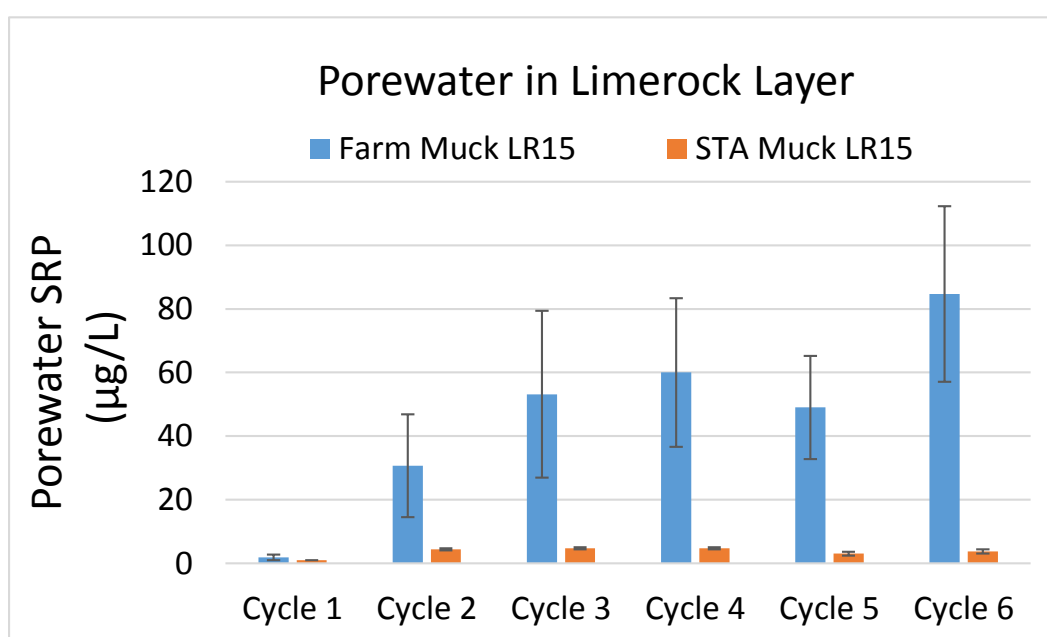


Figure 137. Soluble reactive phosphorus (SRP) concentrations in the porewater of the limerock layer in treatments with 15 cm LR added as a cap above two muck soil types. Error bars denote the standard error around the mean for triplicate cores under each treatment.

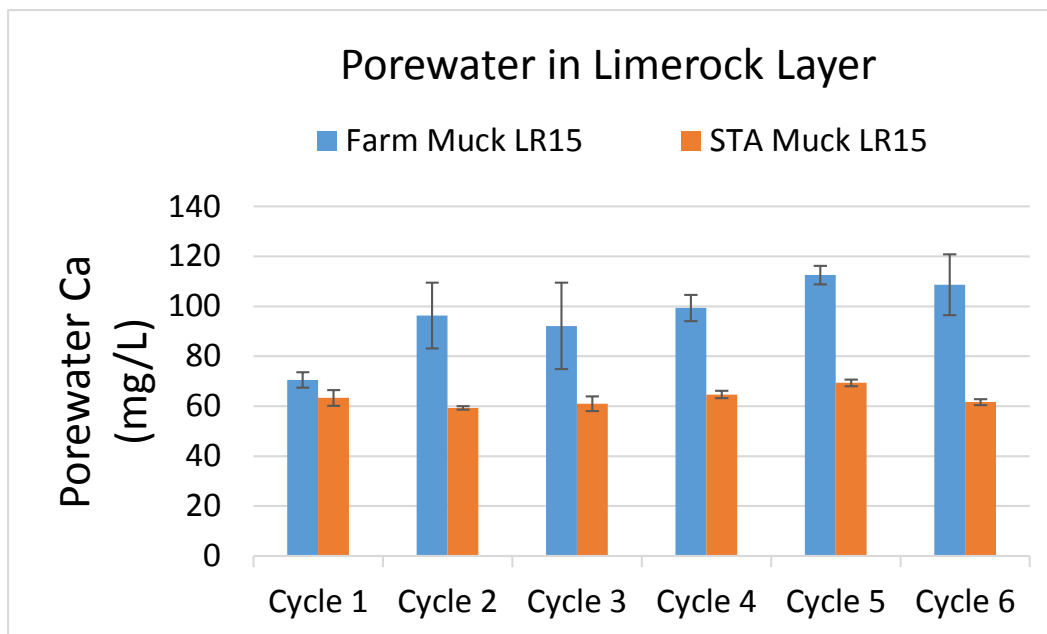


Figure 138. Porewater calcium concentrations in the limerock layer above two muck soil types incubated for six two-week cycles.

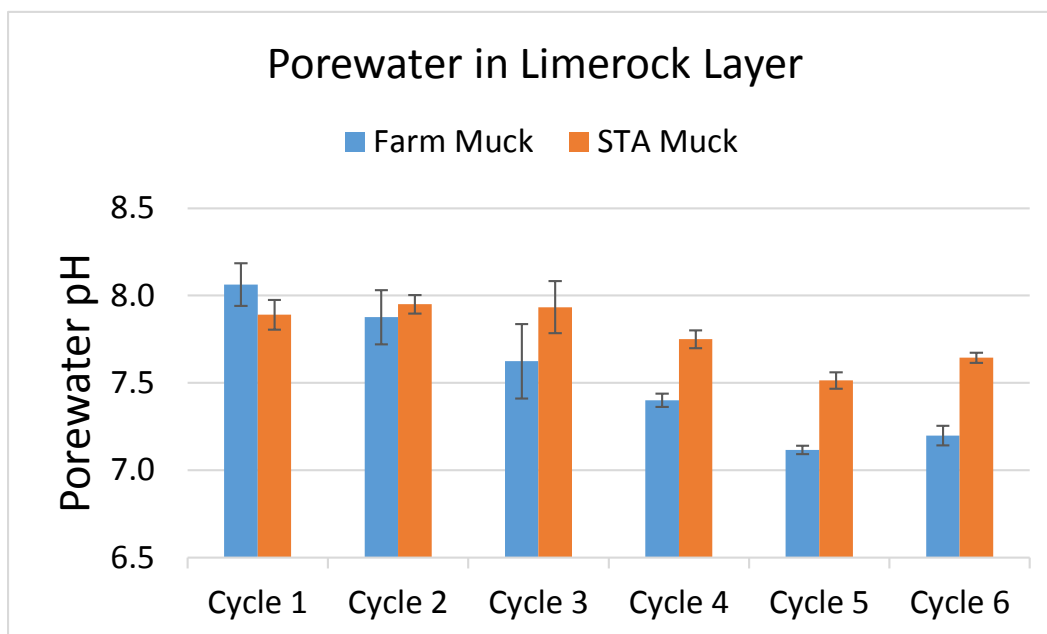


Figure 139. Porewater pH values from limerock over two muck soil types incubated for six two-week cycles.

4.5.4 Discussion

The farm muck was P-enriched relative to the STA muck soils or PSTA sediments, and exhibited greater P release. A limerock cap was effective at both reducing P flux from the farm

muck, and increasing P uptake by the STA muck (during the first cycle), across a range of cap depths (5-15 cm). Porewater SRP and calcium enrichment and lower pH values within the LR layer were observed above farm muck soils.

In order to evaluate the long-term effectiveness of a limerock cap, a follow-up study is planned using larger flow-through mesocosms. This platform will incorporate macrophytes and evaluate the potential adverse effects of macrophyte P uptake from soils (i.e., "mining") on water column P concentration reduction above limerock-capped muck soils.

5 References

- Andreotta, H., M. Chimney, T. DeBusk, B. Garret, G. Goforth, K. Grace, D. Ivanoff, M. Jerauld, M. Kharbanda, N. Larson, S. Miao, D. Marois, W. Mitsch, T. Piccone, K. Pietro, N. Ralph, A. Ramirez, L. Schwartz, L. Toth, S. Xue, Y. Yan, M. Zamorano, L. Zhang, and H. Zhao. 2014. Performance of the Everglades Stormwater Treatment Areas. In 2014 South Florida Environmental Report, Vol. 1, Chapter 5B. South Florida Water Management District, West Palm Beach, FL.
- Andreotta, H., M. Chimney, T. DeBusk, B. Garret, B. Garrett, L. Gerry, J. Henry, D. Ivanoff, M. Jerauld, M. Kharbanda, M. Kirkland, N. Larson, S. Miao, T. Piccone, K. Pietro, L. Schwartz, D. Sierer-Finn, L. Toth, S. Xue, Y. Yan, M. Zamorano, and H. Zhao. 2015. Performance of the Everglades Stormwater Treatment Areas. In Draft 2015 South Florida Environmental Report, Vol. 1, Chapter 5B. South Florida Water Management District, West Palm Beach, FL.
- Barko, J.W., and R.M. Smart. 1980. Mobilization of sediment phosphorus by submersed freshwater macrophytes. *Freshwater Biology*, 10: 229-238.
- Browder, J. A., D Cottrell, M. Brown, M. Newman, R. Edwards, J. Yuska, M. Browder, and J. Krakoski. 1982. Biomass and primary production of macrophytes and macrophytes in periphyton habitats of the Southern Everglades. Report T-662 South Florida Research Center, Homestead, FL. 49 pp.
- Browder, J. A., P.J. Gleason, and D.R. Swift. Periphyton in the Everglades: Spatial variation, environmental correlates, and ecological implications. *Everglades: The Ecosystem and its Restoration*. West Palm Beach, FL: CRC Press. 1994.
- Burkholder, J. M., and R. G. Wetzel. 1990. Epiphytic alkaline phosphatase on natural and artificial plants in an oligotrophic lake: Re-evaluation of the role of macrophytes as a phosphorus source for epiphytes. *Limnology and Oceanography* 35(3): 736-747.
- Carignan, R. and J. Kalff. 1980. Phosphorus sources for aquatic weeds: water or sediments? *Science* 29: 987-989.
- CH2M-Hill 2003. PSTA research and demonstration project Phase 1, 2, and 3 Summary Report. Prepared for SFWMD.
- Craft, C.B., J. Vymazal and C.J. Richardson. 1995. Response of Everglades plant communities to nitrogen and phosphorus additions. *Wetlands* 15:258-271.
- DBE 2002. Vegetation Biomass and Nutrient Analysis for Stormwater Treatment Area - 1West (STA-1W) Final Report. November 2002. Prepared for SFWMD.
- DBE 2015. Water Quality Report: Quantifying Operational Boundaries. Deliverable A-5-b under Agreement No. 4600003125 prepared for the South Florida Water Management District. July 7, 2015.

- DeBusk, T. A., K. A. Grace, F. E. Dierberg, S. D. Jackson, M. J. Chimney, and B. Gu. 2004. An investigation of the limits of phosphorus removal in wetlands: a mesocosm study of a shallow periphyton-dominated treatment system. *Ecol. Eng.* 23: 1-14.
- DeBusk, T. A., M. Kharbanda, S. D. Jackson, K. A. Grace, K. Hillman, and F. E. Dierberg. 2011. Water, Vegetation and Sediment Gradients in Submerged Aquatic Vegetation Mesocosms Used for Low-Level Phosphorus Removal. *Science of the Total Environment* 409 (23):5046-5056.
- Dodds, W. K. 2003. The role of periphyton in phosphorus retention in shallow freshwater aquatic systems. *Journal of Phycology* 39:840-849.
- Doren, R.F. and R.D. Jones. 1996. Conceptual Design of Periphyton-Based STAs. Memo to Col. T. Rice, USACE dated January 30, 1996.
- Gaiser, E. E., D. L. Childers., R. Jones, J. Richards, L. Scinto, and J. Trexler, 2006. Periphyton responses to eutrophication in the Florida Everglades: cross-system patterns of structural and compositional change. *Limnology and Oceanography* 51: 617-630.
- Gaiser, E. E., P. V. McCormick, S. E. Hagerthey, and A. D. Gottlieb. 2011. Landscape patterns of periphyton in the Florida Everglades. *Critical Reviews in Environmental Science and Technology* 41(S1):92-120.
- Goforth, G. 2011. Written Testimony in Case No. 88-1886-Civ-Moreno in the US. District Court, Southern District of Florida. Prepared as an expert witness for the South Florida Water Management District. Prepared by Gary Goforth, Inc., Stuart, FL.
- Gottlieb, A. D., J. H. Richards, and E. E. Gaiser. 2006. Comparative study of periphyton community structure in long and short-hydroperiod Everglades marshes. *Hydrobiologia* 569:195-207.
- Hagerthey, S. E., B. J. Bellinger, K. Wheeler, M. Gantar, and E. Gaiser. (2011) 'Everglades Periphyton: A Biogeochemical Perspective', *Critical Reviews in Environmental Science and Technology*, 41(6): 309-343.
- Helms, J. R., A. Stubbins, J. D. Ritchie, E. C. Minor, D. J. Kieber, and K. Mopper. 2008. Absorption spectral slopes and slope ratios as indicators of molecular weight, source, and photobleaching of chromophoric dissolved organic matter. *Limnol. Oceanogr.* 53:955-969.
- Iwaniec, D. M., D. L. Childers, D. Rondeau, C. J. Madden, and C. Saunders. 2006. Effects of hydrologic and water quality drivers on periphyton dynamics in the Southern Everglades. *Hydrobiologia* 569: 223-235.
- Juston, J. M., and T. A. DeBusk. 2011. Evidence and implications of the background phosphorus concentration of submerged aquatic vegetation wetlands in Stormwater Treatment Areas for Everglades restoration, *Water Resources Research* 47, W01511, doi:10.1029/2010WR009294

- Juston, J. M., T. A. DeBusk, K. A. Grace, S. D. Jackson. 2013. A model of phosphorus cycling to explore the role of biomass turnover in submerged aquatic vegetation wetlands for Everglades restoration. *Ecological Modelling*, 251:135-149
- Kadlec, R. H., and W. W. Walker. 2003. Technology Review of Periphyton Stormwater Treatment. Draft Report dated November 11, 2003.
- Kastovsky, J., K. Rehakova, M. Bastl, J. Vymazal, and R. S. King. 2008. Experimental assessment of phosphorus effects on algal assemblages in dosing mesocosms. In C. J. Richardson (Ed.) *The Everglades Experiments: Lessons for Ecosystem Restoration* Springer, NY.
- McCormick, P. V., and M. B. O'Dell. 1996. Quantifying periphyton response to phosphorus in the Florida Everglades: a synoptic-experimental approach. *J. N. Am. Benthol. Soc.* 15(4): 450-468.
- McCormick, P. V., and L. J. Scinto. 1998. Influence of Phosphorus Loading on Wetland Periphyton Assemblages: A Case Study from the Everglades. In K. R. Reddy, G. A. O'Connor, and C. L. Schelske. (Eds) *Phosphorus Biogeochemistry of Subtropical Ecosystems*. CRC Press. 728 pp.
- McCormick, P. V., M. B. O'Dell, R. B. E. Shuford, J. G. Backus and W. C. Kennedy. 2001. Periphyton responses to experimental phosphorus enrichment in a subtropical wetland. *Aquatic Botany* 71:119-139.
- McCormick, P. V., P. S. Rawlik, K. Lurding, E. P. Smith, F. H. Sklar. 1996. Periphyton-water quality relationships along a nutrient gradient in the northern Florida Everglades. *J. North Am. Benthol. Soc.* 15(4): 433-449.
- McCormick, P. V., R. B. E. Shuford, and M. J. Chimney. 2006. Periphyton as a potential sink in the Everglades Nutrient Removal Project. *Ecological Engineering* 27: 279-289.
- McCormick, P. V., S. Newman, G. Payne, S. Miao, and T. D. Fontaine. 2000. Ecological Effects of phosphorus enrichment in the Everglades. In 2000 Everglades Consolidated Report, Vol. 1, Chapter 3. South Florida Water Management District, West Palm Beach, FL.
- Pietro, K., G. Germain, R. Bearzotti, and N. Iricanin. 2010. Performance and optimization of the Everglades Stormwater Treatment Areas. In 2010 South Florida Environment Report, Vol. 1, Chapter 5. South Florida Water Management District, West Palm Beach, FL.
- Pietro, K. C., R. Bearzotti, M. Chimney, G. Germain, and N. Iricanin. 2008. STA performance, compliance, and optimization. In 2008 South Florida Environment Report, Vol. 1, Chapter 5. South Florida Water Management District, West Palm Beach, FL.
- Scinto, L. J., and K. R. Reddy. 2003. Biotic and abiotic uptake of phosphorus by periphyton in a subtropical freshwater wetland. *Aquatic Botany* 77: 203-222.
- Swift, D. R. 1981. Preliminary investigations of periphyton and water quality relationships in the Everglades Water Conservation Areas. Tech. Publication 81-5, South Florida Water management District, West Palm Beach, 83 pp.

- Swift, D. R., 1984. Periphyton and water quality relationships in Everglades Water Conservation Areas. *In* Gleason, P. J. (Ed.) *Environments of South Florida: Past and Present II* Miami Geological Society, Coral Gables, Florida, pp. 97-117.
- Swift, D. R., and R. B. Nicholas. 1987. Periphyton and water quality relationships in the Everglades Water Conservation Areas. Tech. Publ. 87-2 South Florida Water Management District.
- Vymazal, J. 2003 Periphyton Taxonomic and Abundance Data Analysis in CH2M-Hill 2003.
- Vymazal, J., and C. J. Richardson. 1995. Species composition, biomass, and nutrient content of periphyton in the Florida Everglades. *Journal of Phycology* 31:343-354.
- Wetland Solutions and ANAMAR Environmental Consulting 2011. STA-1E Periphyton Stormwater Treatment Area (PSTA) Final Report (W912-EP-09-E-0013). Prepared for Army Corps of Engineers. Draft dated October 24, 2011.
- Wetzel, R.G. 1991. Extracellular enzymatic interactions: storage, redistribution, and interspecific communication. *In* Chrost, R. (Ed). *Microbial Enzymes in Aquatic Environments*.
- Wetzel, R.G., P.G. Hatcher and T.S. Bianchi. 1995. Natural photolysis by ultraviolet irradiance of recalcitrant dissolved organic matter to simple substrates for rapid bacterial metabolism. *Limnol. Oceanogr.* 40: 1369-1380.
- Wood, E. J. F. & N. G. Maynard, 1974. Ecology of the micro- algae of the Florida Everglades. *In* Gleason, P. J. (ed.), *Environments of South Florida: Past and Present*, Memoir No. 2. Miami Geological Society, Coral Gables, 123-145.